EUROPEAN COMMISSION

Community research

Long-term Performance of Engineered Barrier Systems

PEBS

Long-term Performance of Engineered Barrier Systems PEBS

Engineered Barrier Emplacement Experiment in Opalinus Clay: "EB" Experiment

AS-BUILT OF DISMANTLING OPERATION

(DELIVERABLE-N°: D2.1-4)

Contract (grant agreement) number: FP7 249681

Author(s):

Beatriz Palacios, María Rey and José Luis García-Siñeriz M (AITEMIN) with contributions of María Victoria Villar (CIEMAT), Juan Carlos Mayor (ENRESA) and Manuel Velasco (GOLDER)

Date of issue of this report: **17/09/13**

Start date of project: 01/03/10 Duration: 48 Months

Project co-funded by the European Commission under the Seventh Euratom Framework Programme for Nuclear Research &Training Activities (2007-2011)		
Dissemination Level		
PU	Public	**PU**
RE	Restricted to a group specified by the partners of the [acronym] project	
CO	Confidential, only for partners of the [acronym] project	

PEBS

EURATOM

INDEX

FIGURES

TABLES

1 INTRODUCTION

1.1 THE EB PROJECT

The Engineered Barrier Emplacement Experiment in Opalinus Clay "EB" Experiment aimed the demonstration of a new concept for the construction of HLW repositories in horizontal drifts, in competent clay formations. The principle of the new construction method was based on the combined use of a lower bed made of compacted bentonite blocks, and an upper buffer made of granular bentonite material (GBM).

The project consisted on a real scale isothermal simulation of this construction method in the Opalinus Clay formation at the Mont Terri underground laboratory in Switzerland. A steel dummy canister, with the same dimensions and weight as the Spanish reference canister, was placed on top of a bed of bentonite blocks, and then the upper part of the drift was buffered with the GBM made of bentonite pellets (Figure 1). The drift was sealed with a concrete plug having a concrete retaining wall between the plug and the GBM. Since the end of the test installation the evolution of the different hydro-mechanical parameters were being monitored, both in the barrier and the rock (especially in the EDZ). Relative humidity and temperature in the rock and in the bentonite buffer, rock displacement, pore pressure and total pressure were registered by means of different types of sensors. Due to the short amount of free water available in this formation, an artificial hydration system was installed to accelerate the hydration process in the bentonite.

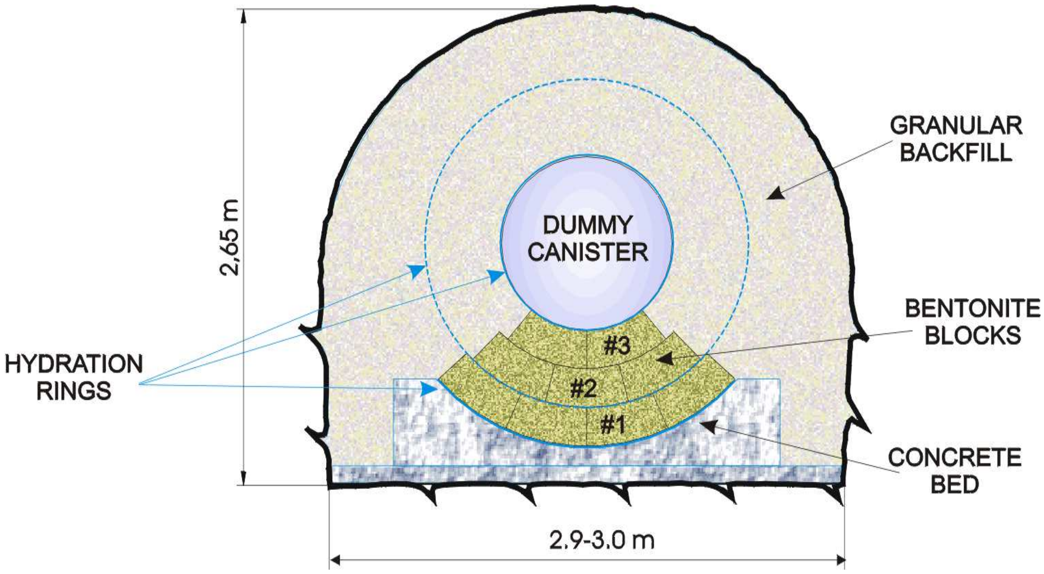

Figure 1: EB experimental layout

The basic objectives of the project were the following:

- Definition of backfill material (composition, grain size distribution ...). Demonstration of the manufacturing process at semi-industrial scale.

- Characterisation of the hydro-mechanical properties of the backfill material.
- Design and demonstration of the emplacement and backfilling technique.
- Quality Assessment of the clay barrier in terms of the achieved geomechanical parameters (homogeneity, dry density, voids distribution ...) after emplacement.
- Characterisation of the Excavation Disturbed Zone (EDZ) in the Opalinus clay, and determination of its influence in the overall performance of the system.
- Investigation of the evolution of the hydro-mechanical parameters in the clay barrier and the EDZ as a function of the progress of the hydration process.
- Development of a hydro-mechanical model of the complete system adjusted and calibrated with the data resulting from the experiment.

After 11 years of operation, the experiment has been dismantled between the 19th of October 2012 and the 1st of February 2013. The aim of this document is to describe the processes, results and conclusions of the dismantling operation.

1.2 BACKGROUND

1.2.1 Funding

The first phase of the EB experiment -years 2000 to 2003–, devoted to the test design, installation and start-up of the operation, was co-financed by the European Commission (contract nº FIKW-CT-2000-00017), under the framework of the research and training programme (Euratom) in the field of nuclear energy, and ENRESA (Spain). Besides ENRESA, BRG (Germany) and NAGRA (Switzerland) were the principal contractors and AITEMIN (Spain) and CIMNE (Spain) the assistant contractors.

Between 2003 and 2009 the project operation continued under the support of the Mont Terri Consortium, project 32.015: EB, phases 10 to 14.

From 2010, the experiment is part of the PEBS[1] project, Work Package 2 Experimentation. The PEBS project is one of the “Small and Medium Projects” forming part of the FP7 Euratom programme. It is a multinational European research project that investigates processes affecting the engineered barrier performance of geological repositories for high-level waste disposal. The PEBS consortium consists of 17 leading nuclear research organisations, radioactive waste management agencies/implementing organisations, universities and companies.

1.2.2 Experiment development

After the preparation of the design document (AITEMIN 2001) and the components procurement, the installation of the experiment was carried out in several steps. The instrumentation was installed from November 2001 to February 2002: in-rock pore pressure sensors, rock displacement sensors and some rock relative humidity sensors, canister

[1] PEBS: Long-term Performance of the Engineered Barrier System

displacement sensors, relative humidity sensors in bentonite and total pressure cells. The artificial hydration system was installed in March 2002. The installation of the experiment was finished in April 2002, including the retaining wall, the concrete plug and the data acquisition system.

The artificial hydration of the bentonite started in May 2002 and ended in June 2007. There was an initial hydration phase with an important amount of water injected (6,700 litres in two days) that was stopped after several water stains appeared on the wall. After that, the hydration was restarted and from September 2002 to June 2007, there were different hydration phases with continuous water injection. The detailed record of effective water inflow for bentonite hydration is included in report SDR EB N19 (AITEMIN 2007).

After the end of the hydration phase, the monitoring of the experiment continued in order to follow the evolution of the bentonite.

The Engineered Barrier Emplacement Experiment test is described in detail in the "EB Experiment Test Plan", Project Deliverable 1, EC contract FIKW-CT2000-00017 (AITEMIN 2001), which includes the preliminary design, the emplacement and the operation.

1.3 CONCEPT OF THE DISMANTLING OPERATION

The main objective of the dismantling of the EB experiment has been to know about the real status of the GBM used after its artificial saturation: degree of saturation, permeability, density, aspect, homogeneity, etc. It has been also important to check the status of the bentonite blocks that support the canister, the rock in contact with the buffer, with especial interest in the EDZ, and the degree of saturation of the concrete in the vicinity of the buffer (plug and blocks support). Therefore, the activities of the dismantling have been coordinated with a sampling programme intended to analyse parameters such as dry density, water content, permeability… in the laboratories of the different organizations as well as in an on-site laboratory. The dismantling has been partial, as the last 120 cm of GBM was left on place, as well as the canister and the last 80 cm of the bed of bentonite blocks in order to show the way the experiment was done (demonstrator).

The Test Plan of the planned operation for the dismantling and sampling is described in the document "EB experiment TEST PLAN & SAMPLING BOOK" Deliverables n°:D2.1-2 and D2.1-3 (AITEMIN 2012).

AITEMIN has been the subcontractor to carry out the dismantling operation including the sampling and on site analyses.

ENRESA, AITEMIN & CIEMAT have been focused in the sampling and analysis of the buffer (GBM and the bentonite blocks), and other participant organizations (BGR, NAGRA and ANDRA) have taken care of the rest of components and interfaces (rock and concrete).

Additionally, the sampling and analysis of the used sensors, to be performed by ENRESA & AITEMIN, and the comparison of the on-site measurements with the last values provided for the installed sensors will help to assess the accuracy of acquired data. Besides, the data resulting from the dismantling will be used for the further adjustment of the H-M model of the complete system.

1.4 CONTENTS OF THE DOCUMENT

This document describes the dismantling and sampling activities carried out. It also shows the results of the dry density and water content obtained in the on site analyses carried out by AITEMIN and in the laboratory ones by the CIEMAT team. In section 2, it starts with a brief chronological description of all the activities that have been carried to accomplish the whole operation. Section 3 describes the dismantling of the concrete plug, the retaining wall and the bentonite removal including the methodology applied and the resources and tools that were used. It also explains the operation to support the canister and to dismantle the data acquisition system.

Section 4 is completely dedicated to the sampling and analysis operation. It describes the different sampling procedures applied depending on the different materials to be sampled, the samples that were taken for the analyses on site and the ones that were taken for the partner organizations. It also explains the analysis procedures carried out in the on-site laboratory, and the obtained results.

The document finishes with the conclusions and the used references.

2 SEQUENCE OF WORKS

The operation started with the partial dismantling of the concrete plug, followed by the sampling and bentonite removal, which were coordinated in order to reach even sections and to alter as minimum as possible the sampling areas. Previously to the dismantling works, the working area was set up.

The dismantling operation itself began on the 23rd of October 2012 with the drilling of a core in the concrete plug in order to have a free inner surface to start breaking it. The bentonite removal and sampling activities started on the 23rd of November 2012 and ended on the 29th of January 2013. The last days of the operation were used to dismantle the data acquisition system (DAS) as well as organizing the shipping of material. The operation was finished on the 1st of February 2013. A more detailed sequence of the whole operation is listed in Table 1.

Table 1. Detailed sequence of works

Date	Activity	Test Plan Phase
October 2012		
19/10/1012-20/10/2012	Preparation of the area of work	Phase 1
23/10/2012	Drilling a 200 mm in diameter core in the concrete plug	Phase 1
24/10/12-31/10/12	Drilling boreholes and use of the splitter to break the concrete plug	Phase 2
November 2012		
6/11/12-13/11/12	Drilling boreholes and use of the splitter to break the concrete plug using a mini-backhoe to help dismantling the plug	Phase 3, 4 and 5
	Taking concrete samples for water content on site analysis	Sampling Phase
14/11/12	The retaining wall and a small area of the bentonite are reached (window)	Phase 6
15/11/12	Testing with different tools to sample the bentonite	Sampling Phase
	Continuing with the plug dismantling works with both methods: splitter and backhoe	Phase 6
16/11/12	Preparation of a plastic cover to protect the bentonite from drying	-
	Testing how to sample concrete and bentonite with a drilling machine.	Sampling Phase
	Continuing with the plug dismantling works using the backhoe	Phase 6
20/11/12	Dismantling of cables box C	Phase 6
	Continuing with the plug dismantling works using the backhoe	Phase 6
21/11/12	Sampling concrete from the retaining wall/bentonite interface	Sampling Phase
22/11/12	Retaining wall/bentonite sampling	Sampling Phase
	Continuing with the plug removal works using the backhoe	Phase 6

Date	Activity	Test Plan Phase
23/11/12-26/11/12	Bentonite removal between retaining wall and the section where the face of the canister is	Bentonite removal
	Taking samples in the section where the face of the canister is for CIEMAT (Geochemical)	Sampling Phase
27/11/12	Testing bentonite sampling and on site dry density and water content analyses	Sampling Phase
28/11/12-30/11/12	Drilling boreholes and use of expansive cement to further break the concrete plug	Phase 6
	Testing bentonite sampling and on site dry density and water content analyses	Sampling Phase
	Continuation of bentonite removal	Bentonite removal
December 2012		
1/12/12-11/12/12	Bentonite removal up to section A1-25	Bentonite removal
12/12/12	Bentonite sampling. Water content and dry density on site analysis section A1-25	Sampling Phase
13/12/12	Sampling section CMT1	Sampling Phase
14/12/12-15/12/12	Sampling for dry density and water content on site analysis of section B1	Sampling Phase
17/12/12-19/12/12	Continuation of bentonite removal	Bentonite removal
	Drilling boreholes and use of expansive cement to further break the concrete plug	Phase 6
January 2013		
9/01/13	Continue bentonite removal	Bentonite removal
10/01/13	Sampling section CMT2	Sampling Phase
11/01/13	Continue bentonite removal	Bentonite removal
12/01/13	Sampling for dry density and water content on site analysis of section E	Sampling Phase
13/01/13-15/01/13	Continue bentonite removal	Bentonite removal
16/01/13	Sampling bentonite blocks from CMT2 section	Sampling Phase
	Nagra's sampling section CMT2	Sampling Phase
17/01/13-18/01/13	Continue bentonite removal	Bentonite removal
22/01/13	Sampling for dry density and water content on site analysis of section B2	Sampling Phase
23/01/13-24/01/13	Continue sampling for dry density and water content on site analysis of section B2 Welding beam to the canister. Canister support works	Canister support
25/01/13	Continue bentonite removal Sampling of blocks section E	Bentonite removal
26/01/13	Sampling for dry density and water content on site analysis of section A2	Sampling Phase
28/01/13-	Continue bentonite removal	Bentonite removal

Date	Activity	Test Plan Phase
29/01/13	DAS dismantling	DAS dismantling
29/01/13	Sampling section CMT3	Sampling Phase
30/01/13-01/02/13	Packing samples and tools	Sampling Phase
	Tiding and cleaning the area. Covering bentonite front with plastic	Closure

Figure 2 represents graphically the evolution of the experiment, taking into account the progress of the excavation, the days that every step took and the milestones of the project.

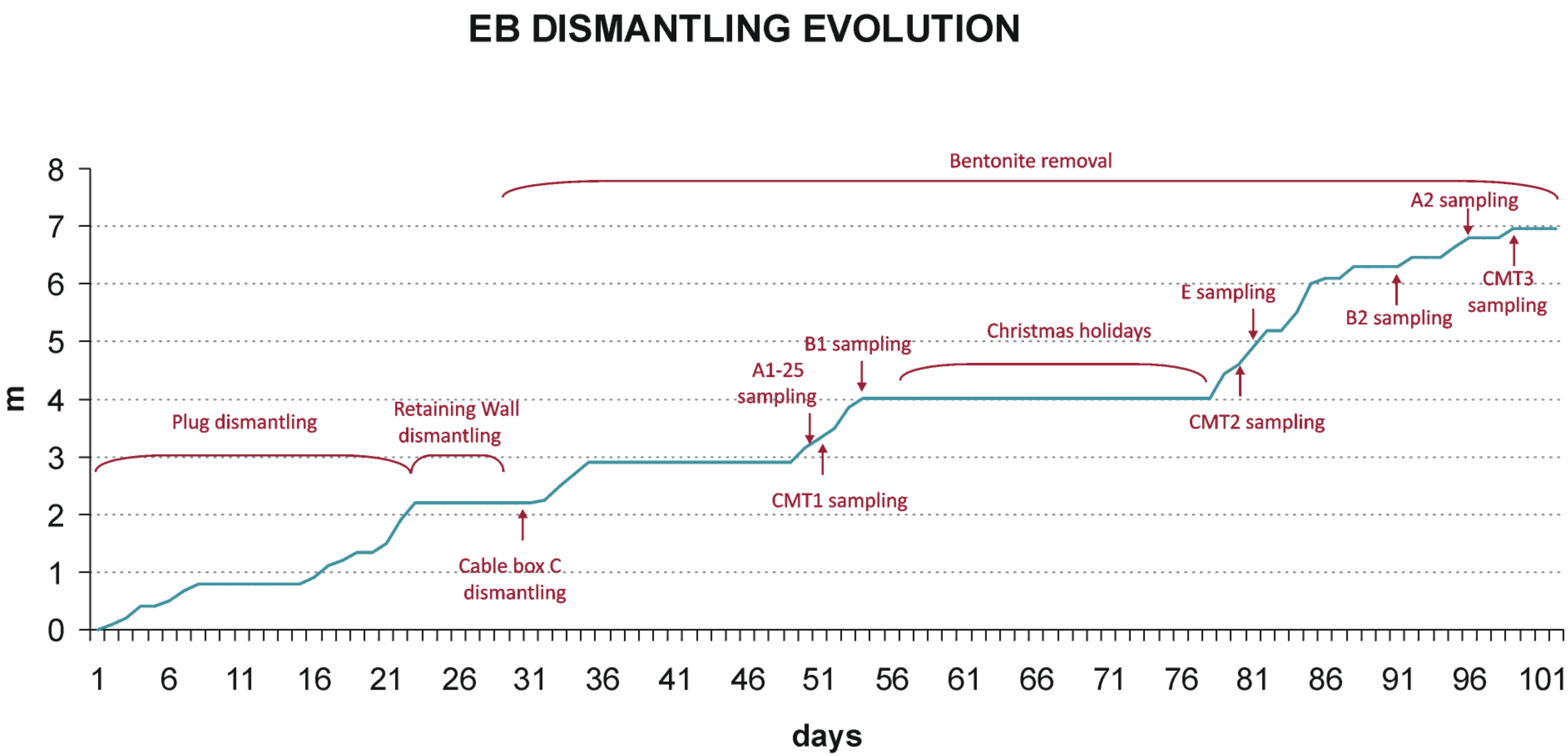

Figure 2: Evolution of the EB experiment. Duration in days of the whole operation (x axis) vs. progress in depth in the gallery (y axis)

3 DISMANTLING OPERATION

3.1 PREPARATION OF THE WORK AREA

On the 19th of October 2012, a team of two people from AITEMIN went on site to prepare the required area for the dismantling works. The purpose of this work was to protect both cables and the Data Acquisition System (DAS) from the dust and damage that the dismantling operations might cause.

The activities carried out were:

- Protection of the seismic cables with metallic tubing cut longitudinally in half. See Figure 3.
- Protection of the DAS cabinets with wooden boards and retro tactile plastic. See Figure 4.
- Positioning of the corresponding safety signs and fence. See Figure 5.
- Removal of the water tank used during the saturation phase.
- Supplying of auxiliary working tables and chairs.

Figure 3: Protection of seismic cables

Figure 4: Protection of the cabinets

Figure 5: Installation of safety signs

3.2 DRILLING OF THE INITIAL BOREHOLE IN THE PLUG

In order to have an inner free surface in the concrete plug to start its dismantling using the drilling/splitter method, it was planned to drill a horizontal borehole of 200 mm in diameter and 2.5 m long over the previous B1 borehole. See Figure 6.

According to the existing drawings*, the thickness of the plug was 2.2 m and of the retaining wall 0.3 m. So in total, the initial core was planned to be 2.5 m long to cover both plug and retaining wall.

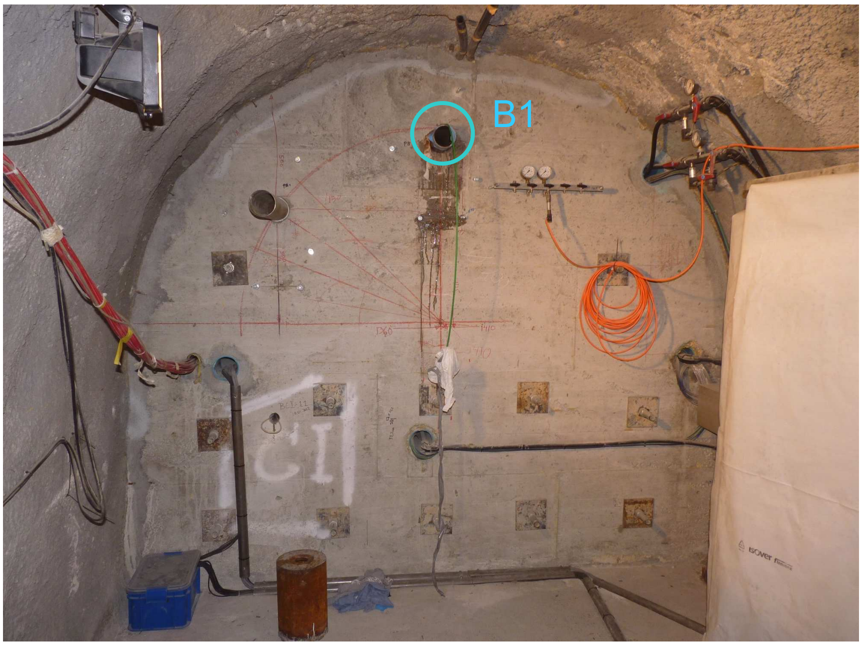

Figure 6: Location of Borehole B1 and planned over coring

The subcontractor company in charge of this operation was Schützeichel GmbH & Co. First of all, they measured the length of the iron pipe in the B1 borehole and it turned out to be 4.3 m long instead of the expected 2.5 m, so it was decided to move the location of the drill 15 cm below the planned one as the initial borehole had to be no longer than 2.5 m. See Figure 7.

* The information from the construction of the plug was very limited and somehow contradictory

Figure 7: Final location of the initial core

Restrictions about the use of water were specified in the Test Plan, but due to communication problems, the company did not bring tools to drill only with air as a refrigerator, so water had to be used during the first 2 m and then the drilling was continued with no water. In order to avoid introducing water in the bentonite everything was protected with plastics and the water was collected during the drilling process. See Figure 8.

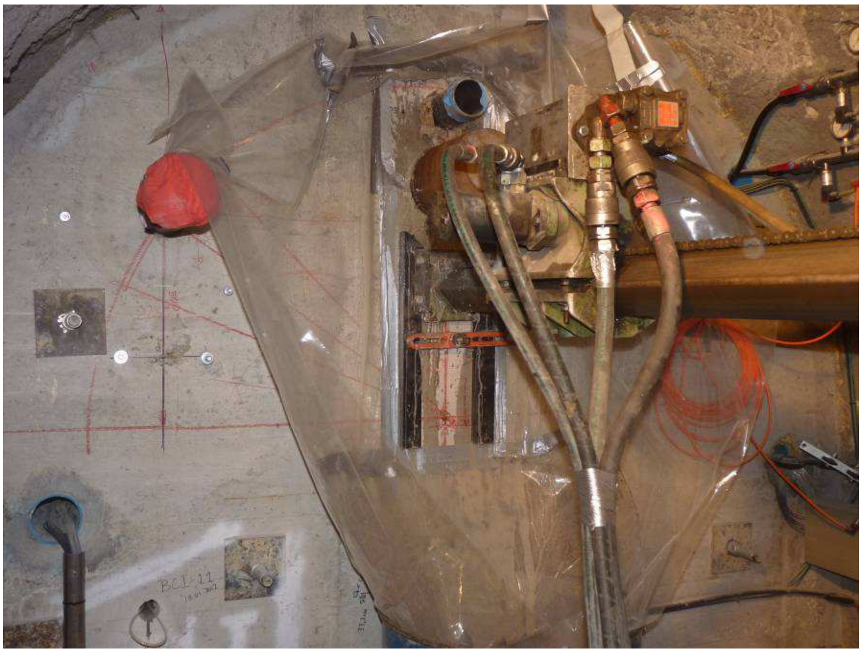

Figure 8: Protection of the experiment to collect the water during the drilling process

During the drilling process, about 30 cm of GBM were drilled because it was found that the plug thickness was 1.9 m and the retaining wall 0.3 m. See Figure 9.

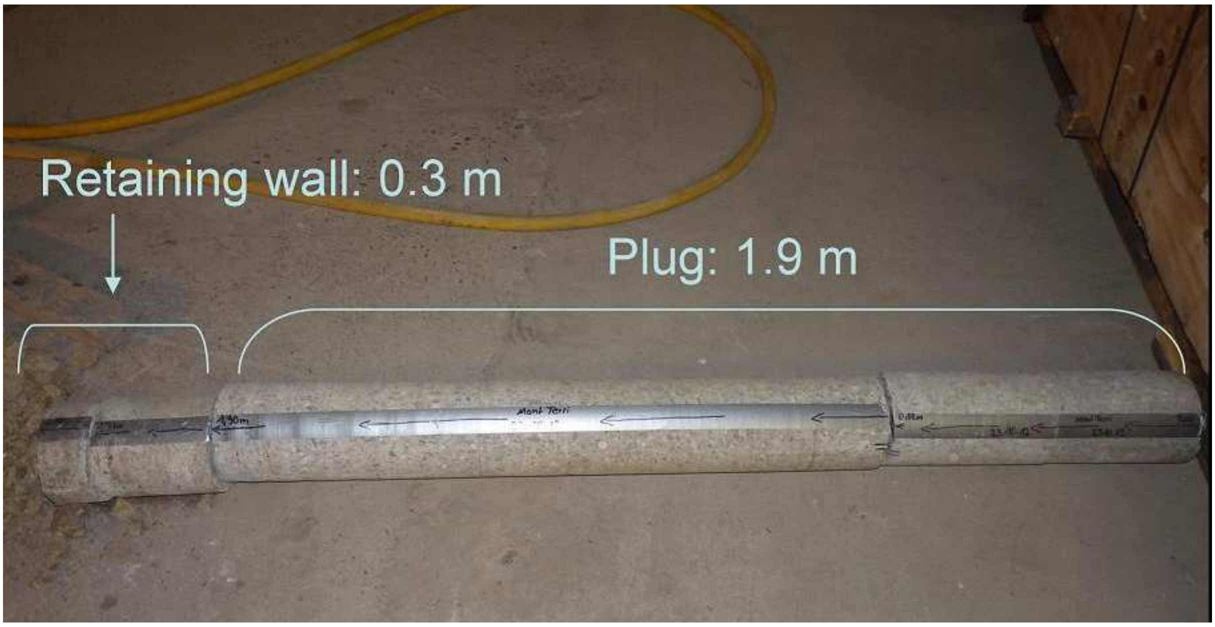

Figure 9: Core from the initial borehole.

3.3 DISMANTLING OF CONCRETE PLUG AND RETAINING WALL

3.3.1 Methodology and equipment

The dismantling of the plug had to be accomplished taking into account that the concrete plug had to be removed in steps in order not to alter the bentonite, not to damage the cables of the sensors and keep the operation as safe as possible. For this reason, the hydraulic splitter method was selected for the concrete dismantling. This method was also succesfully used in the demolition of the plug of the FEBEX experiment. This technique consists of drilling horizontal boreholes and introducing a hydraulic splitter to break the concrete towards an initial big-diameter hole. A pneumatic hammer (Model RH-571) was used to drill the boreholes and a DARDA hydraulic splitter to break the concrete. See technical data of the tools that were used in Appendix I.

The hydraulic splitter was fed by means of a hydraulic compressor. In the first phases, the hydraulic splitter used was the C9 model, which has a length of 30 cm. In the later phases the C12 model with a length of 45 cm was included to the process so both splitters were used in the same working face but not at the same time for safety reasons. See Figure 10.

Figure 10: Hydraulic splitter C9 and C12

A 48 mm in diameter and 800 and 1200 mm long drill bit was assembled to the pneumatic hammer to drill the plug, so the final diameter of the boreholes was around 55 mm. The air compressor supplying the hammer was located in another gallery next to the EB niche. In order to make the drilling activities easier, and due to the high weight of the tool, the pneumatic hammer was attached to a metallic extensible support. See Figure 11.

Figure 11: Pneumatic hammer and compressor (left/right)

The dust from the drilling was collected by means of an industrial vacuum cleaner. See Figure 12.

Figure 12: Vacuum cleaner

Due to the hard resistance of the concrete used to build the plug, this method (hammer+splitter) had to be supplemented with the use of a pneumatic hammer operated by a backhoe. See Figure 13.

Figure 13: Backhoe used for the plug dismantling

The dismantling operation of the plug was also helped with the use of other hand tools such as: a Hilti percussion hammer, a mallet, a pick… See Figure 14.

Figure 14: Handtools

The debris was collected in big bags by means of a shovel, and then it was transported with a forklift to a dump close to the main entrance to the Mont Terri site. See Figure 15.

Figure 15: Loading forklift with debris

3.3.2 Sequence of works

The dismantling of the plug started on the 23rd of October 2012 and it continued along the whole operation due to the difficulties related to the high strength of the concrete.

The plug was planned to be completely dismantled, but later it was decided to leave in place a third of it in the right side as part of the demonstrator.

As the concrete dismantling was moving forward, other components such as fibreglass bolts, metallic tubing… were also dismantled. Concrete samples were also collected and its water content measured on site. Any point regarding the sampling will be extended in section 4.

So the sequence of the works was the following:

1. Drilling the 200 mm diameter borehole so there would be an inner free surface to start with the Splitter breaking method.

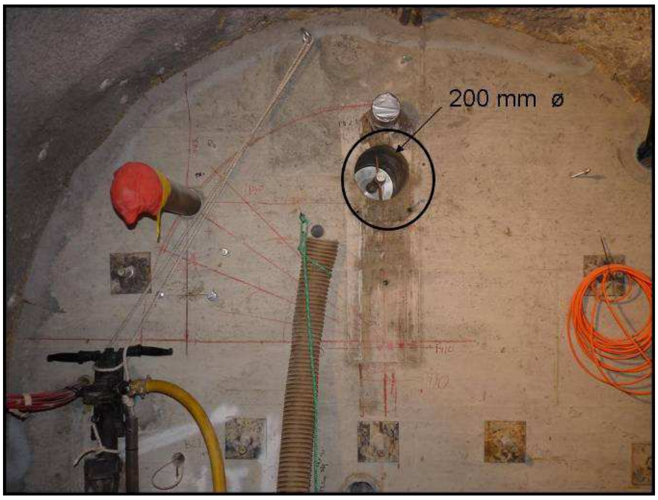

Figure 16: Initial borehole of 200 mm diameter

2. Drilling boreholes around the 200 mm one and use of the splitter to break the concrete. The distance between the boreholes was no longer than 30 cm. The aim was to get a bigger free surface to make breaking the concrete easier. As it was mentioned before, in order to speed up the dismantling, a backhoe was rented from the 6th of November. During this process, the cable box C was also dismantled. All the cables were cut after disconnecting the sensors from the DAS and the box was sent to AITEMIN laboratories to be studied. The following photos compiled in Figure 17 show the evolution of the concrete dismantling up to reaching the granular bentonite material (GBM).

Boreholes around the 200 mm diameter one

Use of the Darda

Holes around the main opening in the plug

Use of the Darda to break the concrete

Progress in breaking the concrete of the plug

Progress in breaking the concrete of the plug

Backhoe working

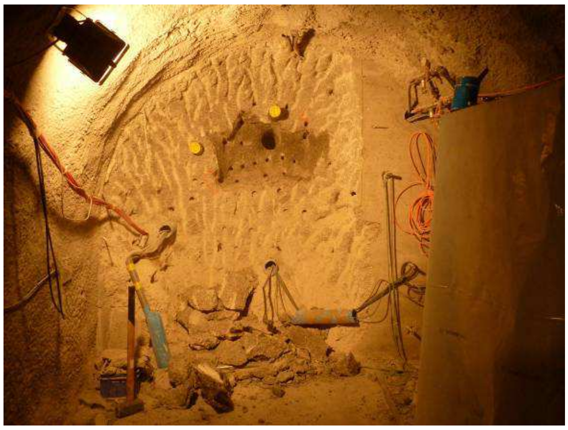

Result of the use of the backhoe

Retaining wall reached

Retaining wall dismantling

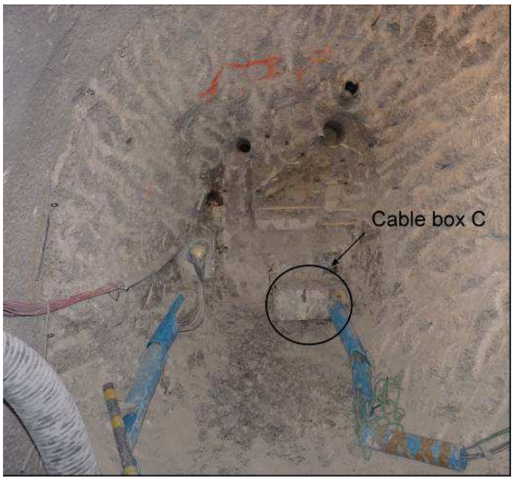

Reaching the cable box C

Cable box C dismantling (I)

Cable box C dismantling (II)

Cable box C dismantling (III). Water spot

Retaining wall dismantling

Bentonite reached

Figure 17: Plug and retaining wall dismantling process

3. The last picture in Figure 17 shows the portion of plug and retaining wall that could be removed before starting to dig the bentonite. Having the inner part of the retaining wall as a free face would help with the dismantling of the remaining concrete. The plug/retaining wall dismantling activities stopped for a week until part of the bentonite behind the plug was removed. Then, the plug dismantling activities continued with the help of expansive cement that was poured in drills that were done for this purpose along the edge of the opening of the Plug/Retaining. The effects of the expansive cement were noticed 72 hours after its placing and part of the plug could be removed with the help of hand tools. The following photos compiled in Figure 18 show this process.

Drilling boreholes for the expansive cement (I)

Drilling boreholes for the expansive cement (II)

Preparation of the liquid expansive cement

Pouring of liquid expansive cement in the floor boreholes

Preparation of the solid expansive cement

Insertion of solid expansive cement in lateral and top boreholes

Use of hand tools to remove the concrete plug after the effect of the expansive cement (I)

Use of hand tools to remove the concrete plug after the effect of the expansive cement (II)

Figure 18. Use of expansive cement to break the plug

3.4 REMOVAL OF BENTONITE

3.4.1 Methodology and equipment

On the 14th of November 2012, the bentonite was reached and tests to find out the best way to remove and sample it were performed.

The conclusion was that the best way to remove the bentonite was with the use of a hammer (for instance a geologist one or an electric percussion hammer with a flat-end bit tool attached) to extract less-disturbed irregular pieces of GBM. See Figure 19.

Figure 19: Tools used for bentonite removal

For the removal of the bentonite blocks, the percussion hammer was provided with a pointy bit in order to separate the blocks between them and remove them in one whole piece. See Figure 20.

Figure 20: Tools for bentonite blocks removal

The removal of the bentonite was done in such way to keep the face of work as much parallel to the plug as possible. Initially the work was slower than expected, but as the team got used to the tools and the material, it went faster. From the moment the bentonite was reached, a fast drying process was observed in the bentonite front (see Figure 21), so after every day of work, the excavation was covered with a protection plastic (see Figure 22). If there were more than 2 days between working days, the team tried to keep the following sampling section as far as possible from the working face. There would be left at least 30 cm of not dismantled bentonite from the working face till the sampling section.

Figure 21: Bentonite front dryness after 5 days exposed

Figure 22: Plastic cover to avoid bentonite drying

The debris was collected in big bags by means of a shovel, and then it was transported with a forklift to a dump close to the main entrance to the Mont Terri site. See Figure 23.

Figure 23: Big bags with bentonite for the dump

3.4.2 Sequence of works

First of all, once the bentonite was reached, a plastic cover was put at the beginning of the concrete plug in order to avoid the loss of humidity of the bentonite as much as possible. See Figure 22.

The removal of the bentonite was done with a team of two people. One of them working in the left side and the other in the right side when the available spaced allowed it. As the dismantling moved forward, all the elements such as hydration pipes, sensors or metallic piping from old boreholes were also dismantled. See Figure 24.

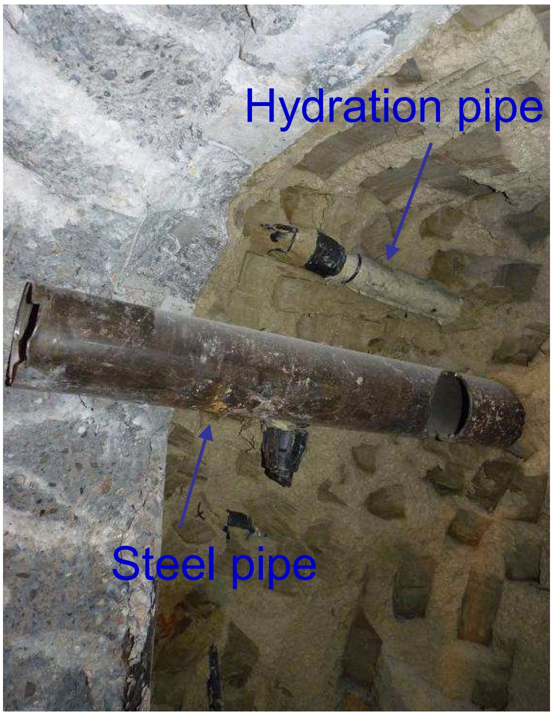

Cutting of the steel pipes located along the experiment

Figure 24: Embedded elements in the GBM

The progress of the bentonite removal was of about 25 cm per day. Pictures in the Figure 25 show its evolution.

Reaching retaining wall and bentonite

Bentonite in contact with the retaining wall

Front face of the canister. A layer of around 75 cm of bentonite already removed

Front face of the canister and vertical extensometer uncovered. Section A1

Removal of the first layer of bentonite blocks

Section CMT2

General view from the gallery

Uncovered canister

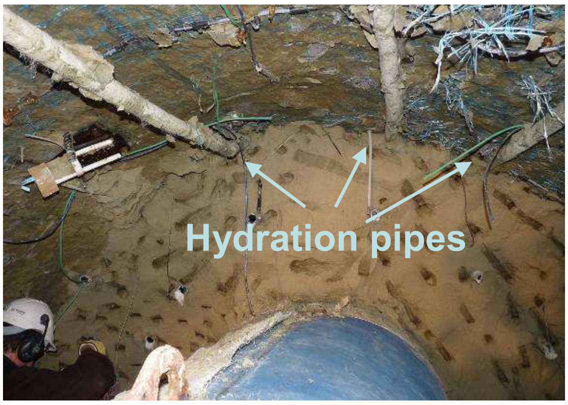

Temporary support of the canister

Section B2

End of the bentonite removal. Z=695 for the GBM

Figure 25: Bentonite removal evolution

At the end, the front of the left bentonite was covered with a plastic in order to keep the humidity until the demonstrator was built. See Figure 26.


Figure 26: Front of the remaining bentonite covered with plastic

3.5 CANISTER SUPPORT OPERATION

As planned in the Test Plan, a custom-made metallic beam for this project was manufactured as the final support solution for the canister. Due to the large dimension of the beam and the narrow entrance initially available through the plug, it was decided it would be placed at the end of the dismantling works. In the mean time, other support works were carried out.

When the first metre of the canister was uncovered, an extensible metallic support was placed at the beginning of the canister. See Figure 27.

Figure 27: Metallic extensible support for canister

As the length of the uncovered canister increased, the metallic support was replaced by a metallic sawhorse able to support up to 10 t, and it was reinforced by two metallic extensible supports holding the left and right sides of the canister. See Figure 28.

Figure 28: Sawhorse support for canister

When the dismantling works finished, the planned final metallic beam was welded to the front face of the canister and fixed to the floor as well as to the concrete bed. As an extra safety measure, two metallic sawhorses were placed along the base of the canister. See representative pictures in Figure 29.

Welding of the beam to the front face of the canister

Metallic beam already welded to the canister front

Attachment of the bottom part of the beam to the floor

Attachment of the lateral part of the metallic beam to the concrete bed

Front view of the metallic beam

Sawhorses supporting the canister

Figure 29: Final support for the canister

3.6 REMOVAL OF THE DATA ACQUISITION SYSTEM (DAS)

The removal of the DAS was left until the very last moment of the dismantling operation as one of the aims was having as many sensors as possible running during the activities. All gathered data were compiled in a final data report that is included as Appendix III.

It consisted in first of all, cutting the cables of the sensors as close as possible to the data logger cabinet. Then, the cabinet containing the computer (PC) was also disconnected.

Finally, both cabinets were appropriately packed to be sent to Spain. See Figure 30.

Data logger cabinet

PC cabinet

DAS Cabinets packed

Figure 30: DAS dismantling

4 SAMPLING OPERATION

4.1 QUALITY DOCUMENTATION

The experiment was run under an internal Quality System. As a result, the following documents were released:

- Inspection Points Program. A log containing all the operations and the person in charge of them was filled in every day during the removal and sampling.
- All the samples taken during the operation were documented. For each sample, a Sample Log was filled in containing all the information regarding the sample: coordinates, sampling procedure, recipient organization, measurements, any relevant incidents… If the sample was also analysed on site, all the processes and results were recorded in the same log.
- For every sampling section, a Section Log was also produced, containing a list of the samples taken, as well as any relevant incidents.

As considered in the quality programme, relevant activity or event was also graphically documented.

The temperature and humidity of the EB niche as well as of the on site laboratory were registered by means of thermo-hygrometers placed in the gallery.

4.2 SAMPLING SECTIONS

There were planned several sampling sections along the experiment. The as built sections, shown in Figure 31, did not differed much from the planned ones in the Test Plan.

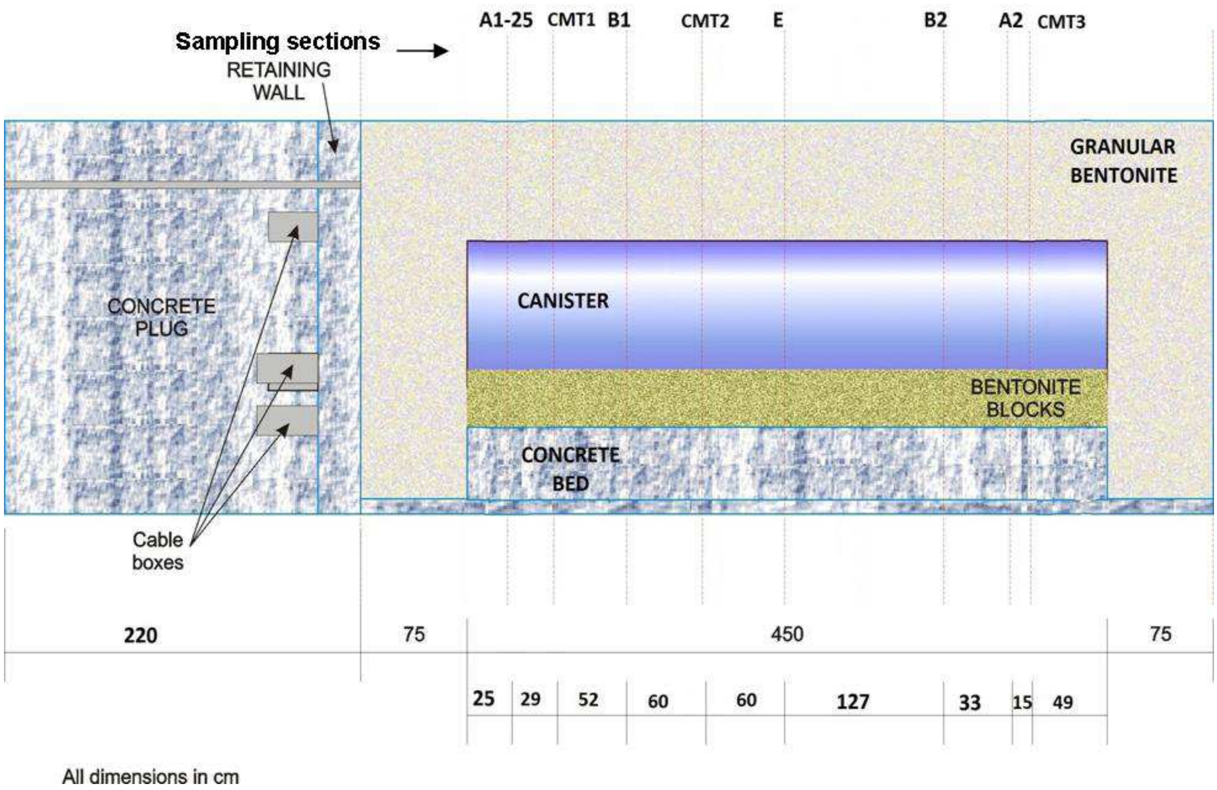

Figure 31: As built sampled sections

The main differences in relation to the Test Plan are:

- The first sampling section was called A1 and it was located in the front face of the canister. Section A1 was moved 25 cm backwards because the analysis method was still under test and the results obtained did not have the desired accuracy. This section has been called A1-25 and the same samples planned in Section A1 were taken.
- In order to leave part of the bentonite on place for the demonstrator, the removal work finished 49 cm before the rear end of the canister. For this reason, sections A2 and CMT3 had to be brought forward. See Figure 31.
- Due to a delay in the delivery of Al-coated paper for the packing of samples in section CMT3, the sampling had to be postponed, so section A2 was sampled before it.
- Due to safety reasons, it was decided not to remove all the bentonite blocks of the bed leaving the last 95 cm (see Figure 32), so the last bentonite blocks to be removed were those in section B2. Because some blocks in section CMT3 were required by the organizations, blocks from section B2 were provided in stead.

Figure 32: Blocks and bentonite left for demonstrator

The origin of coordinates for every section and sample is shown in Figure 33. It was located on the floor, in the centre of the outer face of the concrete plug.

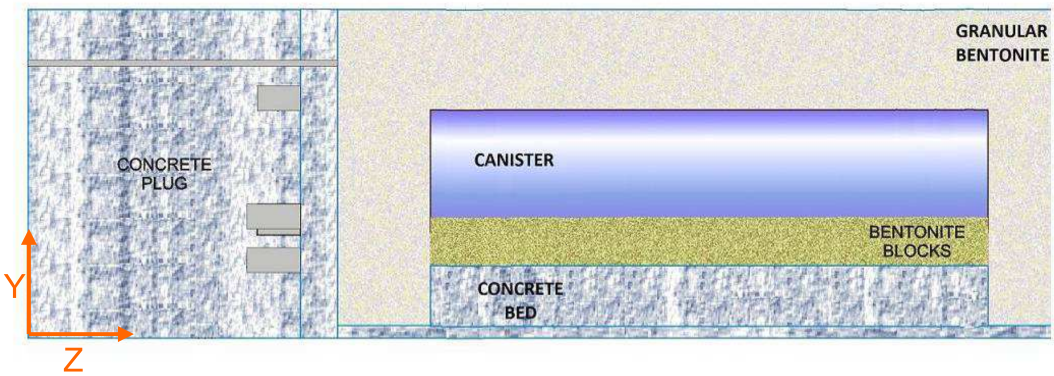

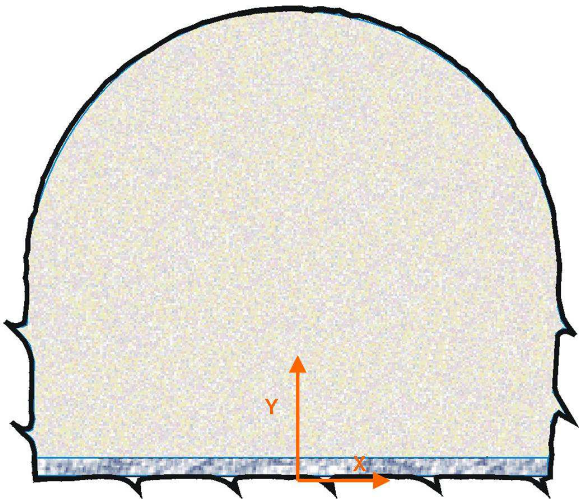

Figure 33: Origin of coordinates

4.3 SAMPLING PROCEDURES

There have been different kinds of samples to be taken. Depending on the sample or the purpose of the analysis to be done, the sampling procedure as well as the packing was adapted.

There were common practices such as:

- Registration of the location of the samples by means of filling the logs T-Y-NNNN-ZZZ (see section 4.3.8 for the codification). One log was filled per sample taken.
- If possible, the transparent film covering the samples was marked with permanent marker, so that their position and especially their orientation and rotation could be established afterwards.
- The sample was identified and the sample log completed as soon as possible. A copy of that file has been attached to the sample container.
- Samples were taken and handled gently to avoid any unnecessary mechanical disturbance.
- The samples were kept properly packed at 17 ºC, in a clean and chemical compounds-free area close to the EB niche. Samples of bentonite, concrete, or Opalinus Clay (OPA) were vacuum-packed in a double Al-coated polyethylene paper. Samples of any other material whose density or water content was not going to be analysed (i.e: sensors, geotextile…) were packed in the same type of paper without being vacuumed.

4.3.1 Samples taken

In total, almost 500 samples were taken. Around 210 of them were analysed on site and the rest was sent to the different partners in the project. Table 2 shows the detailed list of the number and the type of samples taken and the recipient organizations.

Table 2. Samples taken in total

PARTNER	CONCRETE	CONCRETE/ BENTONITE INTERFACE	OPA/BENTONITE INTERFACE	GBM(on site)	GBM(lab)	BENTONITE BLOCKS	SENSORS	WATER	OPA	ELEMENTS
CIEMAT	2	4	6	-	148	10	-	1	-	3
AITEMIN	12	-	-	209	-	-	16	-	-	14
BGR	-	-	-	-	-	-	4	-	-	-
CIEMAT/UAM	-	5	-	-	-	3	-	-	-	-
NAGRA	-	3	3	-	6	1	-	1	-	-
ANDRA	-	4	6	-	12	4	-	-	1	-
RESERVE	-	4	1	-	7	6	-	-	1	-

4.3.2 Concrete

Concrete samples were taken from the plug as well as from the concrete bed.

The samples from the plug were collected as the concrete dismantling was progressing. The demolition process itself generated pieces of concrete suitable for the sampling. The samples were irregular and between 75 and 150 cm3 in volume. See Figure 34.

Figure 34: Plug samples

Some of these samples were packed for the organizations but most of them were analysed on site (water content).

Samples from the concrete bed were taken by means of a circular saw. See Figure 35.

Figure 35: Concrete bed sampling

These samples were properly packed for the recipient organizations.

4.3.3 Concrete/Bentonite interface

Concrete/bentonite samples from the retaining wall and concrete bed were planned to be taken. Samples from the concrete bed in contact with the bentonite were physically impossible to take, so the only samples that were taken of this type were from the retaining wall.

The first samples were taken by means of rotating coring equipment for the concrete part and then a stainless steel pipe used in the bentonite part. See Figure 36.

Use of the rotating coring equipment for the concrete part

Use of a stainless steel pipe for the bentonite part

Figure 36: Retaining wall sampling I

Following samples were taken in blocks with the help of hand tools and then cut in pieces. This way the samples would be completely unaltered. See Figure 37.

Retaining wall. Concrete/bentonite interface

Sampling the concrete/bentonite interface of the retaining wall as a block

Preparing concrete/bentonite interface samples by cutting them

Figure 37: Retaining wall sampling II

4.3.4 OPA/Bentonite interface

Samples of the OPA/Bentonite interface were taken along the dismantling operation as requested by the organizations. For the bentonite, a stainless steel pipe was used to sample up to the OPA by pushing the pipe against the bentonite. Then the rotating coring device adapted with a crown of the same diameter than the stainless steel pipe was used to sample the OPA part (See Figure 38). Then each sample was packed as a whole one keeping the interface between the two materials in contact.

Figure 38: OPA/Bentonite sampling

Due to the difficulties found with the use of the rotating coring device without cooling water, the number of those samples was reduced.

4.3.5 GBM for on site and laboratory analyses

The procedure to sample GBM was the same for the on site analyses as for the laboratory ones (See section 4.4.1). The main difference between them was the size of the taken samples. For the on site analysis it was enough that the weight of the samples were approximately 300 g and for the organizations it was required that the samples weighed over 500 g if possible.

For the sampling, a first attempt was done using a stainless steel tube of 38 mm in diameter and 1.5 mm thickness which was dug into the bentonite by hammering the pipe and then pulled out by hand. This procedure was found not to be appropriate due to the plastic properties of the bentonite, showing a clear disturbance of the sample during the hammering as well as while taking the sample out form the pipe. In order to avoid this, a new attempt was done using the pipe with the help of the backhoe, but it did not work better. It was also tried to sample with a rotating crown attached to the Hilti but the rotation movement heated and dried the sample up. See Figure 39.

The final procedure adopted is described in Section 3.4.1.

Hammering the sampling pipe into the bentonite

Pushing the sampling pipe with the help of the backhoe into the bentonite

Bentonite sample inside the pipe

Sampling with a rotating crown

Figure 39: Testing how to sample GBM

4.3.6 Bentonite blocks

The procedure for sampling the bentonite blocks is the same as for their removal. It has been described in section 3.4.1.

Figure 40: Block of bentonite sample

4.3.7 Sensors

The sampling of the sensors was as expected. First of all, the sensor and cable were uncovered of bentonite and then the cable was cut as far as possible from the head of the sensor. During the sampling, it was observed some different colour in the bentonite surrounding the head of some of the sensors due to corrosion (not relevant). In the case that the sensor was covered with the geotextile (i.e. Total Pressure cells in Section E), the corrosion only affected clearly to the welding points used to attach the sensors to the canister. In this case, a corrosion stain could be observed in the geotextile too. See Figure 41.

Extensometers

Water content sensor

Total Pressure cell

Geotextile covering total pressure cells

Figure 41: Sensors sampling

4.3.8 Codification of samples

The samples were coded as explained in the Test Plan. The codification was as follows:

T-Y-NNNN-ZZZ

T refers to the material of the sample such as:

B: Bentonite

C: Concrete

C/B: Concrete/Bentonite

B/R: Bentonite/Rock

R: Rock

S: Sensor

O: Other

Y refers to the shape of the sample, such as:

B: Block

C: Cores

S: Any shape except blocks or cores. Sensors.

NNNN: Sampling section.

ZZZ: Correlative sample number for same type of samples in each section.

4.3.9 Analysis procedures used in on site laboratory

The procedures explained in this section are related with the on site analysis.

A laboratory in a niche close to the EB experiment was set. See Figure 42.

Figure 42: Laboratory

This laboratory was composed of the following elements.

- Oven
- Balances: One with a precision of 0.1 g and the other 0.01 g
- Density analysis tools: mercury, Pyrex vessels, pipette…
- Cutting tools: knife, cutter…
- Safety accessories: Gloves, masks…

Due to the use of mercury in the analysis procedure, the niche was placed in a ventilated place and the floor was covered with plastic.

Two different measurements were determined in the bentonite samples (blocks and GBM): Water content and dry density. It has been also calculated the degree of saturation of every sample. The specific weight used for these calculations has been 2.7 g/cm^3.

After collecting every GBM sample, it was cut and trimmed into 3 subsamples of between 6 and 12 cm^3 in volume each. The water content was obtained from all the subsamples and the dry density from only 2 of them.

The gravimetric water content (w) is defined as the ratio between the weight of water and the weight of dry solid expressed as a percentage. The weight of water was determined as the difference between the weight of the sample and its weight after oven drying at 110°C for 48 h (weight of solid).

Dry density (ρ_d) is defined as the ratio between the weight of the dry sample and the volume occupied by it prior to drying. The volume of the specimens was determined by immersing them in a recipient containing mercury and by weighting the mercury displaced, as established in UNE Standard 7045 “Determination of soil porosity”. The same samples whose volumes had been determined were used for the water content determination.

Figure 43 shows the analysis procedure:

Original sample

Trimming the sample

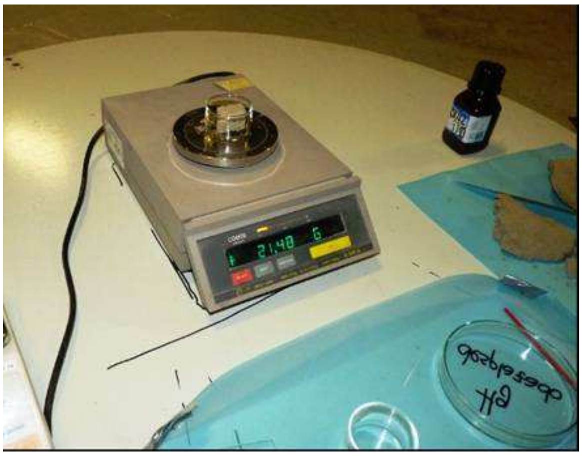

Weighting of the subsamples

Use of mercury to determine the volume of the subsamples

Use of mercury to determine the volume of the subsamples

Drying of the samples in the oven

Figure 43: Analysis procedure

On site analysed samples were disposed of after the analysis.

4.3.10 Packing and transport

Every sample was immediately measured and weighed after the collection. Then the samples were vacuum packed in two successive Al-coated polyethylene sheets. See Figure 44.

Figure 44: Packing of samples

Each package was properly identified and stored in a niche close to the EB experiment until the shipping was organized.

Finally, the samples collected for the different organizations were packed in wooden boxes for its transport (see Figure 45). A copy of the sample logs was included in the parcel.

Figure 45: Transport of samples

4.4 SAMPLING SECTIONS.

4.4.1 Plug

The plug was considered a sampling section itself as a whole. It means that the z coordinate varies from z=0 to z=190 (in centimetres). In the Plug section, two types of samples were collected: concrete and water from the hydration pipes. The sample of water from the hydration pipes was located between the Plug and the Section A1, but it was decided to include it in this section.

Figure 46 shows the location of the samples and the recipient organizations. It also shows some samples of concrete that were taken for water content on site analysis.

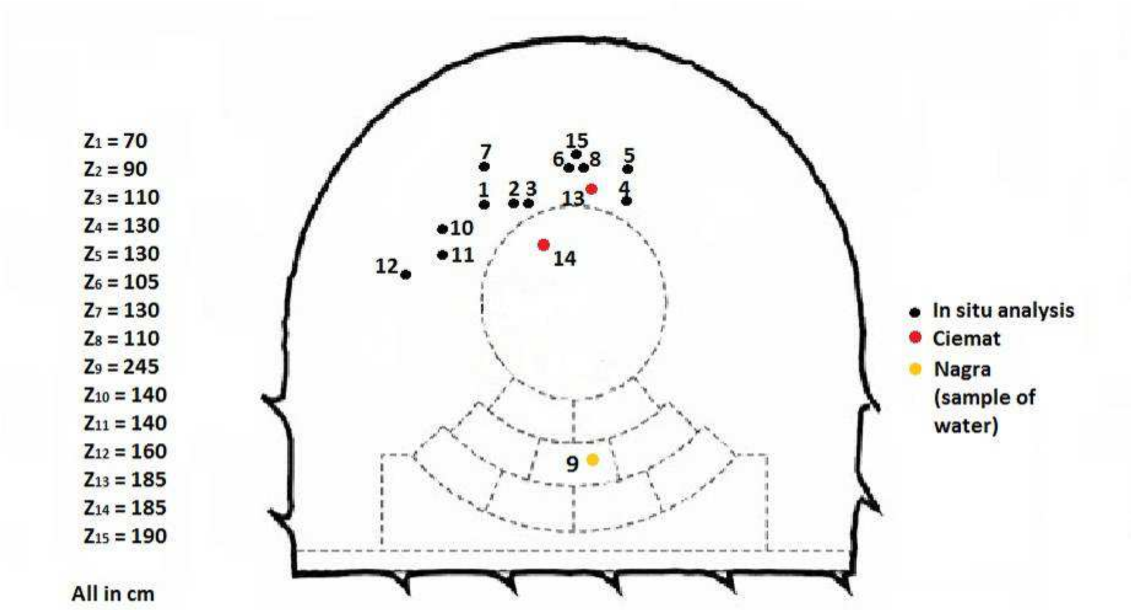

Figure 46: Plug section. Samples

Wet areas were observed while breaking the concrete (See Figure 47).

Figure 47: Wet concrete. Plug

The coordinates of the plug samples taken for on site analysis and the results of the water content obtained are listed below in the Table 3.

Table 3. Results of on site analyses of water content for PLUG samples

ID sample number	Sample	Coordinates			Water content (%)
		x	y	z	
1	C-S-PLUG-001	-20	170	70	3.9
2	C-S-PLUG-002	-10	170	90	4.1
3	C-S-PLUG-003	-10	170	110	3.9
4	C-S-PLUG-004	10	170	130	4.7
5	C-S-PLUG-005	10	175	130	4.7
6	C-S-PLUG-006	0	175	105	4.5
7	C-S-PLUG-007	-20	175	130	4.5
8	C-S-PLUG-008	0	175	110	4.3
9	C-S-PLUG-010	-30	160	140	4.1
10	C-S-PLUG-011	-30	170	140	4.5
11	C-S-PLUG-012	-40	140	160	4.5
12	C-S-PLUG-015	0	175	190	4.7

The values show a high saturation in the concrete, so it can be considered that the plug is practically saturated.

4.4.2 Retaining wall

In the Retaining Wall section, there were taken different types of samples: Bentonite in contact with the concrete, concrete/bentonite interface, and water. Figure 48 shows the location of the samples and the recipient organizations. Table 4 shows the list of the samples and their location coordinates.

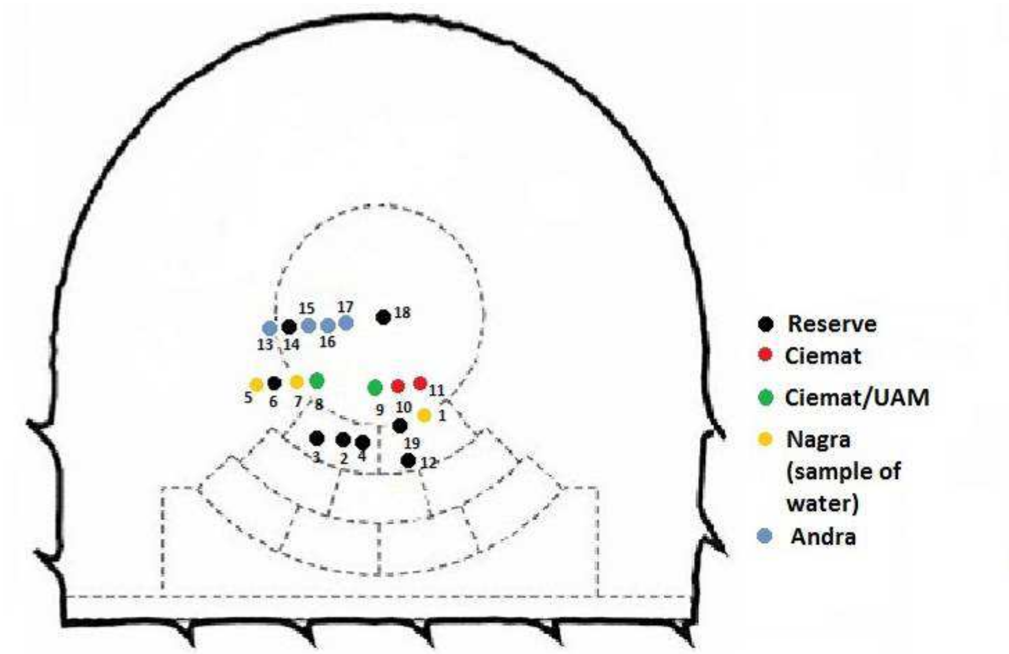

Figure 48: Location of samples in the Retaining Wall

Table 4. List of samples taken in the Retaining Wall

ID sample number	Sample	Coordinates	
		x	y
1	C/B-C-RW-001	20	85
2	C/B-C-RW-002	-25	70
3	C-C-RW-003	-30	75
4	C-C-RW-004	-20	80
5	C/B-S-RW-005	-60	90
6	C/B-S-RW-006	-55	90
7	C/B-S-RW-007	-50	90
8	C/B-S-RW-008	-40	90
9	C/B-S-RW-009	-10	90
10	C/B-S-RW-010	0	90
11	C/B-S-RW-011	10	90
12	C/B-S-RW-012	10	75

ID sample number	Sample	Coordinates	
		x	y
13	B-S-RW-001	-50	120
14	B-S-RW-002	-40	120
15	B-S-RW-003	-35	120
16	B-S-RW-004	-25	120
17	B-S-RW-005	-15	120
18	B-S-RW-006	0	120
19	B-S-RW-007	5	90

None of these samples were analysed on site.

4.4.3 A1-25

The location of the samples taken is shown in Figure 49.

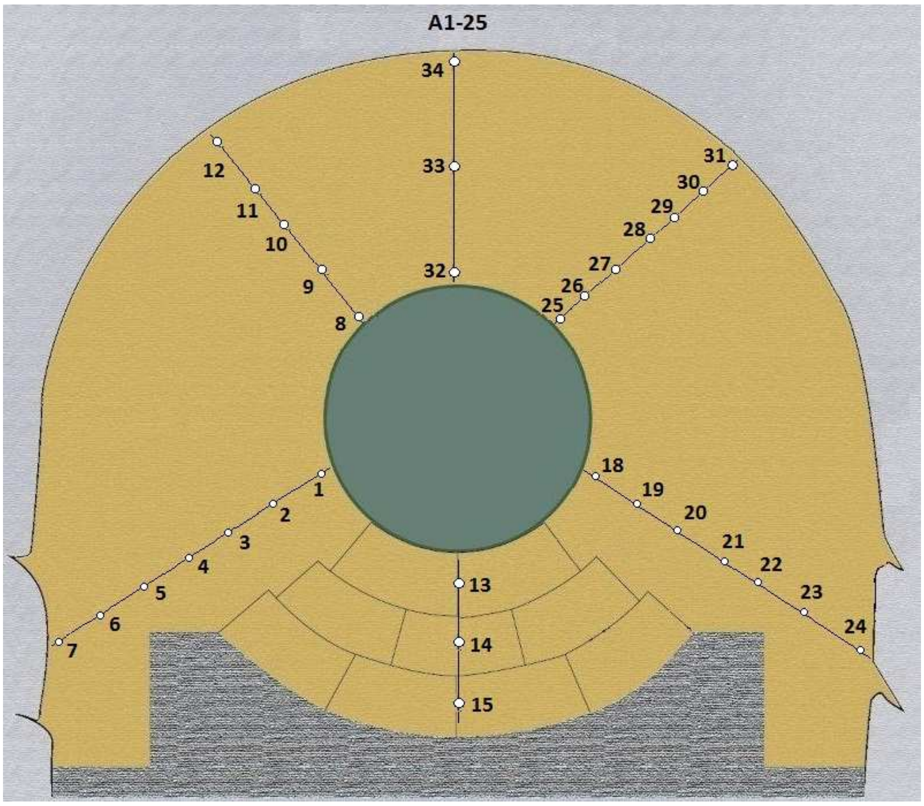

Figure 49: Location of samples in Section A1-25

Table 5 shows the coordinates of the samples and the results of the on site analysis.

Table 5. Water content and dry density obtained from on site analyses in Section A1-25

ID sample number	Sample	Coordinates		Water content (%) mean	Dry density (g/cm^3) mean	Degree of saturation %
		X	Y			
1	B-S-A1_25-001	-42	93	36.3	1.33	95
2	B-S-A1_25-002	-50	82	35.3	1.28	86
3	B-S-A1_25-003	-65	75	36.1	1.32	93
4	B-S-A1_25-004	-88	65	37.4	1.29	93
5	B-S-A1_25-005	-102	55	37.7	1.32	98
6	B-S-A1_25-006	-125	50	39.8	1.26	94
7	B-S-A1_25-007	-140	45	40.8	1.26	97
8	B-S-A1_25-008	-30	167	32.5	1.44	101
9	B-S-A1_25-009	-56	182	31.7	1.44	98
10	B-S-A1_25-010	-83	197	31.9	1.41	95
11	B-S-A1_25-011	-95	204	32.0	1.4	93
12	B-S-A1_25-012	-105	211	32.8	1.37	92
13	B-S-A1_25-013	0	70	33.4	1.36	92
14	B-S-A1_25-014	0	50	34.8	1.3	88
15	B-S-A1_25-015	0	30	34.9	1.33	91
18	B-S-A1_25-018	49	107	37.6	1.32	97
19	B-S-A1_25-019	57	100	35.6	1.36	97
20	B-S-A1_25-020	67	90	34.3	1.35	93
21	B-S-A1_25-021	83	80	34.9	1.39	100
22	B-S-A1_25-022	100	70	35.6	1.4	103
23	B-S-A1_25-023	125	60	35.8	1.37	99
24	B-S-A1_25-024	140	50	37.4	1.28	91
25	B-S-A1_25-025	38	174	32.6	1.42	97
26	B-S-A1_25-026	53	181	31.2	1.43	94
27	B-S-A1_25-027	69	188	31.6	1.43	97
28	B-S-A1_25-028	78	191	32.3	1.42	97
29	B-S-A1_25-029	86	195	31.3	1.42	94
30	B-S-A1_25-030	97	198	30.7	1.43	93
31	B-S-A1_25-031	109	207	32.5	1.39	93
32	B-S-A1_25-032	0	178	31.8	1.43	96
33	B-S-A1_25-033	0	211	30.9	1.46	98
34	B-S-A1_25-034	0	252	31.6	1.46	101

In order to check the reliability of the results obtained on site, some of the samples were taken bigger than the rest so they were divided in two parts: one for the on site laboratory and the other for the laboratory that CIEMAT has in Madrid.

Table 6 shows both results.

Table 6. Comparison of water content and dry density obtained from on site and laboratory analyses in Section A1-25

		Laboratory results			On site results		
ID sample number	Sample	Water content (%) mean	Dry density (g/cm^3) mean	Degree of saturation %	Water content (%) mean	Dry density (g/cm^3) mean	Degree of saturation %
18	B-S-A1_25-018	41.0	1.30	102	37.6	1.32	97
19	B-S-A1_25-019	36.5	1.35	98	35.5	1.36	97
20	B-S-A1_25-020	35.5	1.38	100	34.3	1.35	93
21	B-S-A1_25-021	35.9	1.35	97	34.9	1.39	100
22	B-S-A1_25-022	37.0	1.34	99	35.6	1.40	103
23	B-S-A1_25-023	36.7	1.34	97	35.8	1.37	99
24	B-S-A1_25-024	38.0	1.31	97	37.4	1.28	91

As it can be observed, the water content obtained in the laboratory was 3.8% higher than on site, and the dry density 1.1% lower. This difference is not very significant, and got smaller as the on site analysis progressed given that in this section the methodology was still being improved. See Appendix IV.

4.4.4 CMT1

The location and recipients of these samples are shown in Figure 50.

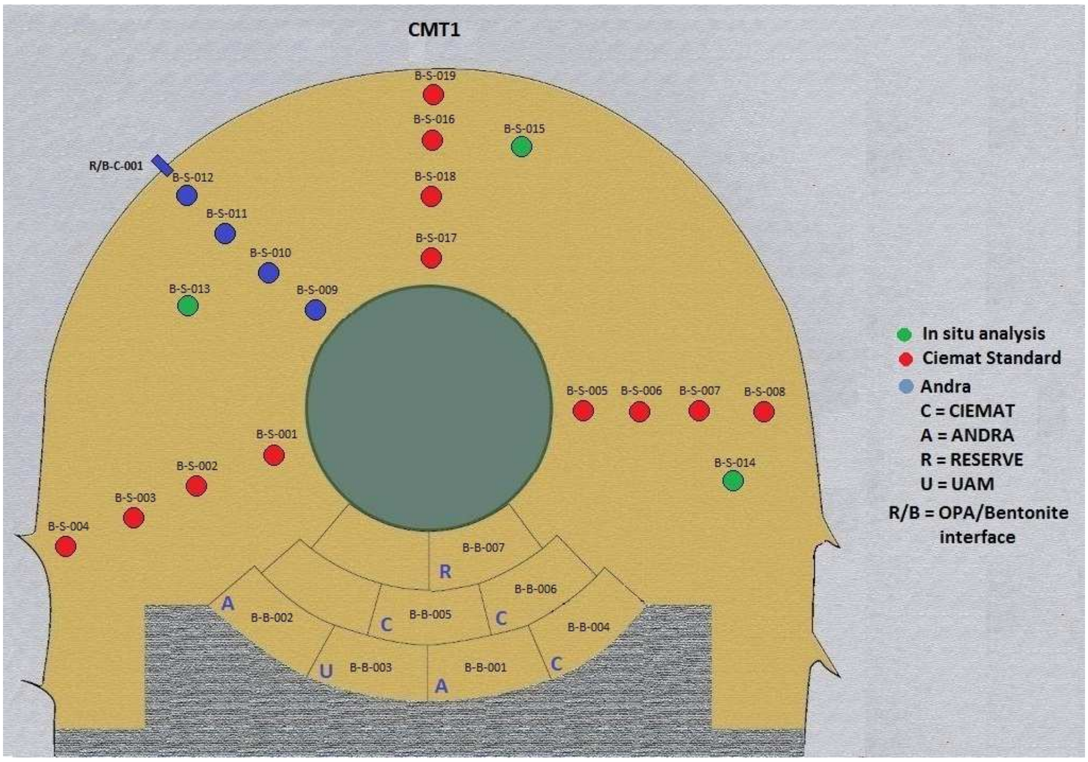

Figure 50: Location of samples in Section CMT1

There were taken few samples to be analysed in the on site laboratory and the rest was sent to the different organizations as requested. The results of the samples analysed on site as well as the ones analysed in the laboratory in CIEMAT facilities are listed below. See also Appendix IV.

Table 7. Water content and dry density on site and laboratory analyses. Section CMT1

			Laboratory results			**On site results**		
Sample	**Coordinates** x	**Coordinates** y	**Water content (%) mean**	**Dry density (g/cm^3) mean**	**Degree of saturation %**	**Water content (%) mean**	**Dry density (g/cm^3) mean**	**Degree of saturation %**
B-B-CMT1-007	-	-	34.2	1.39	98	-	-	-
B-B-CMT1-006	-	-	34.7	1.36	95	-	-	-
B-B-CMT1-004	-	0	37.2	1.34	99	-	-	-
B-S-CMT1-001	-58	105	37.3	1.35	100	-	-	-
B-S-CMT1-002	-78	95	36	1.35	97	-	-	-
B-S-CMT1-003	-105	81	37	1.33	97	-	-	-
B-S-CMT1-004	-130	68	39.8	1.3	100	-	-	-
B-S-CMT1-005	65	112	35.6	1.36	97	-	-	-
B-S-CMT1-006	84	113	36.3	1.36	99	-	-	-
B-S-CMT1-007	111	114	35.3	1.36	97	-	-	-
B-S-CMT1-008	132	114	36.3	1.36	99	-	-	-
B-S-CMT1-017	0	182	34.1	1.41	100	-	-	-

Sample	Coordinates		Laboratory results			On site results		
	x	y	Water content (%) mean	Dry density (g/cm^3) mean	Degree of saturation %	Water content (%) mean	Dry density (g/cm^3) mean	Degree of saturation %
B-S-CMT1-018	0	195	32.8	1.42	98	-	-	-
B-S-CMT1-016	0	235	32.3	1.43	98	-	-	-
B-S-CMT1-019	0	250	34.3	1.4	100	-	-	-
B-S-CMT1-013	-87	167	-	-	-	31.8	1.44	98
B-S-CMT1-014	100	110	-	-	-	31.9	1.45	100
B-S-CMT1-015	20	227	-	-	-	29.3	1.48	96

4.4.5 B1

The physical location of the samples in the section is shown in Figure 51.

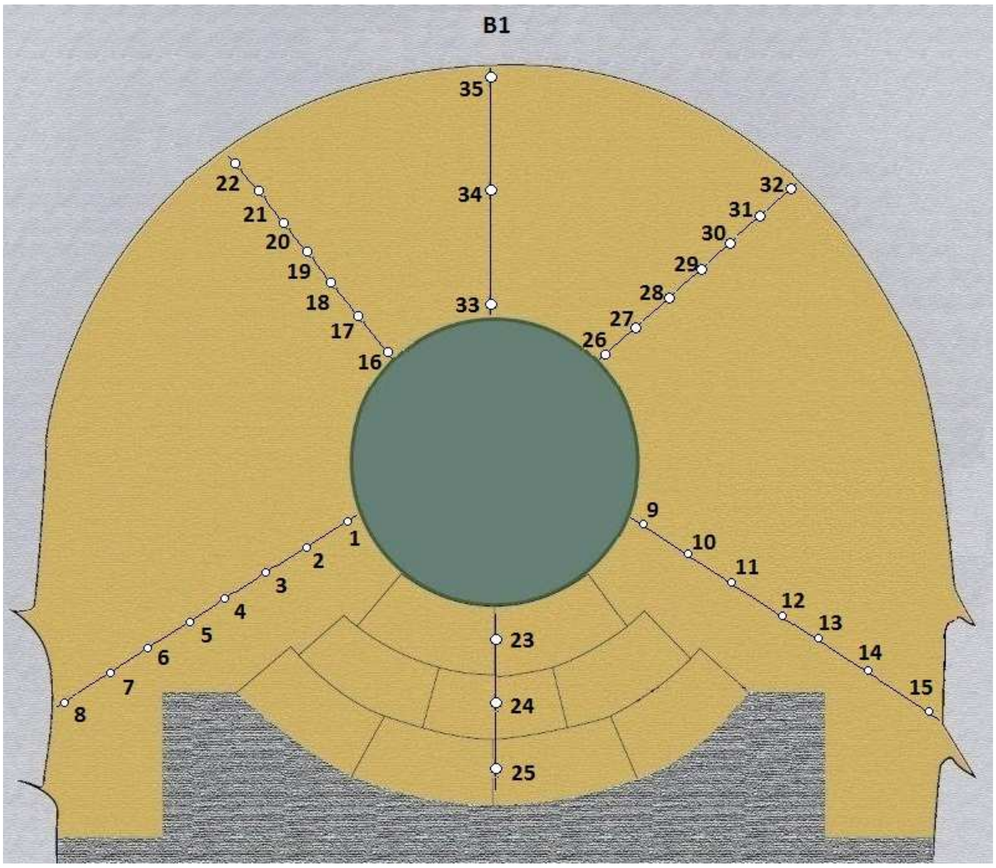

Figure 51: Location of samples in Section B1

Table 8 shows the coordinates of the samples and the results of the on site analysis.

Table 8. Water content and dry density of the on site analyses in Section B1

Sample	Coordinates		Water content (%) mean	Dry density (g/cm^3) mean	Degree of saturation %
	x	y			
B-S-B1-001	-37	92	37.4	1.36	102
B-S-B1-002	-49	86	38.3	1.29	95
B-S-B1-003	-64	77	37.1	1.32	96
B-S-B1-004	-80	66	37.7	1.31	96
B-S-B1-005	-96	57	40.3	1.27	96
B-S-B1-006	-110	49	43.5	1.20	95
B-S-B1-007	-123	45	45.7	1.19	98
B-S-B1-008	-139	43	46.4	1.18	97
B-S-B1-009	51	120	36.9	1.35	100
B-S-B1-010	63	110	36.5	1.32	94
B-S-B1-011	75	102	37.4	1.32	97
B-S-B1-012	91	90	39.4	1.28	96
B-S-B1-013	109	74	39.7	1.27	95
B-S-B1-014	129	61	41.5	1.25	97
B-S-B1-015	144	54	42.4	1.48	138
B-S-B1-016	-29	168	33.8	1.39	97
B-S-B1-017	-37	178	32.7	1.40	96
B-S-B1-018	-44	188	32.8	1.40	95
B-S-B1-019	-52	199	32.6	1.38	92
B-S-B1-020	-60	211	32.4	1.41	95
B-S-B1-021	-67	222	32.7	1.40	95
B-S-B1-022	-71	232	33.1	1.39	95
B-S-B1-023	0	67.5	33.6	1.39	96
B-S-B1-024	0	47.5	33.6	1.37	94
B-S-B1-025	0	25	34.6	1.38	98
B-S-B1-026	41	162	34.6	1.37	96
B-S-B1-027	50	173	33.1	1.35	90
B-S-B1-028	58	186	32.5	1.41	96
B-S-B1-029	68	196	32.3	1.40	94
B-S-B1-030	75	196	31.8	1.43	96
B-S-B1-031	81	214	31.9	1.43	97
B-S-B1-032	88	225	33.2	1.38	93
B-S-B1-033	0	176	33.3	1.43	102
B-S-B1-034	0	212	32.3	1.42	96
B-S-B1-035	0	246	32.5	1.43	98

4.4.6 CMT2

The location and recipients of the samples are shown in Figure 52.

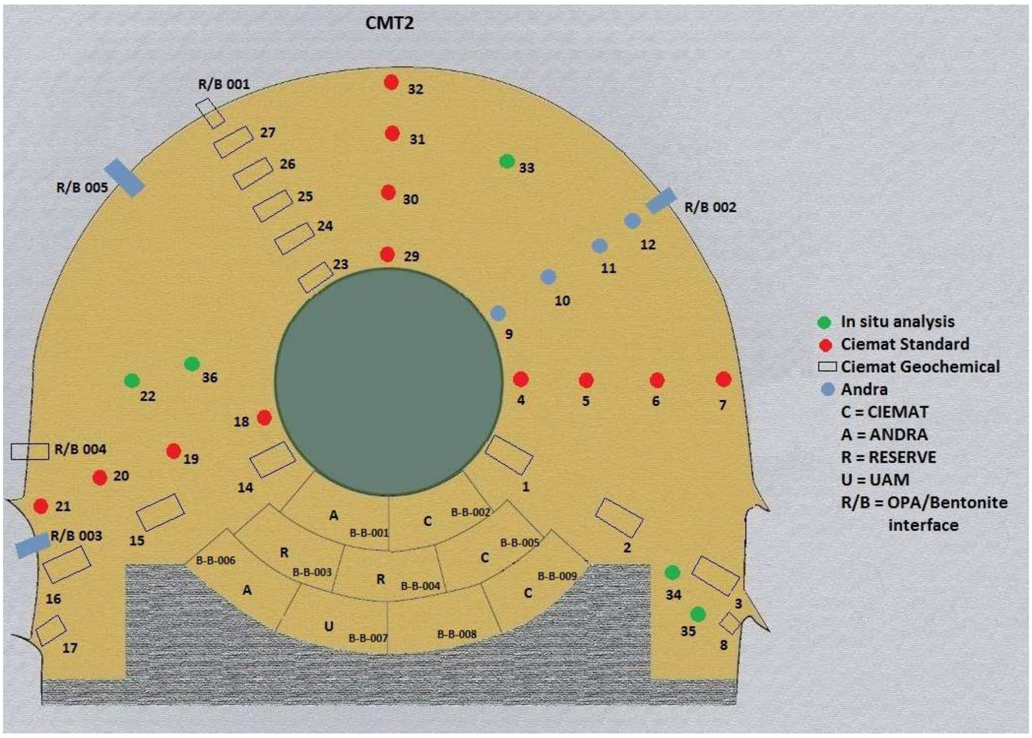

Figure 52: Location of samples in Section CMT2

There were taken few samples to be analysed on site and the rest was sent to the different organizations as requested. The results of the samples analysed on site as well as the ones analysed in the laboratory in CIEMAT facilities are listed in Table 9. See also Appendix IV.

Table 9. Water content and dry density obtained from on site and laboratory analyses in Section CMT2

				Laboratory results			On site results		
ID sample number	Sample	Coordinates x	Coordinates y	Water content (%) mean	Dry density (g/cm^3) mean	Degree of saturation %	Water content (%) mean	Dry density (g/cm^3) mean	Degree of saturation %
B-B-002	B-B-CMT2-002	-	-	33.2	1.39	95	-	-	-
B-B-005	B-B-CMT2-005	-	-	35.1	1.38	99	-	-	-
B-B-009	B-B-CMT2-009	-	-	35.7	1.37	99	-	-	-
4	B-S-CMT2-004	55	127	37.2	1.33	98	-	-	-
5	B-S-CMT2-005	81	127	37.4	1.33	98	-	-	-
7	B-S-CMT2-007	134	127	36.2	1.35	98	-	-	-
18	B-S-CMT2-018	-53	127	37.7	1.34	100	-	-	-
19	B-S-CMT2-019	-81	127	38.3	1.3	96	-	-	-

				Laboratory results			On site results		
ID sample number	Sample	Coordinates		Water content (%) mean	Dry density (g/cm^3) mean	Degree of saturation %	Water content (%) mean	Dry density (g/cm^3) mean	Degree of saturation %
		x	y						
20	B-S-CMT2-020	-111	103	39.2	1.29	97	-	-	-
21	B-S-CMT2-021	-120	95	46.2	1.18	97	-	-	-
29	B-S-CMT2-029	0	187	32	1.42	96	-	-	-
30	B-S-CMT2-030	0	207	33.3	1.39	95	-	-	-
31	B-S-CMT2-031	0	227	32.8	1.42	98	-	-	-
32	B-S-CMT2-032	0	250	33.5	1.42	100	-	-	-
26	B-S-CMT2-026	95	189	35.5	1.38	100	-	-	-
17	B-S-CMT2-017	-129	57	48.3	1.17	100	-	-	-
22	B-S-CMT2-022	-100	123	-	-	-	31.2	1.39	90
36	B-S-CMT2-036	-90	123	-	-	-	30.9	1.40	90
33	B-S-CMT2-033	75	195	-	-	-	30.8	1.39	89
34	B-S-CMT2-034	113	41	-	-	-	35.1	1.31	90
35	B-S-CMT2-035	113	30	-	-	-	35.4	1.33	93

4.4.7 E

The reference location of the samples is shown in Figure 53.

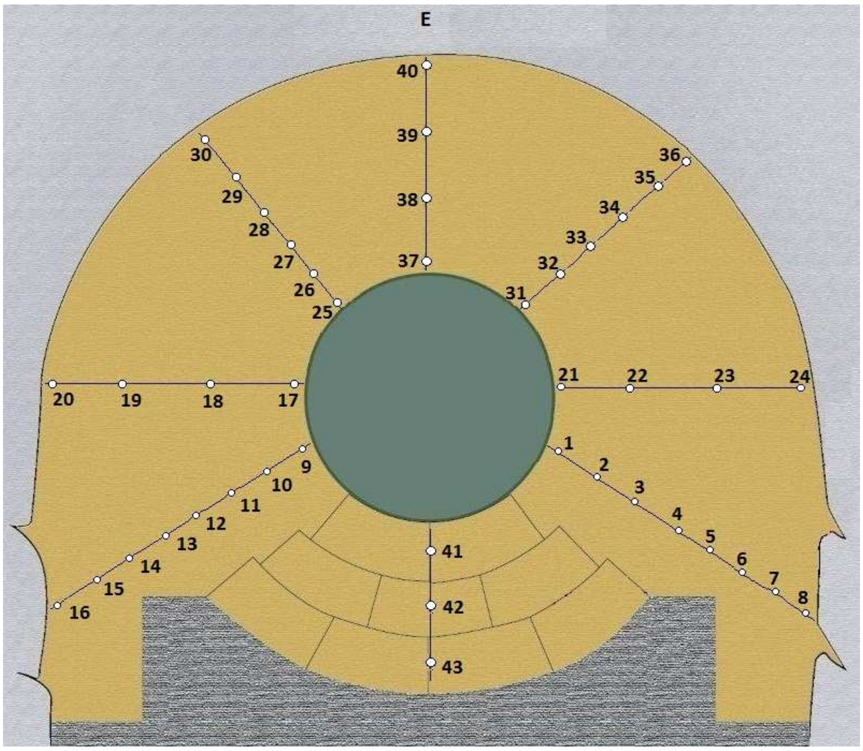

Figure 53: Location of samples in Section E

Table 10 shows the coordinates of the samples and the results of the on site analysis.

Table 10. Water content and dry density from on site analyses in Section E

ID sample number	Sample	Coordinates		Water content (%) mean	Dry density (g/cm^3) mean	Degree of saturation %
		x	y			
1	B-S-E-001	51	112	36.88	1.33	97.35
2	B-S-E-002	62	104	34.98	1.36	96.26
3	B-S-E-003	72	95	35.02	1.31	88.49
4	B-S-E-004	85	83	36.48	1.36	99.98
5	B-S-E-005	100	70	37.31	1.32	96.93
6	B-S-E-006	115	56	40.49	1.28	98.43
7	B-S-E-007	128	45	45.43	1.20	97.58
8	B-S-E-008	143	23	47.81	1.14	94.90
9	B-S-E-009	-54	111	37.30	1.28	91.45
10	B-S-E-010	-64.5	101	36.44	1.34	96.57
11	B-S-E-011	-76	92	35.52	1.33	92.96
12	B-S-E-012	-87	81	36.42	1.33	95.30
13	B-S-E-013	-96	73	39.64	1.25	92.85
14	B-S-E-014	-106	63	41.59	1.25	97.09
15	B-S-E-015	-117	46	45.05	1.20	97.57
16	B-S-E-016	-133	25	51.15	1.12	97.19
17	B-S-E-017	-67	128	36.90	1.36	100.47
18	B-S-E-018	-89	128	35.02	1.35	94.54
19	B-S-E-019	-112	127	34.98	1.34	93.05
20	B-S-E-020	-135	127	34.94	1.35	94.57
21	B-S-E-021	55	127	36.36	1.34	97.13
22	B-S-E-022	79.5	127.5	35.33	1.35	96.05
23	B-S-E-023	105	128	34.56	1.32	89.84
24	B-S-E-024	132	128.5	34.73	1.35	93.49
25	B-S-E-025	49	143	34.55	1.38	97.51
26	B-S-E-026	58	150	33.56	1.38	95.07
27	B-S-E-027	69	159	33.06	1.38	93.49
28	B-S-E-028	81	169	34.45	1.37	96.37
29	B-S-E-029	96	178	34.72	1.37	96.33
30	B-S-E-030	106	190	34.08	1.40	98.56
31	B-S-E-031	-45.5	159	34.18	1.43	103.26
32	B-S-E-032	-57	170	34.42	1.37	95.74
33	B-S-E-033	-71	185	34.22	1.37	94.82
34	B-S-E-034	-80	195	33.56	1.38	95.07
35	B-S-E-035	-89	202	33.78	1.40	97.73
36	B-S-E-036	-99	213	34.73	1.37	96.60
37	B-S-E-037	0	180	35.28	1.35	95.19
38	B-S-E-038	0	203	33.85	1.36	92.35
39	B-S-E-039	0	219	32.72	1.40	95.00
40	B-S-E-040	0	240	33.25	1.37	92.75

ID sample number	Sample	Coordinates		Water content (%) mean	Dry density (g/cm^3) mean	Degree of saturation %
		x	y			
41	B-S-E-041	0	67.5	31.84	1.42	95.86
42	B-S-E-042	0	47.5	32.64	1.33	85.41
43	B-S-E-043	0	25	34.40	1.38	96.82

In order to check the reliability of the results obtained on site, some of the samples were taken bigger than the rest so they could be divided in two parts and analysed two times: on site and in the laboratory that CIEMAT has in Madrid.

Table 11 shows both results.

Table 11. Comparison of water content and dry density results obtained from on site and laboratory analyses in Section E

		Laboratory results			On site results		
ID sample number	Sample	Water content (%) mean	Dry density (g/cm^3) mean	Degree of saturation %	Water content (%) mean	Dry density (g/cm^3) mean	Degree of saturation %
10	B-S-E-010	35.4	1.36	97	36.4	1.34	97
12	B-S-E-012	35.5	1.36	97	36.4	1.33	95
14	B-S-E-014	42.5	1.24	97	41.6	1.25	97
16	B-S-E-016	51.7	1.13	100	51.1	1.12	97
17	B-S-E-017	34.9	1.37	97	36.9	1.36	100
19	B-S-E-019	34.2	1.37	95	35.0	1.34	93
22	B-S-E-022	35.6	1.36	98	35.3	1.35	96
23	B-S-E-023	36	1.36	99	34.6	1.32	90
24	B-S-E-024	35.4	1.38	100	34.7	1.35	93
28	B-S-E-028	35.5	1.37	99	34.5	1.37	96
29	B-S-E-029	33.8	1.41	100	34.7	1.37	96
32	B-S-E-032	34.2	1.38	97	34.4	1.37	96
37	B-S-E-037	34.3	1.39	98	35.3	1.35	95
38	B-S-E-038	33.8	1.39	97	33.8	1.36	92
38	B-S-E-039	33.1	1.42	99	32.7	1.40	95
40	B-S-E-040	35.3	1.36	97	33.2	1.37	93

As the results show, the water contents obtained in the laboratory were on average the same as the on site results, and the dry densities 1.4 % higher. The differences are very small so they are not considered significant. See Appendix IV.

4.4.8 B2

The reference location of the samples is shown in Figure 54.

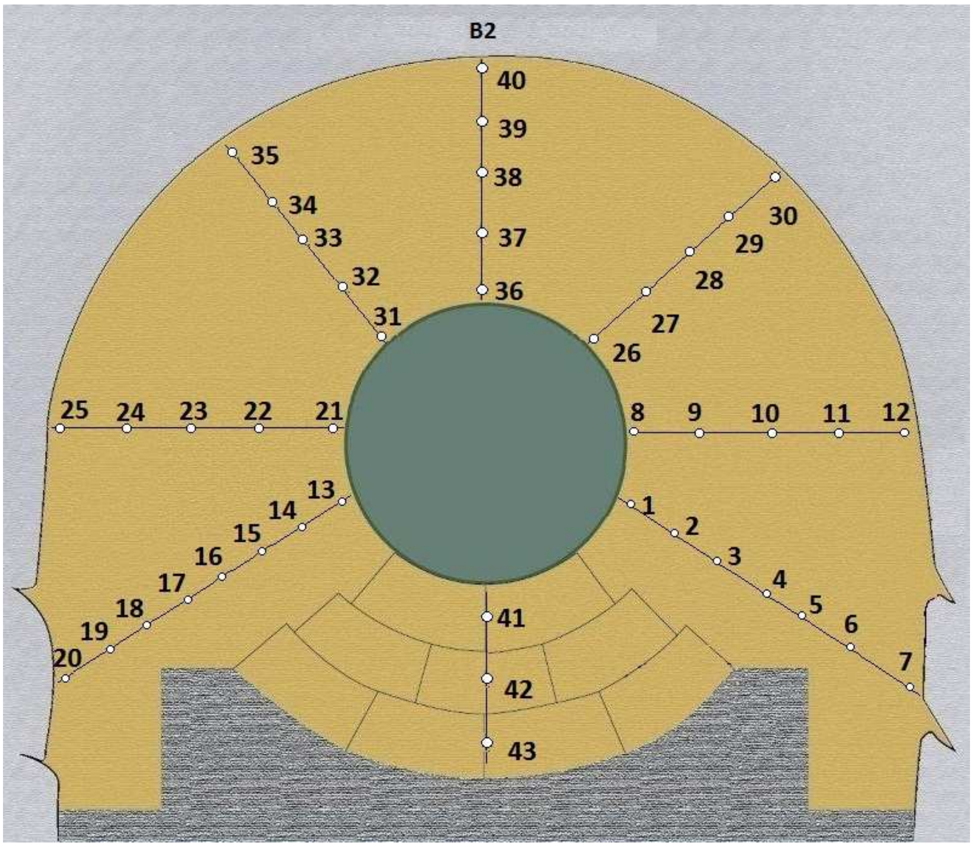

Figure 54: Location of samples in Section B2

Table 12 shows the coordinates of the samples and the results of the on site analysis.

Table 12. Water content and dry density obtained from on site analyses in Section B2

Sample	Coordinates		Water content (%) mean	Dry density (g/cm3) mean	Degree of saturation %
	x	y			
B-S-B2-001	48	101	39.0	1.27	93
B-S-B2-002	58	95	37.8	1.31	96
B-S-B2-003	67	85	37.8	1.31	96
B-S-B2-004	82	75	37.9	1.33	99
B-S-B2-005	102	62	40.8	1.27	97
B-S-B2-006	119	50	43.8	1.22	97
B-S-B2-007	129	40	44.9	1.18	95
B-S-B2-008	55	127	37.1	1.33	96
B-S-B2-009	70	127	35.7	1.33	94
B-S-B2-010	90	127	35.8	1.33	93
B-S-B2-011	115	127	37.5	1.29	93

Sample	Coordinates		Water content (%) mean	Dry density (g/cm3) mean	Degree of saturation %
	x	y			
B-S-B2-012	140	127	40.3	1.27	97
B-S-B2-013	-47	99	39.2	1.31	100
B-S-B2-014	-56	91	37.7	1.32	98
B-S-B2-015	-70	79	37.9	1.32	98
B-S-B2-016	-82	69	38.7	1.31	98
B-S-B2-017	-94	59	39.6	1.29	97
B-S-B2-018	-104	49	49.6	1.19	105
B-S-B2-019	-114	39	47.4	1.20	103
B-S-B2-020	-124	29	50.3	1.14	100
B-S-B2-021	-53	127.5	36.1	1.32	93
B-S-B2-022	-69	127	36.3	1.31	93
B-S-B2-023	-91	127	38.3	1.32	99
B-S-B2-024	-111	128	37.4	1.34	100
B-S-B2-025	-134	127	37.9	1.31	97
B-S-B2-026	46	166	34.2	1.37	95
B-S-B2-027	59	175	33.2	1.39	95
B-S-B2-028	71	185	32.8	1.39	94
B-S-B2-029	86	197	33.7	1.40	98
B-S-B2-030	99	212	32.9	1.38	93
B-S-B2-031	-35	168	35.5	1.38	100
B-S-B2-032	-45	176	34.8	1.36	95
B-S-B2-033	-55	186	34.7	1.36	96
B-S-B2-034	-65	199	35.3	1.35	95
B-S-B2-035	-75	214	35.2	1.36	96
B-S-B2-036	0	177	33.5	1.38	95
B-S-B2-037	0	197	33.0	1.39	95
B-S-B2-038	0	211	33.0	1.44	102
B-S-B2-039	0	229	32.9	1.45	104
B-S-B2-040	0	246	33.3	1.39	96
B-S-B2-041	0	67.5	34.1	1.36	94
B-S-B2-042	0	47.5	33.7	1.36	92
B-S-B2-043	0	25	35.3	1.35	95

As in sections A1-25 and E, some of the samples in section B2 were split in two so they were analysed on site as well as in the laboratory (CIEMAT) to check the consistency of the analysis.

Table 13 shows both results.

Table 13. Comparison of water content and dry density obtained from on site and laboratory analyses in Section B2

		Laboratory results			On site results		
ID sample number	Sample	Water content (%) mean	Dry density (g/cm^3) mean	Degree of saturation %	Water content (%) mean	Dry density (g/cm^3) mean	Degree of saturation %
31	B-S-B2-031	35.0	1.37	97	35.5	1.38	100
32	B-S-B2-032	35.2	1.36	96	34.8	1.36	95
33	B-S-B2-033	35.3	1.37	98	34.7	1.36	96
34	B-S-B2-034	35.0	1.37	97	35.3	1.35	95
35	B-S-B2-035	35.2	1.37	98	35.2	1.36	96
1	B-S-B2-001	39.6	1.29	98	39.0	1.27	93
2	B-S-B2-002	38.7	1.3	97	37.8	1.31	96
3	B-S-B2-003	38.8	1.31	99	37.8	1.31	96
4	B-S-B2-004	40.2	1.29	99	37.9	1.33	99
5	B-S-B2-005	39.6	1.29	98	40.8	1.27	97
6	B-S-B2-006	44.5	1.21	98	43.8	1.22	97
7	B-S-B2-007	45.6	1.19	97	44.9	1.18	95
20	B-S-B2-020	50.3	1.12	96	50.3	1.14	100

The values of the water content obtained in the laboratory are 0.7 % higher that the on site ones, and the dry densities are also higher in a 0.2 %. The differences are very small so they are not considered significant. See Appendix IV.

4.4.9 A2

No samples from the bentonite blocks were taken as explained in section 1.3.

The reference location of the samples is shown in Figure 55.

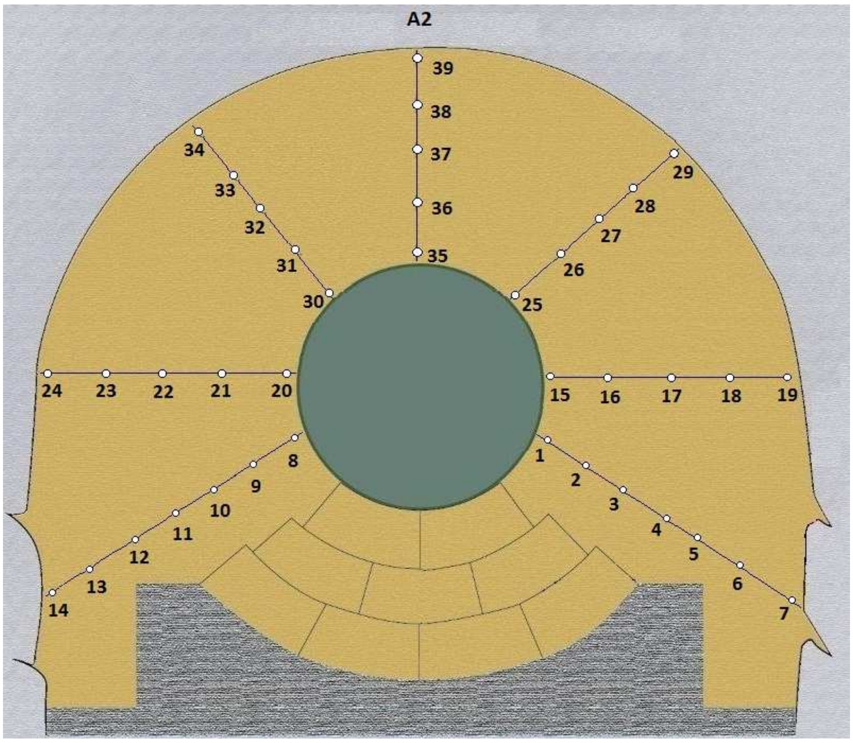

Figure 55: Location of samples in Section A2

Table 14 shows the coordinates of the samples and the results of the on site analysis.

Table 14. Water content and dry density obtained from on site analyses in Section A2

ID sample number	Sample	Coordinates		Water content (%) mean	Dry density (g/cm3) mean	Degree of saturation %
		x	y			
1	B-S-A2-001	49	113	40.3	1.28	98
2	B-S-A2-002	69	105	37.4	1.32	97
3	B-S-A2-003	89	95	38.5	1.29	95
4	B-S-A2-004	102	87	37.8	1.32	98
5	B-S-A2-005	115	79	40.6	1.26	96
6	B-S-A2-006	127	64	43.9	1.20	95
7	B-S-A2-007	147	44	46.8	1.17	97
8	B-S-A2-008	-48	113	41.0	1.23	93
9	B-S-A2-009	-66	105	38.8	1.28	95
10	B-S-A2-010	-82	95	38.9	1.28	94
11	B-S-A2-011	-95	86	39.6	1.27	94
12	B-S-A2-012	-111	75	46.0	1.19	98
13	B-S-A2-013	-126	63	48.3	1.14	95
14	B-S-A2-014	-141	52	49.2	1.13	96

ID sample number	Sample	Coordinates		Water content (%) mean	Dry density (g/cm3) mean	Degree of saturation %
		x	y			
15	B-S-A2-015	55	127	37.2	1.33	98
16	B-S-A2-016	72	127	36.1	1.36	99
17	B-S-A2-017	95	127	36.4	1.32	94
18	B-S-A2-018	115	127	38.4	1.27	92
19	B-S-A2-019	138	127	39.1	1.29	97
20	B-S-A2-020	-55	127	37.4	1.31	95
21	B-S-A2-021	-74	127	36.6	1.34	98
22	B-S-A2-022	-95	127	38.3	1.31	98
23	B-S-A2-023	-118	127	37.3	1.30	94
24	B-S-A2-024	-135	127	38.2	1.30	96
25	B-S-A2-025	35	165	34.7	1.37	97
26	B-S-A2-026	47	177	33.5	1.39	96
27	B-S-A2-027	63	187	34.3	1.38	97
28	B-S-A2-028	79	201	34.9	1.38	98
29	B-S-A2-029	95	211	35.7	1.36	98
30	B-S-A2-030	-32	169	35.0	1.37	97
31	B-S-A2-031	-42	179	34.5	1.37	96
32	B-S-A2-032	-52	190	33.5	1.39	96
33	B-S-A2-033	-65	201	34.0	1.38	96
34	B-S-A2-034	-77	211	35.6	1.35	96
35	B-S-A2-035	0	182	33.3	1.39	95
36	B-S-A2-036	0	196	32.3	1.38	91
37	B-S-A2-037	0	210	32.4	1.38	91
38	B-S-A2-038	0	228	32.5	1.41	97
39	B-S-A2-039	0	245	34.2	1.37	95

4.4.10 CMT3

Most of the samples taken in section CMT3 were for the organizations involved in the project. The location and recipients of these samples are shown in Figure 56.

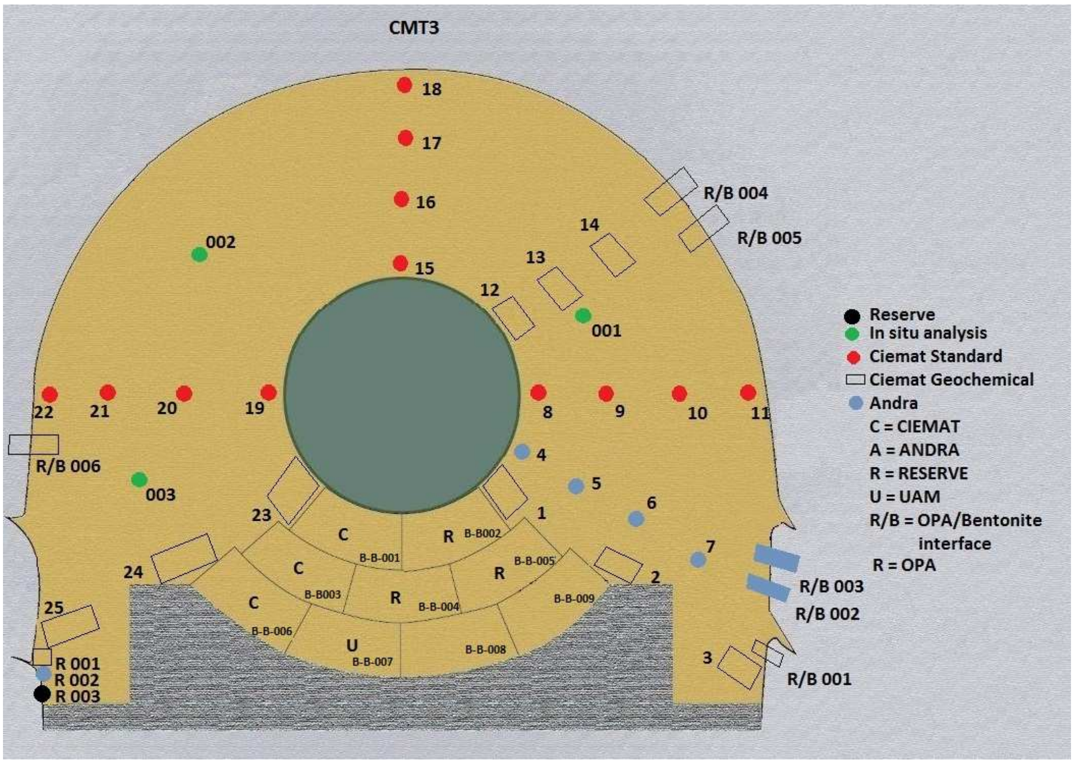

Figure 56: Location of samples in Section CMT3

There were taken few samples to be analysed on site. The rest was sent to the different organizations as requested. The results of the samples analysed on site as well as the ones analysed in the laboratory in CIEMAT facilities are listed in Table 15.

Table 15. Water content and dry density obtained from on site analyses in Section CMT3

ID sample number	Sample	Coordinates		Laboratory results			On site results		
		x	y	Water content (%) mean	Dry density (g/cm³) mean	Degree of saturation %	Water content (%) mean	Dry density (g/cm³) mean	Degree of saturation %
B-B-001	B-B-CMT3-001	-	-	35.5	1.36	97	-	-	-
B-B-003	B-B-CMT3-003	-	-	35.9	1.35	97	-	-	-
B-B-006	B-B-CMT3-006	-	-	35.1	1.36	96	-	-	-
8	B-S-CMT3-008	65	127	35.6	1.35	96	-	-	-
9	B-S-CMT3-009	90	127	36	1.34	96	-	-	-
10	B-S-CMT3-010	110	127	36	1.35	97	-	-	-
11	B-S-CMT3-011	125	127	35.6	1.34	95	-	-	-
14	B-S-CMT3-014	65	200	34.6	1.38	98	-	-	-
15	B-S-CMT3-015	0	180	35.7	1.38	101	-	-	-
16	B-S-CMT3-016	0	195	34.6	1.39	99	-	-	-
17	B-S-CMT3-017	0	215	34.7	1.39	99	-	-	-
18	B-S-CMT3-018	0	235	35.3	1.39	101	-	-	-

ID sample number	Sample	Coordinates		Laboratory results			On site results		
		X	Y	Water Content (%) mean	Dry Density (g/cm^3) mean	Degree of Saturation %	Water Content (%) mean	Dry Density (g/cm^3) mean	Degree of Saturation %
19	B-S-CMT3-019	-55	127	38.7	1.31	98	-	-	-
20	B-S-CMT3-020	-60	127	38	1.32	98	-	-	-
21	B-S-CMT3-021	-82	127	39.6	1.29	98	-	-	-
22	B-S-CMT3-022	-124	127	43.8	1.23	99	-	-	-
1	B-S-CMT3-001	41	90	41.3	1.3	104	-	-	-
2	B-S-CMT3-002	94	55	43.1	1.27	103	-	-	-
3	B-S-CMT3-003	129	30	47.8	1.17	99	-	-	-
23	B-S-CMT3-023	-40	105	41.4	1.26	98	-	-	-
24	B-S-CMT3-024	-95	70	40.9	1.27	98	-	-	-
25	B-S-CMT3-025	-135	35	50.1	1.14	99	-	-	-
001	BR-S-CMT3-001	50	185	-	-	-	34.7	1.37	97
002	BR-S-CMT3-002	-90	185	-	-	-	34.0	1.39	97
003	BR-S-CMT3-003	-100	100	-	-	-	44.5	1.22	99

4.5 ADDITIONAL TESTS, COMMENTS AND EVALUATION OF THE RESULTS

4.5.1 Test behavior of bentonite samples at air conditions

In order to evaluate the impact of the time spent handling the samples in the results, an expansion test was done. It consisted in taking a big sample and dividing it in 7 subsamples. Water content and dry density was measured in this subsamples after 2, 15, 30, 60 120, 240 and 360 minutes. Figure 57 and Figure 58 show the obtained results.

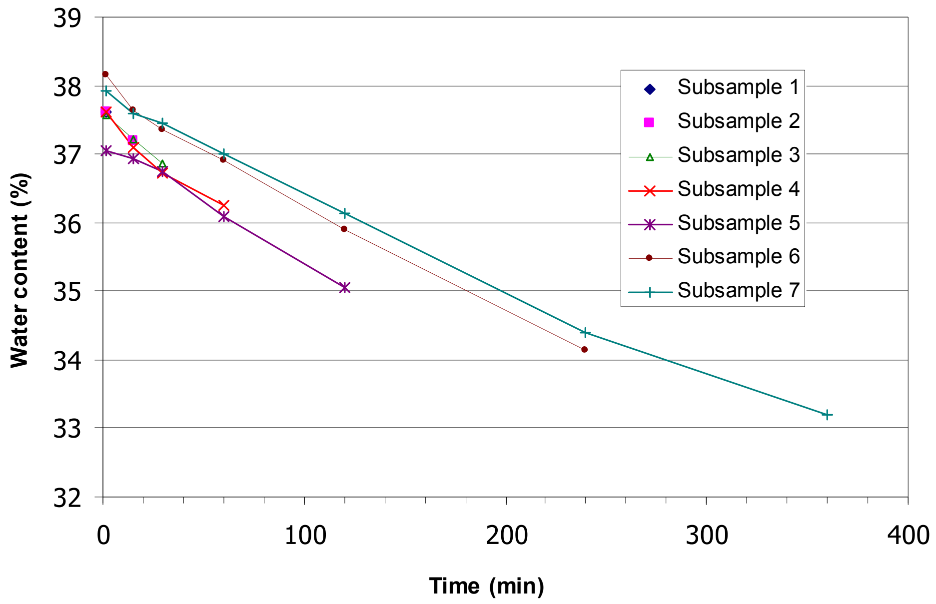

Figure 57: Evolution of the water content in the samples at air conditions in the on site laboratory

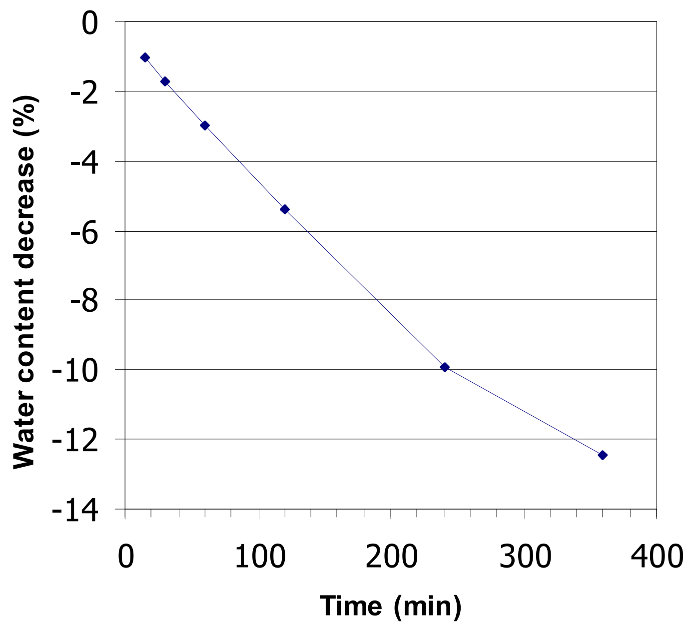

Figure 58: Evolution of the average water content loss

The results of this test show that there would be an average of a 1.2% decrease of the water content after 20 minutes of the sample being exposed to air conditions. 20 minutes is approximately the time spent trimming and handling the samples to be analysed. This would have an impact on the values of the degree of saturation, decreasing the percentage in approximately 3 points in most of the cases.

Apart from this, the expansion of the bentonite mass as a whole before the sampling should also be taken into account when calculating the degree of saturation. This would increase the porosity of the mass and therefore, the density would decrease and the degree of saturation. However, this effect can not be quantified with the expansion test it was carried out or by other tests.

4.5.2 Water content, dry density and degree of saturation

During the sampling campaigns of sections CMT1 CMT2 and CMT3, some samples were taken to be analysed on site in order to get reference values of water content and dry density for the future laboratory analyses. These samples were located in places between planned samples in order to cover as much as possible the surface of the section (See Figure 50, Figure 52 and Figure 56) as it was thought that the results would be homogeneous in every part of the section.

As the dismantling was moving forward and the on site analyses were being made, it was observed that the lower parts of the experiment were wetter than the upper ones and that the dry density was lower at the bottom than in the top. Table 16 shows the average values of water content, dry density and degree of saturation in every section and in every area of each section (upper, intermediate, lower and blocks). The total average in the experiment of water content is 36%, of dry density is 1.34 g/cm^3 and a 95.5% of degree of saturation.

Table 16. Average values of water content, dry density and degree of saturation in every section obtained from on site analysis.

Position		Amount of samples	Water content (%)	Dry density (g/cm^3)	Degree of Saturation (%)
A1_25	GBM Lower	14	36.8	1.32	95
	GBM Upper	15	31.8	1.42	96
	Blocks	3	34.4	1.33	90
B1	GBM Lower	15	40.0	1.29	99
	GBM Upper	17	32.8	1.40	96
	Blocks	3	34.0	1.38	96
E	GBM Lower	16	39.8	1.28	96
	GBM Intermediate	8	35.4	1.35	95
	GBM Upper	16	34.0	1.38	96
	Blocks	3	33.0	1.38	93
B2	GBM Lower	15	41.5	1.26	98
	GBM Intermediate	10	37.2	1.32	96
	GBM Upper	15	33.9	1.39	96
	Blocks	3	34.4	1.36	94
A2	GBM Lower	14	41.9	1.24	96
	GBM Intermediate	10	37.5	1.31	96
	GBM Upper	15	34.0	1.38	96

This results also show that the water content was higher and the dry density lower in the sections that are farther away from the concrete plug.

Regarding the degree of saturation, no differences were observed between areas in the same section or between sections. The values remain stable close to 96% in most of the cases.

These results are applicable to both the GBM and the blocks.

4.5.3 Tentative correction of the on site results

If the impact of the drying of the samples before they are analysed is taken into account (see section 4.5.1) in the final results of the experiment, then the actual water content of the samples could be about 1.2 % higher than the obtained results; and the degree of saturation would increase between 2 and 4 points in percentage.

In order to show the results as real as possible, the values obtained in the on site laboratory have been tentatively corrected by means of rising 1.2 % more in the water content measurements and recalculating the degree of saturation. These values are gathered in Appendix II as well as the isoline graphs for every parameter in every cross section. Regarding the isoline graphs, note that the amount of data taken on the field should have been much higher in order to have a more accurate image so they show an approximate distribution but the general trends are representative.

To build the contour and shaded maps, Surfer 10 software has been used. Surfer is a grid-based mapping program that interpolates irregularly spaced XYZ data into a regularly spaced grid. This grid is used to produce different types of maps (contour, shaded relief, vector, image, 3D wireframe maps, 3D surface...). As gridding methods, Kriging has been used. Kriging produces visually appealing maps from irregularly spaced data, expressing trends suggested in the data.

These maps are also shown in a smaller scale in Figures 60, 61 and 62. The red numbers in every chart refer to the identification number of the samples.

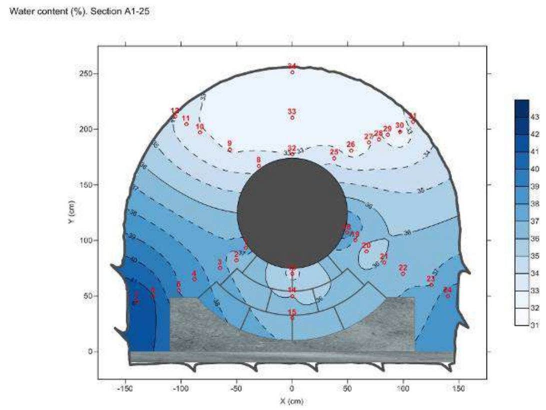

SECTION A1-25

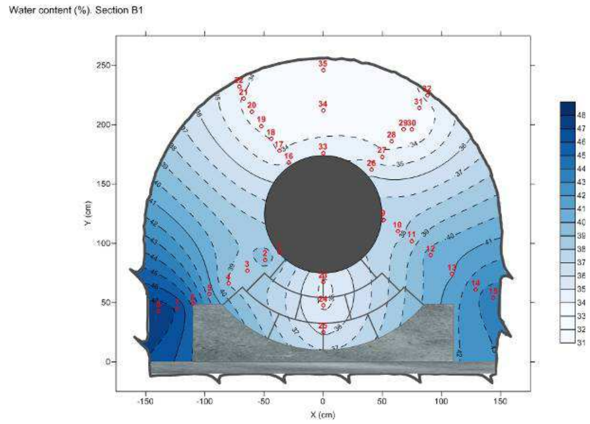

SECTION B1

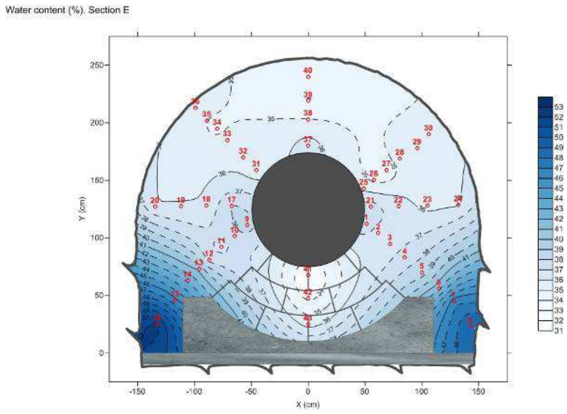

SECTION E

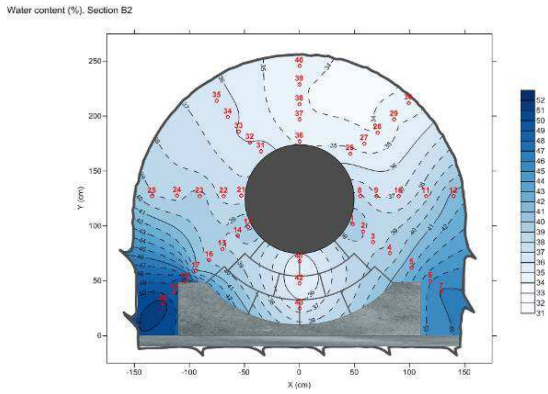

SECTION B2

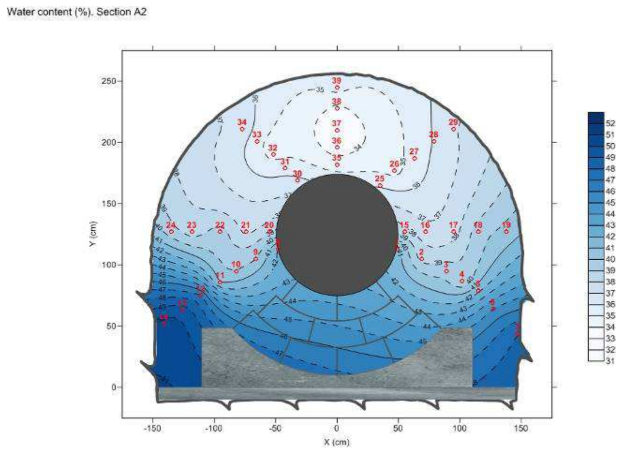

SECTION A2

Figure 59: Evolution of the Water Content. Cross sections. Values corrected according to section 4.4.3.

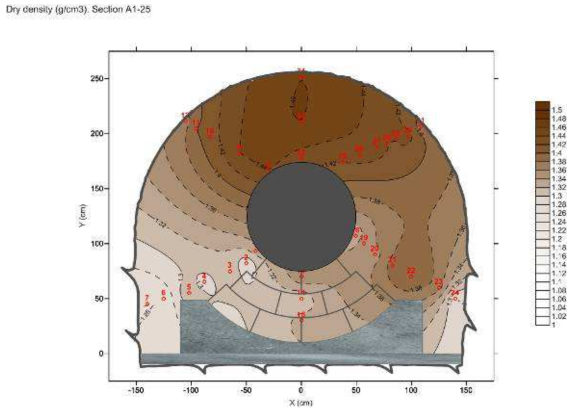

SECTION A1-25

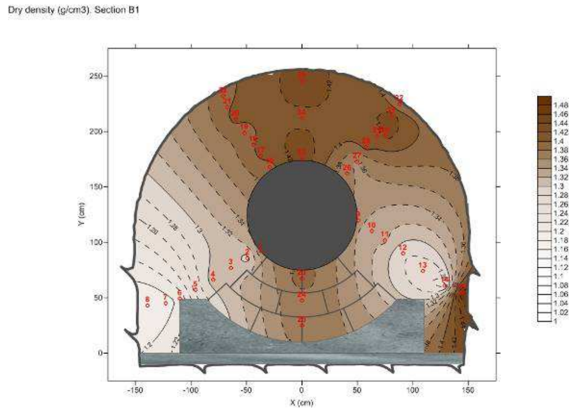

SECTION B1

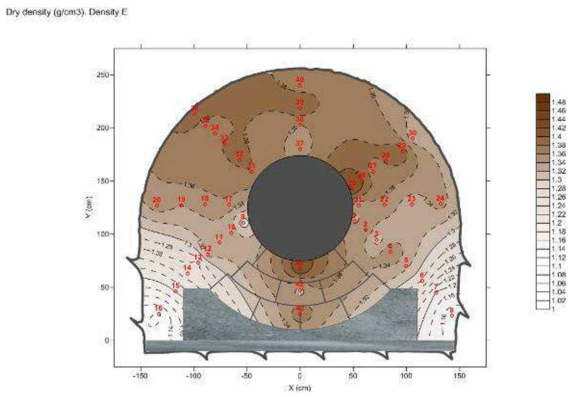

SECTION E

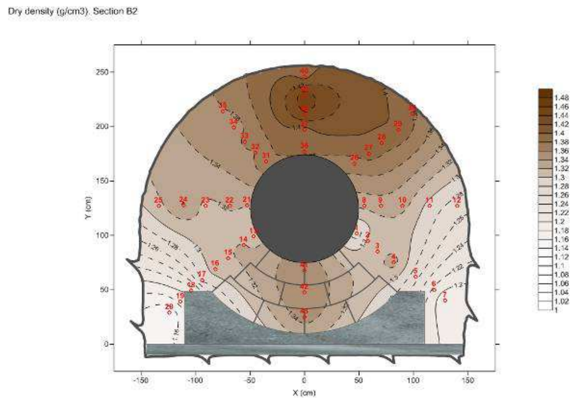

SECTION B2

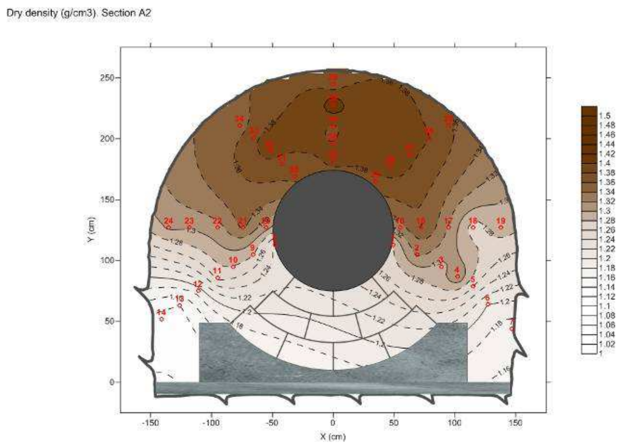

SECTION A2

Figure 60: Evolution of the Dry Density. Cross sections. Values corrected according to section 4.4.3.

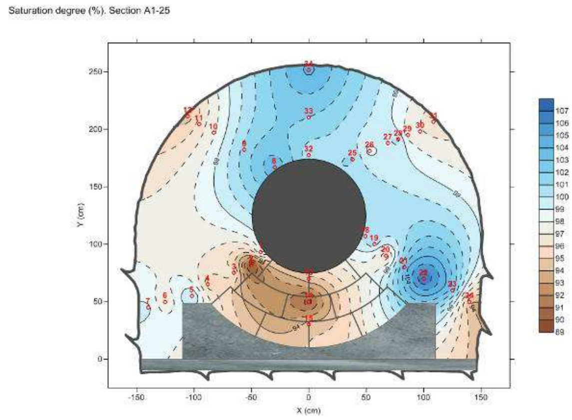

SECTION A1-25

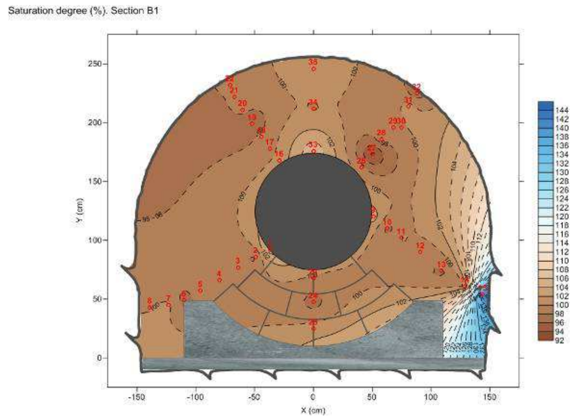

SECTION B1

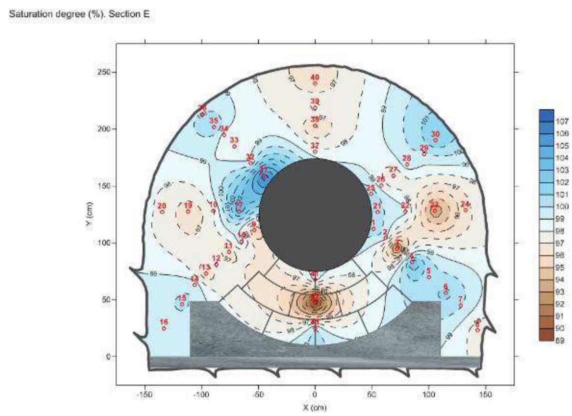

SECTION E

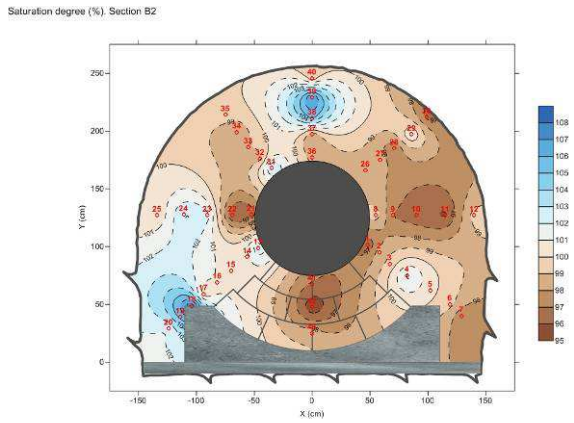

SECTION B2

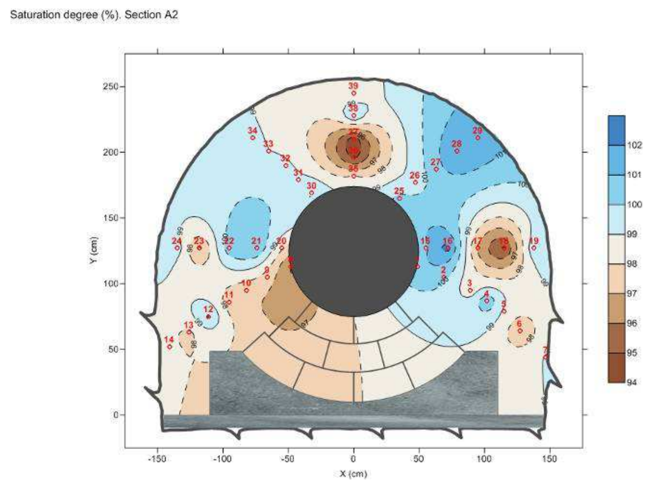

SECTION A2

Figure 61: Evolution of the degree of saturation. Cross sections. Values corrected according to section 4.4.3.

Since an increasing trend for the water content and decreasing trend for the dry density with the Y coordinate was observed, isoline maps corresponding to different longitudinal sections were also drawn. In order to have more data in the longitudinal sections, every section was defined to cover few cm thick (i.e. Y 44-54 represents a section of 10 cm thickness between z= 44cm and z=54 cm). See Appendix II and also Figures 63, 64 and 65.

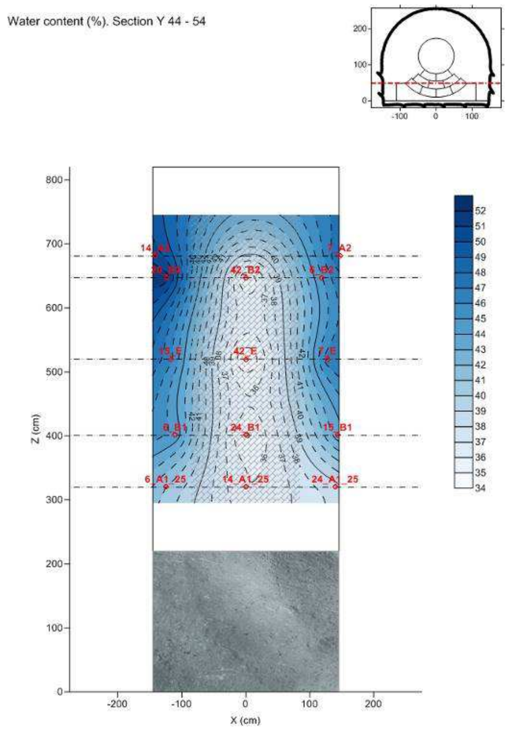

SECTION Y 44-54

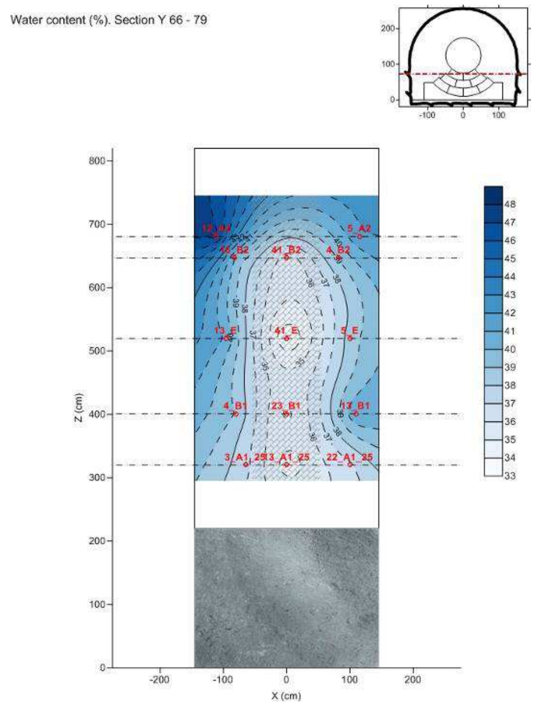

SECTION Y 66-79

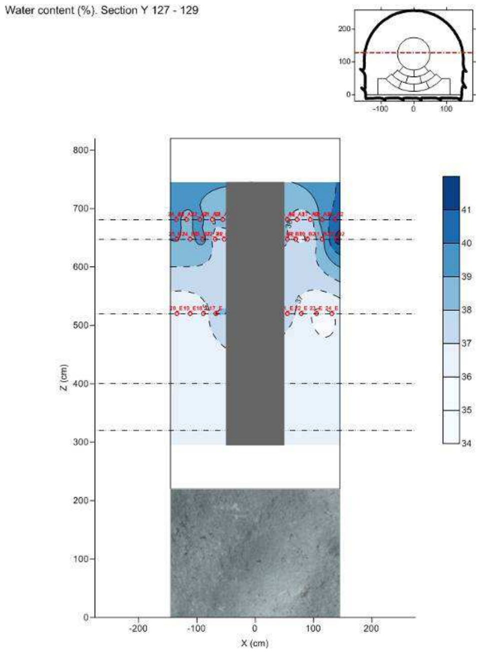

SECTION Y 127-129

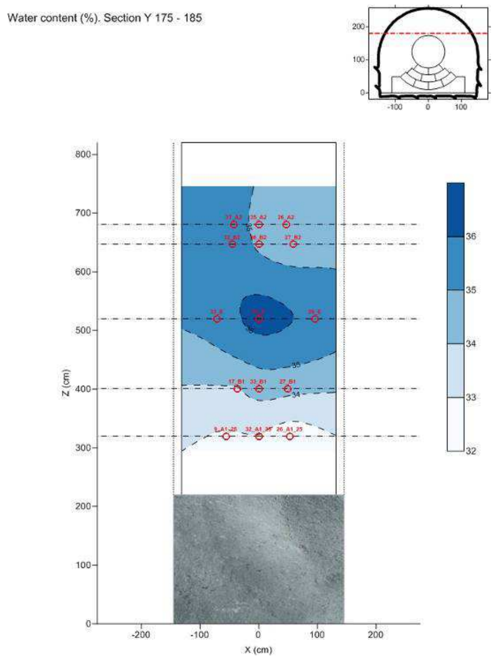

SECTION Y 175-185

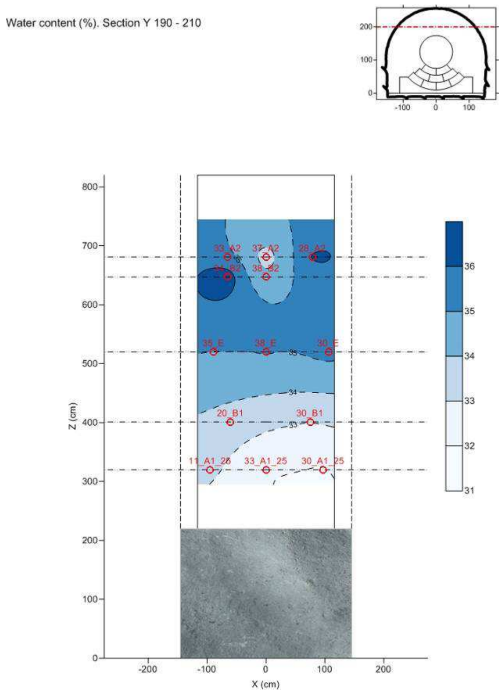

SECTION Y 190-210

Figure 62: Evolution of the Water Content. Longitudinal sections. Values corrected according to section 4.4.3.

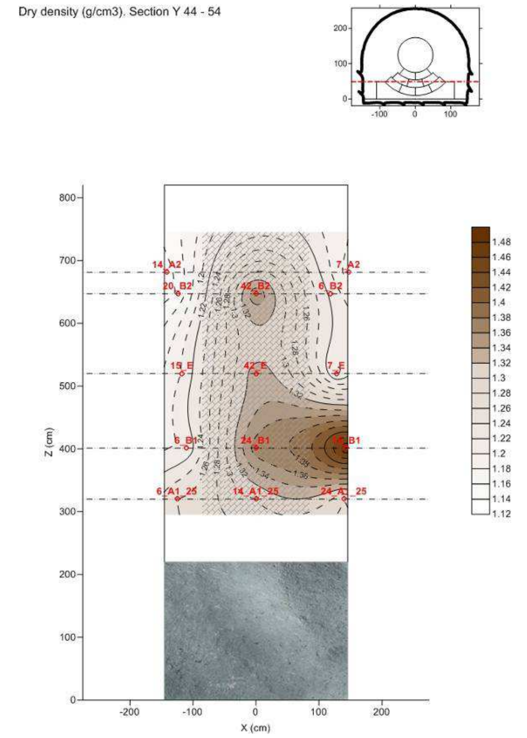

SECTION Y 44-54

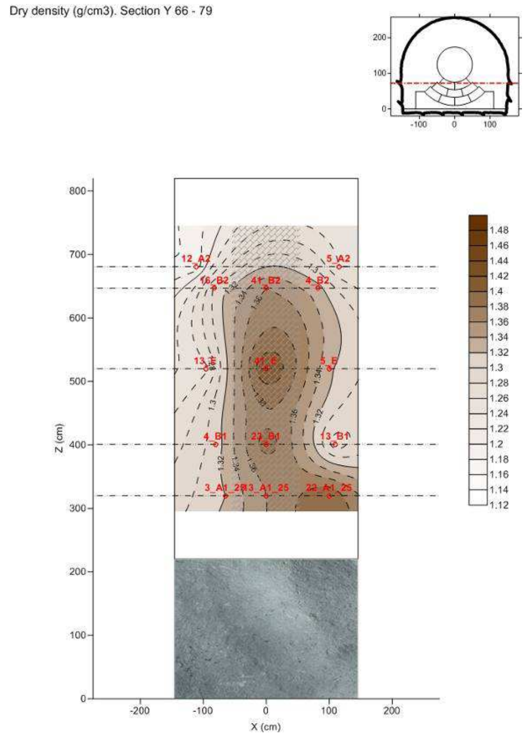

SECTION Y 66-79

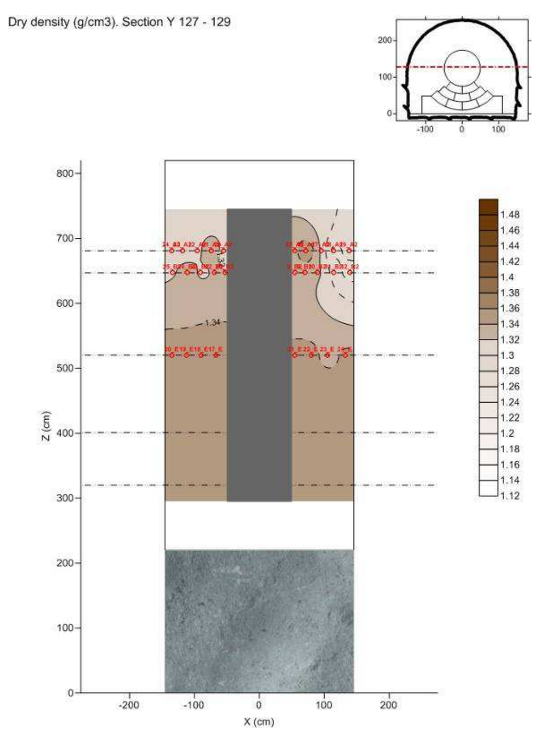

SECTION Y 127-129

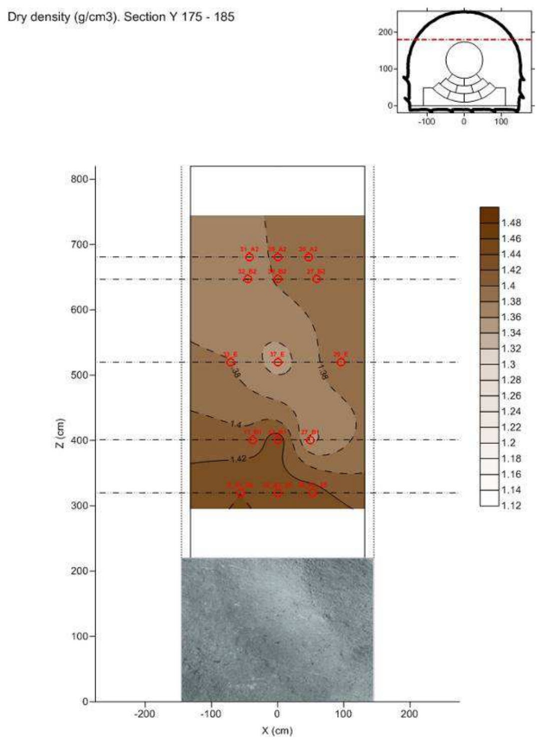

SECTION Y 175-185

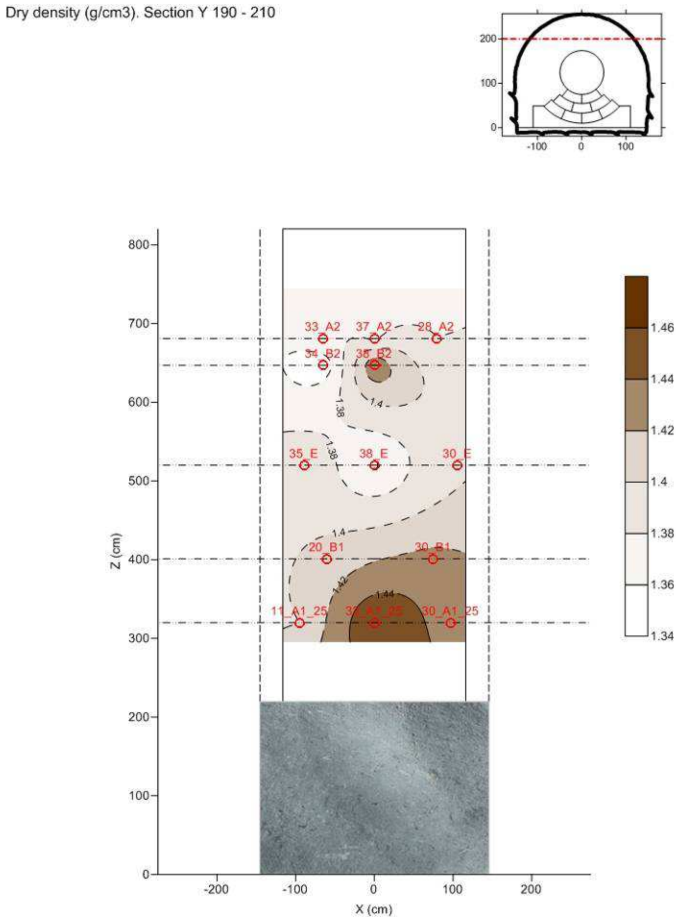

SECTION Y 190-210

Figure 63: Evolution of the Dry Density. Longitudinal sections. Values corrected according to section 4.4.3.

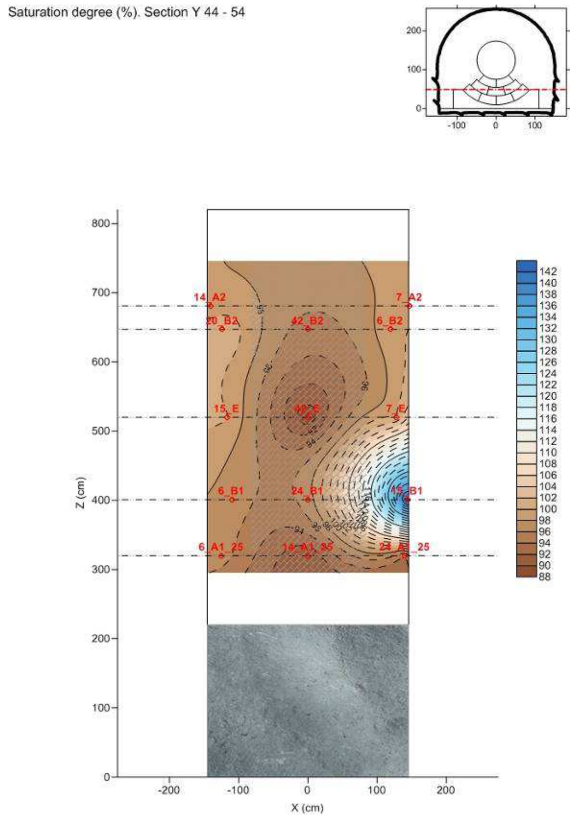

SECTION Y 44-54

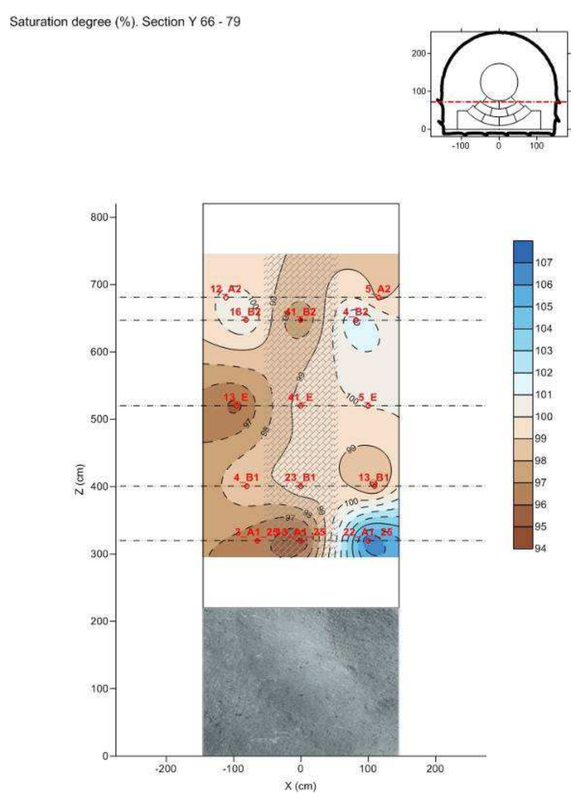

SECTION Y 66-79

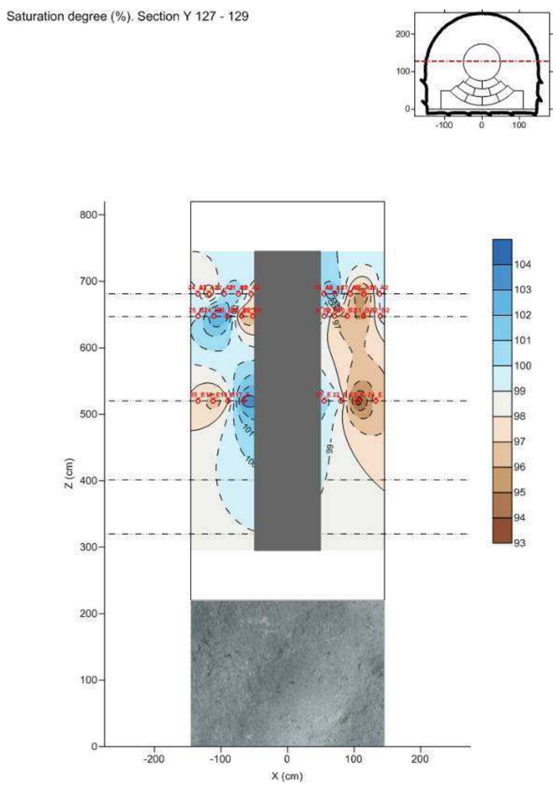

SECTION Y 127-129

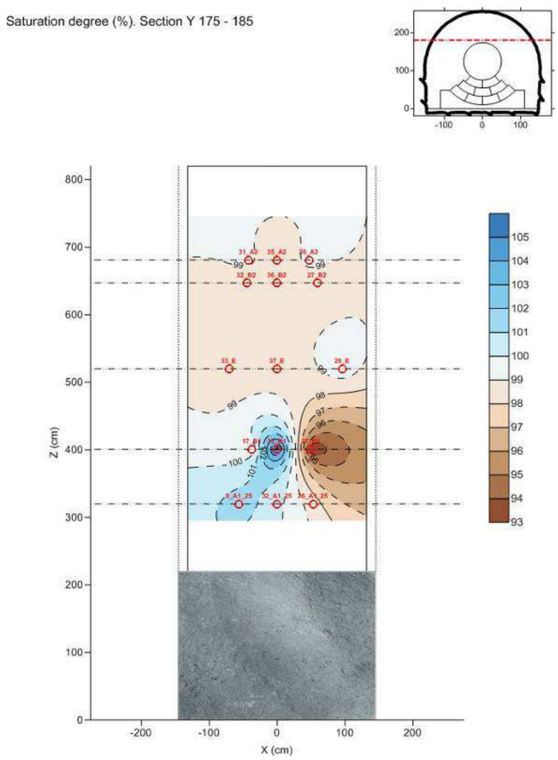

SECTION Y 175-185

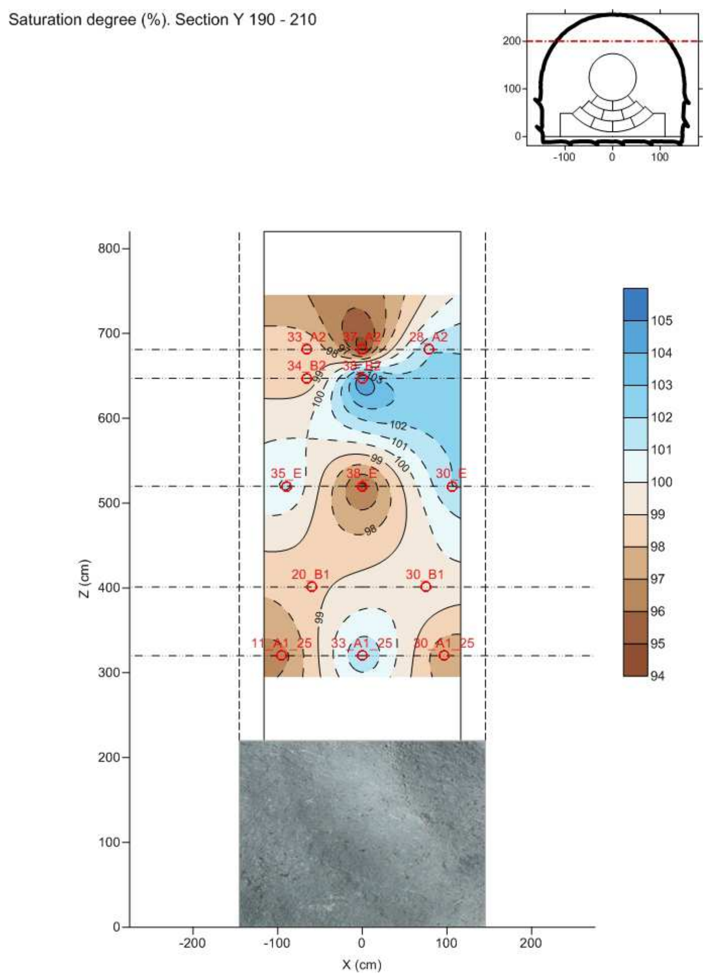

SECTION Y 190-210

Figure 64: Evolution of the degree of saturation. Longitudinal sections. Values corrected according to section 4.4.3.

4.5.4 Bentonite blocks and canister displacement

According to the results, the density of the bentonite blocks decreased from an initial value of 1.7 g/cm^3 in the installation phase to a value rating from 1.33 to 1.38 g/cm^3 (on site analyses). The lower densities corresponded to the sections closer to the concrete plug. This only can be explained by an expansion of the blocks.

There were 3 different levels of bentonite blocks (#01, #02 and #03) and their dimensions measured on site as the dismantling was moving forward. The distance from the centre of the canister to the floor was also measured. Figure 65 shows the dimensions of the blocks when they were installed. Figure 66 shows the obtained measurements from blocks along different sections during the dismantling.

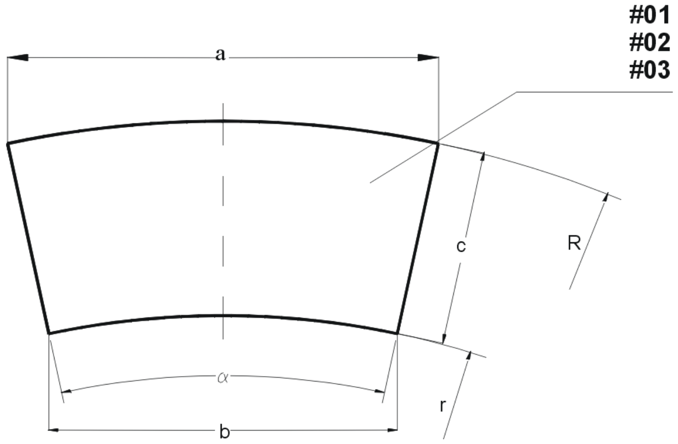

Block type	a (mm)	b (mm)	c (mm)	Thickness (mm)	External Radius R (mm)	Internal Radius r (mm)	α (°)	Weight (kg)
#01	$470.0^{+2,0}_{-5,0}$	$380.0^{+2,0}_{-4,0}$	$214.0^{+2,0}_{-3,0}$	$125.0^{+2,0}_{-2,0}$	1.133	919	24°	22.1
#02	$473.0^{+2,0}_{-5,0}$	$361.0^{+2,0}_{-4,0}$	$214.0^{+2,0}_{-3,0}$	$125.0^{+2,0}_{-2,0}$	917	703	30°	21.8
#03	$478.0^{+2,0}_{-5,0}$	$330.0^{+2,0}_{-4,0}$	$214.0^{+2,0}_{-3,0}$	$125.0^{+2,0}_{-2,0}$	701	487	40°	21.3

Figure 65: Original bentonite blocks dimensions

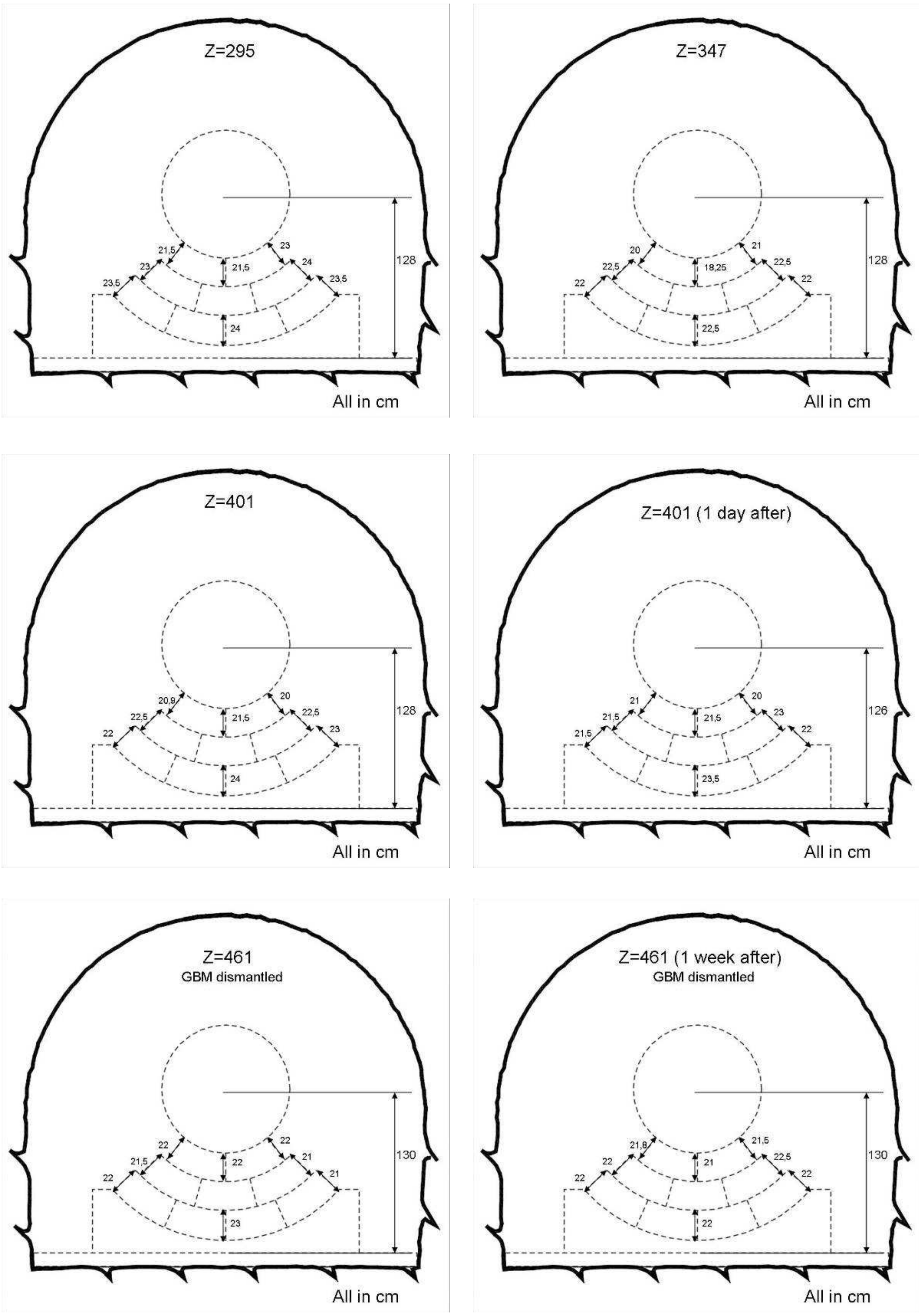
Z=295
128
21,5
23
21,5
24
23,5
23
23,5
24
23
All in cm
Z=347
128
20
21
22,5
18,25
22,5
22
22
22,5
All in cm
Z=401
128
20,9
20
22,5
21,5
22,5
22
23
24
All in cm
Z=401 (1 day after)
126
21
20
21,5
21,5
23
21,5
22
23,5
All in cm
Z=461
GBM dismantled
130
22
22
21,5
22
21
22
21
23
All in cm
Z=461 (1 week after)
GBM dismantled
130
21,8
21,5
22
21
22,5
22
22
22
All in cm

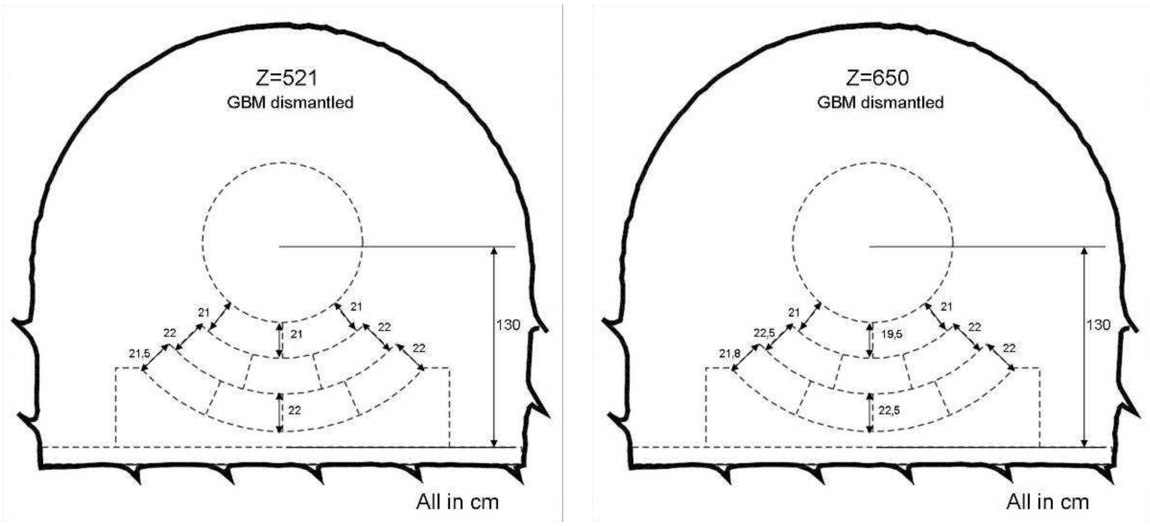

Figure 66: Bentonite blocks on site measurements

As seen in Figure 66 , the parameter measured in the blocks (‘c’ parameter in Figure 65) had an initial value of 21.4 cm, and in most of the cases this value increased showing that a vertical expansion (Y axis) of the block took place.

The expansion along the Y axis was also assessed by the evolution of the distance between the centre of the canister and the floor, which shows an uplift of the canister of approximately 3 cm from its original position. As it can be seen in Figure 66, this expansion took place from Z=461, when a complete section of bentonite was not dig at the same time because the bentonite blocks bed was left on place while the GBM front was being removed.

The expansion of the blocks along the Z axis was also proved by the evolution of the distance between the front face of the canister and the front face of the concrete bed. They were aligned when the EB experiment started and at the end of the dismantling operation there was a gap of around 4 cm between both. See Figure 67.

All these observations indicate that apart from the expansions developed in the bentonite blocks during the operational phase they had an additional expansion during the dismantling operation.

Figure 67: Longitudinal expansion of the bentonite

4.5.5 Other observations

In general, the aspect of the GBM was homogeneous and consistent along the whole operation. No risk of collapse was observed. This same observation can be applied to the Opalinus clay as it seemed to have kept all its physical properties intact. See Figure 68.

Figure 68: OPA after the dismantling operation

The rest of elements of the experiment such as hydration pipes, cables, geotextile…all of them were in perfect conditions. If any cable was damaged, it was during the bentonite removal operation as it was no possible to exactly predict the location of them after the swelling of the bentonite due to the hydration. The tools used to remove the bentonite were powerful and sharp and by the time the cables were reached, sometimes it was already too late to save them. See Figure 69.

Figure 69: Broken cables during the bentonite removal

The geotextile used for the hydration system always looked clean with no intrusions of bentonite. There were some corrosion stains from the welding points used to attach the total pressure cells to the canister in section E but in general the corrosion effects on metallic parts were negligible. See Figure 41.

5 SUMMARY AND CONCLUSIONS

Despite the initial delay due to the difficulties met to dismantle the concrete plug the operation as a whole went very well and it was concluded in a reasonable time, less than 100 working days.

The laboratory analyses show a clear trend of higher water contents from top to bottom in every section, and from sections closer to the plug to sections towards the end of the experiment. This trend was also followed by the dry density results but in a reverse way: the results showed lower densities at the bottom of every section. These trends can be explained by two events. One is the material segregation that probably happened during the construction of the experiment (NAGRA 2004, see Figure 70). The bigger pellets would lay at the bottom and the smaller ones filling the gaps, only on the top, so the initial values of density were lower at the bottom.

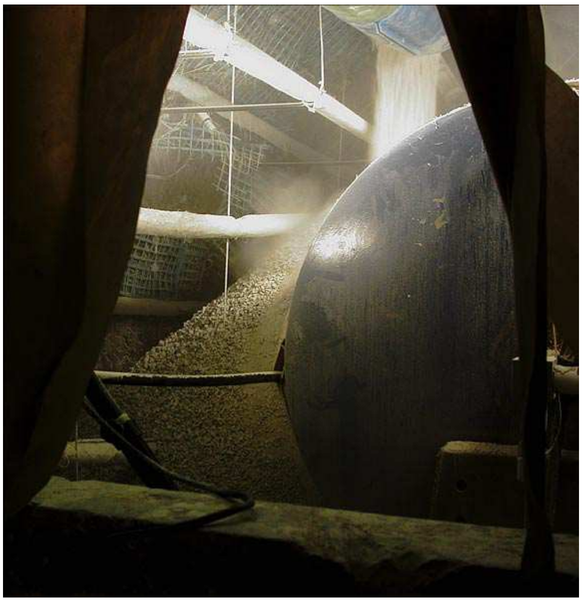

Figure 70: GBM emplacement with gravity fall from the auger during EB installation

The other fact is the gravity effect. During the hydration process, injected water would be affected by gravity and it might have accumulated preferentially at the bottom of the experiment. This explanation matches quite well with the up levelling recorded for the dummy canister during the operational phase and with the dry density distribution found, because the accumulation of the water at the bottom would have promoted the expansion of the blocks and GBM at the bottom increasing the initial heterogeneity due to the emplacement.

Observations indicated that the front of bentonite dried quickly, with a clear effect in 1-2 days after exposure. Besides, there was an expansion of the bentonite buffer along the Z axis, which correlates with the decreasing pressure trend of the total pressure cells recorded as the dismantling works were advancing. This expansion would have affected to the dry density of the bentonite in the experiment by dropping the results obtained in the laboratory, and therefore, the results of the degree of saturation. These laboratory results ranged from 90% to 99% and after applying a correction due to the handling of the samples, these results might range from 98 % to 100.5%. The decrease of the dry density due to the same reasons has not been possible to quantify, but taking the whole in consideration the values of the degree of saturation of the bentonite would probably show a complete saturation of it. This is in line with the operational results, which showed that no additional water could be introduced in the buffer after 5 years of artificial saturation.

In conclusion, the dismantling operation provided the information requested: it was possible to inspect and analyse "in-situ" the GBM in order to determine its properties. Despite the initial heterogeneity due to the emplacement its aspect and homogeneity were very good and the registered degree of saturation almost complete taking into account the uncertainties due to bentonite expansion and drying during the dismantling. Obtained dry density and most probably permeability (laboratory analyses are still on-going) are well correlated with the expected initial heterogeneity (not measured during the emplacement due to operational reasons) but the obtained values indicate that low enough buffer permeability was achieved everywhere and that higher than expected total pressures were developed. Furthermore, almost 300 samples more were taken and sent to the different partners in the project to carry out different laboratory analyses, which results will be reported in specific documents.

6 REFERENCES

- AITEMIN 2001. Engineered Barrier Emplacement Experiment in Opalinus Clay "EB" Experiment. TEST PLAN. Madrid, 76 pp.
- ENRESA 2005. "Engineered barrier emplacement experiment in Opalinus Clay for the disposal of radioactive waste in underground repositories" Final Report. *Publicación Técnica ENRESA* 02/05. Madrid, 101 pp.
- AITEMIN 2007. Engineered Barrier Emplacement Experiment in Opalinus Clay "EB" Experiment. Sensors data report Nº 19 and Mont Terri TN2007-11. Period 22/11/2001 to 30/06/2007, 38 pp.
- UNE 7045(1952): Determinación de la porosidad de un terreno.
- AITEMIN 2012. Engineered Barrier Emplacement Experiment in Opalinus Clay "EB" Experiment. Test Pland and sampling book. Madrid, 64 pp.
- NAGRA 2004, K. Kennedy. TECHNICAL NOTE TN 2004-19 October 2004. Engineered Barrier Emplacement (EB) Experiment in Opalinus Clay: Granular Material Backfill QA Report with Emplacement Description. Project Deliverable D 12. EC contract FIKW-CT-2000-00017, 78 pp.

7 APPENDIX I TOOLS DATA SHEET

DARDA - Splitting cylinder

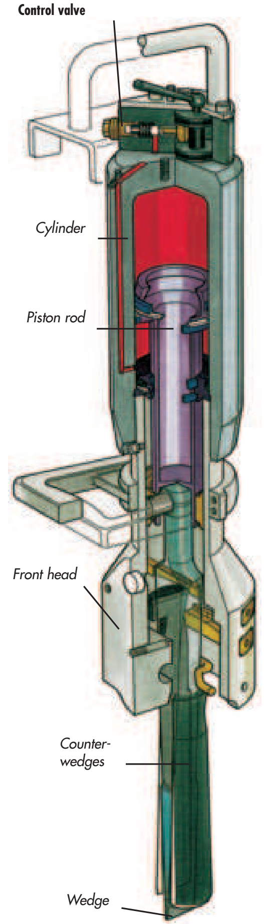

Darda general survey

Splitting cylinders

Type	Wedge set	Required drill hole diameter mm	Minimal drill hole depth mm	Splitting distance mm	Splitting force theoretical kN	to	Splitting force effective kN	to	Weight kg	Length splitting cylinder mm	Length wedge set mm	Order-No
C 2 S	N	31 - 32	270	9	3490	355	1913	195	18	745	140	8381 0402 10
C 4 S	N	34 - 36	430	10 - 40	4524	461	2256	230	22	995	250	8381 0405 25
C 4 S	WL	35 - 38	540	14	3267	333	1864	190	23	1145	400	8381 0405 40
C 9	N	45 - 48	410	18 - 53[1]	2995	305	1962	200	22	1020	230	8381 0409 00
C 9	L	48 - 50	580	18 - 53[1]	2995	305	1962	200	23	1190	400	8381 0409 40
C 10 S	N	41 - 43	630	18 - 58[1]	4948	504	2551	260	32	1400	380	8381 0408 00
C 12	N	45 - 48	610	19 - 60[1]	6061	618	3507	358	31	1290	380	8381 0412 38
C 12	L	45 - 48	680	15 - 44[1]	8082	824	4048	413	32	1360	450	8381 0412 45
C 12	W	45 - 48	550	24 - 80[1]	4849	494	3150	321	31	1250	340	8381 0412 50

[1] With 1 enlarging counter wedge and 1 special enlarging counter wedge

Hydraulic pump units

Type	Model	Type of motor	Rating kW	Suitable for splitting cylinders	Weight kg	Length mm	Width mm	Height mm	Pump capacity l/min	Volume of tank l	Order-No
A 1	mobile	Air motor[1]	3,8	1 - 4	113	1180	720	730	5,0	10,0	8381 0501 12
D 4	mobile	Diesel motor	5,6	1 - 5	137	1180	720	730	5,4	10,0	8381 0502 40
D 4 E	mobile	Diesel motor[2]	5,6	1 - 5	156	1180	720	730	5,4	10,0	8381 0502 41
E 2	mobile	Electro motor[3]	4,0	1 - 5	117	1180	720	800	4,8	10,0	8381 0503 12
A P	portable	Air motor[4]	1,8	1 - 2	41	460	400	500	2,0	5,0	8381 0503 53
B P	portable	Gasoline motor	4,7	1 - 2	38	460	400	500	2,0	5,0	8381 0503 38
E P	portable	Electro motor[3]	1,5	1 - 2	40	460	400	500	2,3	5,0	8381 0503 46

[1] Air consumption: 3,9 m^3/min (at 6 bar); [2] With electro-starter; [3] Electro motor: 3 phases, 400 V, 50 cycles per second; [4] Air consumption: 2,4 m^3/min (at 6 bar)

Transport racks

Type	Type of motor	Suitable for splitting cylinders	Weight kg	Length mm	Width mm	Height mm	Pump capacity l/min	Volume of tank l	Order-No
T 1 D	Diesel motor D 4	1 - 6	193	1200	800	1700	5,4	10,0	8381 0503 60
T 1 DE	Diesel motor D 4 E (with electro-starter)	1 - 6	212	1200	800	1700	5,4	10,0	8381 0503 63

Hydraulic hoses

Type	Length m	Suitable for cylinders	Order-No
S 1	10	1	8381 0504 02
S 1	20	1	8381 0504 03
S 2	20	2	8381 0504 11
S 3	20	3	8381 0504 29
S 4	20	4	8381 0504 37
S 5	20	5	8381 0504 45

[1] Distance between cylinder and pump unit

Enlarging counter wedges

Type	Enlarging counter wedges Order-No	Special enlarging counter wedges Order-No
C 4 SN	3390 0141 03	–
C 9 N	3390 0246 11	3390 0246 21
C 9 L	3390 0246 31	3390 0246 51
C 10 SN	3390 0261 00	3390 0261 11
C 12 N	3390 0236 00	3390 0427 00
C 12 L	3390 0236 21	3390 0280 21
C 12 W	3390 0236 11	3390 0280 11

Pressure shells

suitable for	Required drill hole diameter mm	Minimal drill hole depth mm	Order-No
C 9 N	100	410	3390 0357 00
C 12 N/W	100	610	3390 0429 00

Special Lubricant

Quantity/Tin	Order-No
0,25 kg	3391 0928 00
1,00 kg	3391 0942 00
30,00 kg	3391 0980 00

darda®

We've got the power.

Darda GmbH
Im Tal 1, D-78176 Blumberg
Fon + 49 (0) 77 02 / 43 91 - 0
Fax + 49 (0) 77 02 / 43 91 - 12
info@darda.de
www.darda.de

Our distributor :

SPLITTER C2-C12

Hydraulic rock and concrete splitters

- Splitting force up to 413 tons (4048 kn)
- Dust free
- Quiet performance
- Also applicable at places of difficult access
- Vibration free
- Easy handling
- Easy to transport
- Splits in seconds
- Controlled splitting
- Dimensionally accurate working

darda®

We've got the power.

QUEBRANTADORES HIDRÁULICOS

C2 C4 C9 C10 C12

El nombre DARDA simboliza competencia y experiencia en el desarrollo, la producción y la comercialización de herramientas hidráulicas de demolición especiales que no dañen el medio ambiente.

Funcionamiento

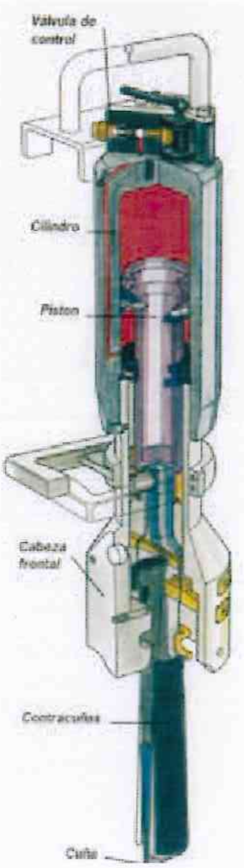

Los quebrantadores hidráulicos pueden sustituir a otros métodos de demolición, como las voladuras y el cemento expansivo.

Estos equipos se distiguen por su habilidad para quebrar roca y hormigón sin producir ondas de choque, vibraciones, polvo ni ruidos.

Su fuerza de quebrantación, que se controla fácilmente con una sola mano, es superior a las 413 toneladas.

Son equipos ligeros, con gran precisión y aptos para ser utilizados en espacios cerrados o lugares de difícil acceso.

Ventajas

- Fuerza de rotura de hasta 413 toneladas por unidad
- No produce polvo ni ruidos
- No produce vibraciones
- Aplicable en lugares de difícil acceso
- Facilidad de manejo
- Facilidad de transporte
- Produce la rotura en segundos
- Control de la dirección de rotura
- Precisión de trabajo

Datos técnicos

Modelo	Tipos de cuñas	Diámetro de barreno mm	Profundidad mínima del barreno mm	Distancia de quebrantación mm	Fuerza real de quebrantación kN / Ton.	Peso kg	Longitud del cilindro mm	Longitud del conjunto de cuñas mm
C 2 S	N	32	270	9	1913 / 195	18	745	140
C 4 S	N	35 - 38	430	10 - 40	2256 / 230	22	995	250
C 9	N	45 - 48	410	18 - 44	1962 / 200	22	1020	230
C 9	L	48 - 50	580	18 - 40	1962 / 200	23	1190	400
C 10 S	N	41 - 43	630	18 - 45	2551 / 260	32	1400	380
C 12	N	45 - 48	610	20 - 50	3507 / 358	31	1290	380
C 12	L	45 - 48	680	15 - 35	4048 / 413	32	1360	450

darda

QUEBRANTADORES HIDRÁULICOS

Proceso de quebrantación

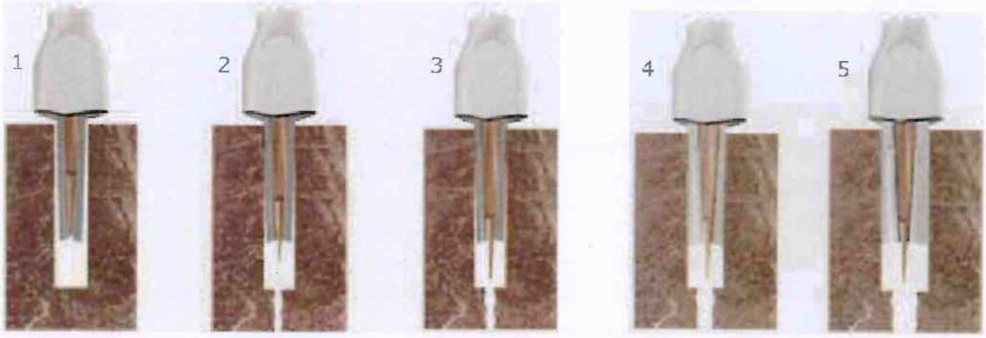

Con contracuñas estándar (pasos 1-3) y con contracuñas de ampliación (pasos 4-5)

Aplicaciones

Excavación y vaciado

Quebrantado y demolición de hormigón

Zanjeo

Túneles y galerías

Descabezamiento de pilotes

Canteras

Demoliciones submarinas

Demolición en interiores

Perforadoras de roca manuales RH, BBD y DKR

Herramientas que hacen el trabajo más rápido

Atlas Copco

Trabaje mejor, trabaje más rápido

¿Agobiado por la falta de tiempo? ¿Trabaja con frecuencia con un apretado calendario? Si es así, no deje de ver las perforadoras de roca de Atlas Copco. Los clientes nos dicen que una alta productividad es decisiva, así que hemos incorporado funciones que le ayudarán a trabajar más rápido.

Descarga de aire integrada

Vamos a comenzar, por ejemplo, por el barrido de aire integrado. Mientras perfora, el barreno se mantiene limpio gracias a un potente chorro de aire. Esto permite aumentar la productividad de dos modos. En primer lugar, acelera el proceso de perforación ya que la punta perfora sobre una superficie más limpia. En segundo lugar, al terminar de perforar, no tendrá que limpiar el agujero antes de la voladura.

Perforación de barrenos más sencilla

También hemos acelerado y simplificado el emboquille. Las perforadoras de Atlas Copco son potentes, pero esta potencia es fácil de manejar gracias a un control gradual de la puesta en marcha. Esto le ayudará a mantener la punta de la herramienta justo en el lugar que desea, desde el comienzo.

Estos son tan solo dos ejemplos entre otros muchos. Como puede apreciar el aumento de la productividad forma parte de nuestra filosofía de diseño. Si desea obtener más información, siga leyendo y descubra el modo en que las perforadoras de roca de Atlas Copco pueden ayudarle a trabajar más rápido.

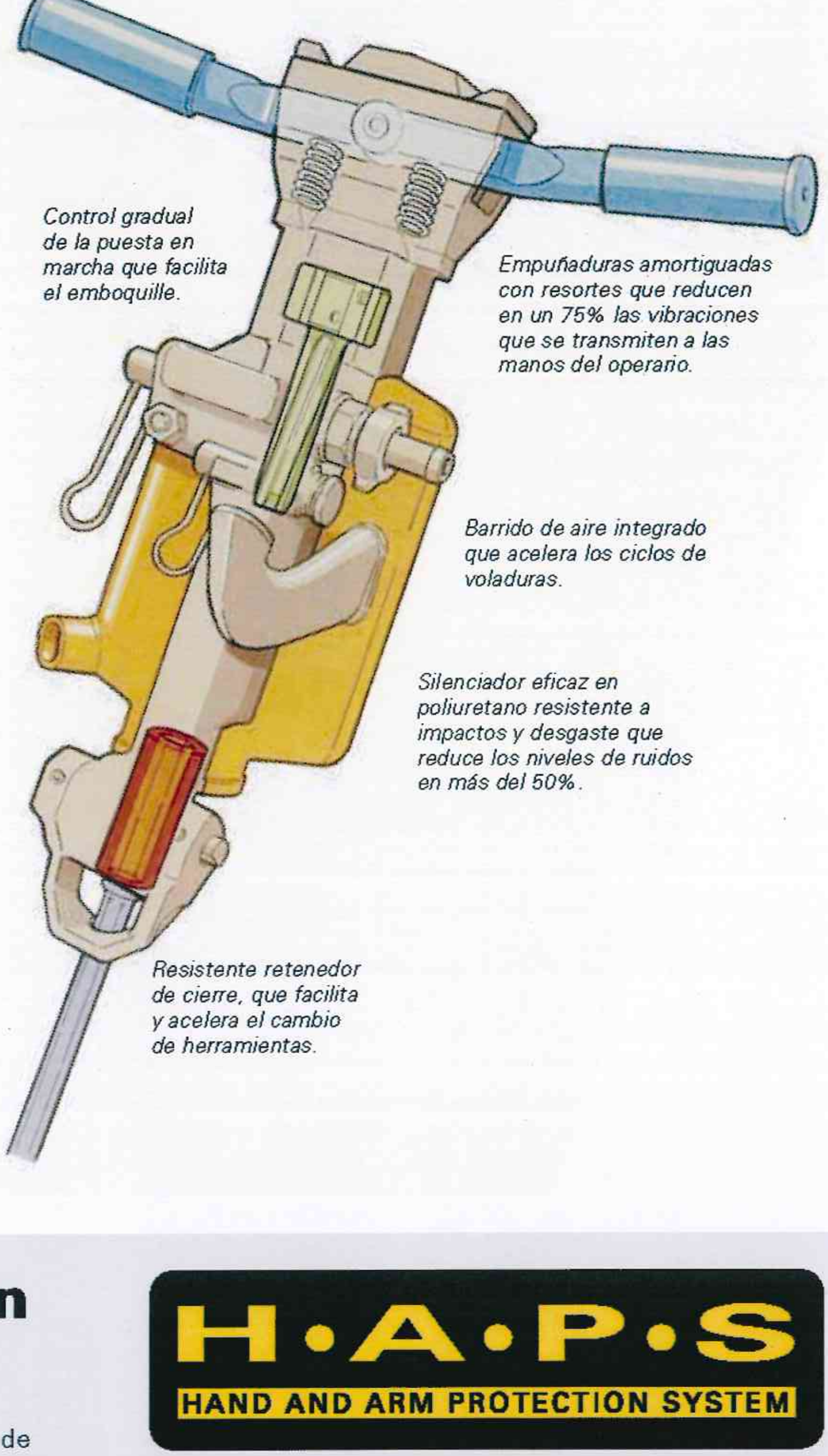

Niveles de vibración más bajos

Desarrollamos herramientas con niveles reducidos de vibración y sonido desde 1970. En la actualidad, somos líderes del sector y nuestras perforadoras con sistema de amortiguación de vibraciones satisfacen la última directiva europea de 2006 (2002/44/CE).

El exclusivo sistema de protección de manos y brazos (HAPS, Hand and Arm Protection System) le ayudará a reducir la exposición del operario a las vibraciones. Esto se traduce en una reducción del 75% de las vibraciones que se transmiten a las manos del operario. Además, nuestro sistema de amortiguación de sonido, reduce los ruidos de baja frecuencia más de un 50%.

H•A•P•S
HAND AND ARM PROTECTION SYSTEM

El exclusivo sistema de protección de manos y brazos (HAPS) de Atlas Copco le ayudará a reducir la exposición del operario a las vibraciones.

Perforadoras RH, para roca dura y grandes agujeros

Las perforadoras RH se han diseñado para trabajos más pesados como perforación secundaria y banqueo. También para la perforación en voladuras de esponjamiento.

Las perforadoras RH poseen un resistente mecanismo de rotación y una alta energía de impacto para la perforación en roca dura.

Dónde utilizarlas

- Perforación secundaria y banqueo, perforación para voladuras de esponjamiento
- RH 571 para trabajos ligeros
- RH 658 para perforación de barrenos más profundos

La perforada adecuada para su aplicación

La perforadora ligera RH 571 es perfecta para los trabajos más ligeros. La RH 658, un poco más pesada y potente, es adecuada para la perforación de barrenos más profundos. La RH 572E combina su poco peso con más confort parta el operario gracias a sus empuñaduras con sistema de amortiguación de vibraciones y su eficaz silenciador.

Todos los modelos están equipados con empuñaduras en T para poder agarrarlas con más fuerza y de un modo más cómodo.

- Barrido de aire integrado que acelera los ciclos de voladuras
- Control gradual de la puesta en marcha que facilita la perforación de agujeros
- Resistente retenedor de cierre, que facilita y acelera el cambio de herramientas
- Empuñaduras amortiguadas con resortes que reducen en un 75% las vibraciones
- Silenciador en poliuretano resistente a impactos y desgaste que reduce los niveles de ruidos en más del 50%

Datos técnicos

Modelo	Peso	Long.[1]	Consumo de aire a 6 bares	Buje porta-herramienta (hex)	Frecuencia de impacto	Velocidad de rotación	Velocidad de penetración	Conexión de manguera	Designación
	kg	mm	l/s	mm	impactos/min	rpm	mm/min	mm	
RH 572E	22,8	583	37	22x108	2040	170	260[2]	19	8311 0301 17
RH 571-5L	17,8	510	39	22x108	2100	190	295[2]	19	8311 0301 29
RH 571-5LS	18,9	510	39	22x108	1980	190	275[2]	19	8311 0301 37
RH 658L	24	565	58	22x108	2040	215	425[2]	19	8311 0302 86
RH 658LS	25	565	58	22x108	2040	215	410[2]	19	8311 0302 87

1) Incluye retenedor de herramienta
2) Perforación en granito con una barrena integral de 33 mm (a una presión de trabajo de 6 bares.)

Equipo opcional

Descripción	Designación
Manguera, 19 mm x 3 m completa con acoplamientos de garras y abrazaderas para la manguera	9030 2047 00

Perforadoras BBD, para trabajos más ligeros

Ligeras y fáciles de manejas, las perforadoras de roca BBD son ideales para trabajos rápidos o en zonas de difícil acceso. Se suministran equipadas con empuñaduras en T o en D.

La acción de la rueda de trinquete acelera la rotación y aumenta la frecuencia de impacto al perforar en roca blanda y semi-dura.

Dónde utilizarlas

- Empuñadura en D: Perforación horizontal de roca y hormigón, realización de orificios de desagüe
- Empuñadura en T: Trabajos en posición vertical en hormigón, perforación de agujeros, voladuras de esponjamiento y perforación de filones

La perforada adecuada para su aplicación

La perforadora ligera de roca BBD 12 está disponible en dos versiones. Una versión está equipada con una empuñadura en D que se utiliza principalmente en perforaciones horizontales, hasta una profundidad máxima de 1 metro en hormigón, y para la realización de agujeros de desagüe. La otra versión, equipada con empuñaduras en T, es la BBD 12T, y se ha diseñado para perforar en vertical hasta una profundidad máxima de 3 metros.

La perforadora BBD 15E, de peso medio, posee una "empuñadura combinada T/D" para facilitar su transporte. Ofrece una alta relación potencia-peso, además de una alta seguridad en su manejo. La BBD 15E está equipada con empuñaduras amortiguadas por resortes y un silenciador altamente eficaz.

La perforadora más grande BBD está disponible en una versión con accionamiento mediante palanca en la empuñadura, la BBD 15ET. Las máquinas más antiguas pueden actualizarse con un kit de conversión.

- Poco peso que facilita su manejo
- Barrido de aire integrado que acelera los ciclos de voladuras
- Control gradual de la puesta en marcha que facilita la perforación de agujeros
- Resistente retenedor de cierre, que facilita y acelera el cambio de herramientas
- Empuñaduras amortiguadas con resortes que reducen en un 75% las vibraciones
- Silenciador en poliuretano resistente a impactos y desgaste que reduce los niveles de ruidos en más del 50%

Datos técnicos

Modelo	Peso	Long.[1]	Consumo de aire a 6 bares	Buje porta-herramienta (hex)	Frecuencia de impacto	Velocidad de rotación	Velocidad de penetración	Conexión de manguera	Designación
	kg	mm	l/s	mm	impactos/min	rpm	mm/min	mm	
BBD 15E	15,5	575	22	19x108	2520	220	220[3]	19	8311 0104 02
BBD 15E	15,5	575	22	22x108	2520	220	220[3]	19	8311 0104 10
BBD 15ET	15,6	575	22	19x108	2520	220	220[3]	16	8311 0104 12
BBD 15ET	15,6	575	22	22x108	2520	220	220[3]	16	8311 0104 13
BBD 12T-01	11,1	505	24	22x108	2580	220	150[3]	19	8311 0102 95
BBD 12TS-01	12,1	505	22	22x108	2520	220	150[3]	19	8311 0102 98
Horizontal									
BBD 12D	9,8	565	24	19x108	2580	220	250[2]	13	8311 0102 47
BBD 12DS	10,7	565	22	19x108	2520	220	230[2]	13	8311 0102 80

1) Incluye retenedor de herramienta
2) Perforación en granito con una barrena integral de 28 mm (a una presión de trabajo de 6 bares.)
3) Perforación en granito con una barrena integral de 33 mm (a una presión de trabajo de 6 bares.)

Equipo opcional

Descripción	Designación
Manguera, 13 mm x 3 m completa con acoplamientos de garras y abrazaderas para la manguera	9030 2066 00
Manguera, 16 mm x 3 m completa con acoplamientos de garras y abrazaderas para la manguera	9030 2046 00
Manguera, 19 mm x 3 m completa con acoplamientos de garras y abrazaderas para la manguera	9030 2047 00
Kit de conversión de BBD 15E a BBD 15ET	8311 0104 95

Perforación más rápida y costes de perforación más bajos

Los equipos perforación con barrenas cónicas ofrecen numerosas ventajas frente a las de acero integral. La primera y más importante es que la velocidad de penetración es más rápida, hasta un 50% en algunos tipos de roca. Las barrenas cónicas son también más fáciles de utilizar: el emboquille es más rápido, la perforación de agujeros rectos es más sencilla y el nivel de vibraciones es considerablemente más bajo. Y, quizás, lo mejor de todo, es que las herramientas cónicas reducen los gastos totales de perforación. ¿Aún no está convencido? Haga una prueba y juzgue por sí mismo.

Reducción de polvo en el lugar de trabajo y aumento de la productividad

El polvo que genera la perforación oscurece la visión y supone un riesgo para la salud. El colector de polvo DCT reduce la cantidad de polvo generado en el entorno de trabajo. También aumenta la productividad ya que continuamente se eliminan los residuos que se generan durante la perforación. El colector de polvo DCT puede utilizarse con toda la gama de perforadoras neumáticas de mano de Atlas Copco.

El colector de polvo DCT funciona sobre la base del principio de eyección, que crea una subpresión en todo el sistema de filtros. Ya que el eyector está integrado en la unidad de filtro, no puede dañarse por causas externas o por el polvo generado durante la perforación.

Datos técnicos

Modelo	Presión máx. de aire	Requisitos de aire del eyector	Capacidad de succión	Área de filtrado	Peso total	Manguera de succión	Designación
	bars	*l/s*	*l/s*	*m²*	*kg*	*mm*	
DCT 10	7	9.5	47	1.3	22	38	8092 0407 84

Equipo opcional

Descripción	Designación
Bolsas (25 uds.)	3217 0578 91

Ligereza y gran potencia de impacto

La DKR 36 es una herramienta neumática de función dual cinceladora/perforadora que pesa tan solo 4 kilos.

Es una máquina que perfora con gran potencia. A pesar de su poco peso y de su tamaño compacto, podrá trabajar más rápido – hasta dos y tres veces más – que con una perforadora eléctrica similar. También es mucho más resistente y no se quemará cuando la empuje con fuerza.

Dos en una

Esta máquina de función dual puede utilizarse tanto para cincelar, como para perforar. El cambio entre los distintos modos es sencillo: solo tendrá cambiar el cincel por una barrena y la DKR36 cambiará automáticamente a la función de perforación.

Dónde utilizarla

- Trabajos generales de cincelado y rebaje
- Perforación de agujeros con un diámetro de 8-38 mm
- Perforación de agujeros con una profundidad máxima de 300 mm
- Material: hormigón o ladrillo, paredes y techos para entubado de cables e instalación de conductos de ventilación
- Partición de rocas mediante cuñas/contracuñas
- Perforación subacuática

- Más productiva que una cinceladora/perforadora eléctrica
- Potente y ligera
- Dos funciones en la misma máquina
- Engrasador integrado que facilita su mantenimiento
- Portaherramientas de acoplamiento rápido que acelera los cambios de herramienta

Datos técnicos

Modelo	Peso	Long.	Consumo de aire a 6 bares	Buje porta-herramientas	Frecuencia de impacto	Velocidad de rotación	Velocidad de penetración	Conexión de manguera	Designación
	kg	*mm*	*l/s*	*mm*	*impactos/min*	*rpm*	*mm/min*	*mm*	
DKR 36	4,5	375	10	R19xH14,7x89	2820	250	180[1] / 160[2]	19	8463 0103 60
DKR 36R	4,5	375	10	R19x95	2820	250	180[1] / 160[2]	19	8463 0103 50

1) Barrena de 19 mm en granito
2) Barrena de 19 mm en hormigón

Equipo opcional

Descripción	Designación
Kit DKR 36	8463 0103 61
Contenido del kit:	
Maletín metálico	3315 1449 00
DKR 36	8463 0103 60
Lubricador neumático Air-Oil (0,2 l)	8099 0202 40
Manguera, 10 mm x 3 m completa con acoplamiento de garra y acoplamiento rápido con boquilla	9030 2042 00
Adaptador para barrenas de 8, 10, 12 mm	0701 1001 32
Útil de extracción para barrenas de 8, 10, 12 mm	3085 0210 00
Cincel plano	3083 3045 00
Juego de piezas de repuesto (17 bolas de acero)	3315 1294 00

La DKR 36 puede suministrarse con un resistente y práctico maletín de transporte metálico, con un set completo de manguera y accesorios. El peso total de este kit es de 10 kg.

Siempre se deben utilizar piezas originales. Cualquier fallo o defecto originado por la utilización de piezas no originales produce la consecuente pérdida de garantía.

www.atlascopco.com

8 APPENDIX II TENTATIVE CORRECTION OF THE ON SITE ANALYSES DATA. ISOLINES GRAPHS

APPENDIX II TENTATIVE CORRECTION OF ON SITE ANALYSES DATA. ISOLINES GRAPHS

Table AII-1: Tentative correction of the on site values in cross section A1-25

Sample	Coordinates		Water content (%) mean	Dry density (g/cm^3) mean	Degree of saturation %
	X	Y			
B-S-A1_25-001	-42	93	37.5	1.33	98
B-S-A1_25-002	-50	82	36.5	1.28	89
B-S-A1_25-003	-65	75	37.3	1.32	96
B-S-A1_25-004	-88	65	38.6	1.29	95
B-S-A1_25-005	-102	55	38.9	1.32	100
B-S-A1_25-006	-125	50	41.0	1.26	97
B-S-A1_25-007	-140	45	42.0	1.26	99
B-S-A1_25-008	-30	167	33.7	1.44	104
B-S-A1_25-009	-56	182	32.9	1.44	101
B-S-A1_25-010	-83	197	33.1	1.41	98
B-S-A1_25-011	-95	204	33.2	1.4	97
B-S-A1_25-012	-105	211	34.0	1.37	94
B-S-A1_25-013	0	70	34.6	1.36	95
B-S-A1_25-014	0	50	36.0	1.3	90
B-S-A1_25-015	0	30	36.1	1.33	95
B-S-A1_25-018	49	107	38.8	1.32	100
B-S-A1_25-019	57	100	36.8	1.36	101
B-S-A1_25-020	67	90	35.5	1.35	96
B-S-A1_25-021	83	80	36.1	1.39	103
B-S-A1_25-022	100	70	36.8	1.4	107
B-S-A1_25-023	125	60	37.0	1.37	103
B-S-A1_25-024	140	50	38.6	1.28	94
B-S-A1_25-025	38	174	33.8	1.42	101
B-S-A1_25-026	53	181	32.4	1.43	99
B-S-A1_25-027	69	188	32.8	1.43	100
B-S-A1_25-028	78	191	33.5	1.42	100
B-S-A1_25-029	86	195	32.5	1.42	97
B-S-A1_25-030	97	198	31.9	1.43	97
B-S-A1_25-031	109	207	33.7	1.39	96
B-S-A1_25-032	0	178	33.0	1.43	100
B-S-A1_25-033	0	211	32.1	1.46	102
B-S-A1_25-034	0	252	32.8	1.46	104

Table AII-2: Tentative correction of the on site values in cross section B1

Sample	Coordinates		Water content (%) mean	Dry density (g/cm^3) mean	Degree of saturation %
	x	y			
B-S-B1-001	-37	92	38.6	1.36	105
B-S-B1-002	-49	86	39.5	1.29	98
B-S-B1-003	-64	77	38.3	1.32	99
B-S-B1-004	-80	66	38.9	1.31	99
B-S-B1-005	-96	57	41.5	1.27	99
B-S-B1-006	-110	49	44.7	1.20	97
B-S-B1-007	-123	45	46.9	1.19	100
B-S-B1-008	-139	43	47.6	1.18	100
B-S-B1-009	51	120	38.1	1.35	103
B-S-B1-010	63	110	37.7	1.32	97
B-S-B1-011	75	102	38.6	1.32	100
B-S-B1-012	91	90	40.6	1.28	99
B-S-B1-013	109	74	40.9	1.27	98
B-S-B1-014	129	61	42.7	1.25	100
B-S-B1-015	144	54	43.6	1.48	142
B-S-B1-016	-29	168	35.0	1.39	101
B-S-B1-017	-37	178	33.9	1.40	99
B-S-B1-018	-44	188	34.0	1.40	99
B-S-B1-019	-52	199	33.8	1.38	96
B-S-B1-020	-60	211	33.6	1.41	99
B-S-B1-021	-67	222	33.9	1.40	98
B-S-B1-022	-71	232	34.3	1.39	98
B-S-B1-023	0	67.5	34.8	1.39	100
B-S-B1-024	0	47.5	34.8	1.37	97
B-S-B1-025	0	25	35.8	1.38	101
B-S-B1-026	41	162	35.8	1.37	99
B-S-B1-027	50	173	34.3	1.35	93
B-S-B1-028	58	186	33.7	1.41	99
B-S-B1-029	68	196	33.5	1.40	98
B-S-B1-030	75	196	33.0	1.43	100
B-S-B1-031	81	214	33.1	1.43	101
B-S-B1-032	88	225	34.4	1.38	97
B-S-B1-033	0	176	34.5	1.43	106
B-S-B1-034	0	212	33.5	1.42	100
B-S-B1-035	0	246	33.7	1.43	102

Table AII-3: Tentative correction of the on site values in cross section E

Sample	Coordinates		Water content (%) mean	Dry density (g/cm^3) mean	Degree of saturation %
	x	y			
B-S-E-001	51	112	38.1	1.33	101
B-S-E-002	62	104	36.2	1.36	100
B-S-E-003	72	95	36.2	1.31	92
B-S-E-004	85	83	37.7	1.36	103
B-S-E-005	100	70	38.5	1.32	100
B-S-E-006	115	56	41.7	1.28	101
B-S-E-007	128	45	46.6	1.20	100
B-S-E-008	143	23	49.0	1.14	97
B-S-E-009	-54	111	38.5	1.28	94
B-S-E-010	-64.5	101	37.6	1.34	100
B-S-E-011	-76	92	36.7	1.33	96
B-S-E-012	-87	81	37.6	1.33	98
B-S-E-013	-96	73	40.8	1.25	96
B-S-E-014	-106	63	42.8	1.25	100
B-S-E-015	-117	46	46.3	1.20	100
B-S-E-016	-133	25	52.3	1.12	99
B-S-E-017	-67	128	38.1	1.36	104
B-S-E-018	-89	128	36.2	1.35	98
B-S-E-019	-112	127	36.2	1.34	96
B-S-E-020	-135	127	36.1	1.35	98
B-S-E-021	55	127	37.6	1.34	100
B-S-E-022	79.5	127.5	36.5	1.35	99
B-S-E-023	105	128	35.8	1.32	93
B-S-E-024	132	128.5	35.9	1.35	97
B-S-E-025	49	143	35.8	1.38	101
B-S-E-026	58	150	34.8	1.38	98
B-S-E-027	69	159	34.3	1.38	97
B-S-E-028	81	169	35.7	1.37	100
B-S-E-029	96	178	35.9	1.37	100
B-S-E-030	106	190	35.3	1.40	102
B-S-E-031	-45.5	159	35.4	1.43	107
B-S-E-032	-57	170	35.6	1.37	99
B-S-E-033	-71	185	35.4	1.37	98
B-S-E-034	-80	195	34.8	1.38	98
B-S-E-035	-89	202	35.0	1.40	101
B-S-E-036	-99	213	35.9	1.37	100
B-S-E-037	0	180	36.5	1.35	98
B-S-E-038	0	203	35.0	1.36	96
B-S-E-039	0	219	33.9	1.40	98
B-S-E-040	0	240	34.4	1.37	96
B-S-E-041	0	67.5	33.0	1.42	99
B-S-E-042	0	47.5	33.8	1.33	89
B-S-E-043	0	25	35.6	1.38	100

Table AII-4: Tentative correction of the on site values in cross section B2

Sample	Coordinates		Water content (%) mean	Dry density (g/cm^3) mean	Degree of saturation %
	x	y			
B-S-B2-001	48	101	40.2	1.27	96
B-S-B2-002	58	95	39.0	1.31	99
B-S-B2-003	67	85	39.0	1.31	99
B-S-B2-004	82	75	39.1	1.33	102
B-S-B2-005	102	62	42.0	1.27	100
B-S-B2-006	119	50	45.0	1.22	99
B-S-B2-007	129	40	46.1	1.18	97
B-S-B2-008	55	127	38.3	1.33	100
B-S-B2-009	70	127	36.9	1.33	97
B-S-B2-010	90	127	37.0	1.33	97
B-S-B2-011	115	127	38.7	1.29	96
B-S-B2-012	140	127	41.5	1.27	99
B-S-B2-013	-47	99	40.4	1.31	103
B-S-B2-014	-56	91	38.9	1.32	101
B-S-B2-015	-70	79	39.1	1.32	101
B-S-B2-016	-82	69	39.9	1.31	101
B-S-B2-017	-94	59	40.8	1.29	100
B-S-B2-018	-104	49	50.8	1.19	108
B-S-B2-019	-114	39	48.6	1.20	105
B-S-B2-020	-124	29	51.5	1.14	102
B-S-B2-021	-53	127.5	37.3	1.32	96
B-S-B2-022	-69	127	37.5	1.31	96
B-S-B2-023	-91	127	39.5	1.32	103
B-S-B2-024	-111	128	38.6	1.34	103
B-S-B2-025	-134	127	39.1	1.31	100
B-S-B2-026	46	166	35.4	1.37	99
B-S-B2-027	59	175	34.4	1.39	99
B-S-B2-028	71	185	34.0	1.39	97
B-S-B2-029	86	197	34.9	1.40	101
B-S-B2-030	99	212	34.1	1.38	97
B-S-B2-031	-35	168	36.7	1.38	103
B-S-B2-032	-45	176	36.0	1.36	99
B-S-B2-033	-55	186	35.9	1.36	99
B-S-B2-034	-65	199	36.5	1.35	98
B-S-B2-035	-75	214	36.4	1.36	100
B-S-B2-036	0	177	34.7	1.38	99
B-S-B2-037	0	197	34.2	1.39	98
B-S-B2-038	0	211	34.2	1.44	105
B-S-B2-039	0	229	34.1	1.45	107
B-S-B2-040	0	246	34.5	1.39	99
B-S-B2-041	0	67.5	35.3	1.36	97
B-S-B2-042	0	47.5	34.9	1.36	95
B-S-B2-043	0	25	36.5	1.35	99

Table AII-5: Tentative correction of the on site values in cross section A2

Sample	Coordinates		Water content (%) mean	Dry density (g/cm^3) mean	Degree of saturation %
	x	y			
B-S-A2-001	49	113	41.5	1.28	101
B-S-A2-002	69	105	38.6	1.32	100
B-S-A2-003	89	95	39.7	1.29	98
B-S-A2-004	102	87	39.0	1.32	101
B-S-A2-005	115	79	41.8	1.26	99
B-S-A2-006	127	64	45.1	1.20	97
B-S-A2-007	147	44	48.0	1.17	99
B-S-A2-008	-48	113	42.2	1.23	96
B-S-A2-009	-66	105	40.0	1.28	98
B-S-A2-010	-82	95	40.1	1.28	97
B-S-A2-011	-95	86	40.8	1.27	97
B-S-A2-012	-111	75	47.2	1.19	100
B-S-A2-013	-126	63	49.5	1.14	98
B-S-A2-014	-141	52	50.4	1.13	98
B-S-A2-015	55	127	38.4	1.33	101
B-S-A2-016	72	127	37.3	1.36	102
B-S-A2-017	95	127	37.6	1.32	97
B-S-A2-018	115	127	39.6	1.27	95
B-S-A2-019	138	127	40.3	1.29	100
B-S-A2-020	-55	127	38.6	1.31	98
B-S-A2-021	-74	127	37.8	1.34	101
B-S-A2-022	-95	127	39.5	1.31	101
B-S-A2-023	-118	127	38.5	1.30	97
B-S-A2-024	-135	127	39.4	1.30	100
B-S-A2-025	35	165	35.9	1.37	100
B-S-A2-026	47	177	34.7	1.39	99
B-S-A2-027	63	187	35.5	1.38	101
B-S-A2-028	79	201	36.1	1.38	102
B-S-A2-029	95	211	36.9	1.36	102
B-S-A2-030	-32	169	36.2	1.37	100
B-S-A2-031	-42	179	35.7	1.37	99
B-S-A2-032	-52	190	34.7	1.39	99
B-S-A2-033	-65	201	35.2	1.38	99
B-S-A2-034	-77	211	36.8	1.35	99
B-S-A2-035	0	182	34.5	1.39	98
B-S-A2-036	0	196	33.5	1.38	95
B-S-A2-037	0	210	33.6	1.38	94
B-S-A2-038	0	228	33.7	1.41	100
B-S-A2-039	0	245	35.4	1.37	98

Table AII-6: Tentative correction of the on site values in longitudinal section Y 44-54

ID sample number	Coordinates		Water content (%) mean	Dry density (g/cm^3) mean	Degree of saturation %
	x	z			
6_A1_25	-125	320	41.0	1.26	97
14_A1_25	0	320	36.0	1.3	90
24_A1_25	140	320	38.6	1.28	94
6_B1	-110	401	44.7	1.20	97
15_B1	144	401	43.6	1.48	142
24_B1	0	401	34.8	1.37	97
7_E	128	520	46.6	1.20	100
15_E	-117	520	46.3	1.20	100
42_E	0	520	33.8	1.33	89
6_B2	119	647	45.0	1.22	99
20_B2	-124	647	51.5	1.14	102
42_B2	0	647	34.9	1.36	95
7_A2	147	681	48.0	1.17	99
14_A2	-141	681	50.4	1.13	98

Table AII-7: Tentative correction of the on site values in longitudinal section Y 66-129

ID sample number	Coordinates		Water content (%) mean	Dry density (g/cm^3) mean	Degree of saturation %
	x	z			
3_A1_25	-65	320	37.3	1.32	96
13_A1_25	0	320	34.6	1.36	95
22_A1_25	100	320	36.8	1.4	107
5_E	100	520	38.5	1.32	100
13_E	-96	520	40.8	1.25	96
41_E	0	520	33.0	1.42	99
4_B2	82	647	39.1	1.33	102
16_B2	-82	647	39.9	1.31	101
41_B2	0	647	35.3	1.36	97
4_B1	-80	401	38.9	1.31	99
13_B1	109	401	40.9	1.27	98
23_B1	0	401	34.8	1.39	100
5_A2	115	681	41.8	1.26	99
12_A2	-111	681	47.2	1.19	100

Table AII-8: Tentative correction of the on site values in longitudinal section Y 127-129

ID sample number	Coordinates		Water content (%) mean	Dry density (g/cm^3) mean	Degree of saturation %
	x	z			
17_E	-67	520	38.10	1.36	104
18_E	-89	520	36.22	1.35	98
19_E	-112	520	36.18	1.34	96
20_E	-135	520	36.14	1.35	98
21_E	55	520	37.56	1.34	100
22_E	79.5	520	36.53	1.35	99
23_E	105	520	35.76	1.32	93
24_E	132	520	35.93	1.35	97
8_B2	55	647	38.3	1.33	100
9_B2	70	647	36.9	1.33	97
10_B2	90	647	37.0	1.33	97
11_B2	115	647	38.7	1.29	96
12_B2	140	647	41.5	1.27	99
21_B2	-53	647	37.3	1.32	96
22_B2	-69	647	37.5	1.31	96
23_B2	-91	647	39.5	1.32	103
24_B2	-111	647	38.6	1.34	103
25_B2	-134	647	39.1	1.31	100
15_A2	55	681	38.4	1.33	101
16_A2	72	681	37.3	1.36	102
17_A2	95	681	37.6	1.32	97
18_A2	115	681	39.6	1.27	95
19_A2	138	681	40.3	1.29	100
20_A2	-55	681	38.6	1.31	98
21_A2	-74	681	37.8	1.34	101
22_A2	-95	681	39.5	1.31	101
23_A2	-118	681	38.5	1.30	97
24_A2	-135	681	39.4	1.30	100

Table AII-9: Tentative correction of the on site values in longitudinal section Y 175-185

ID sample number	Coordinates		Water content (%) mean	Dry density (g/cm^3) mean	Degree of saturation %
	x	z			
9_A1_25	-56	320	32.9	1.44	101
26_A1_25	53	320	32.4	1.43	99
32_A1_25	0	320	33.0	1.43	100
29_E	96	520	35.9	1.37	100
33_E	-71	520	35.4	1.37	98
37_E	0	520	36.5	1.35	98
27_B2	59	647	34.4	1.39	99
32_B2	-45	647	36.0	1.36	99
36_B2	0	647	34.7	1.38	99
17_B1	-37	401	33.9	1.40	99
27_B1	50	401	34.3	1.35	93
33_B1	0	401	34.5	1.43	106
26_A2	47	681	34.7	1.39	99
31_A2	-42	681	35.7	1.37	99
35_A2	0	681	34.5	1.39	98

Table AII-10: Tentative correction of the on site values in longitudinal section Y 190-210

ID sample number	Coordinates		Water content (%) mean	Dry density (g/cm^3) mean	Degree of saturation %
	x	z			
11_A1_25	-95	320	33.2	1.4	97
30_A1_25	97	320	31.9	1.43	97
33_A1_25	0	320	32.1	1.46	102
30_E	106	520	35.3	1.40	102
35_E	-89	520	35.0	1.40	101
38_E	0	520	35.0	1.36	96
34_B2	-65	647	36.5	1.35	98
38_B2	0	647	34.2	1.44	105
20_B1	-60	401	33.6	1.41	99
30_B1	75	401	33.0	1.43	100
28_A2	79	681	36.1	1.38	102
33_A2	-65	681	35.2	1.38	99
37_A2	0	681	33.6	1.38	94

Figure AII-1: Water content (%). Cross section A1-25

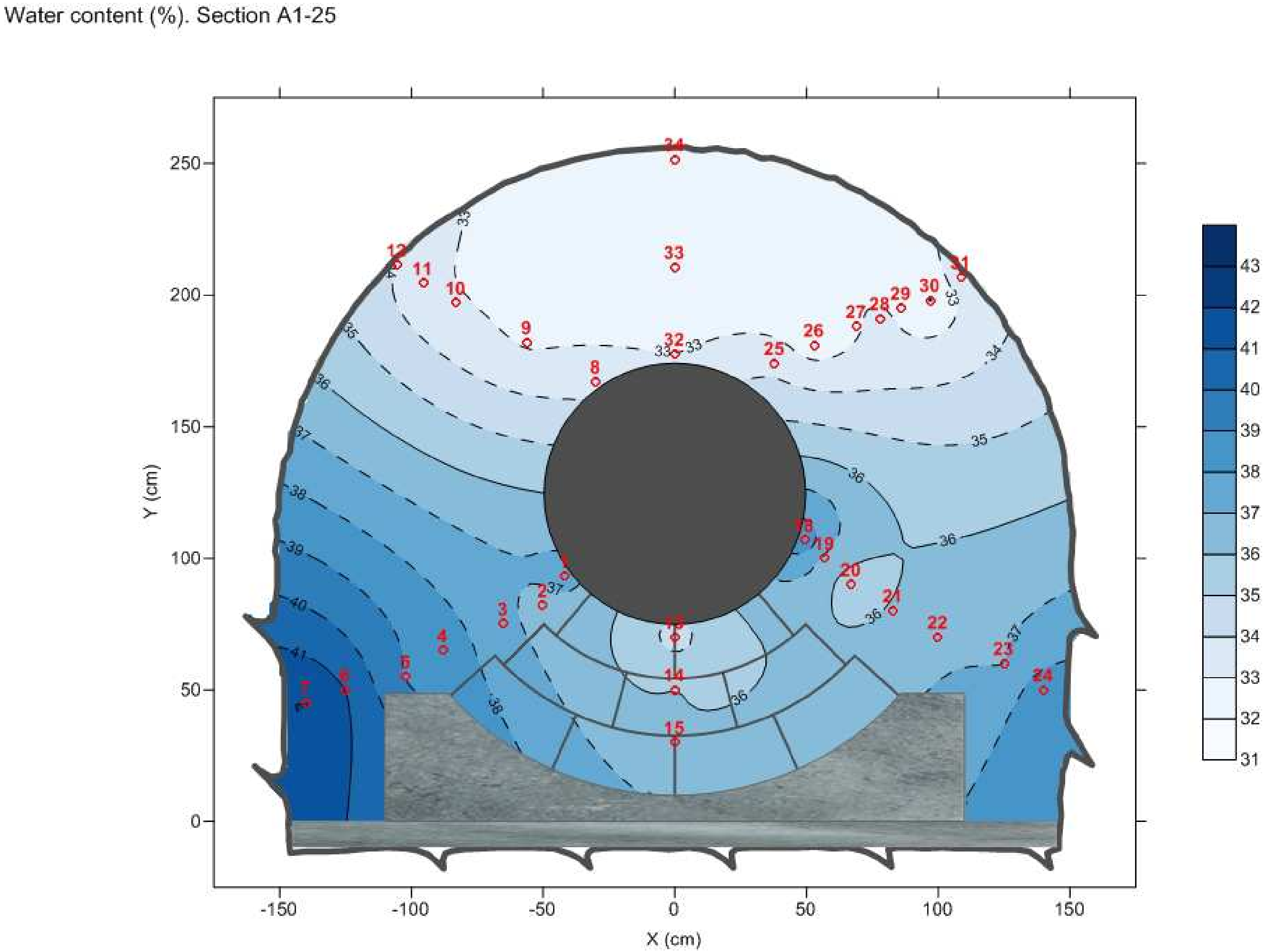

Figure AII-2: Water content (%). Cross section B1

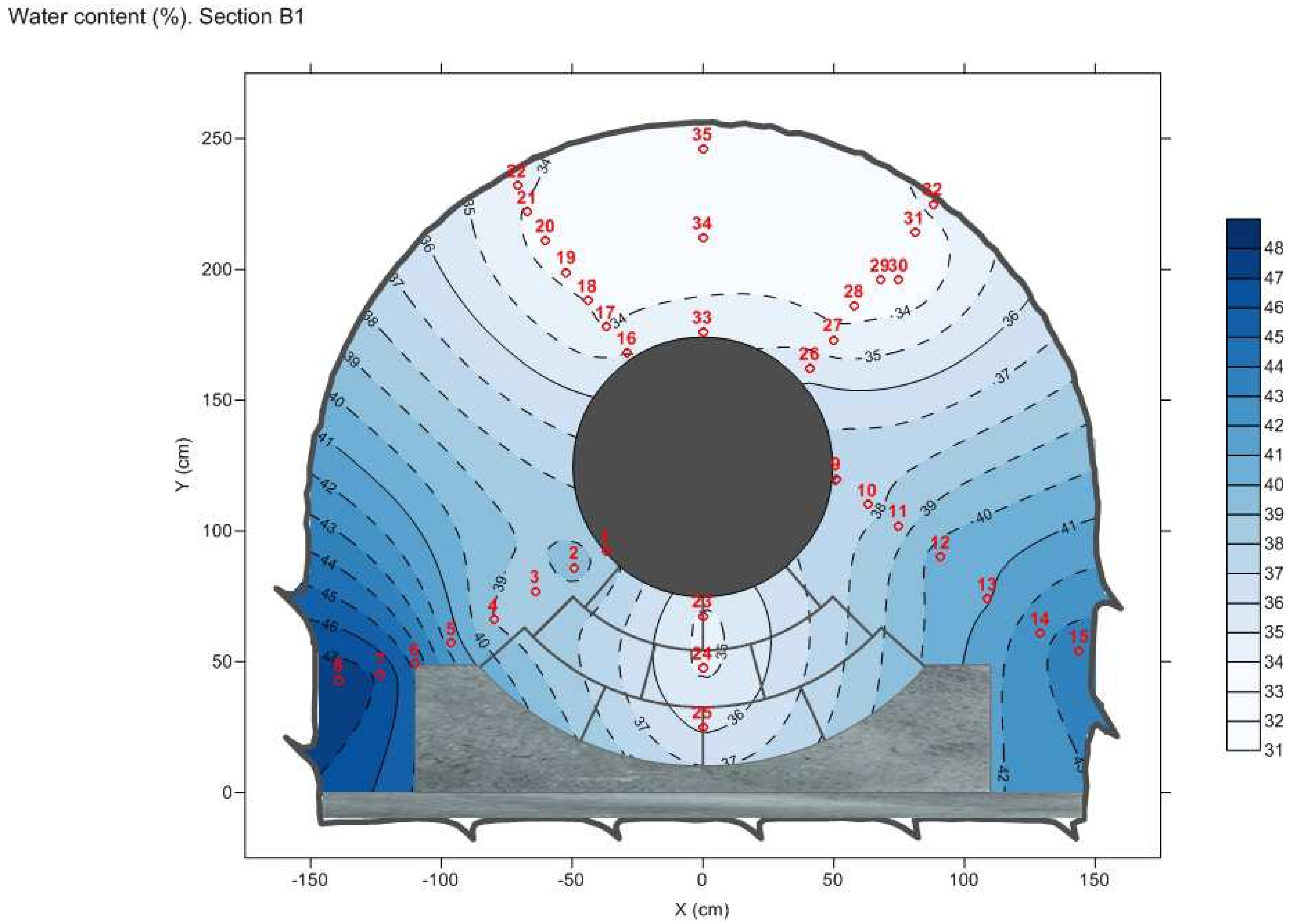

Figure AII-3: Water content (%). Cross section E

Water content (%). Section E

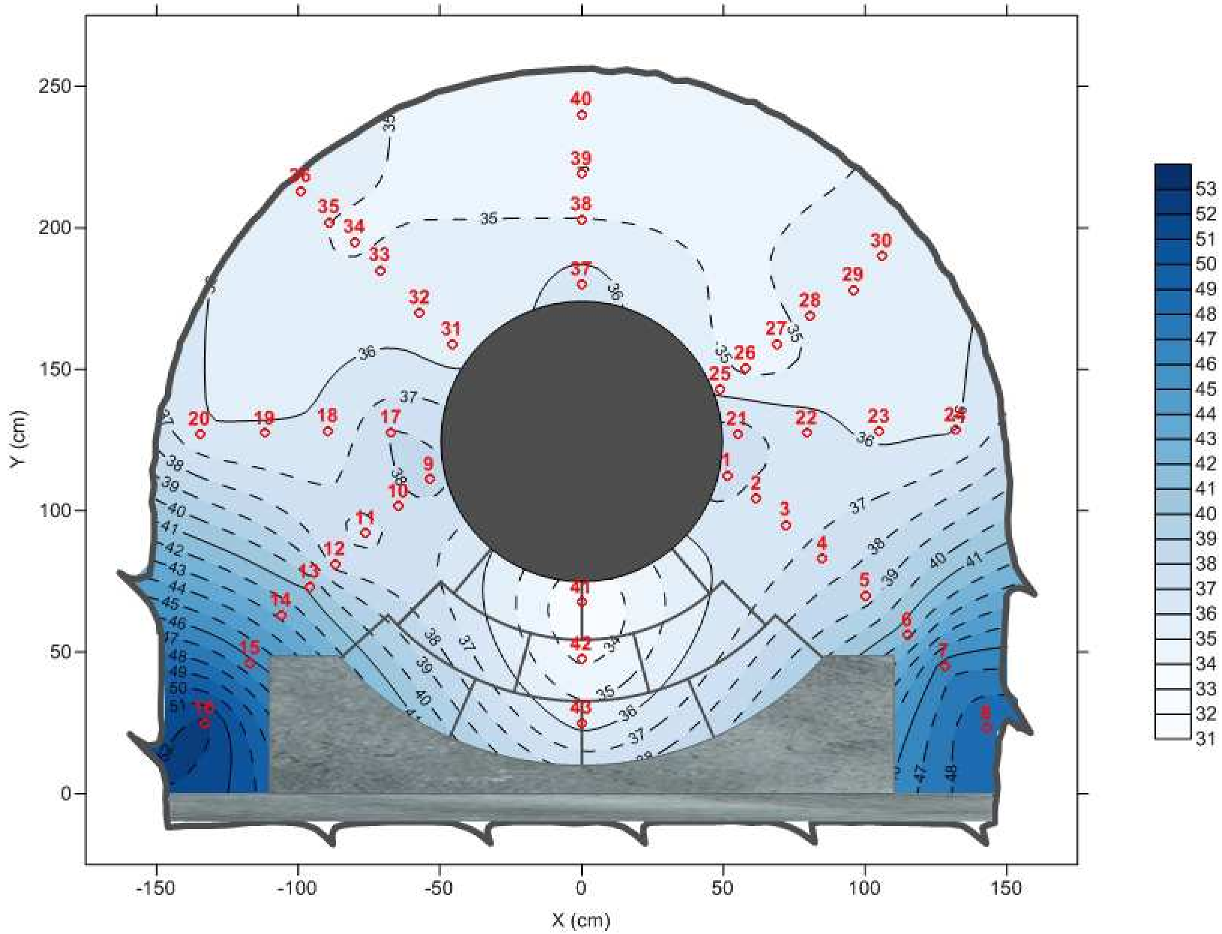

Figure AII-4: Water content (%). Cross section B2

Water content (%). Section A2

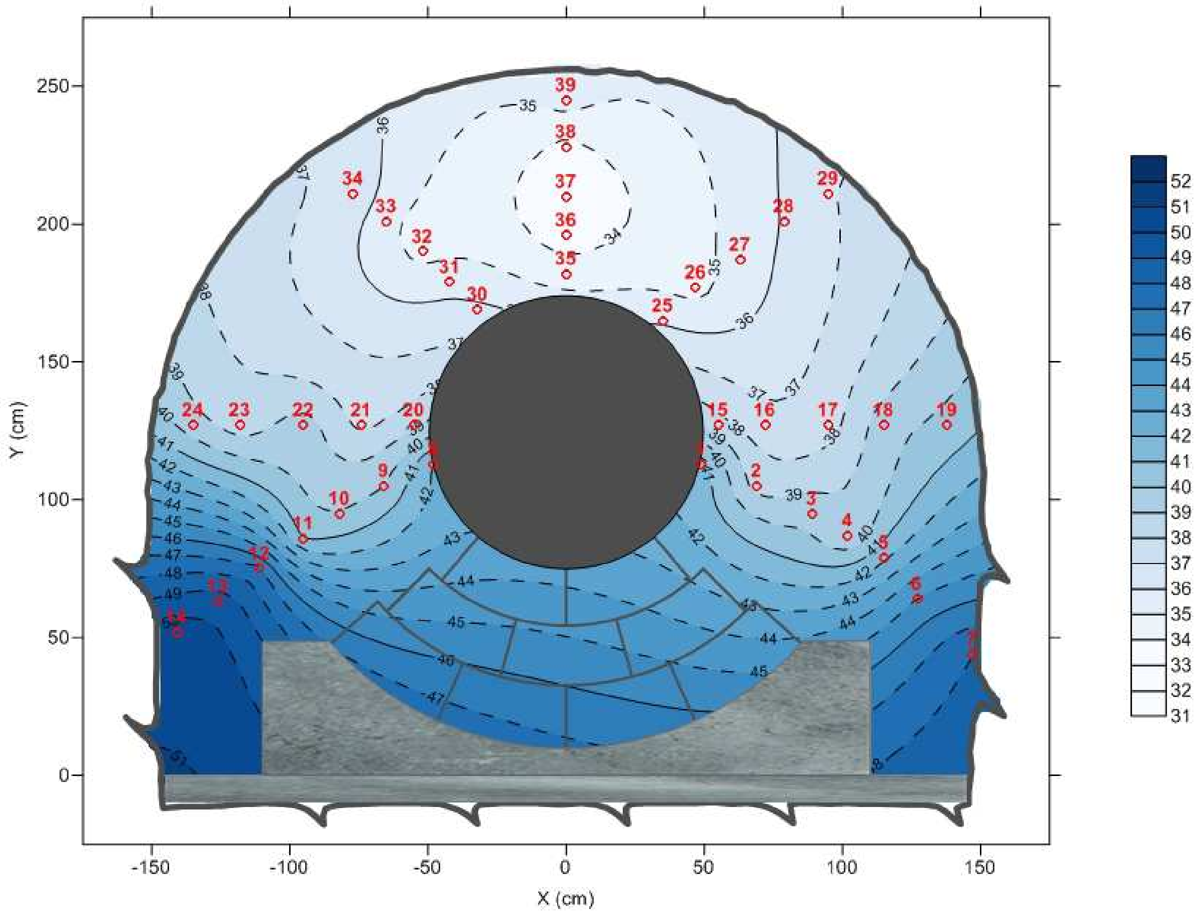

Figure AII-5: Water content (%). Cross section A2

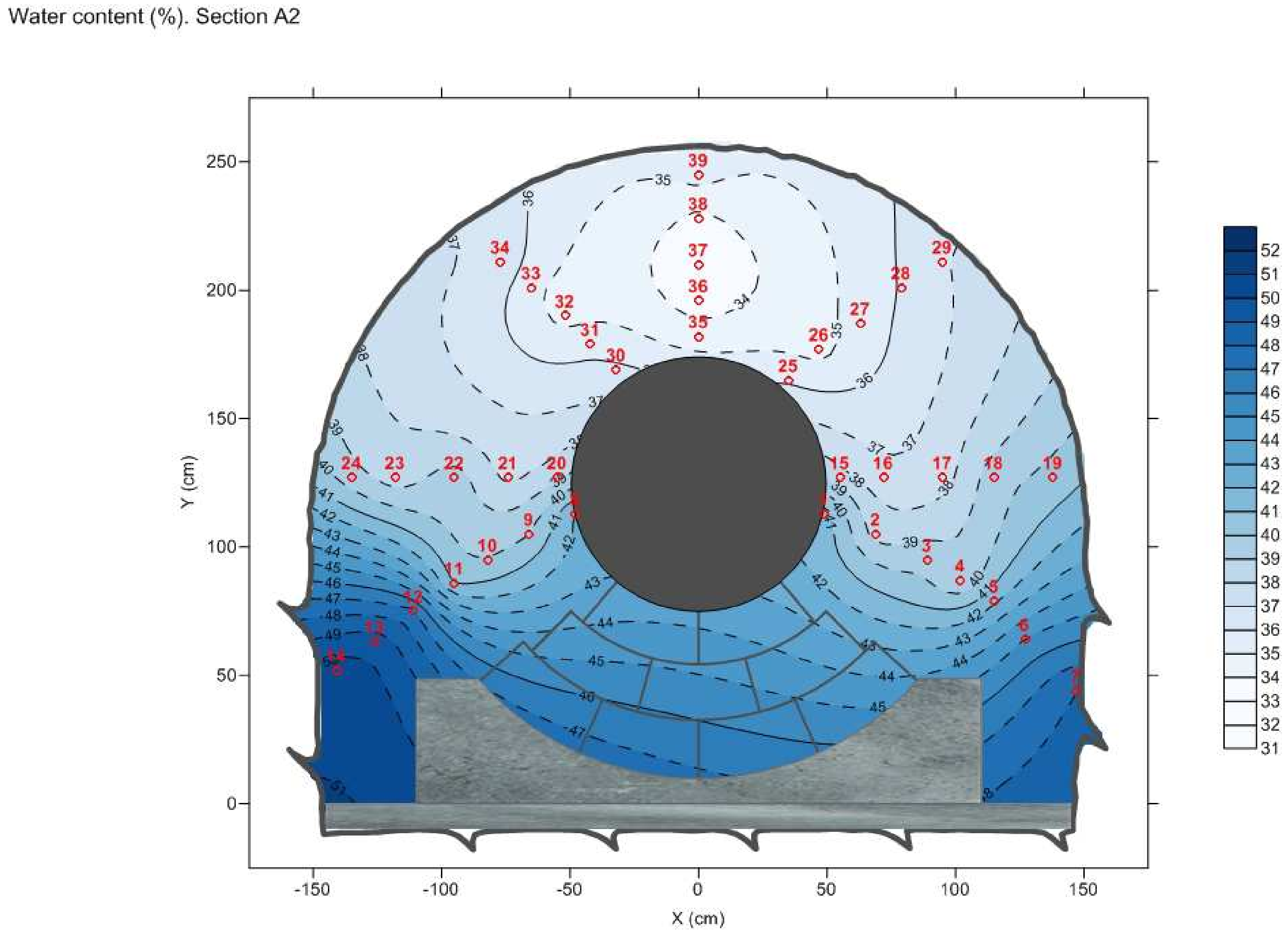

Figure AII-6: Dry density (g/cm3) Cross section A1-25

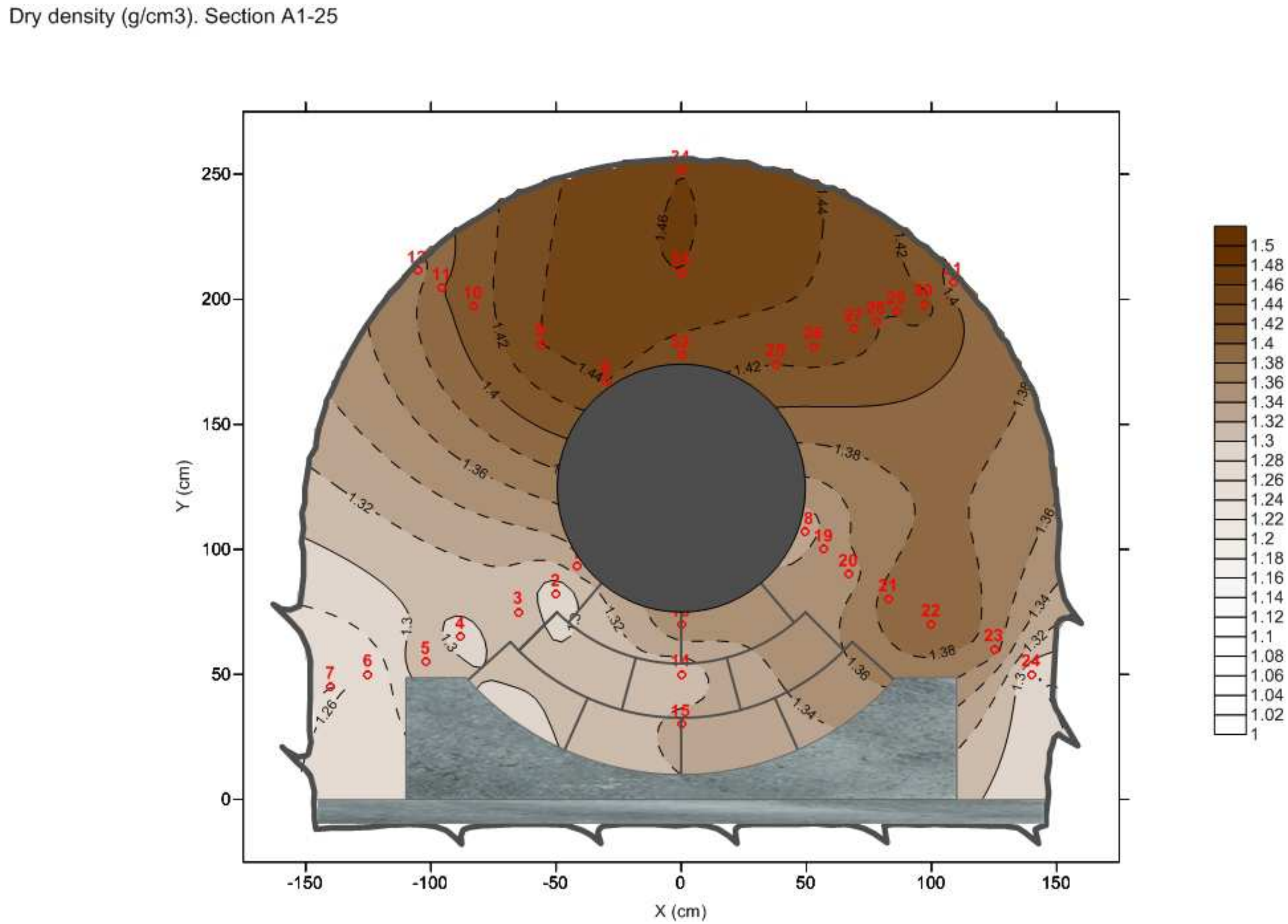

Figure AII-7: Dry density (g/cm3) Cross section B1

Dry density (g/cm3). Section B1

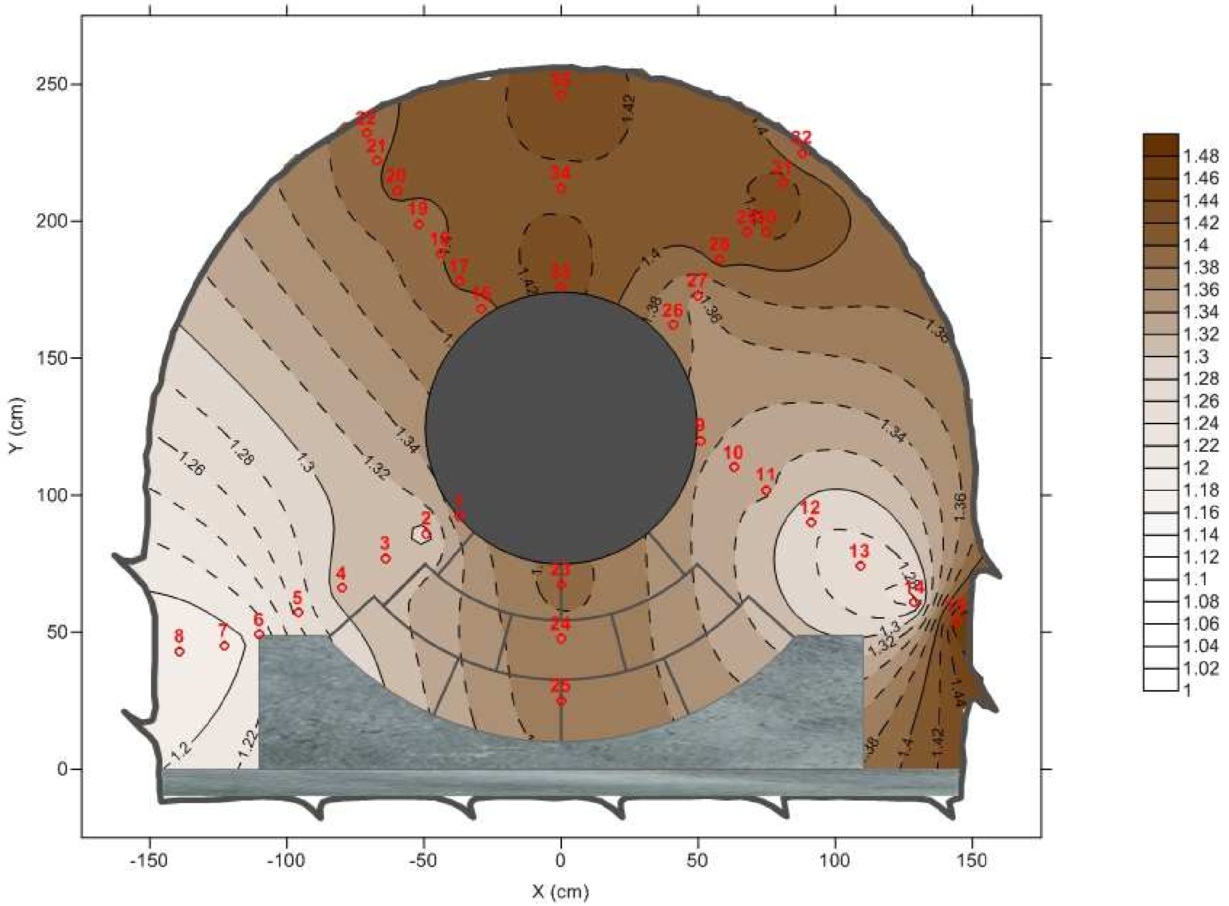

Figure AII-8: Dry density (g/cm3) Cross section E

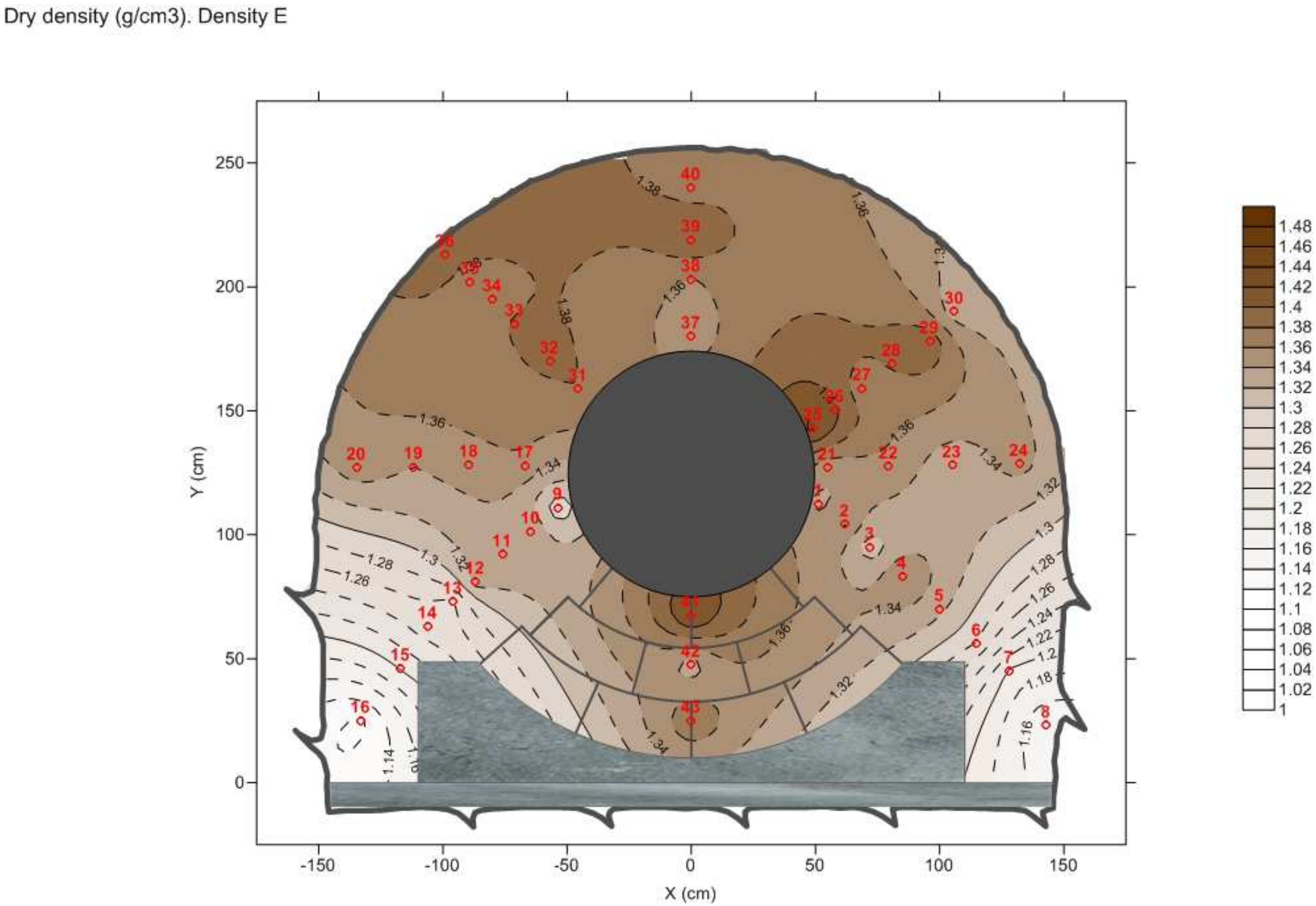

Figure AII-9: Dry density (g/cm3) Cross section B2

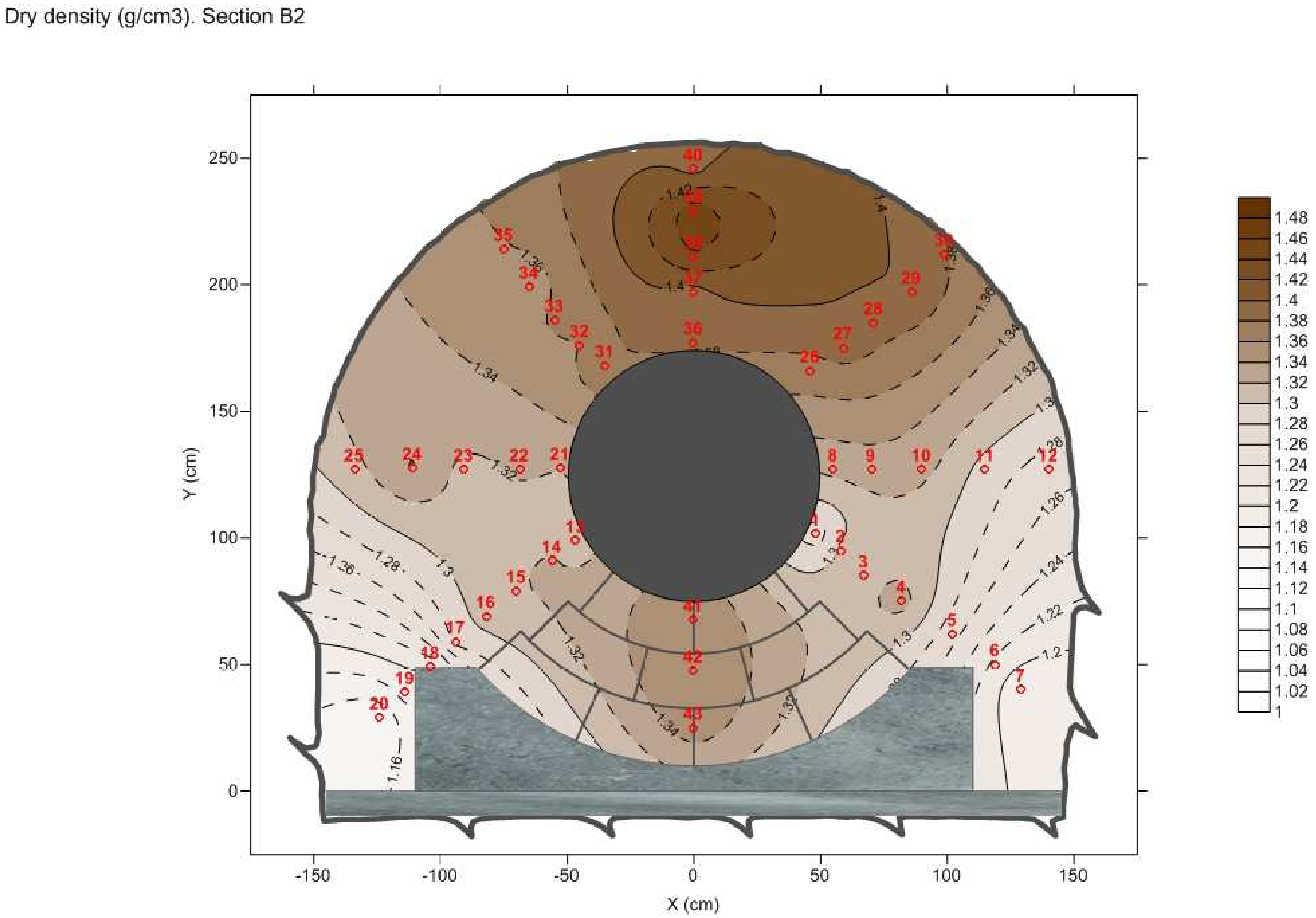

Figure AII-10: Dry density (g/cm3) Cross section A2

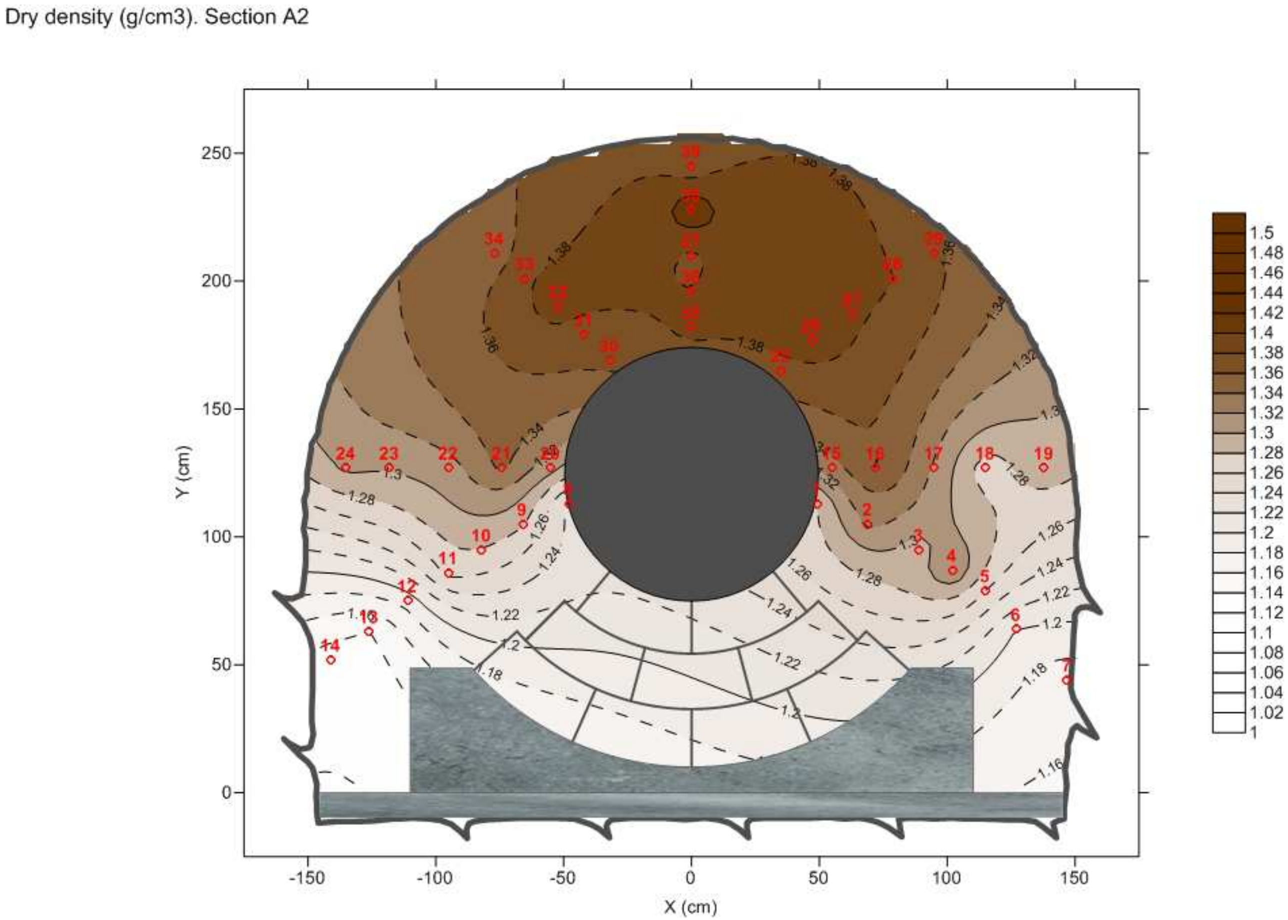

Figure AII-11: Degree of saturation (%) Cross section A1-25

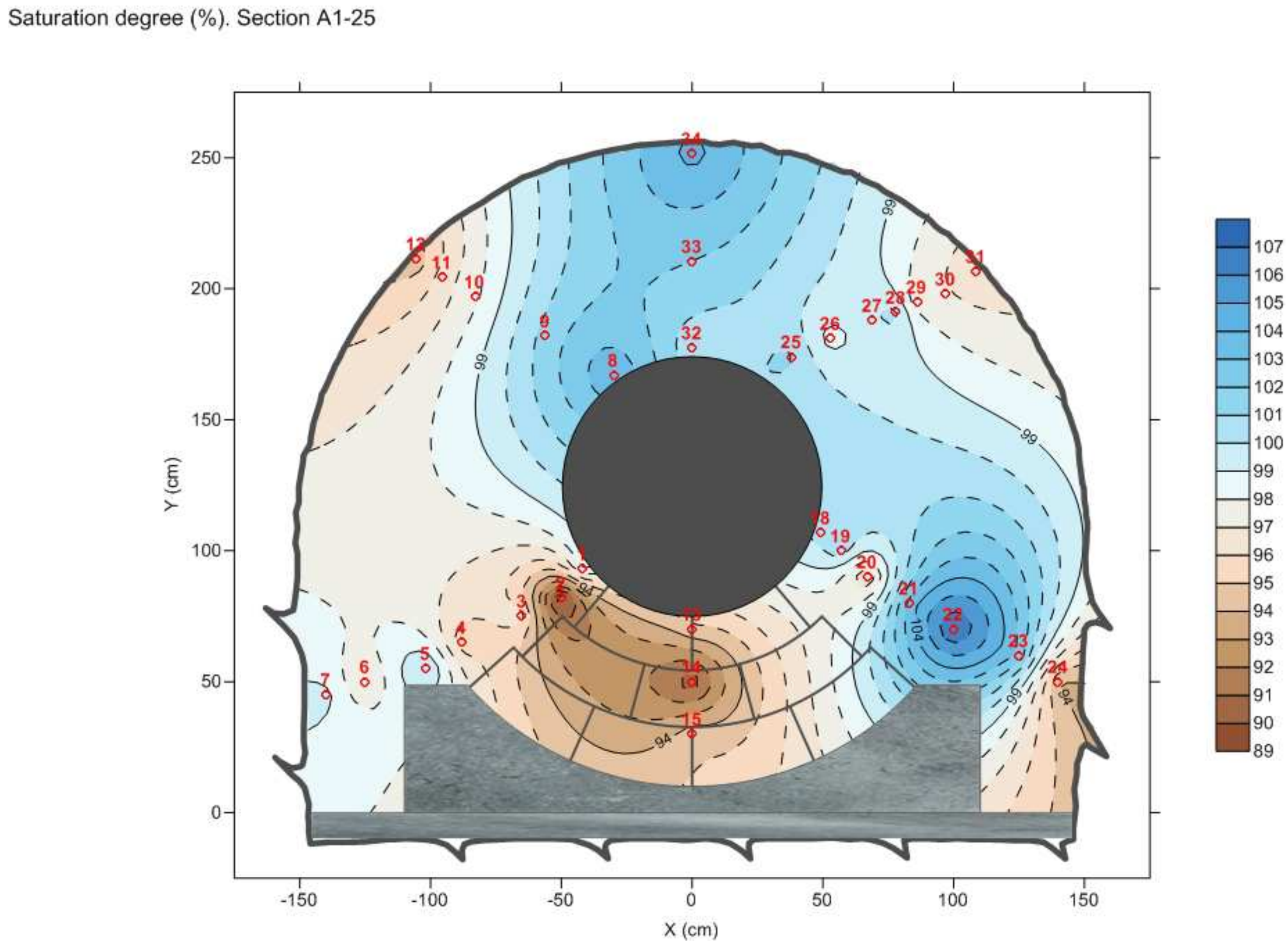

Figure AII-12: Degree of saturation (%) Cross section B1

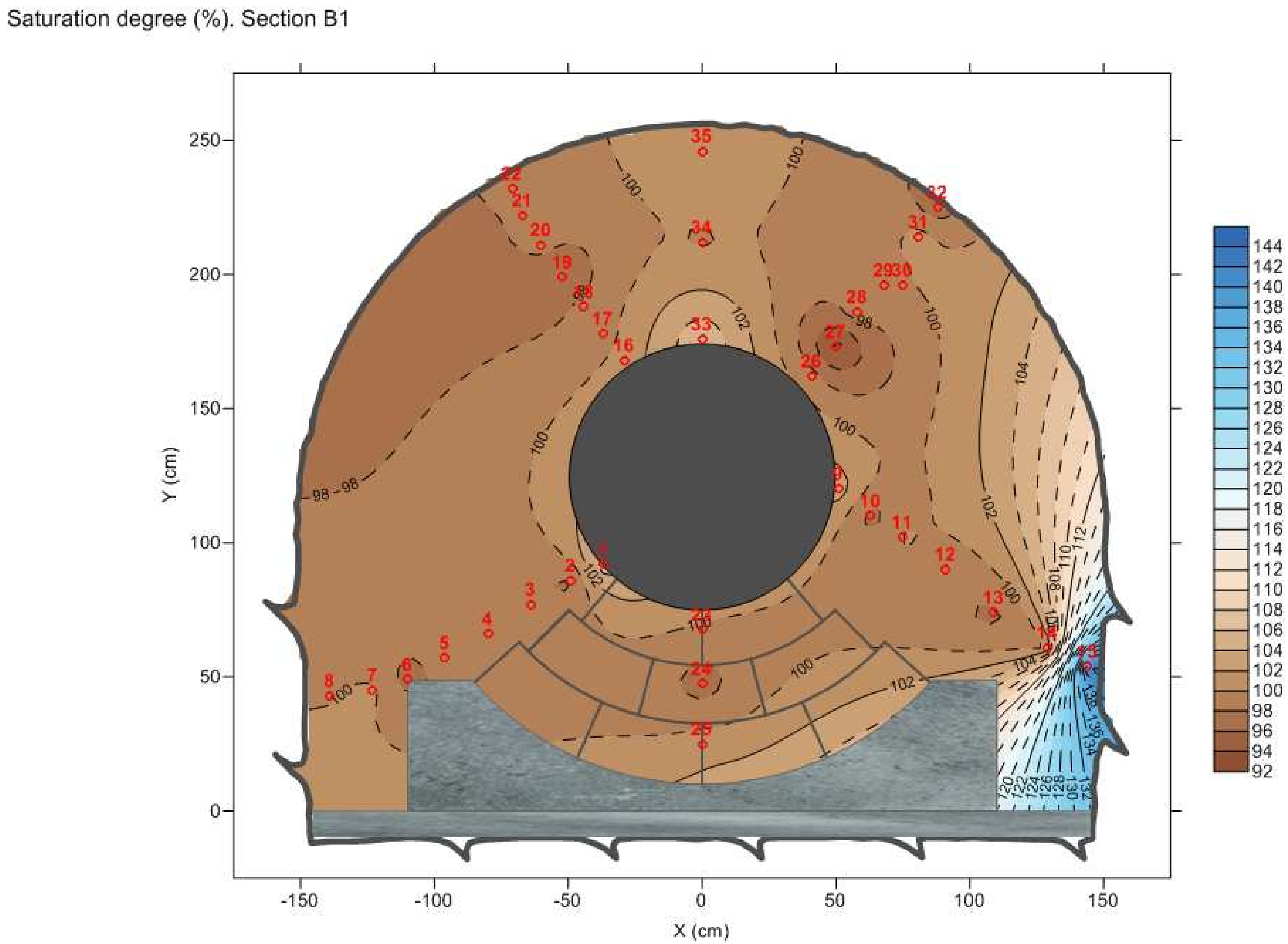

Figure AII-13: Degree of saturation (%) Cross section E

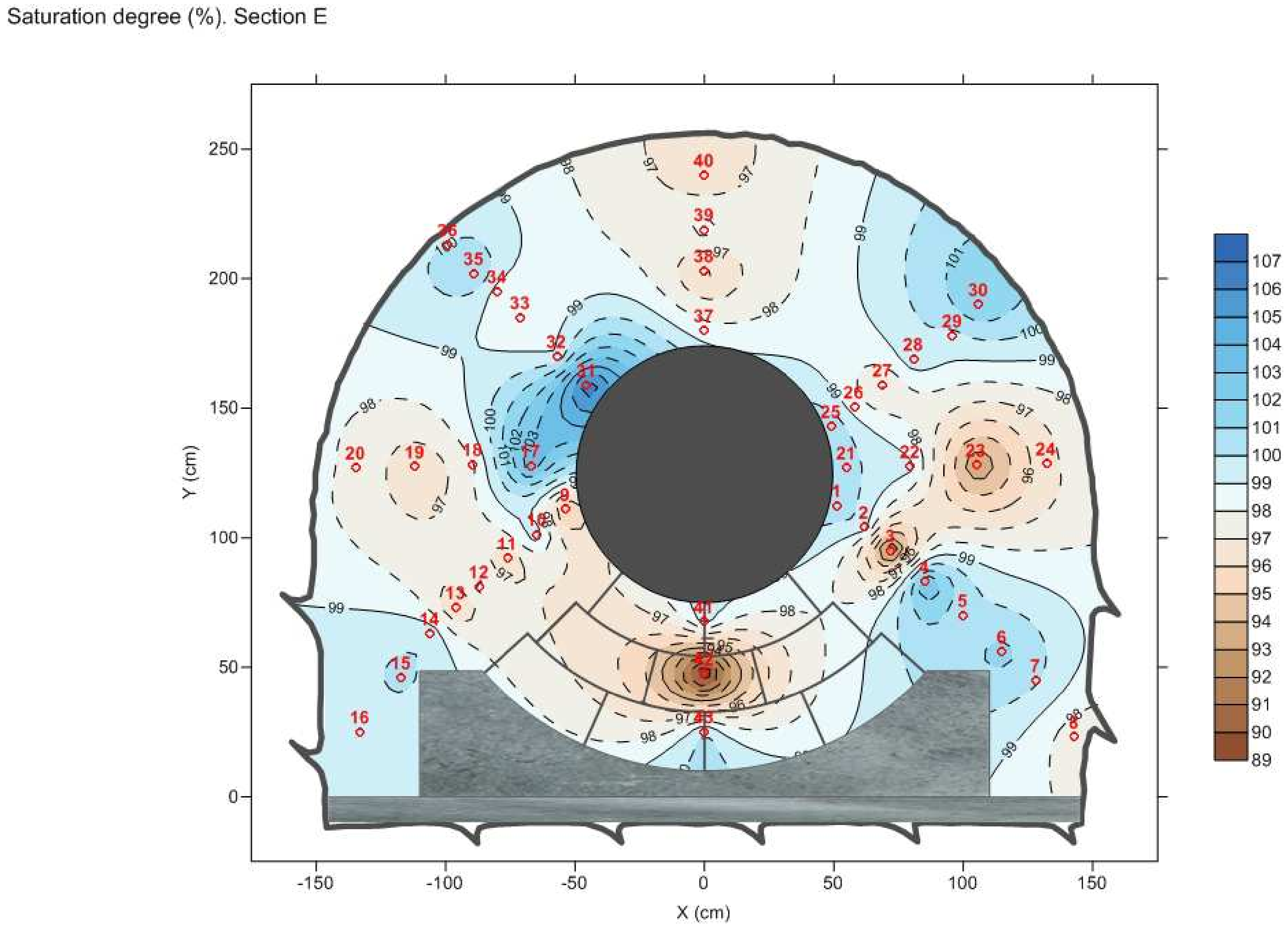

Figure AII-14: Degree of saturation (%) Cross section B2

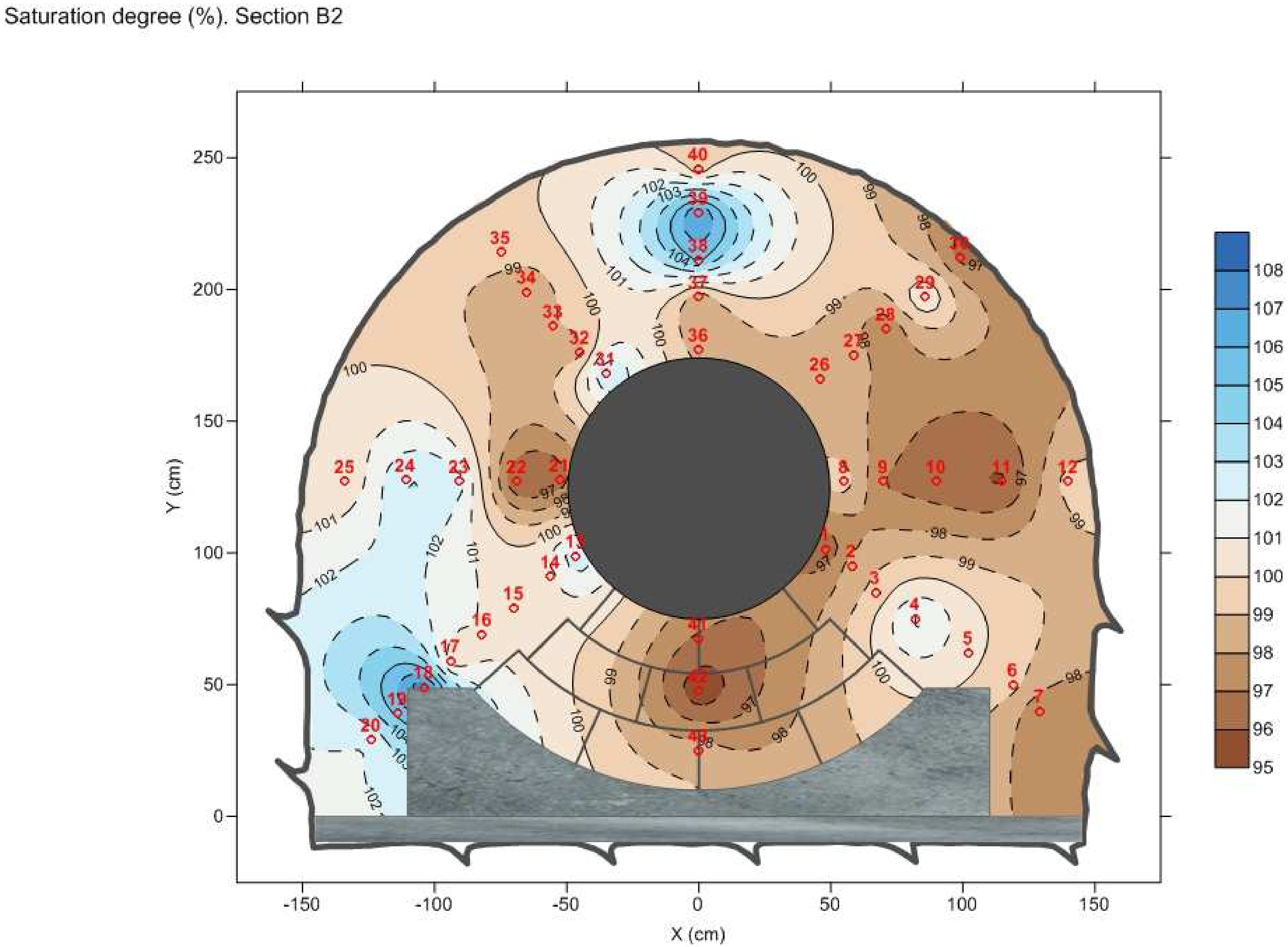

Figure AII-15: Degree of saturation (%) Cross section A2

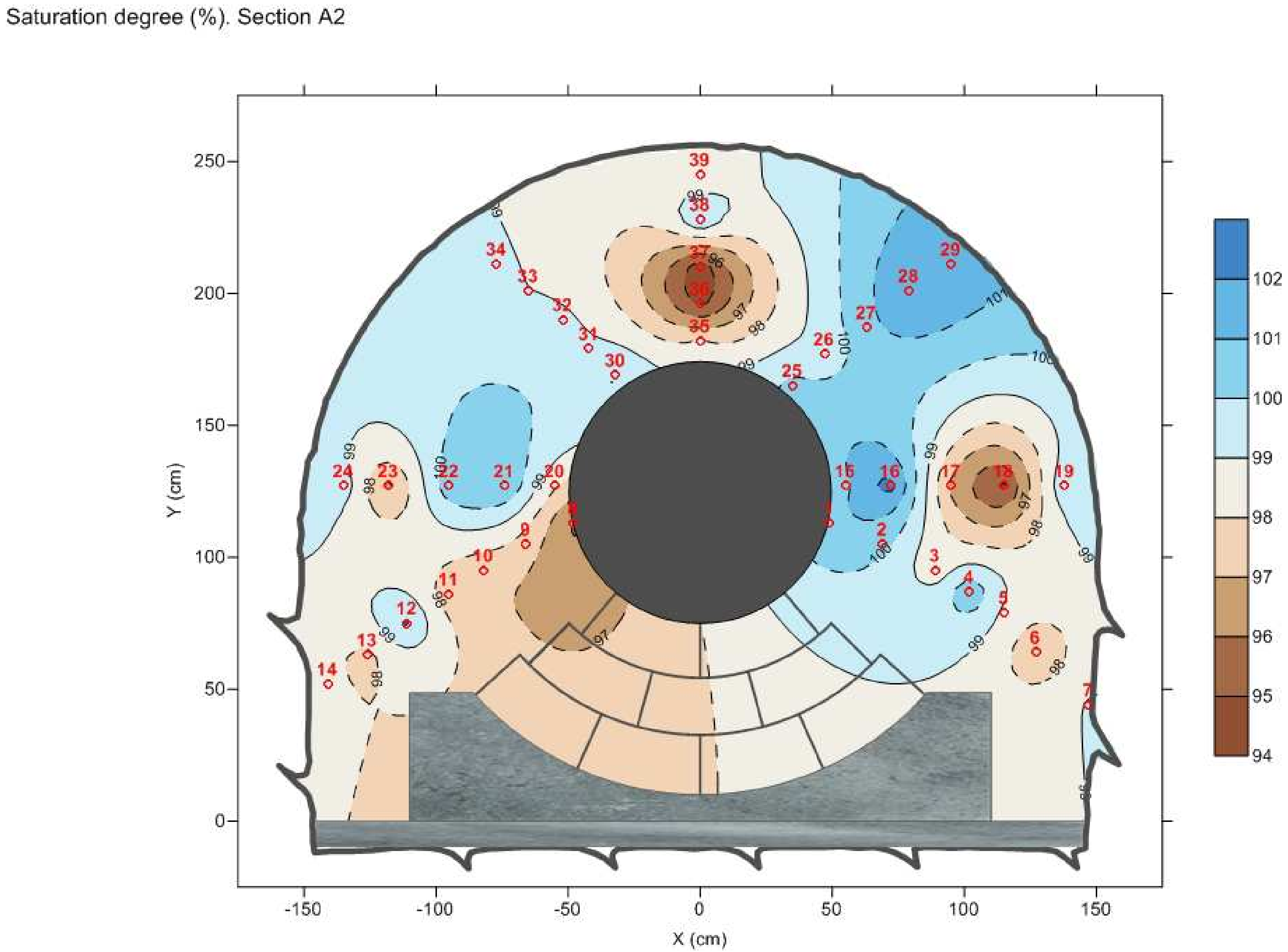

Figure AII-16: Water content (%) Longitudinal section Y 44-54

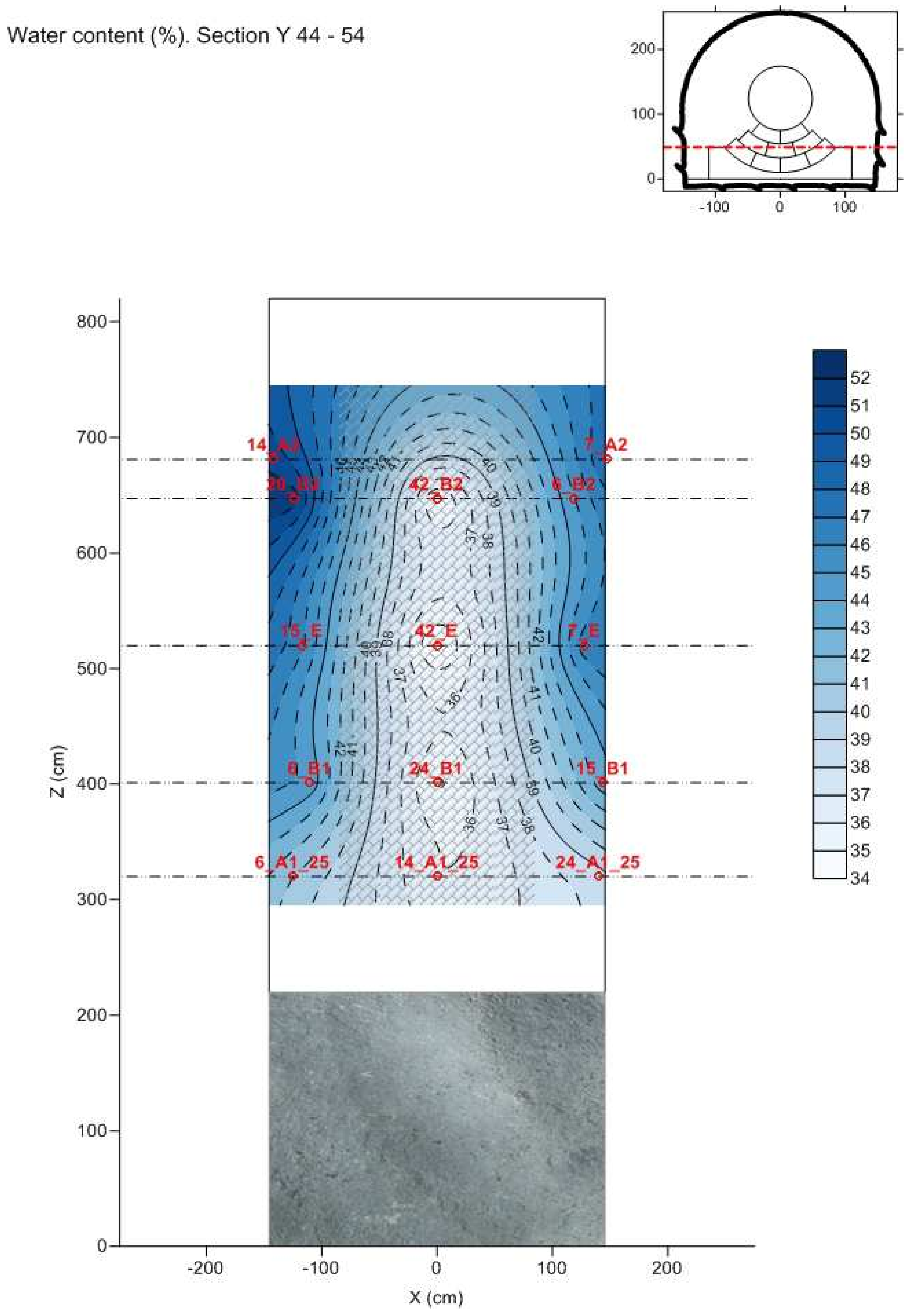

Figure AII-17: Water content (%) Longitudinal section Y 66-79

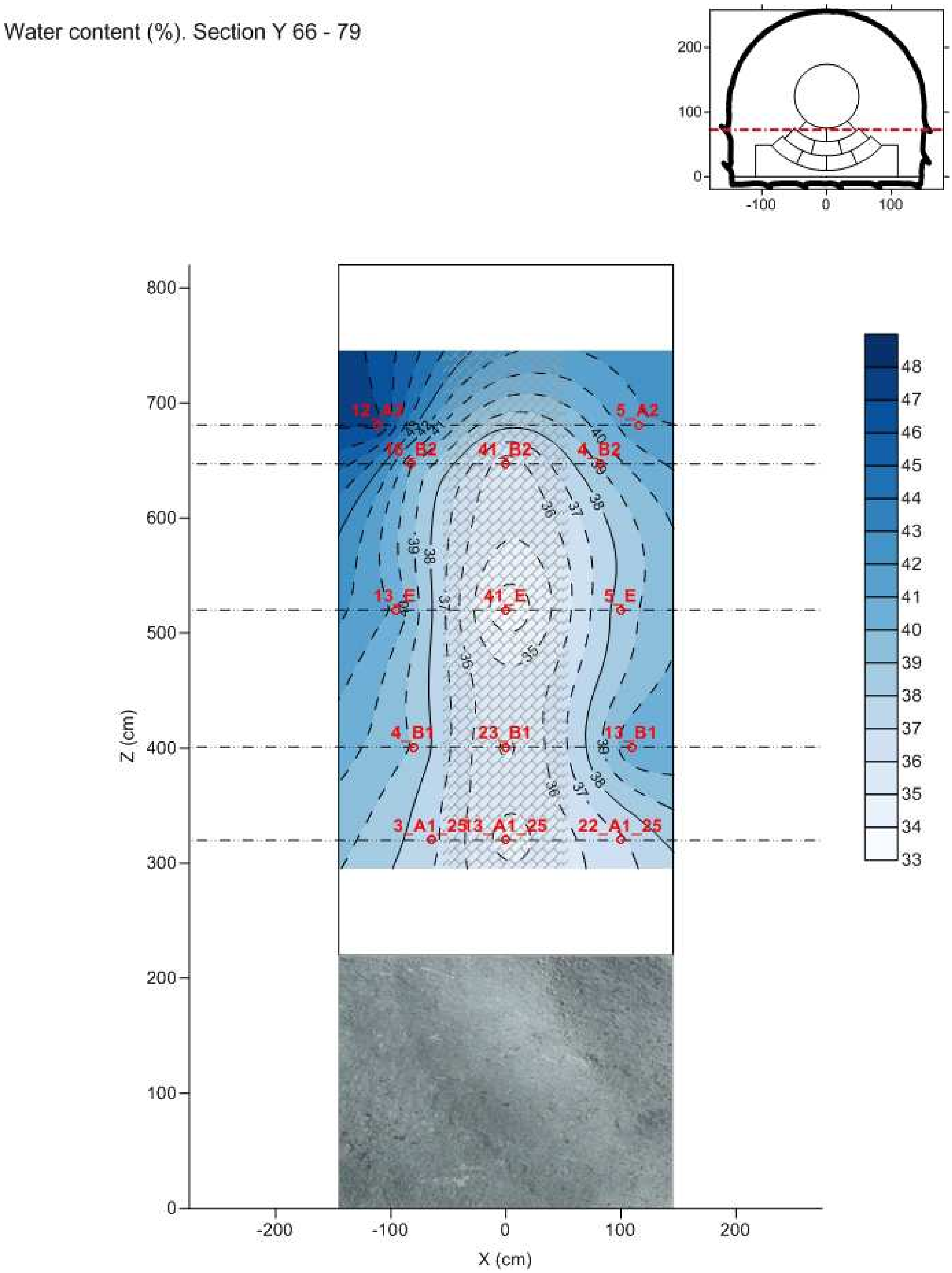

Figure AII-18: Water content (%) Longitudinal section Y 127-129

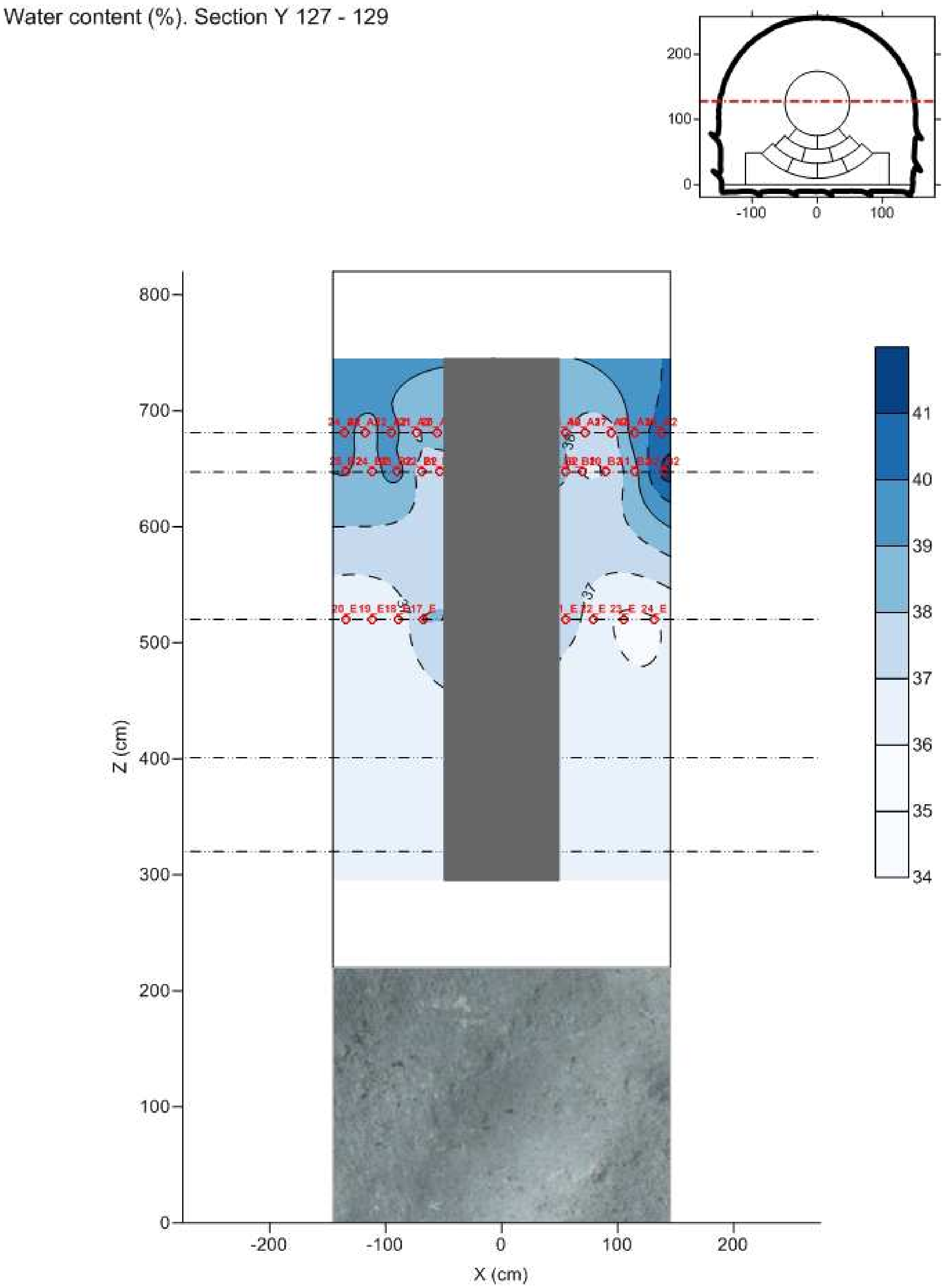

Figure AII-19: Water content (%) Longitudinal section Y 175-185

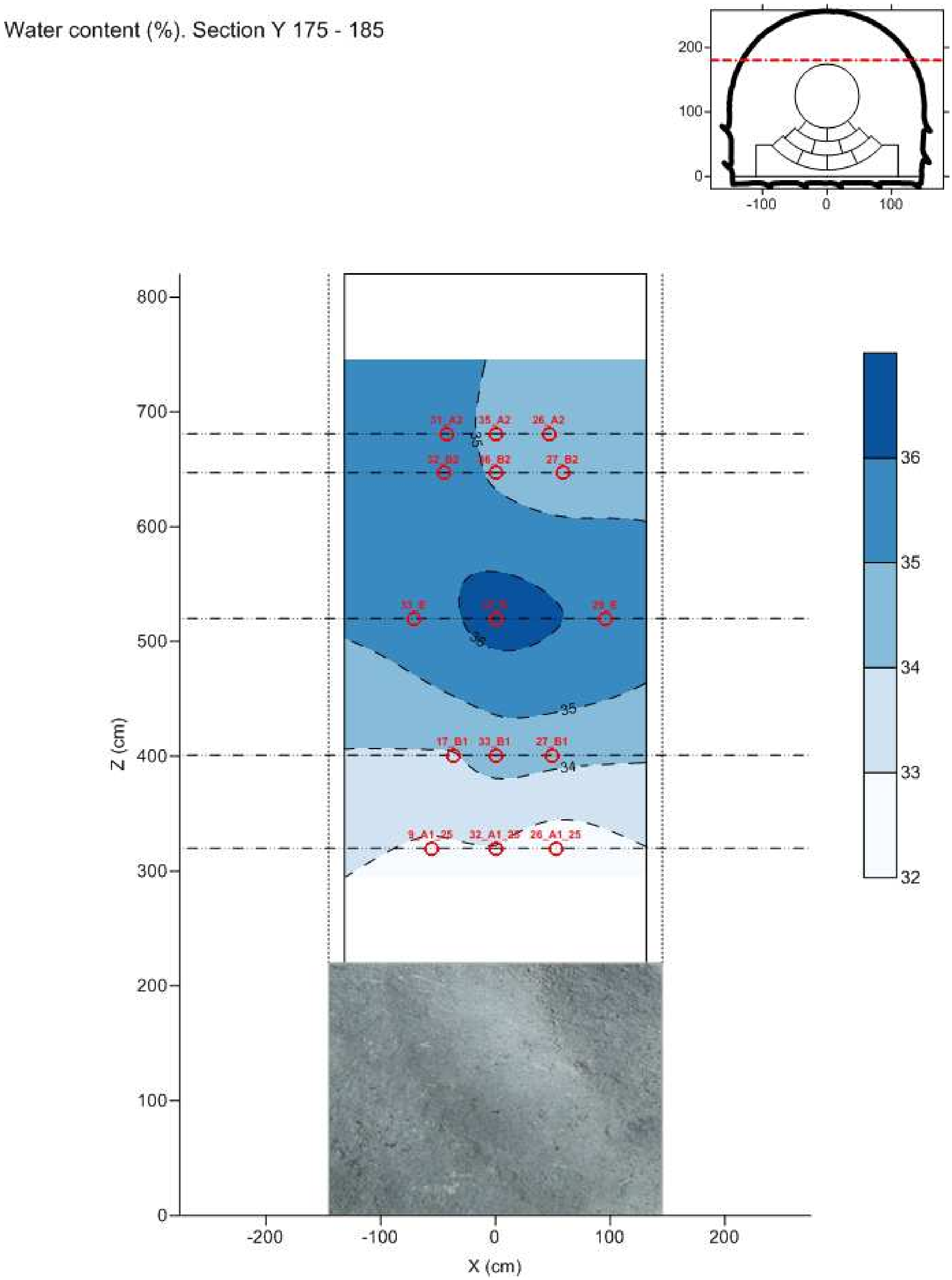

Figure AII-20: Water content (%) Longitudinal section Y 190-210

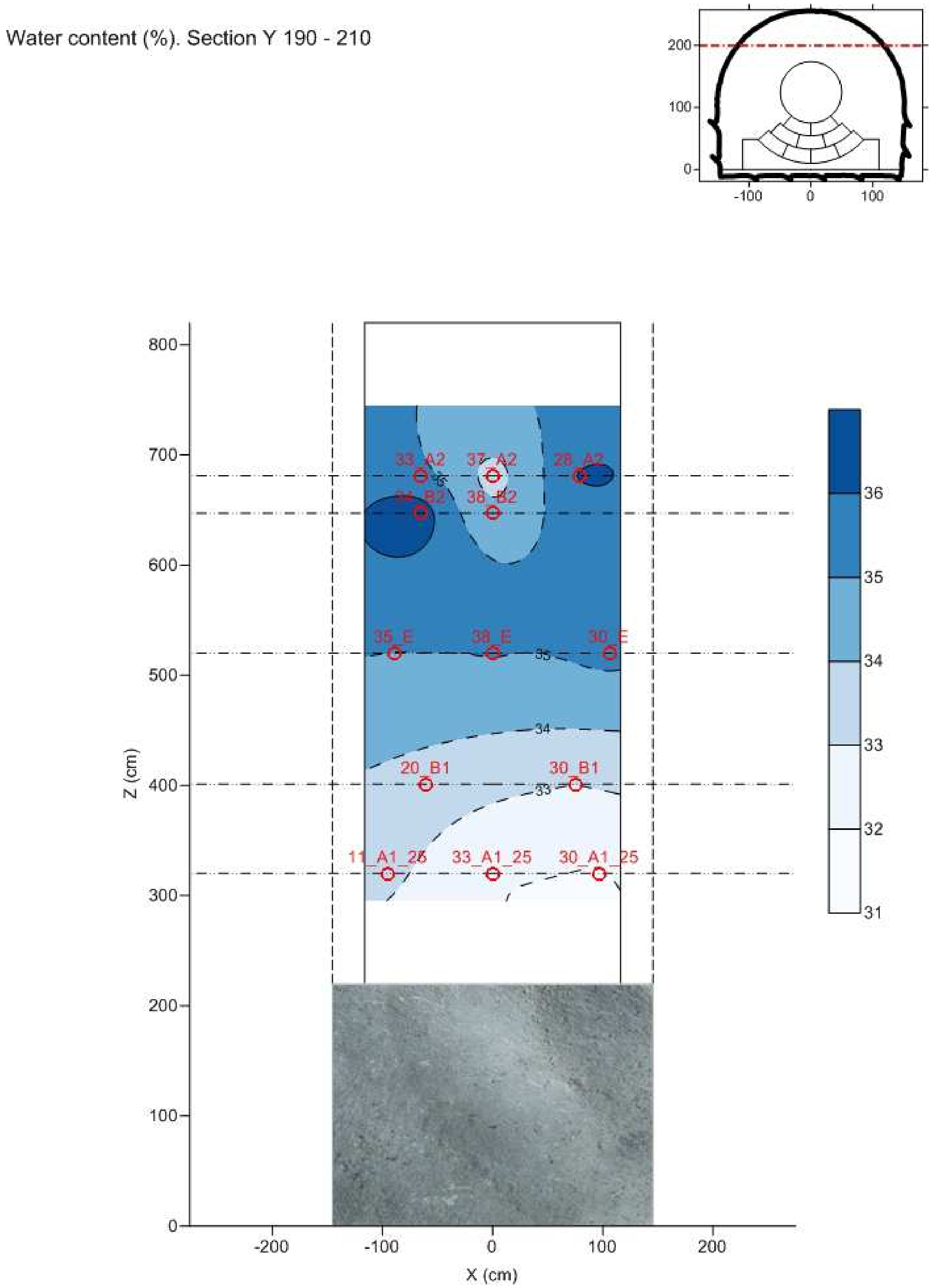

Figure AII-21: Dry density (g/cm3) Longitudinal section Y 44-54

Dry density (g/cm3). Section Y 44 - 54

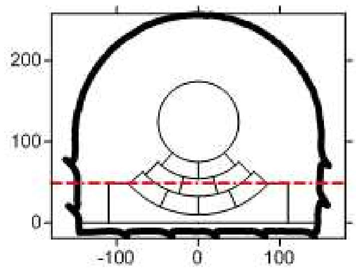

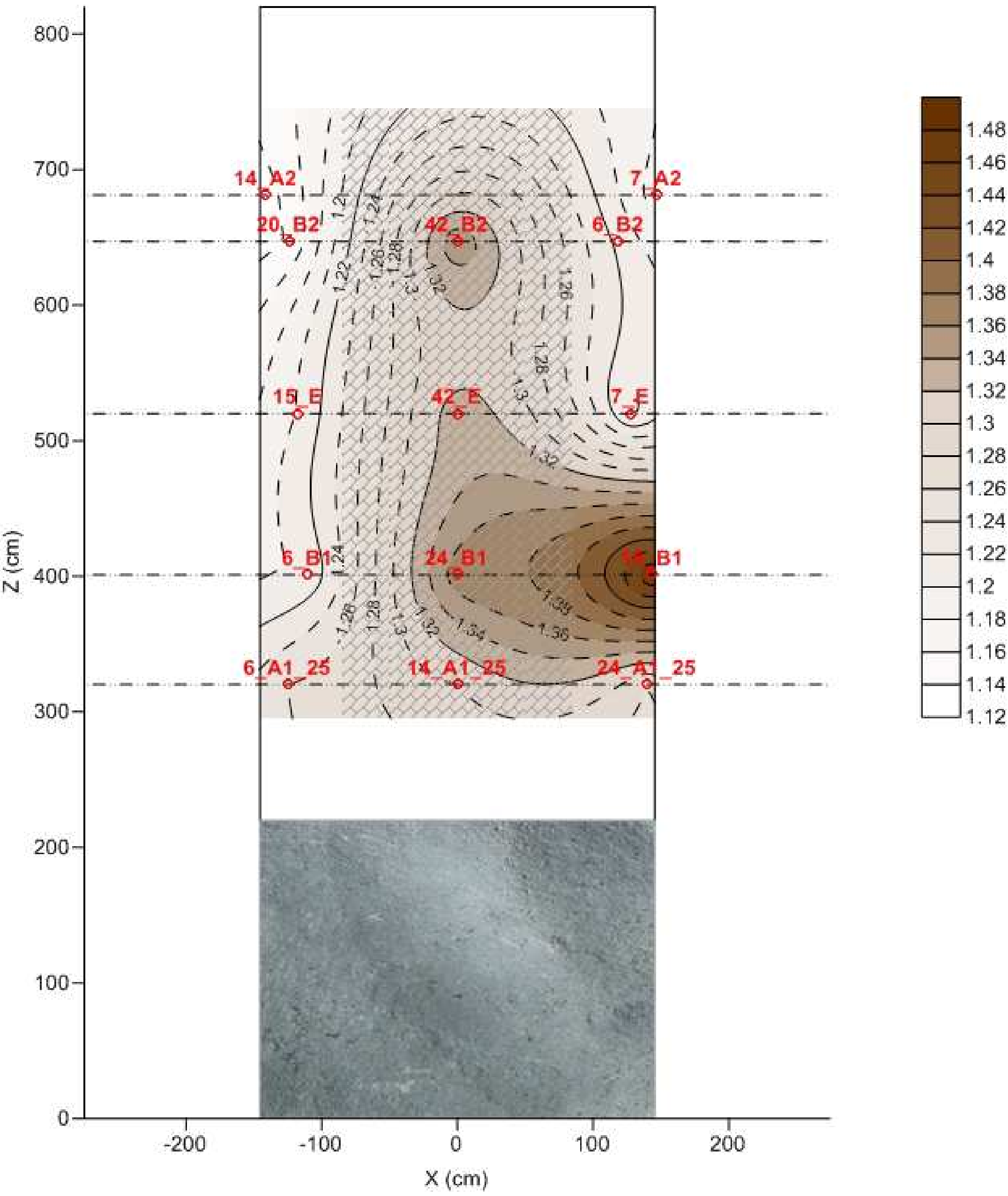

Figure AII-22: Dry density (g/cm3) Longitudinal section Y 66-79

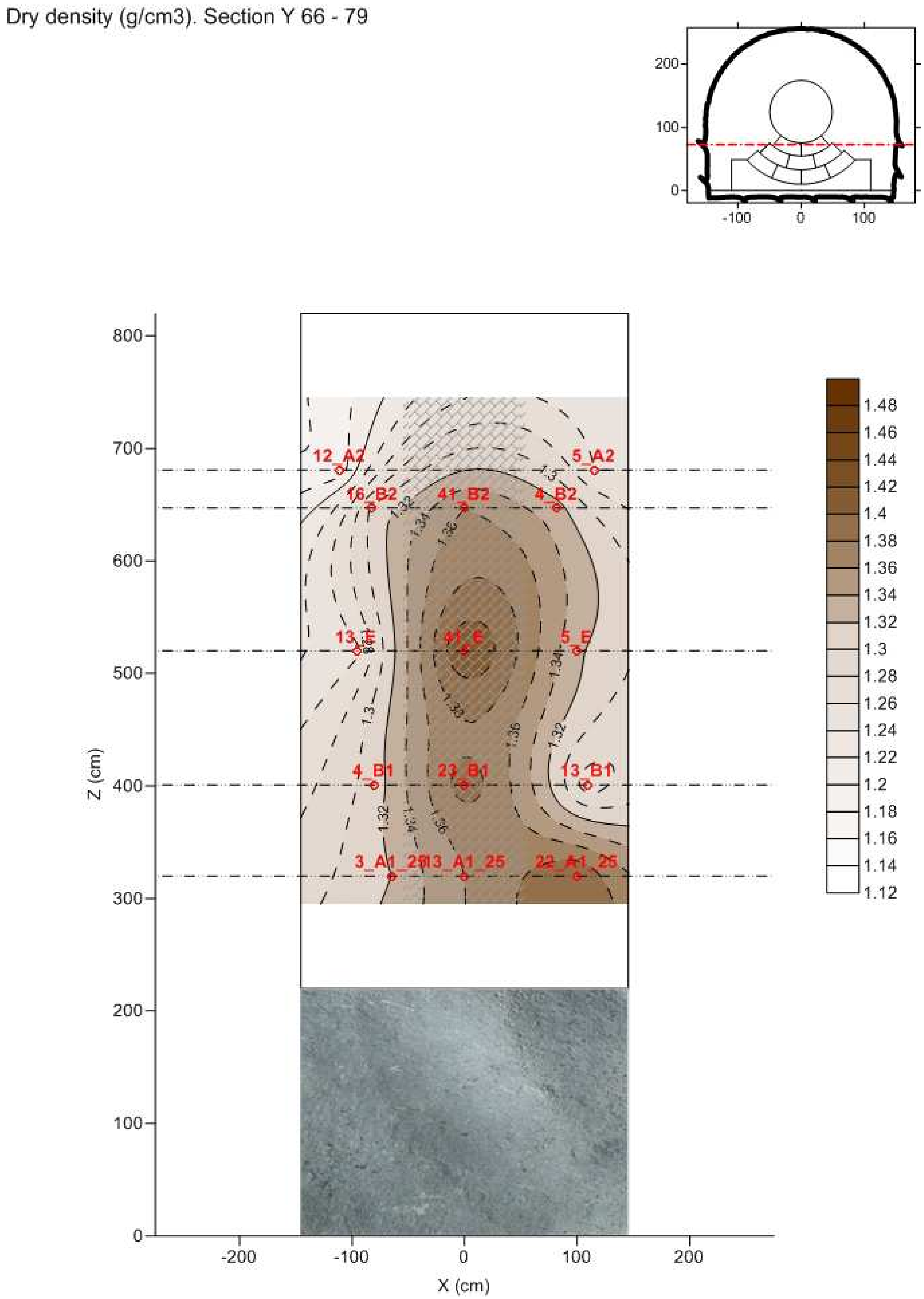

Figure AII-23: Dry density (g/cm3) Longitudinal section Y 127-129

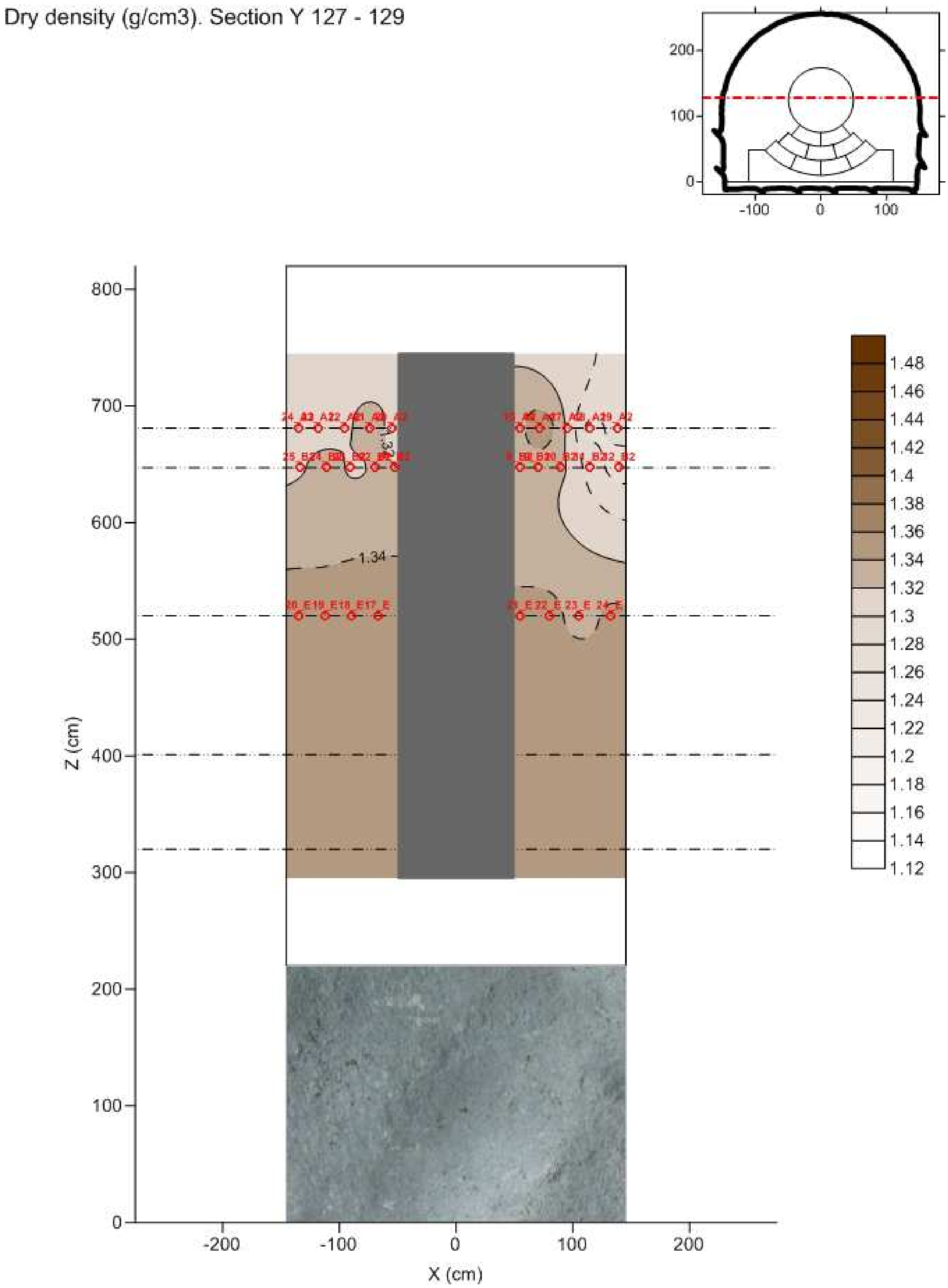

Figure AII-24: Dry density (g/cm3) Longitudinal section Y 175-185

Dry density (g/cm3). Section Y 175 - 185

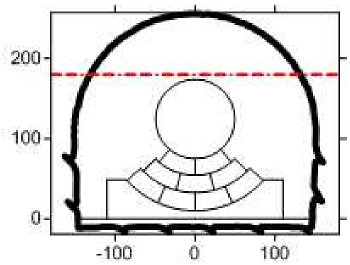

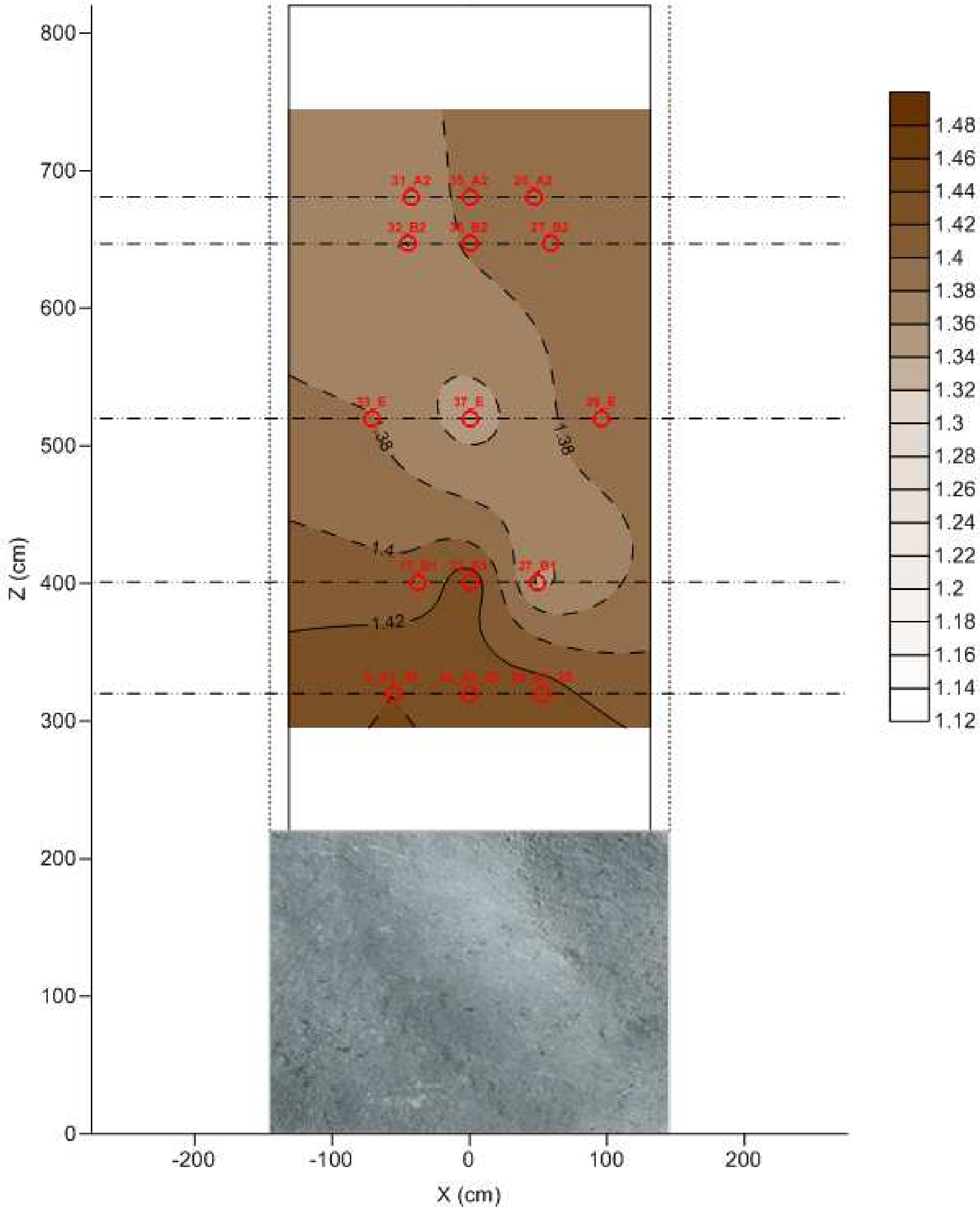

Figure AII-25: Dry density (g/cm3) Longitudinal section Y 190-210

Dry density (g/cm3). Section Y 190 - 210

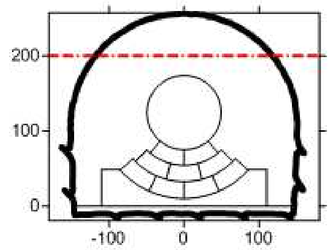

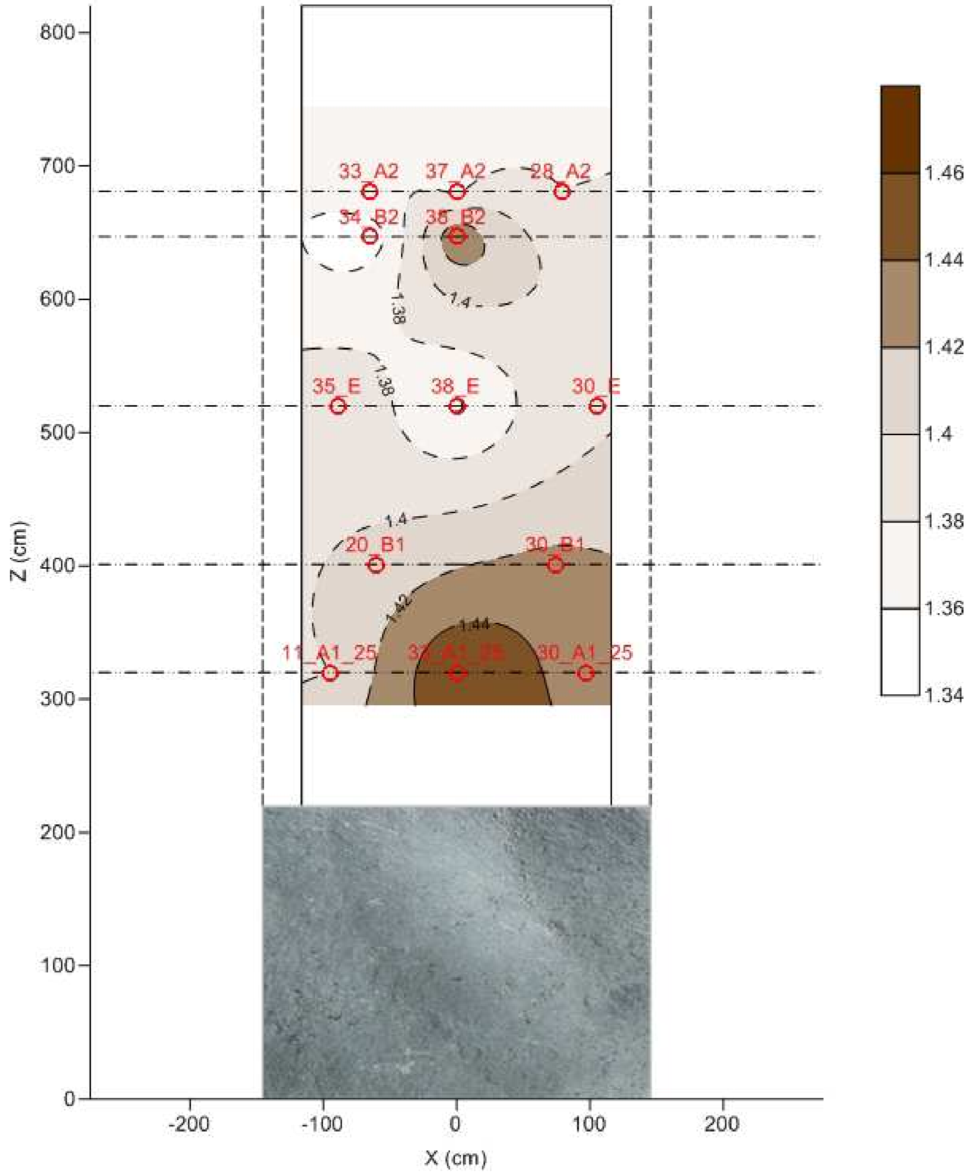

Figure AII-26: Degree of Saturation (%) Longitudinal section Y 44-54

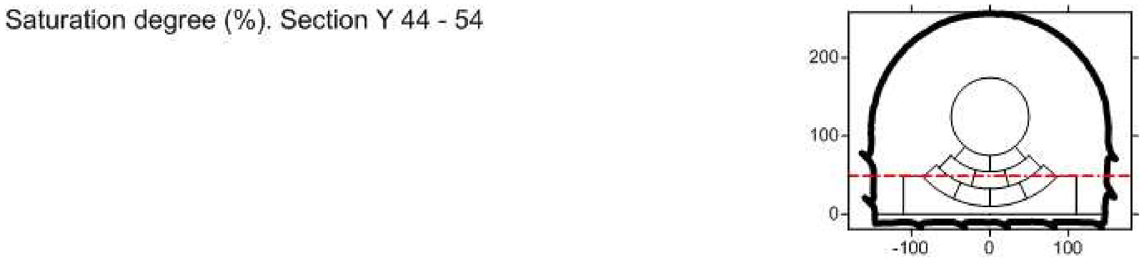

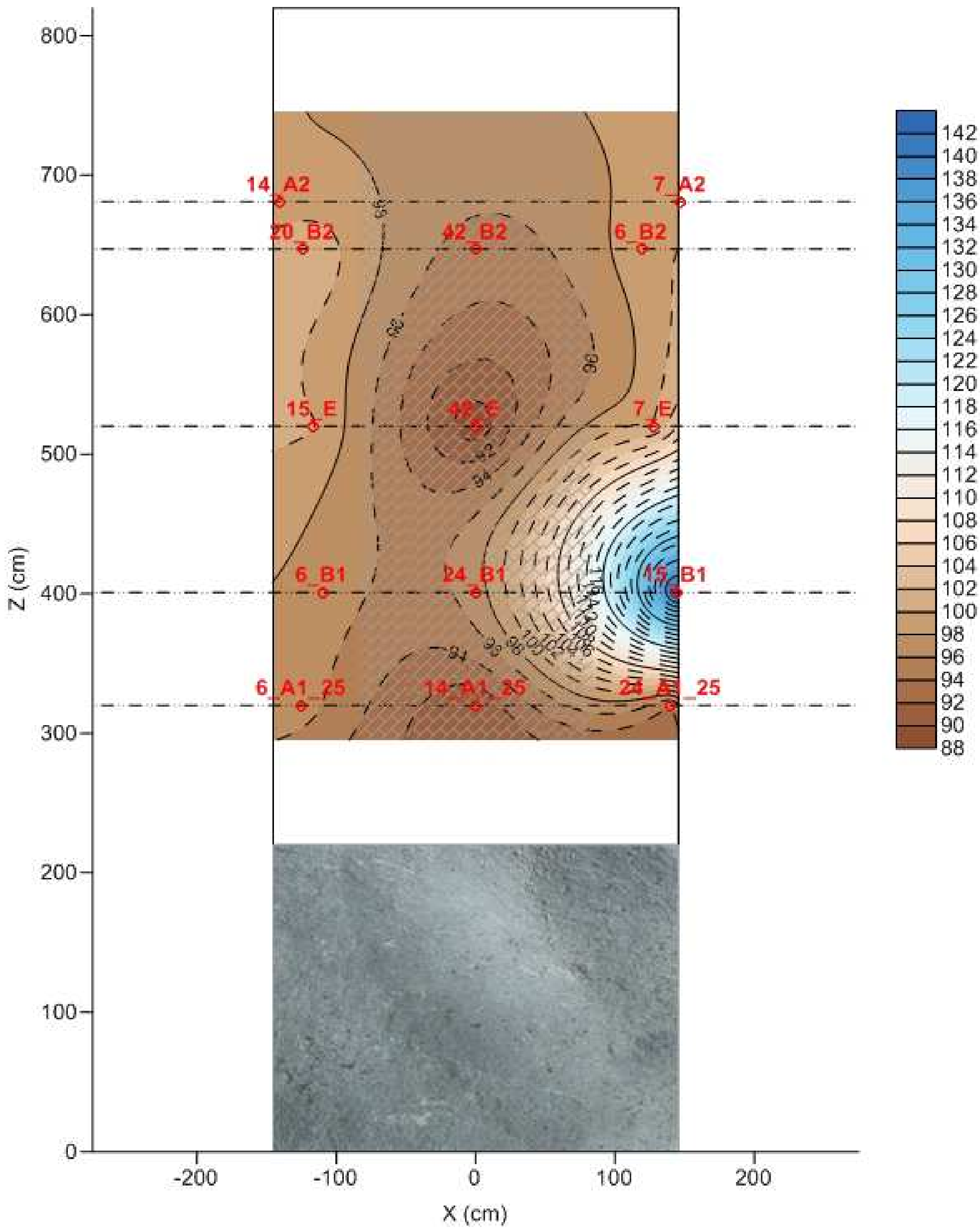

Figure AII-27: Degree of Saturation (%) Longitudinal section Y 66-79

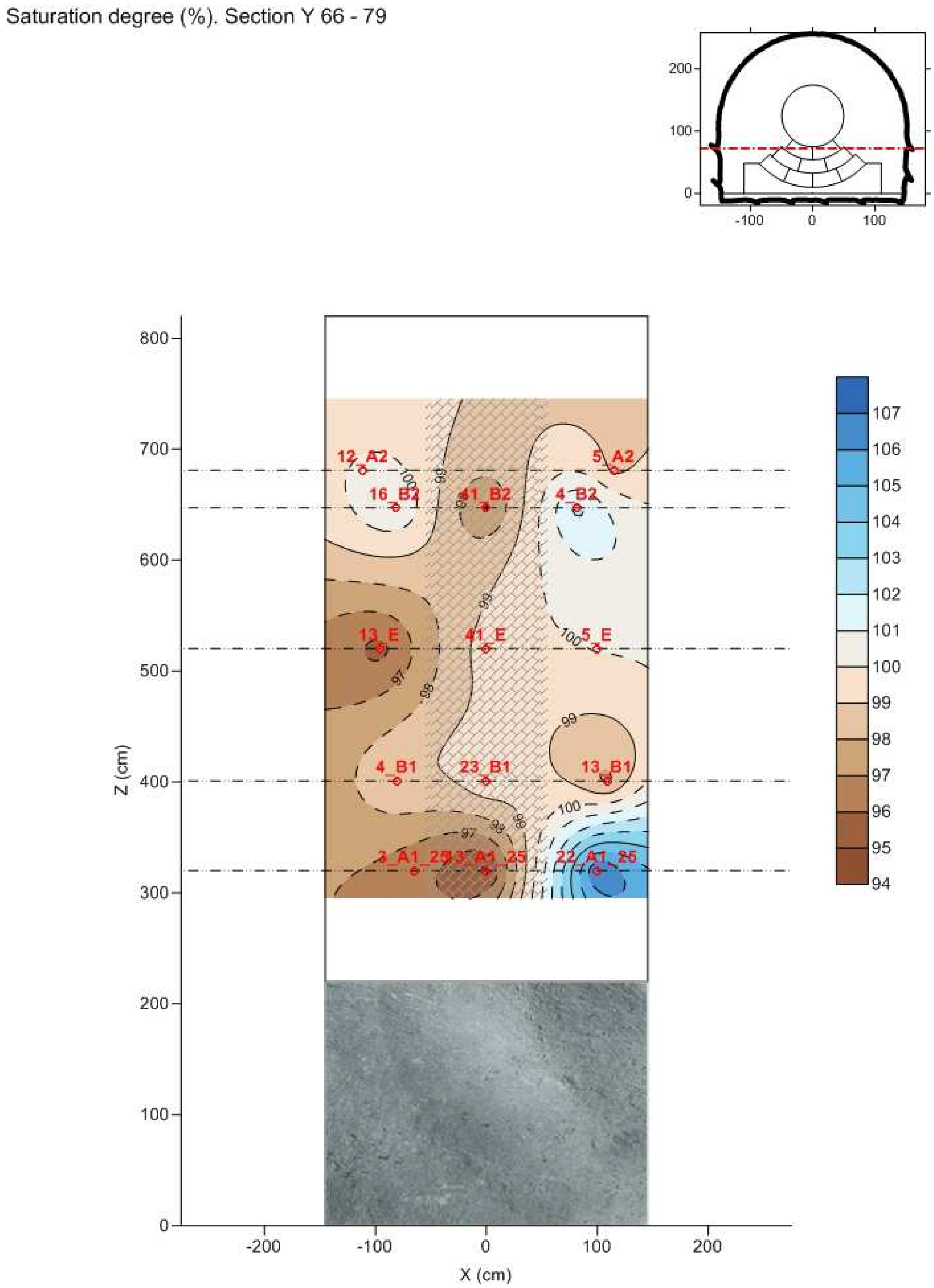

Figure AII-28: Degree of Saturation (%) Longitudinal section Y 127-129

Saturation degree (%). Section Y 127 - 129

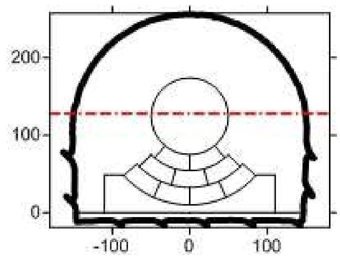

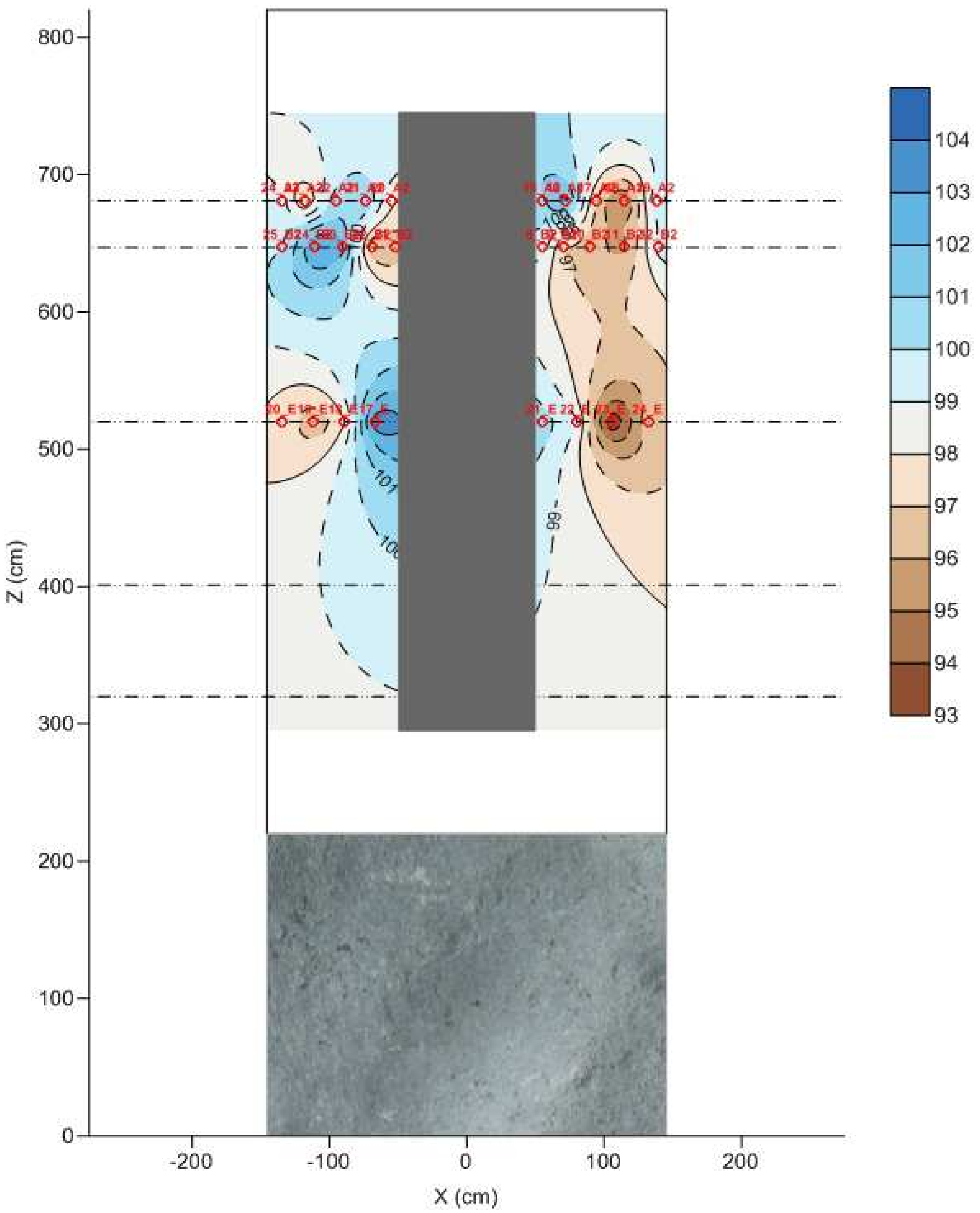

Figure AII-29: Degree of Saturation (%) Longitudinal section Y 175-185

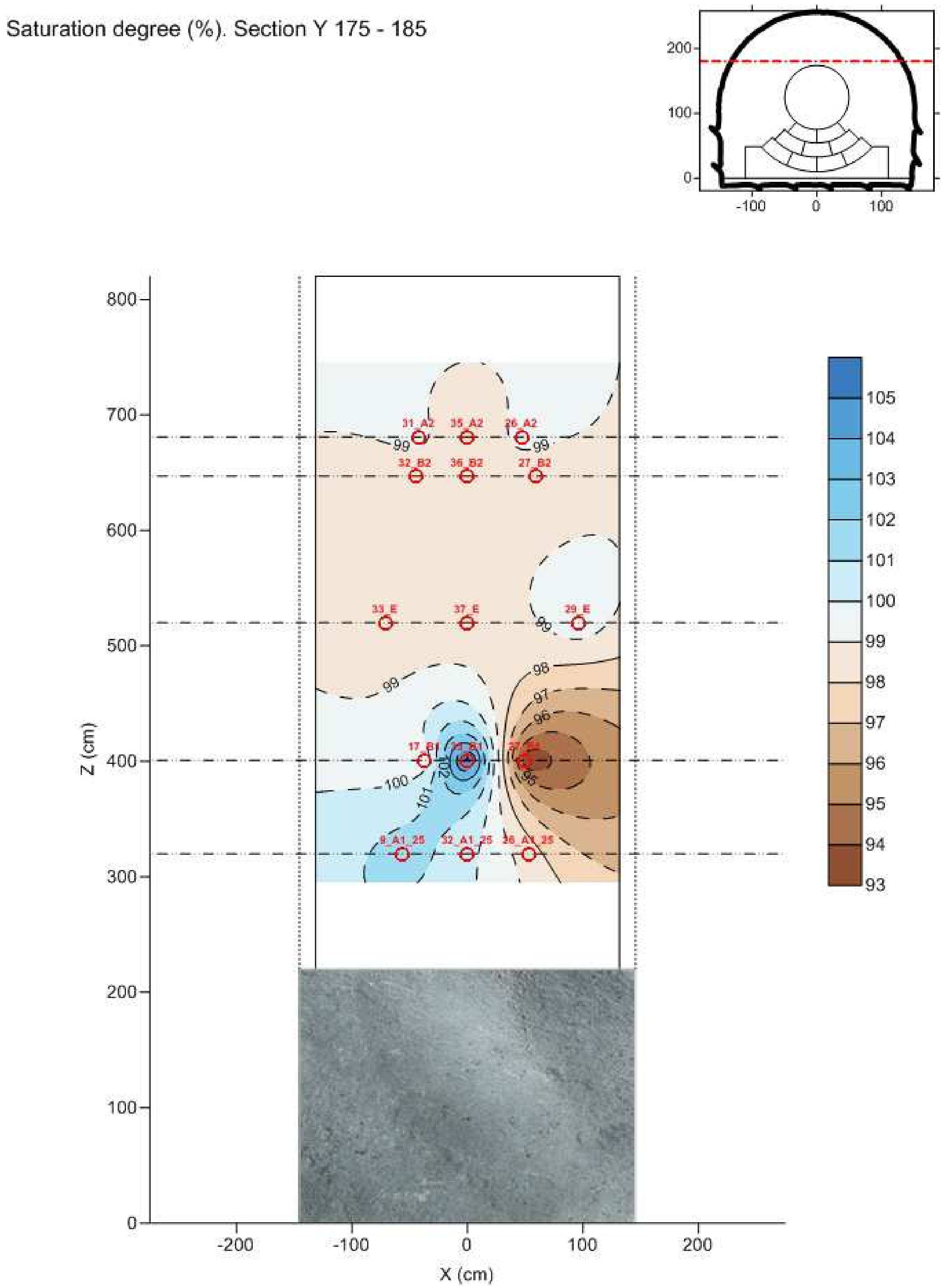

Figure AII-30: Degree of Saturation (%) Longitudinal section Y 190-210

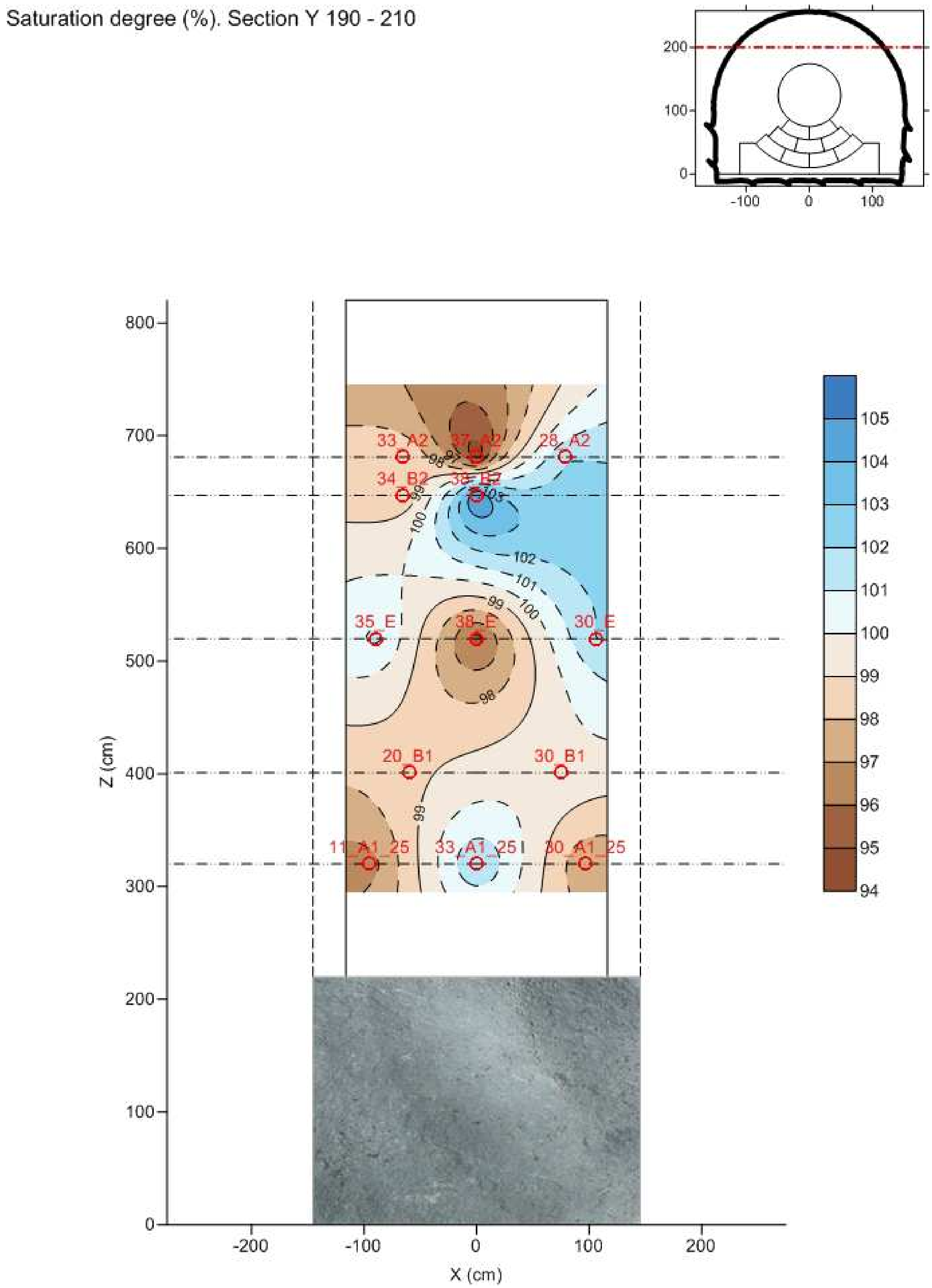

9 APPENDIX III FINAL SENSORS DATA REPORT SDR N30

Aitemin

Centro Tecnológico

Engineered Barrier Emplacement Experiment in Opalinus Clay. "EB" Experiment

SENSORS DATA REPORT No. 30 (LAST ONE)

Period: 22/11/01 to 14/01/2013 (4071 days)

Sensors: All installed at the EB niche

July 2013

C.D.: Sensor Data Report No. 30	PREPARADO/*Prepared*:	REVISADO/*Revised*:	APROBADO/*Approved*:
	Fecha/*Date* 31/07/13	Fecha/*Date*: 31/07/13	Fecha/*Date*: 31/07/13
No. pages: 37	Firma/*Signature*:	Firma/*Signature*:	Firma/*Signature*:
SDR EB N30 Final.doc	María Rey		

INDEX

1 INTRODUCTION

1.1 THE EB PROJECT

The Engineered Barrier Emplacement Experiment in Opalinus Clay “EB” Experiment aimed the demonstration of a new concept for the construction of HLW repositories in horizontal drifts, in competent clay formations. The principle of the new construction method was based on the combined use of a lower bed made of compacted bentonite blocks, and an upper buffer made of granular bentonite material (GBM). The project is a real scale isothermal simulation of the method in the Opalinus Clay formation at the Mont Terri underground laboratory in Switzerland.

A steel dummy canister, with the same dimensions and weight as the reference canister, was placed on top of a bed of bentonite blocks, and then the upper part of the drift was buffered with the GBM made of bentonite pellets (Figure 1). The drift was sealed with a concrete plug having a concrete retaining wall between the plug and the GBM.

Since the end of the test installation the evolution of the different hydro-mechanical parameters was monitored, both in the barrier and the rock (especially in the EDZ). Relative humidity and temperature in the rock and in the bentonite buffer, rock displacement, pore pressure and total pressure are registered by means of different types of sensors. Due to the short amount of free water available in this formation, an artificial hydration system was installed to accelerate the hydration process in the buffer.

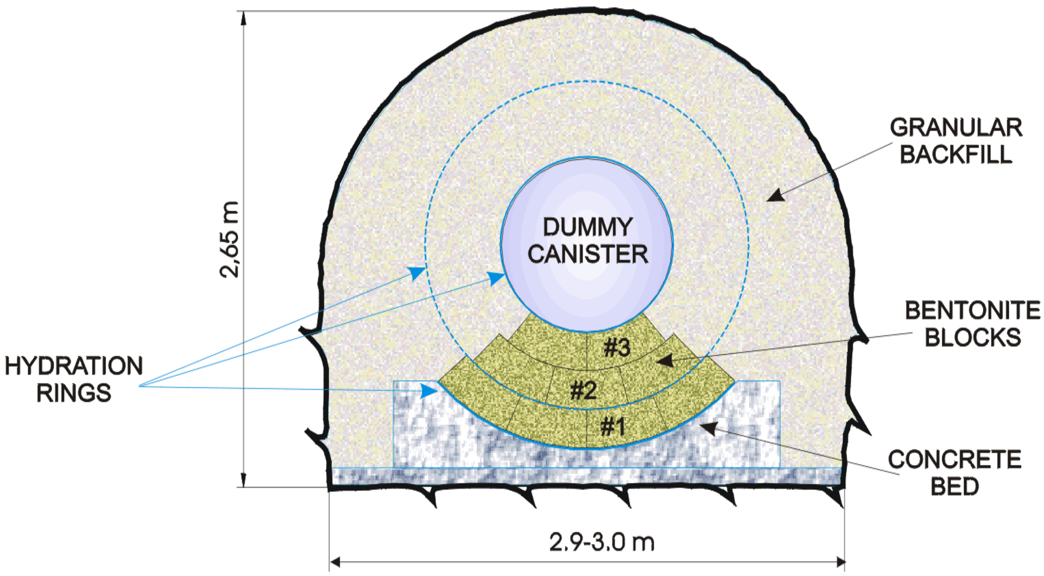

Figure 1: EB experimental layout

1.2 SENSORS DATA REPORT

This is the thirtieth and final data report of the Engineered Barriers Project (EB). It has been prepared under the support of PEBS[1] research project, FP7 Euratom. The report covers the period from 1st May 2002 to 14th January 2013 (129 months), including data collected during the dismantling operation carried out between October 2012 and January 2013. However, as in previous reports, the data available from dataloggers for some sensors installed in November 2001 have also been included.

The previous ninety-nine reports were published as shown in Table 1, which also details the funding of each phase of the project.

Table 1. Published Sensors Data Reports

Name	Date	Funding
SDR EB D16-1	October 2002	EC contract FIKW-CT2000-00017
SDR EB D16-2	November 2002	
SDR EB D16-3	March 2003	
SDR EB D16-4	June 2003	
SDR EB D16-5	December 2003	
SDR EB N6	March 2004	Mont Terri Consortium 32.015:EB1_PH9
SDR EB N7	June 2004	
SDR EB N8	September 2004	Mont Terri Consortium 32.015:EB1_PH10
SDR EB N9	November 2004	
SDR EB N10	May 2005	
SDR EB N11	August 2005	
SDR EB N12	October 2005	Mont Terri Consortium 32.0150.EB1_PH11
SDR EB N13	February 2006	
SDR EB N14	April 2006	
SDR EB N15	July 2006	
SDR EB N16	November 2006	Mont Terri Consortium 32.0150.EB1_PH12
SDR EB N17	March 2007	
SDR EB N18	April 2007	
SDR EB N19 (TN2007-11)	August 2007	
SDR EB N20	December 2007	Mont Terri Consortium 32.0150.EB1_PH13
SDR EB N21	January 2008	
SDR EB N22	May 2008	
SDR EB N23	July 2008	
SDR EB N24	December 2008	Mont Terri Consortium 32.0150.EB1_PH14
SDR EB N25	July 2009	
SDR EB N26	December 2009	Mont Terri Consortium 32.0150.EB1_PH15
SDR EB N27	August 2010	
SDR EB N28	August 2011	EURATOM FP7, project PEBS “Long-term performance of Engineered Barrier Systems”
SDR EB N29	August 2012	

[1] PEBS: Long-term Performance of the Engineered Barrier System (multinational European research project that investigates processes affecting the engineered barrier performance of geological repositories for high-level waste disposal).

2 CHRONOLOGY

The installation of the experiment was carried out in several steps. The instrumentation was installed from November 2001 to February 2002: in-rock pore pressure sensors, rock displacement sensors and some rock relative humidity sensors, canister displacement sensors, relative humidity sensors in bentonite and total pressure cells. The artificial hydration system was installed in March 2002. The installation of the experiment was finished in April 2002, including the retaining wall, the concrete plug and the data acquisition system.

2.1 INSTALLATION OF SENSORS

The installation of the EB experiment instrumentation to which this report is focused was carried out in several steps:

- First phase: last week of November 2001. Installation of all in-rock pore pressure sensors, rock displacement sensors and some rock relative humidity sensors. Data loggers installed to collect pressure, relative humidity and some temperature data.
- Second phase: February 2002. Installation of canister displacement sensors, relative humidity sensors in bentonite and total pressure cells, as well as the hydration system and its support structure.

After the construction of the concrete plug, the installation of the data acquisition system was carried out and the connection of all sensors to it. It was finished on 30th April 2002.

Day 0 considered for data collection is 1st May 2002. Therefore, data collected by means of dataloggers from November 2001 to April 2002 correspond to days -160 to -1. Hydration of bentonite buffer started on 6th May 2002.

2.2 HYDRATION OF BUFFER

The hydration of the bentonite buffer started in May 2002 and ended in June 2007. There was an initial hydration phase with an important amount of water injected (6,700 litres in two days) that was stopped after several water stains appeared on the wall. After that, and from September 2002 to June 2007, there were different hydration phases with continuous water injection.

The historical record of the water inflow is the following:

- Start of buffer hydration: 6th May 2002 (day 5). A total of 6,700 litres of Pearson's water were injected to the system during the first hydration phase, from 6th May to 8th May 2002 (day 5 to day 7). It had been planned to keep on with the continuous hydration for several months, but it was faster than initially expected and it was stopped after some water stains appeared on the walls (see 1st Status Report, 10th May 2002). 50 more litres were added during several injection tests made in July 2002. It was not possible to quantify the amount of water lost through the plug and the adjacent rock.

- Start of second phase of buffer hydration: 11th September 2002 (day 133). Several electrovalves were installed to allow the injection be automatic, at a rate of 25 litres per day approximately. The daily injection failed on days 23rd, 28th to 30th September 2002 (days 145, 150 to 152), 7th to 10th, 14th and 26th to 29th October 2002 (days 159 to 161 and 166 to 178) and from 8th to 15th November 2002 (days 191 to 198).

The injection rate was 25 litres per day during the months of May, June and July 2003. In August 2003 the rate decreased as a consequence of a decrease of the injection pressure. From 1st to 18th September 2003 the rate increased again, with a value of 20 litres per day.

Due to the leaks and the increase of pressure, there was no injection from 19th September to 2nd October 2003 and from this day the injection was reduced to 10 litres per day until 21st October 2003.

- Third phase of buffer hydration: Installation of continuous injection system the 22ndOctober 2003. The hourly rate was approximately 0.25 litres at that moment.

  The continuous injection system was designed to inject water constantly at low pressure. It consisted of a steel tank suspended by means of a support and a load cell that allows the continuous measurement of the water loss weight (injected water). The tank was periodically refilled with Pearson's water. The tank's output was connected to the bentonite buffer, being Nitrogen the gas used to pressurise it up to 0.5 bar.

  Due to unknown causes, the injection pressure increased accidentally up to 1.44 bar the 1st December 2003 (day 579). As the injection rate is related to the injection pressure, and to avoid undesired pressure increases, a new pressure regulator was installed in April 2004.

  The injection was stopped from 11th to 20th February 2005 (days 1017 to 1026) due to an obstruction in the injection valve. An increase in the injection rate was detected after the cleaning of the valve.

  Although it cannot be considered as an independent injection phase, from 21st February 2006 (day 1392), the injection was made at a pressure value of approximately 1 bar.

- Fourth phase of buffer hydration: Start of buffer hydration at atmospheric pressure from 18th May 2006 (day 1478). A decrease in the injection rate was observed during the first days of this phase, with inversion of the flow.

  The evolution of the pressure values registered by both rock pore pressure sensors and EDZ sensors in the previous year suggested a possible connection of these sensors with the injection water. Therefore, it was decided to continue the injection at atmospheric pressure and the gas tank was disconnected.

  This injection phase was temporarily interrupted due to the maintenance activities carried out by the GI in September 2006. The injection tank was disconnected from 19th September 2006 (day 1602) to 17th October 2006 (day 1630).

  The injection at atmospheric pressure continued from day 1630. A temporary increase of the injection rate was observed (see Figure 2, page 9) after the re-start of water injection at atmospheric pressure, but the value soon recovered a stable value.

- Fifth phase: Injection valve was closed the 18th June 2007 (day 1874). There was no water injection to the bentonite buffer after that day.

Table 2 shows in detail the effective water inflow.

Table 2. Record of effective inflow to the system for buffer hydration

Date/Phase	Total days of water injection	Volume (litres)	Mean Rate (litres/day)
1st Hydration phase			
6-8 May 2002	2 days	6,700	
2-4 July 2002 (Manual injection)	2 days	50	
Automatic injection			
11-30 September 2002	14 days	287	20.5
October 2002	22 days	473	21.5
November 2002	22 days	524	23.8
December 2002	29 days	742	25.6
January 2003	24 days	732	30.5
February 2003	28 days	730	26.0
March 2003	31 days	820	26.5
April 2003	30 days	730	24.3
May 2003	31 days	666	21.5
June 2003	30 days	768	25.6
July 2003	31 days	751	24.2
August 2003	31 days	151	4.8
September 2003	30 days	681	22.7
1-21 October 2003	21 days	263	12.5
Continuous automatic injection			
22-31 October 2003	10 days	99	9.9
November 2003	30 days	188	6.3
December 2003	30 days	203	6.8
January 2004	20 days	132	6.6
February 2004	28 days	209	7.5
March 2004	31 days	218	7.0
April 2004	30 days	188*	6.3
May 2004	31 days	149	4.8
June 2004	30 days	131	4.4
July 2004	31 days	129	4.2
August 2004	31 days	133	4.3
September 2004	30 days	123	4.1
October 2004	31 days	123	4.0
November 2004	30 days	117	3,9
December 2004	31 days	115	3.7
January 2005	31 days	106	3.4
February 2005	19 days	80	4.2
March 2005	31 days	119	3.8

Date/Phase	Total days of water injection	Volume (litres)	Mean Rate (litres/day)
April 2005	30 days	108	3.6
May 2005	31 days	126	4.1
June 2005	30 days	125	4.1
July 2005	31 days	130	4.2
August 2005	31 days	121	3.9
September 2005	30 days	111	3.7
October 2005	31 days	107	3.4
November 2005	30 days	96	3.2
December 2005	31 days	96	3.1
January 2006	31 days	98	3.2
February 2006	28 days	79	2.8
March 2006	31 days	31	1.0
April 2006	30 days	35	1.2
Continuous injection atmospheric pressure			
May 2006	31 days	-32**[2]	-1.0
June 2006	30 days	4	0.14
July 2006	31 days	9	0.30
August 2006	31 days	1	0.04
September 2006	18 days	1	0.04
October 2006	15 days	5	0.33
November 2006	30 days	0	0.00
December 2006	31 days	0	0.00
January 2007	31 days	0	0.00
February 2007	28 days	0	0.01
March 2007	31 days	0	0.01
April 2007	30 days	0	0.00
May 2007	31 days	0	0.00
June 2007	18 days	0	0.00
Total	**1,660 days**	**18,882 litres**	

[2] There was a temporary inversion of flow, filling the water tank and registering these negative values (positive values mark the water injected to buffer).

Figure 2 shows the daily injection rate versus the average value.

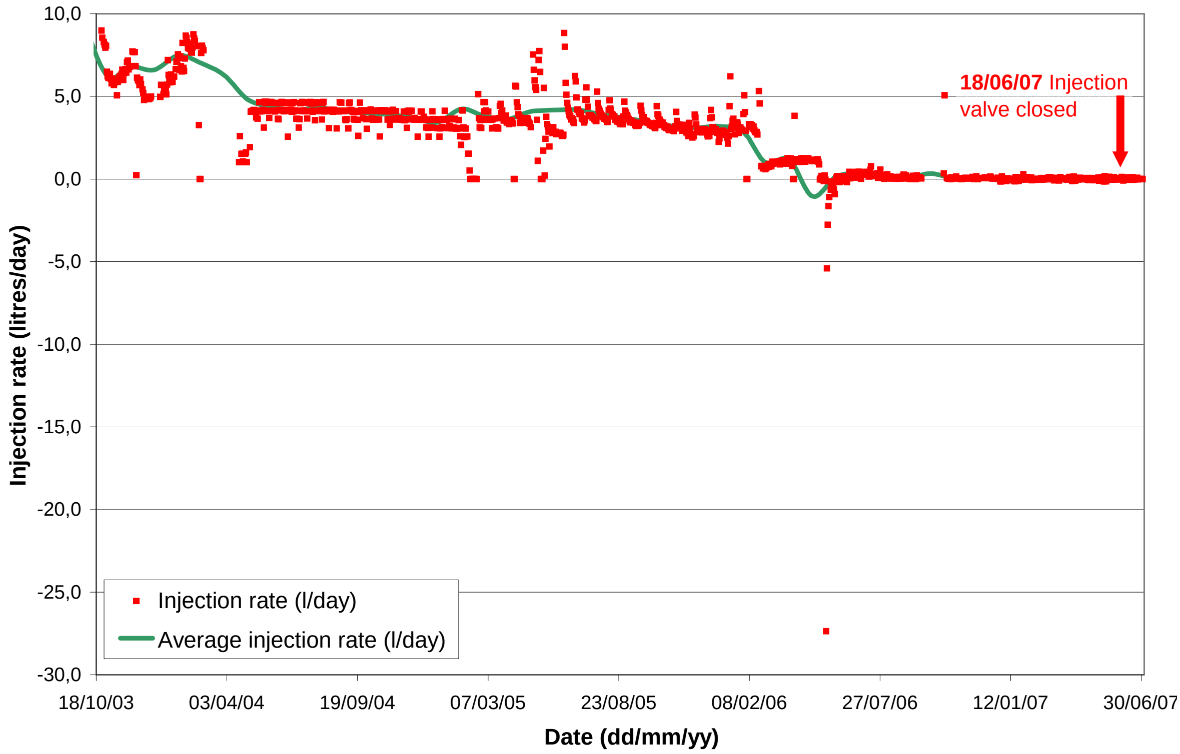

Figure 2. Daily injection rate versus average daily injection rate

Figure 3 shows the temporal evolution of the injection rate and the injection pressure, from the beginning of the continuous injection.

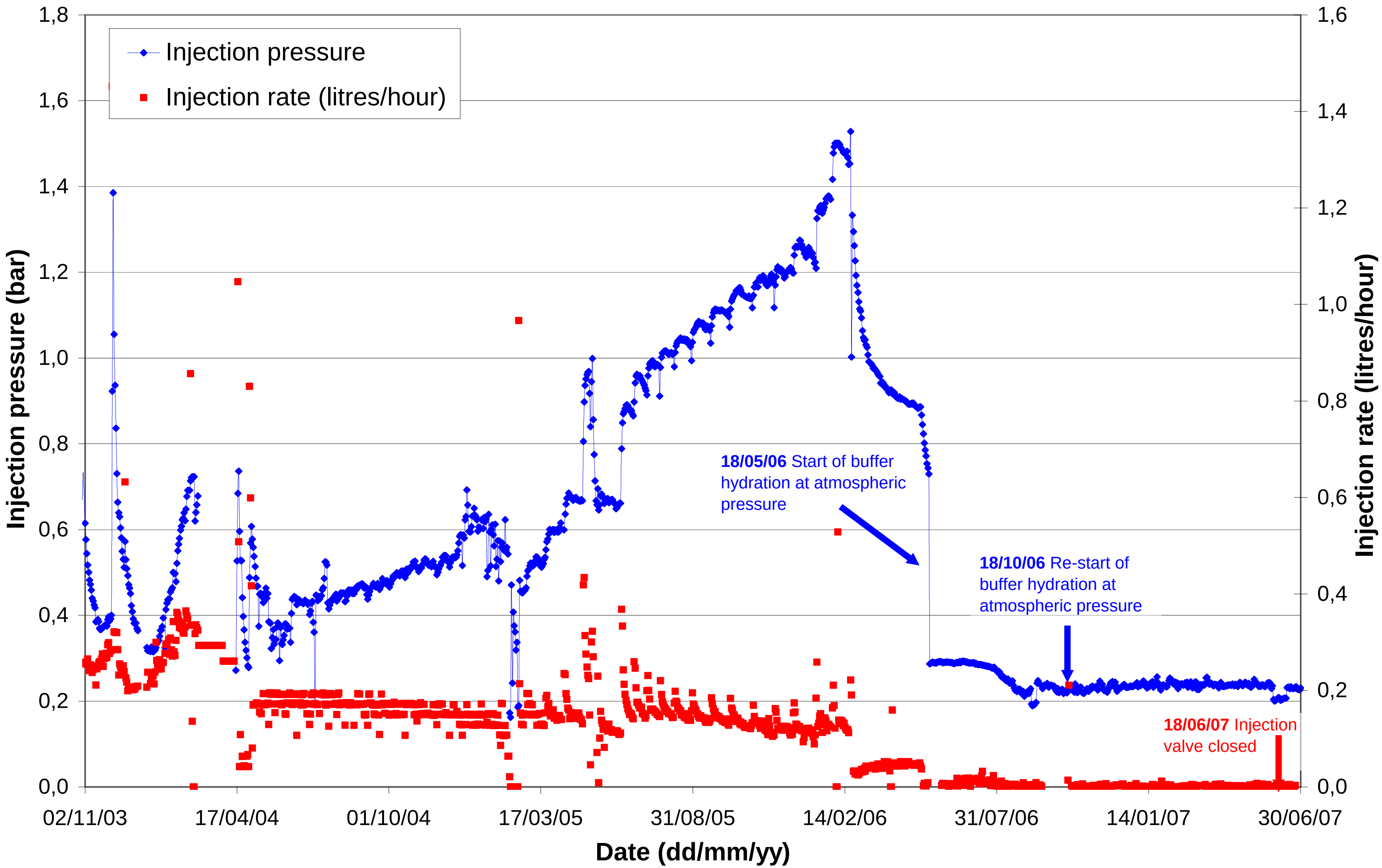

Figure 3. Injection rate versus injection pressure from the start of continuous injection

2.3 EXCAVATION OF GALLERY08

The excavation works performed for Gallery08 from October 2007 to December 2008 influenced some of the parameters measured in the EB experiment. Table 3 details the sequence of the operations carried out, according to information provided by Mont Terri weekly reports elaborated by the Geotechnical Institute.

Table 3. Excavation sequence of Gallery08

Date	Activity / excavation distance reached
29 October 2007	Start of excavation works (enlargement of the ceiling DI niche)
16 November 2007	Tunnel metre Ga08 GM 6
23 November 2007	Tunnel metre Ga08 GM 13
30 November 2007	Tunnel metre Ga08 GM 18.5
7 December 2007	Tunnel metre Ga08 GM 24
14 December 2007	Tunnel metre Ga08 GM 29
21 December 2007	Tunnel metre Ga08 GM 34.5
22 December 07-6 January 08	Christmas holidays
7 January 2008	Re-start after Xmas break
11 January 2008	Tunnel metre Ga08 GM 39
18 January 2008	Tunnel metre Ga08 GM 43.5
January 2008	Tunnel metre Ga08 GM 46
1 February 2008	Tunnel metre Ga08 GM 50.5
1 February 2008	Start of Mine-by test (20 m long section)
8 February 2008	Tunnel metre Ga08 GM 58
February 15 2008	Tunnel metre Ga08 GM 66
20-26 February 2008	Break A (Drilling and instrumentation Mine-by Test (MB) experiment)
27 February 2008	Excavation of SE part of the entrance Niche 1
7 March 2008	Tunnel metre Ga08 GM 79
14 March 2008	Tunnel metre Ga08 GM 86.50
20 March 2008	Tunnel metre Ga08 GM 93
21 to 24 March 2008	Eastern holidays
25 and 26 March 2008	RC experiment niche
26 March 2008	Tunnel metre Ga08 GM 93.5
31 March to 21 April	Break B (drilling campaign RC and MB experiments)
22 April 2008	Re-start of excavation
25 April 2008	Tunnel metre Ga08 GM 101
30 April 2008	Tunnel metre Ga08 GM 105.1
9 May 2008	Tunnel metre Ga08 GM 111
14 May 2008	Tunnel metre Ga08 GM 114
15 May 2008	Stop of excavation. Lining installation Ga08 GM 98 to GM 110
15 and 16 May 2008	8 cm of shotcrete
19 May 2008	7 cm thick shotcrete
22 and 23 May 2008	No excavation (holidays in Canton of Jura)
30 May 2008	Tunnel metre Ga08 GM 124
6 June 2008	Tunnel metre Ga08 GM 127
20 June 2008	Tunnel-metre Ga08 GM 138

Date	Activity / excavation distance reached
27 June 2008	Tunnel metre Ga08 GM 144
05 July 2008	Tunnel metre Ga08 GM 151
11 July 2008	Tunnel metre Ga08 GM 159
17 July 2008	No excavation (emplacement of invert concrete GM 88 - GM 130)
25 July 2008	No excavation
5 August 2008	Excavation from 29 of July, tunnel metre Ga08 GM 163
22 August 2008	Tunnel metre Ga08 GM 166.5
25 August 2008	End of Ga08 excavation
1 to 5 of September 2008	Enlargement of the Gallery 08 from GM 167 to GM 157
8 to 17 of September 2008	Excavation of Niche 1 (DR-A)
22 September to 10 Oct 2008	Excavation of Niche 4 up to GM 12
13 October to 7 Nov 2008	Excavation of Niche 2 (MB)
10 to 26 November 2008	Excavation of Niche 4 from GM 12 to GM 22
27 Nov to 5 of Dec 2008	Excavation of Niche 3
8 to 17 December 2008	Renovation works. New shotcrete applied (rear end of the DR-A Niche, entrance of Niche 3 and 4, RC and DI Niches and ceiling between the MB RC Niches
18 December 2008	End of construction and renovation works

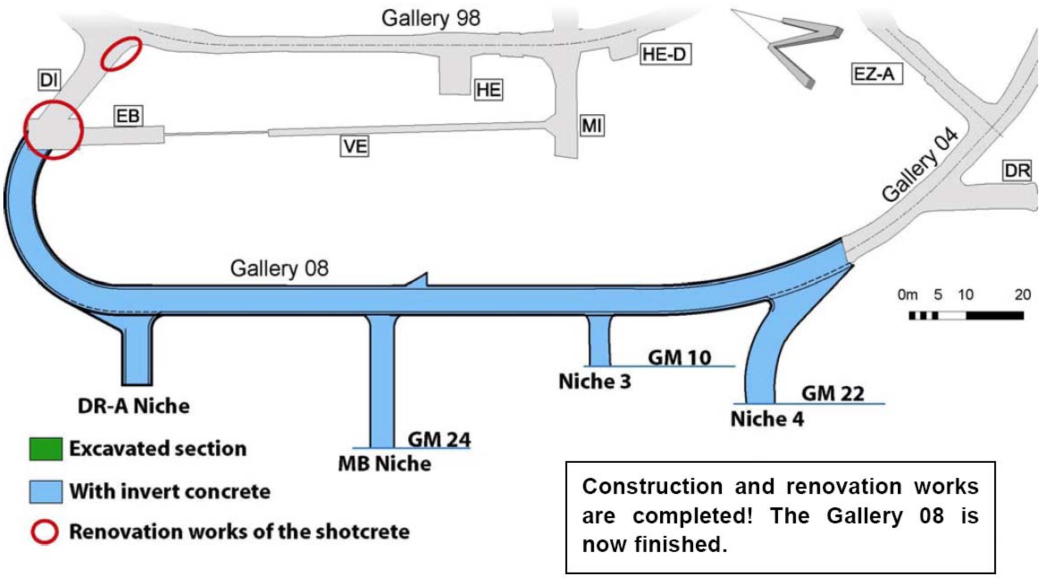

Figure 4. Gallery08 layout. Status of construction and renovation works 18/12/08

3 STATUS

The situation of EB experiment buffer saturation was quite stable since the stop of water injection on the 18th June 2007, day 1874.

Temperature and relative humidity measured by rock and bentonite buffer sensors remained steady and no significant movements were detected in any of the extensometers (rock and canister).

Total pressure cells' values were also stable up to the start of the dismantling operation.

3.1 DATA LOSSES

The record of all data losses is detailed below; there was one data loss during this period.

Data losses from the start of the data acquisition:

- 10th to 21st July 2002 (days 70 to 81): software problems, solved by re-installation.
- 31st December 2002 to 2nd January 2003 (days 244 to 246): failure in PC re-start.
- 31st December 2003 to 7th January 2004 (days 610 to 616): failure of the data logging unit. The water injection continued.
- 6th March 2004 to 15th April 2004 (days 675 to 715): general failure of the computer. Computer changed.
- 2nd to 10th September 2007 (days 1950 to 1958): failure of driver due to electrical failures.
- 3rd to 29th November 2007 (days 2012 to 2038): power supply problems in MT URL.
- 9th to 20th May 2008 (days 2200 to 2211): failure of automatic re-start of PC and consequent driver failure.
- 7th to 16th June 2008 (days 2229 to 2238): general power failure in MT URL.
- 21st July 2008 (day 2273): general power failure in Jura region.
- 1st to 3rd August 2008 (days 2284 to 2286): general power failure in MT URL.
- 3rd to 19th March 2009 (days 2498 to 2514): general power failure in MT URL.
- 31st March to 1st April 2009 (days 2526 and 2527): driver failure after re-start of PC.
- 10th to 13th July 2009 (days 2627 to 2630): driver failure.
- 9th September to 14th October 2009 (days 2688 to 2724): driver failure.
- 14th and 15th October 2009 (days 2724 and 2725): PC failure[3].
- 27th to 30th November 2009 (days 2767 to 2770): PC failure.
- 23rd to 27th December 2009 (days 2793 to 2797): PC failure.
- 9th to 11th April 2010 (days 2900 to 2902): PC failure.
- 13th to 16th July 2010 (days 2995 to 2998), 11th August 2010 (day 3024): PC failure.
- 8th September 2010 (day 3052): PC failure.
- 4th June to 8th June 2012 (days 3687 to 3691): driver failure.
- 24th July to 25th July 2012 (days 3737 and 3738): driver failure.

Web based connection via Andra's SAGD network was available since the 27th Nov2009.

[3] There was a problem with the laboratory's telephone line which left the EB computer out of remote control via modem, from the 1st Sept. to the 16th Nov. 2009, preventing the solution of data acquisition errors.

There was an additional data loss the last week of April 2002 in those sensors whose data were collected from November 2001 by means of data loggers, and it corresponds to the temporary disconnection from the dataloggers for their connection to the data acquisition system.

4 SENSOR DATA

The data acquisition system started to collect data the 30 April 2002 (day -1 in the graphs), after the completion of the installation and connection of all sensors. Data available for some sensors previously installed in rock were collected from November 2001 to April 2002 by means of data loggers specially provided for this purpose.

Temperature

All the sensors used in the experiment include temperature probes, except the in-rock pore pressure ones.

Sections A1, B1, E, B2 & A2 (pages 19 to 23): After the start of water injection there was a clear temperature increase that might be due to plug's concrete curing and previous preparatory works, reaching a maximum peak of 28 ºC in Section A2. In general, after that initial peak –after the curing process– the temperature registered after the starting of buffer's hydration remained at about 4 ºC above than the values recorded in the beginning of data collection for a period of three months. After this time, temperature did progressively recover the initial values and was almost constant until the end of the recording phase. The average temperature value in the buffer was 16.23 ºC on the 31st October 2013, previous to the dismantling operation.

Relative Humidity

Relative humidity sensors of the capacitive type were installed in sections A1, B1, A2 and B2. These sensors were placed inside several boreholes excavated in rock, in the bentonite blocks and in the granular bentonite backfilling.

The saturation state was gradually achieved by all sensors after the start of the hydration phase; 100% R.H. was reached in all sensors after three years of operation. At the end of the operation phase all sensors were reliable except *WB1/2, WB1/4, WB2/4 and WB24-1.0.* See graphs in pages 24 to 30.

Displacement

There are two kinds of displacement sensors installed: extensometers placed to measure the movements of the canister and extensometers installed in rock to track possible deformations.

Canister movements

Sections A1&A2 (pages 28 and 29). The canister moved upwards in the beginning of data acquisition period.

In section A1 (canister front end), the initial up levelling movement had a value of around 2 mm (see EA1/2) and no horizontal movement was registered up to October 2002 (start-up of the second phase of hydration, day 153). Afterwards, the displacement continued but the movement seemed to have stopped again from September 2005. The displacement in EA1/2 (vertical position) re-started in October 2006 and continued up to December 2007. Since the start of year 2008 the movement was almost negligible (less than 0.35 mm per year).

Besides, the front part of the canister seemed to move to the left, clearer from October 2002.

As in section A1, the position reached in section A2 (canister rear end) with the mentioned initial up levelling movement was of 8 mm in EA2/2 and it was maintained from the start of hydration until October 2005, when the trend changed. From this month, small movements were detected in EA2/2.

A left to right movement was recorded in section A2 up to December 2006. There are no data from EA2/1 since 11/12/08 (day 2416). The sensor was considered out of order from that date.

Note: The horizontal movements might be related to the different densities of the granular material at both sides of the dummy canister. The vertical movements might be caused by the difference of density between the blocks and the granular material.

Relative displacements have been represented versus time (see Figure 5).

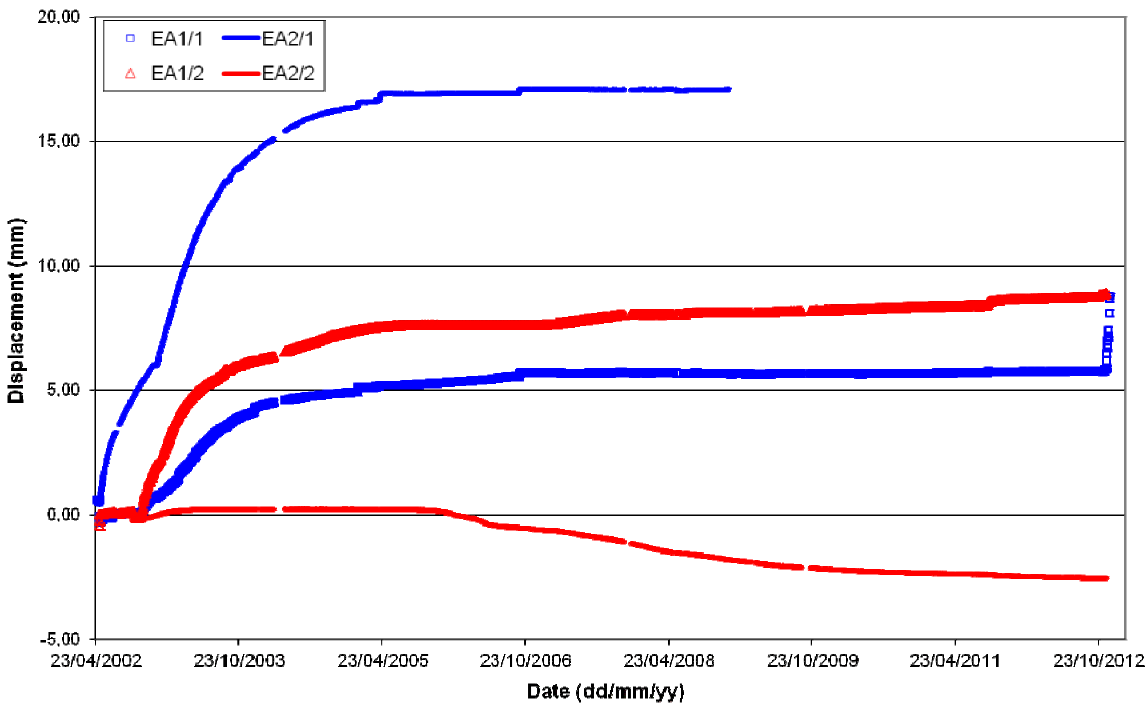

Figure 5. Relative movement of canister displacement transducers (Sections A1 & A2)

According to recorded data there was a total up levelling of the dummy canister of almost 1 cm in the front while a sinking of 2-3 mm in the rear part. In parallel there was a movement towards the left hand side (looking from gallery entry) of 6 mm in the front and of around 17 mm towards the right hand side in the rear part.

Rock movements

Section E (page 30). Three pairs of rock extensometers anchored to the rock surface and to depths of 1 m and 2 m were installed, one pair at the ceiling of the gallery and another one at each side of the wall.

From the start of data recording period, and stated that deeper anchors are fixed points, a small elevation of the upper part of the niche was detected, stabilising in May 2003 at 1.7 mm from the original position (EB13-1.0 and EB13-2.0). Afterwards, a change in this trend was registered, and both sensors started to move backwards. Since the end of 2004 the rock extensometers are almost stabilized and no significant changes have been detected, with no appreciable variation in any of them for the last seven years.

Accumulated displacements are an elevation of the roof of less than 1.2 mm and a closing of the gallery walls of around 1.5 mm in the left hand side and of 1 mm in the right one.

Rock Pore Pressure

Two types of pore pressure sensors were installed, in the rock and in the EDZ. The evolution of pressures is shown in their corresponding data plots (see pages 31 to 34).

Rock sensors

Inclined boreholes: BEB-2, section B1 (page 31) and BEB-21, section B2 (page 33), both located in the same position of the two boreholes: All sensors detected gradual pressure increases from the start of data recording period until the end of water injection, being the increase cause of the recovery of the rock water pressures. Pressure was almost stable in the last three years with small variations. The maximum final pressure value was recorded by sensor QB21-3.0, 10.55 bar abs.

Vertical boreholes: BEB-3, section B1 (page 32) and BEB-22, section B2 (page 34): As in the case of inclined boreholes, the pressure increase was gradual in all sensors. The maximum final pressure value was recorded by sensor QB22-3.0, 11.30 bar abs, being the general evolution the expected for this kind of clay. An additional pressure change can be seen in August 2011 (23rd to 25th August, days 3767 to 3769), during the drilling of the investigation pilot borehole previous to the dismantling.

EDZ sensors

Sections C1&C2 (pages 35 and 36): the pressure evolution along the recording period was related with the rock pressure recovery for deepest ones and with the buffer injection water for those closer to the surface[4]. The maximum pressure was registered by sensor QB17-0.9, 2.81 bar abs.

The excavation works of Gallery08 caused several perturbations to pore pressures, which seem now to stabilize values to those present before the works. The variations can be seen in the pore pressure graphs from 29th October 2007 (day 2007) to 18th December 2008 (day 2423). These sensors also detect the pressure variations caused by the drilling of investigation borehole in August 2011.

Except for the variations explained due to mentioned external reasons the remaining ones are considered normal in this type of rock.

[4] Data from piezometer QB5-0.5 were considered not reliable since October 2003. However, from 16th June 2007 (day 1872), data seem to be valid and have been included in the graph.

Total pressure

Eight total pressure cells were installed in section E (page 37). In general, pressures showed a gradual increase from the start of buffer hydration the 6th May 2002 (day 5) up to reach values that range roughly from 1.5 to 2.2 MPa.

Total pressure increased gradually in all sensors from the start of the hydration of the buffer. The maximum total pressure was registered in the sensors installed on the top of the canister (PE/1) and under the bentonite blocks' bed (PE/6), with values of 22.06 and 22.08 bar abs respectively the 31st October 2012, last day of operation before the dismantling started.

The drilling of investigation borehole in August 2011 (23rd to 25th August, days 3767 to 3769) was "seen" in the total pressure cells with a small variation, showing the buffer is sensitive to small changes in the conditions.

Several changes were detected during dismantling operation. The possible explanation is that bentonite barrier was continuously swelling after being uncompressed with the consequent increase of volume and proportional decrease of saturation degree. See Figure 6 for further detail.

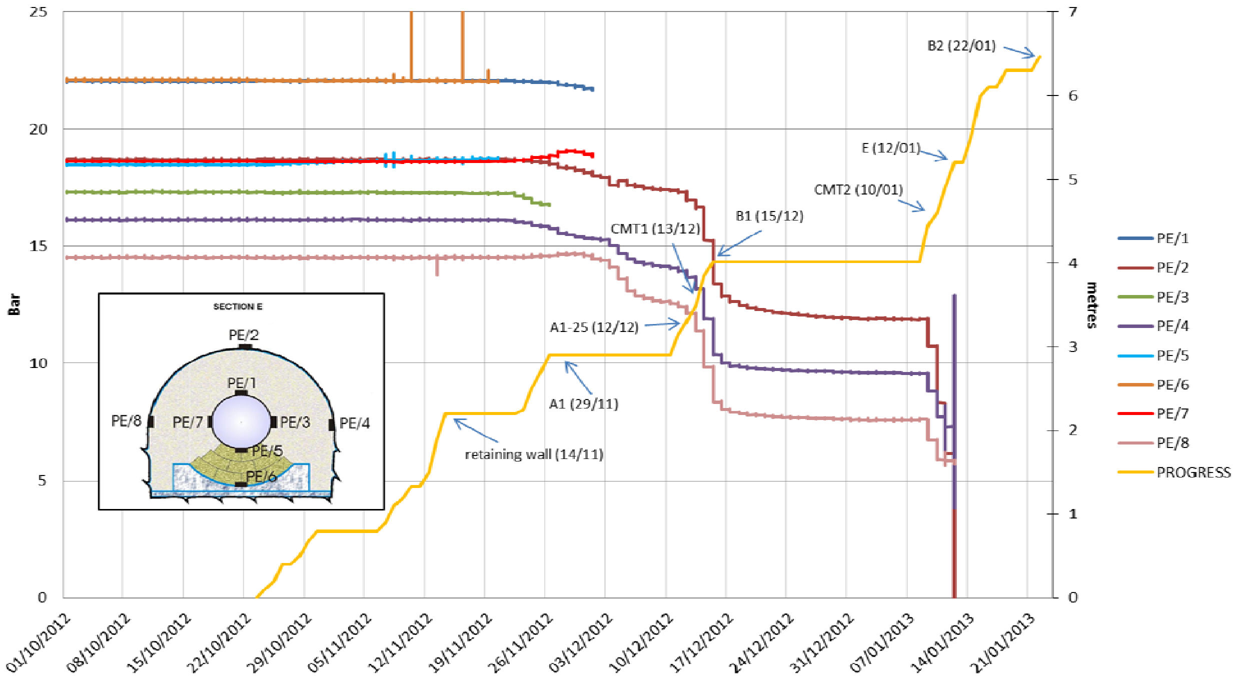

Figure 6. Total pressure evolution versus progress of dismantling operation

Failure of sensors

Before the start of the dismantling operation, the following sensors had failed:

- WB1/2 and WB1/2T: Last data on 31st October 2005 (day 1440);
- WB1/4 and WB1/4T: Last data on 31st October 2005 (day 1440);
- WB2/4 and WB2/4T: Last data on 10th February 2006 (day 1542);
- WB24-1.0 and WB24-1.0T. Last data 4th October 2007 (day 1982);
- EA2/1: Last data 10th December 2008 (day 2415).

LOCATION Section A1

SENSOR TYPE: Temperature (Buffer and Rock) *UNITS: ºC*

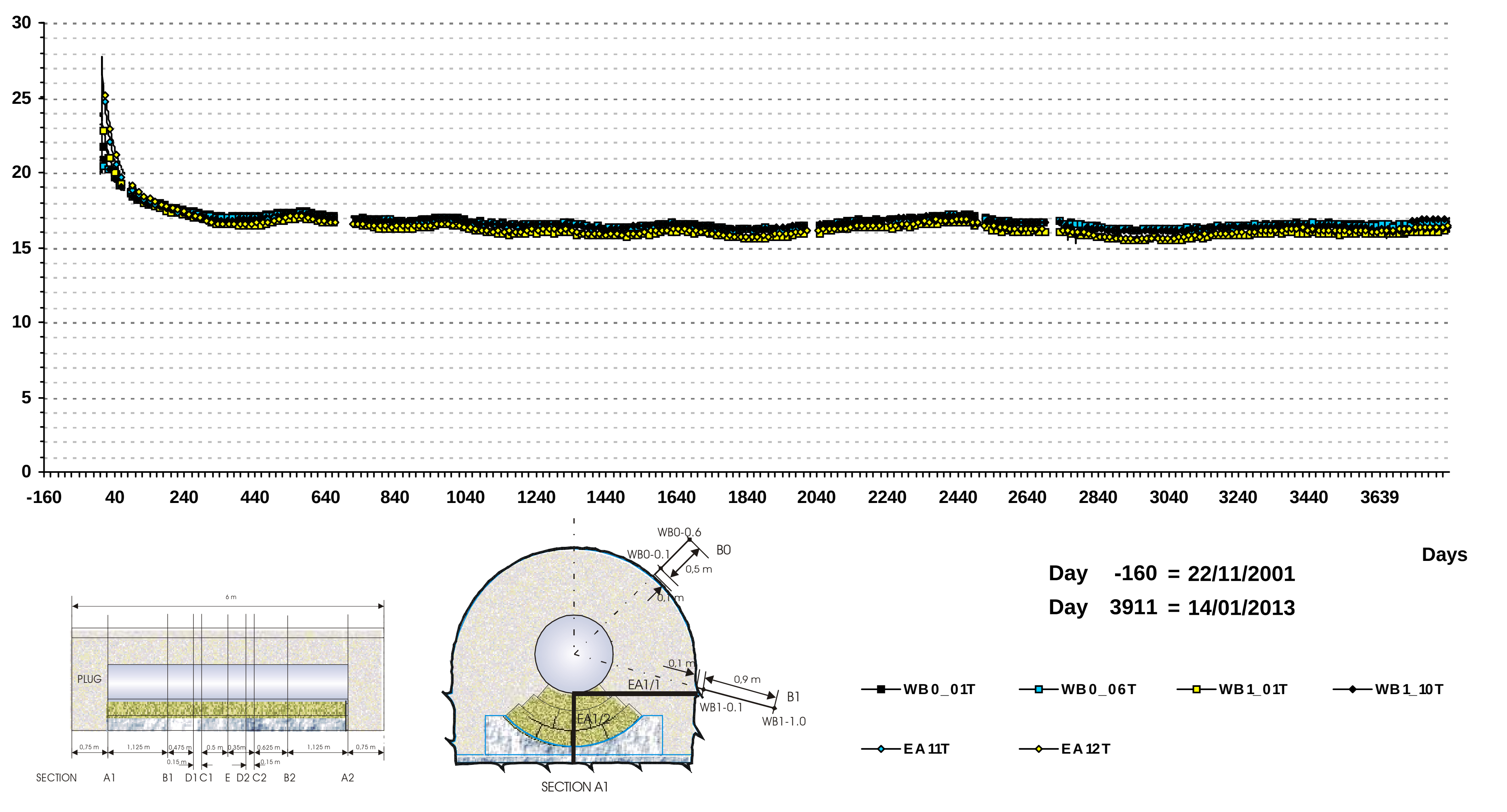

COMMENTS:

Rock sensors installed 20 November 2001, but temperature data recorded from 30 April 2002 (day -1).

Buffer sensors installed April 2002 and data recorded from 30 April 2002 (day -1).

LOCATION ***Section B1***

SENSOR TYPE: Temperature (Buffer) ***UNITS: ºC***

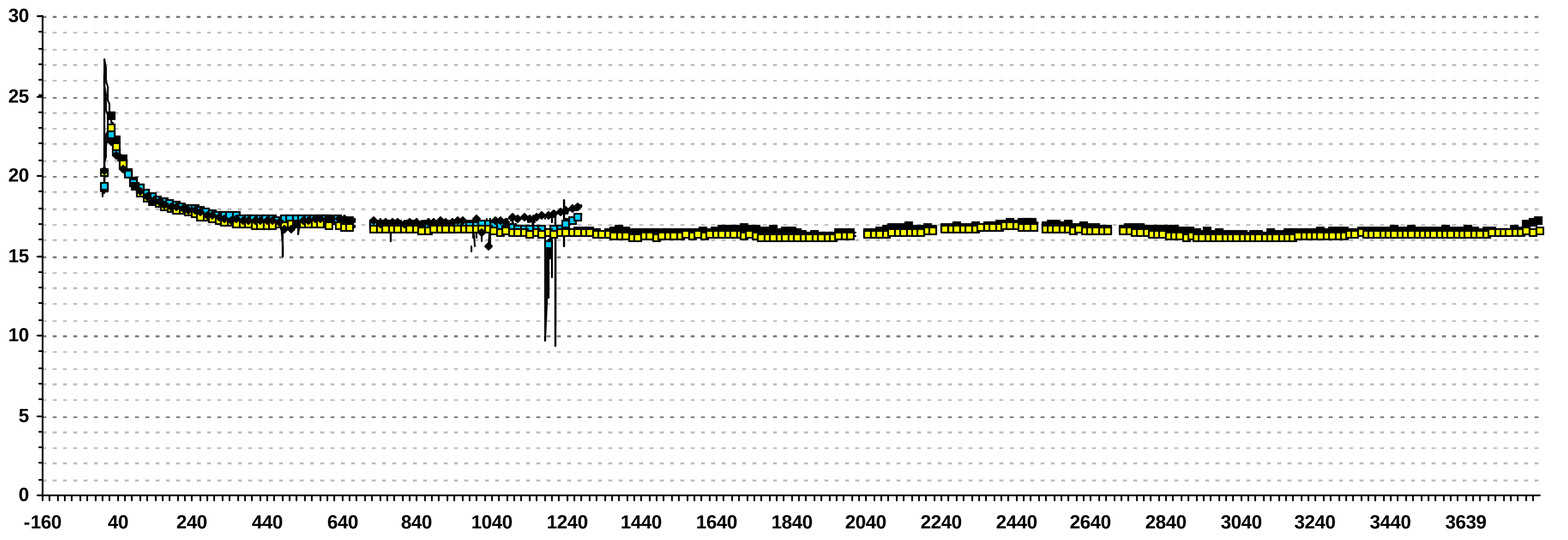

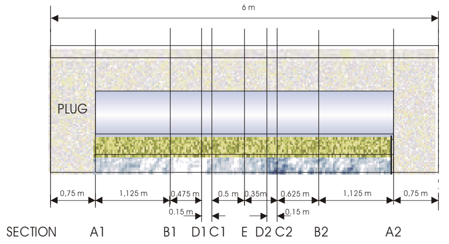

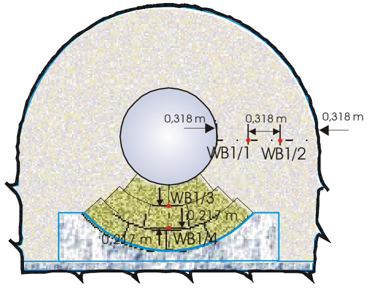

SECTION B1

COMMENTS:

Sensors installed April 2002. Data recorded from 30 April 2002 (day -1).

WB1/4T: Data not reliable from 22nd August to 4th December 2003 (days 478 to 482).

WB1/2T and WB1/4T: Data not reliable from 1st November 2005 (day 1280). Data eliminated from graph.

LOCATION **Section E**

SENSOR TYPE: Temperature (Buffer) **UNITS: ºC**

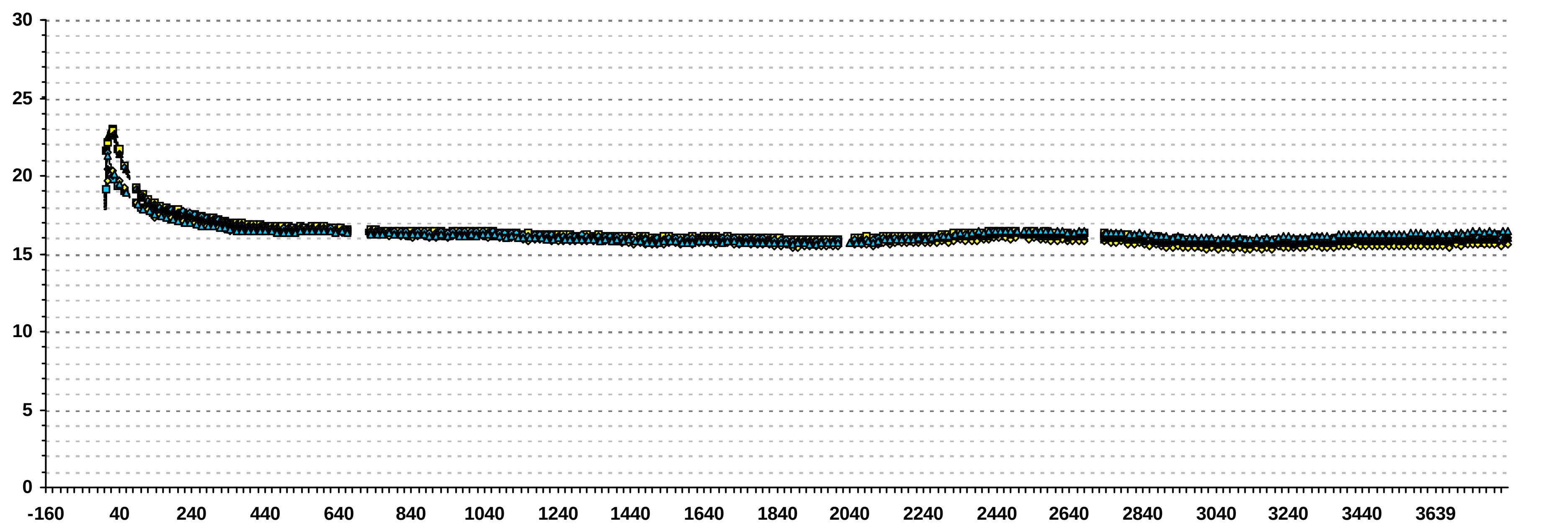

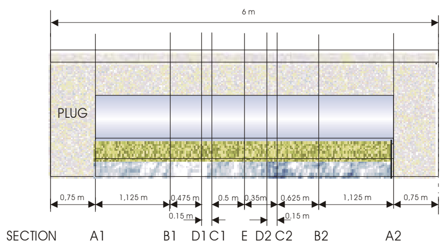

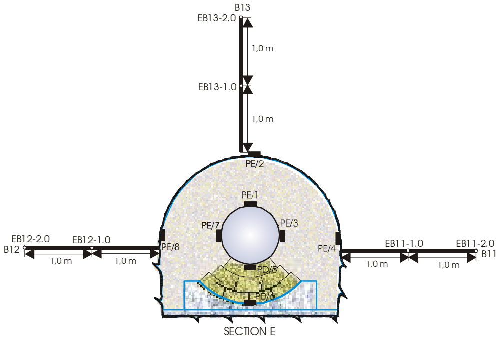

COMMENTS:
Pressure cells installed February 2002. Data recorded from 30 April 2002 (day -1).

LOCATION **Section B2**

SENSOR TYPE: Temperature (Buffer) **UNITS: ºC**

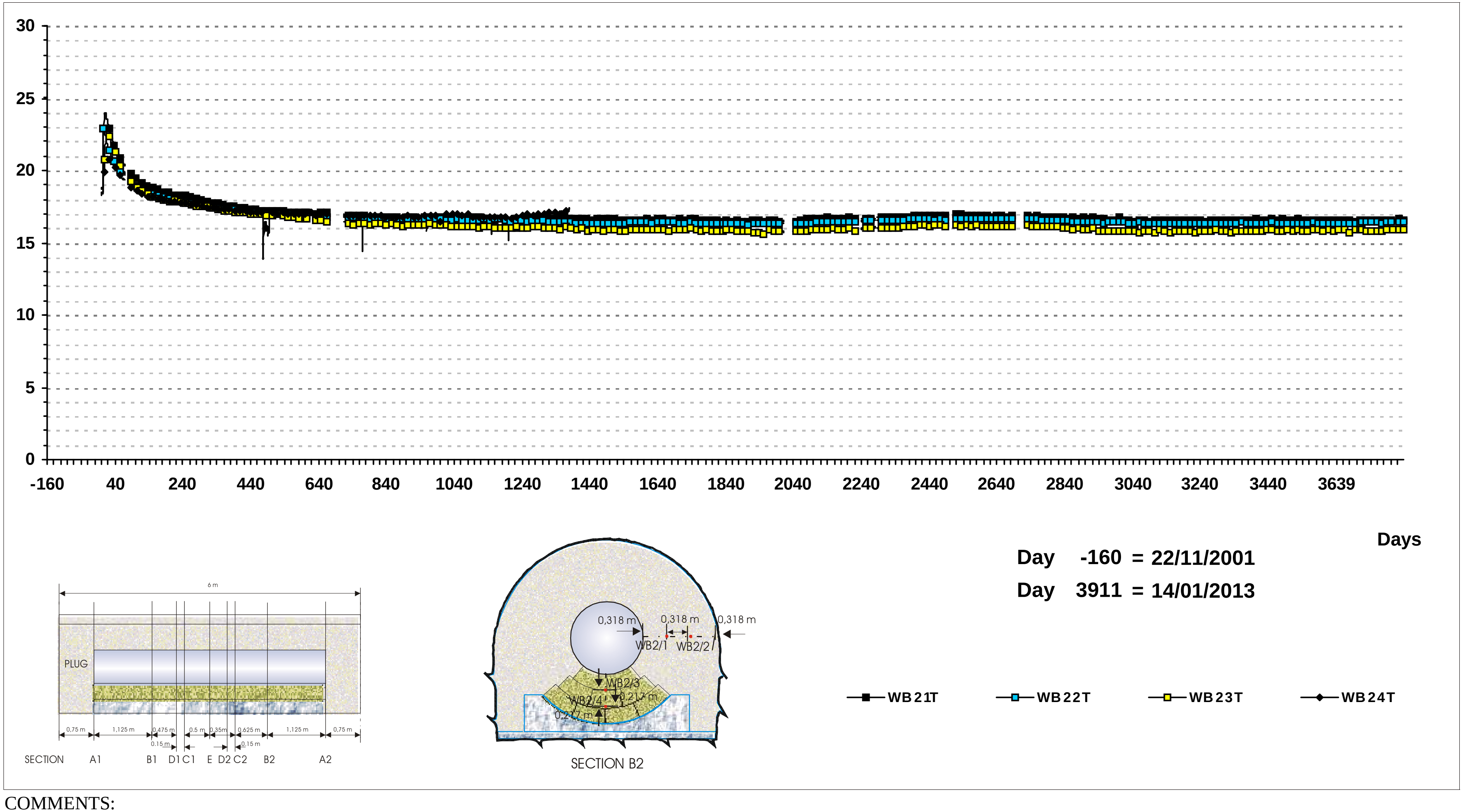

COMMENTS:

Sensors installed April 2002 but temperature data recorded from 30 April 2002 (day -1).

WB2/4T: Data not reliable from 20th August 2003 to 4th December 2003 (days 476 to 482).

WB2/4T: Data not reliable from 11th February 2006 (day 1383). Data eliminated from graph.

LOCATION **Section A2**

SENSOR TYPE: Temperature (Buffer and Rock) **UNITS: ºC**

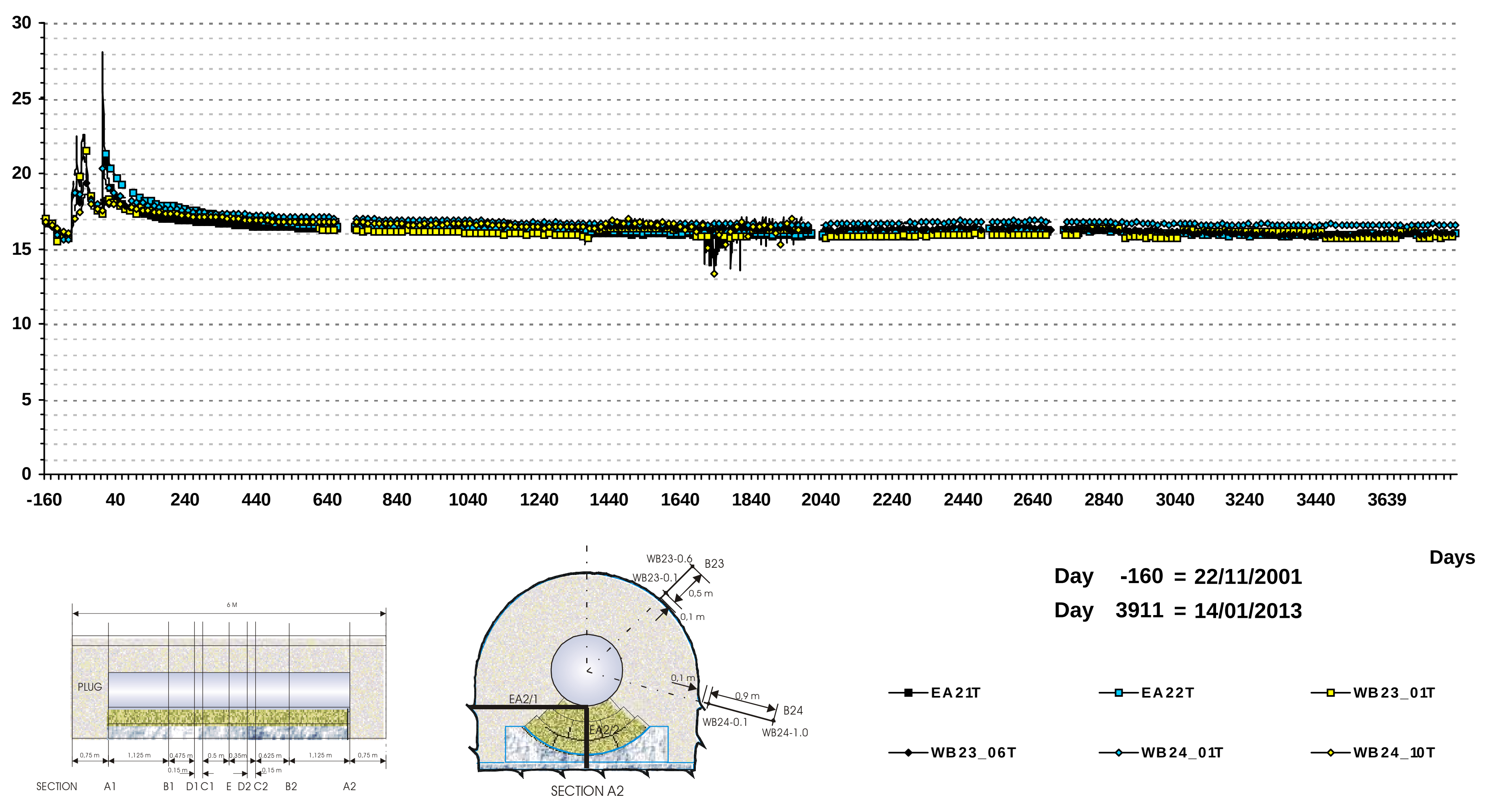

COMMENTS:
Sensors installed 20 November 2001. Temperature data available from 22 November 2002 (day -160).
No data from 28th April to 5th May 2002 (days -3 to 4) during connection of sensors to Data Acquisition System.
No data from 31st December 2003 to 7th January 2004 (days 610 to 616) due to failure of data logging unit.
WB24-1.0T: Data not reliable from 5th October 2007 (day 1983). Data eliminated from graph.

LOCATION **Section A1**

SENSOR TYPE: Relative Humidity (Rock) **UNITS: % R.H.**

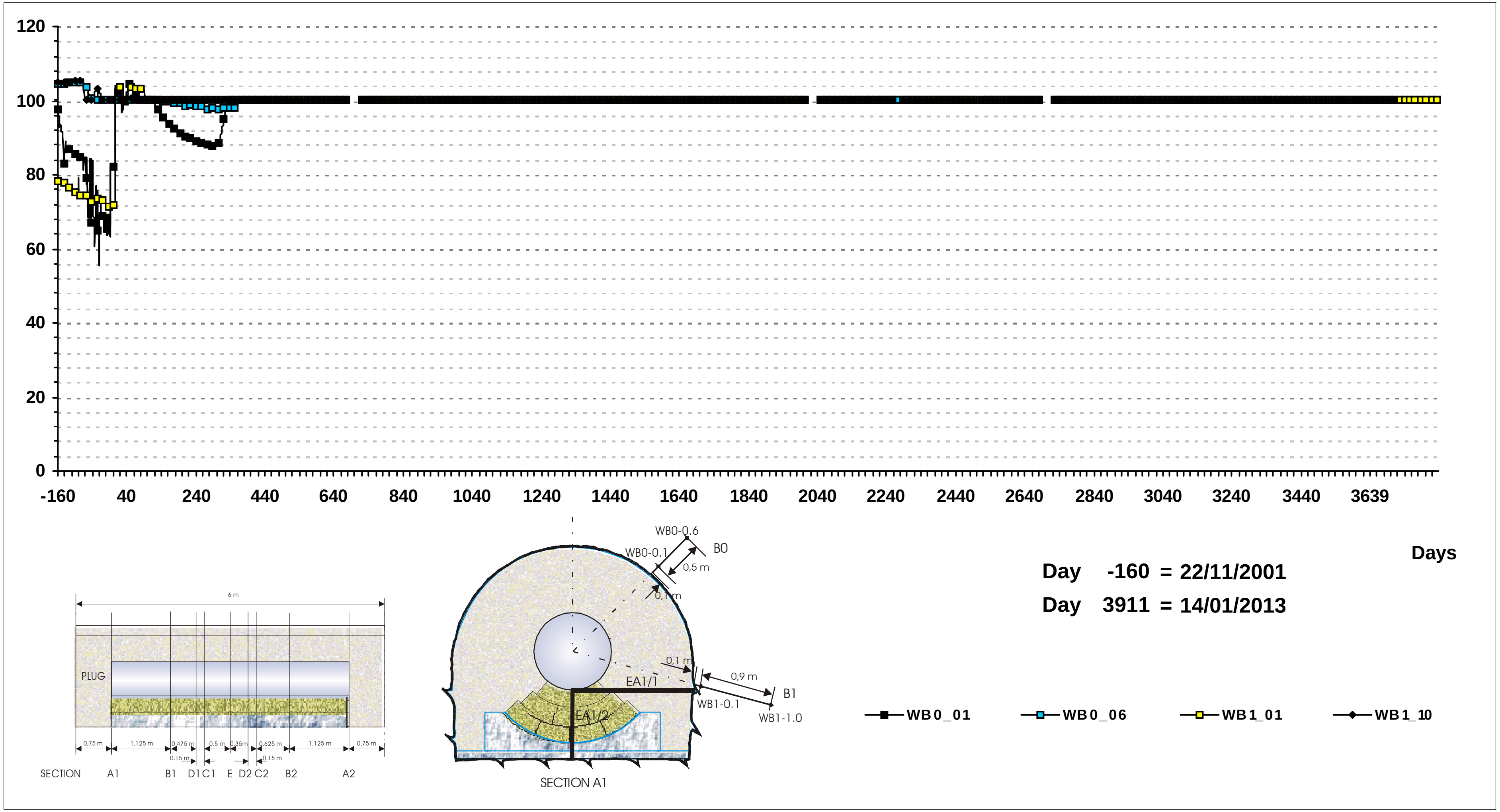

COMMENTS:

Sensors installed 20 November 2001. Data available from 22 November 2002 (day -160).

No data from 28th April to 5th May 2002 (days -3 to 4) during connection of sensors to Data Acquisition System.

No data from 31st December 2003 to 7th January 2004 (days 610 to 616): failure of data logging unit.

LOCATION **Section B1**

SENSOR TYPE: Relative Humidity (Buffer) **UNITS: % R.H.**

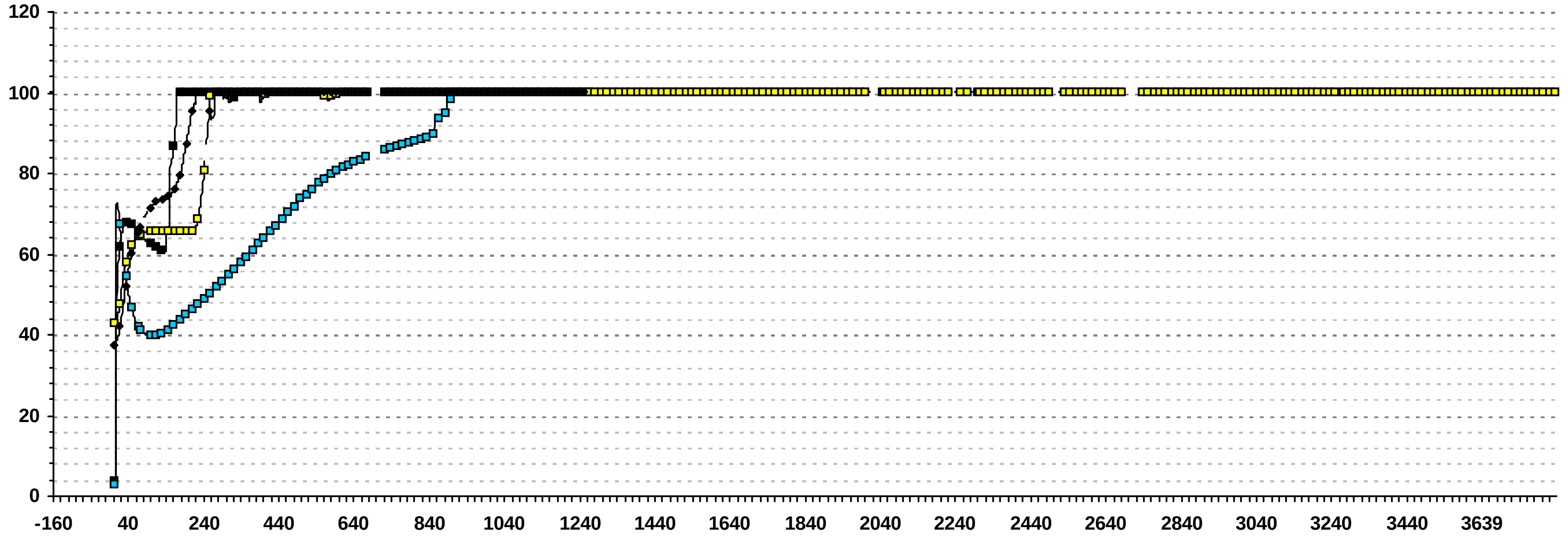

Day -160 = 22/11/2001
Day 3911 = 14/01/2013

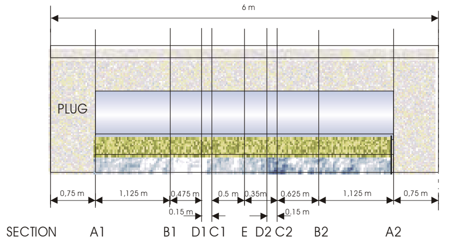

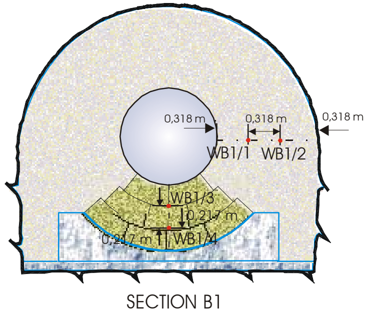

WB 11 WB 12 WB 13 WB 14

COMMENTS:

Sensors installed February 2002. Data available from 30 April 2002 (day -1).

WB1/2 and WB1/4: Data not reliable from 1st November 2005 (day 1280). Data eliminated from graph.

LOCATION Section B2

SENSOR TYPE: Relative Humidity (Buffer) ***UNITS: % R.H.***

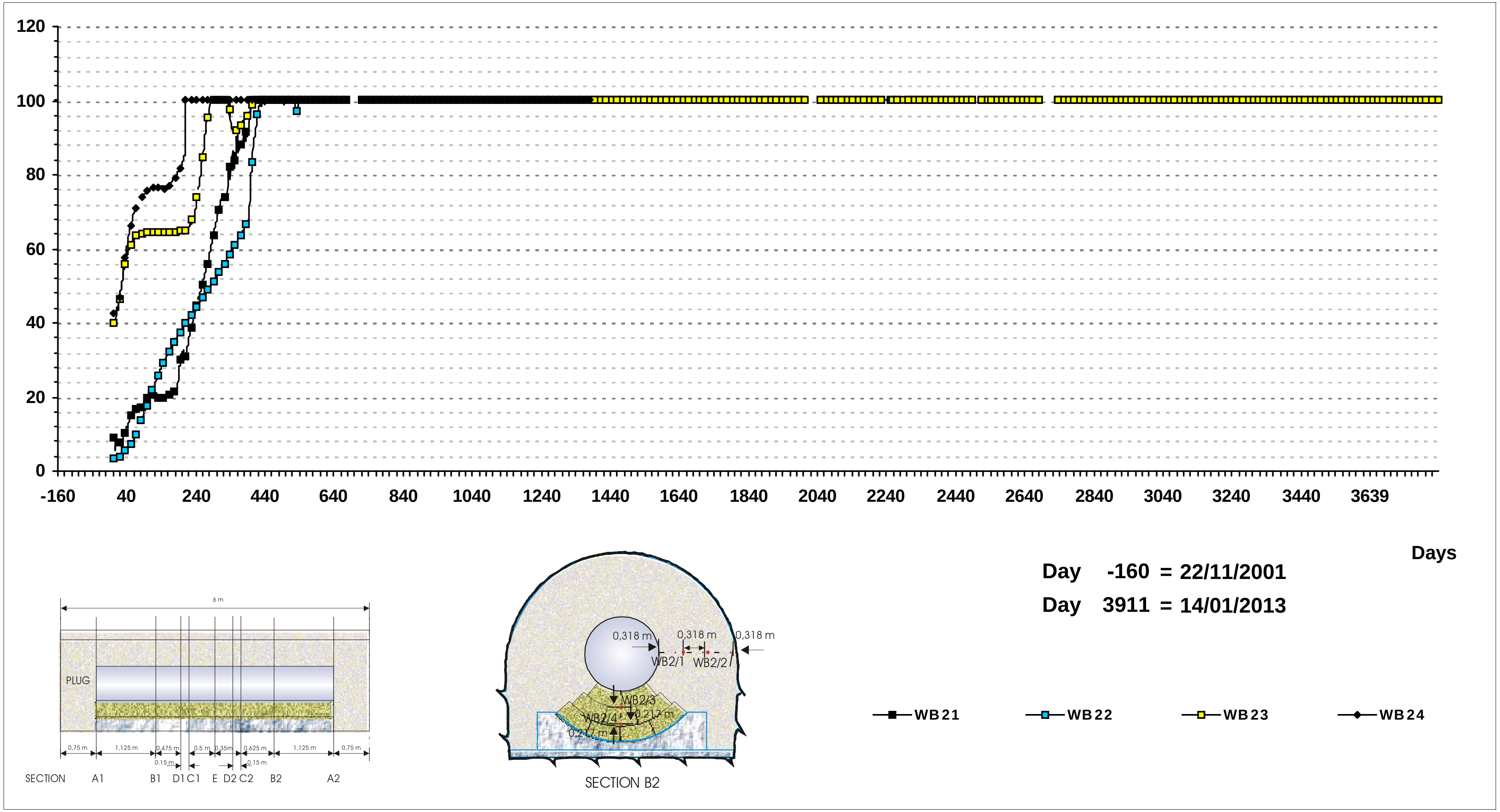

COMMENTS:

Sensors installed February 2002. Data available from 30 April 2002 (day -1).

WB2/4: Data not reliable from 11th February 2006 (day 1383). Data eliminated from graph

LOCATION Section A2

SENSOR TYPE: Relative Humidity (Rock) **UNITS: % R.H.**

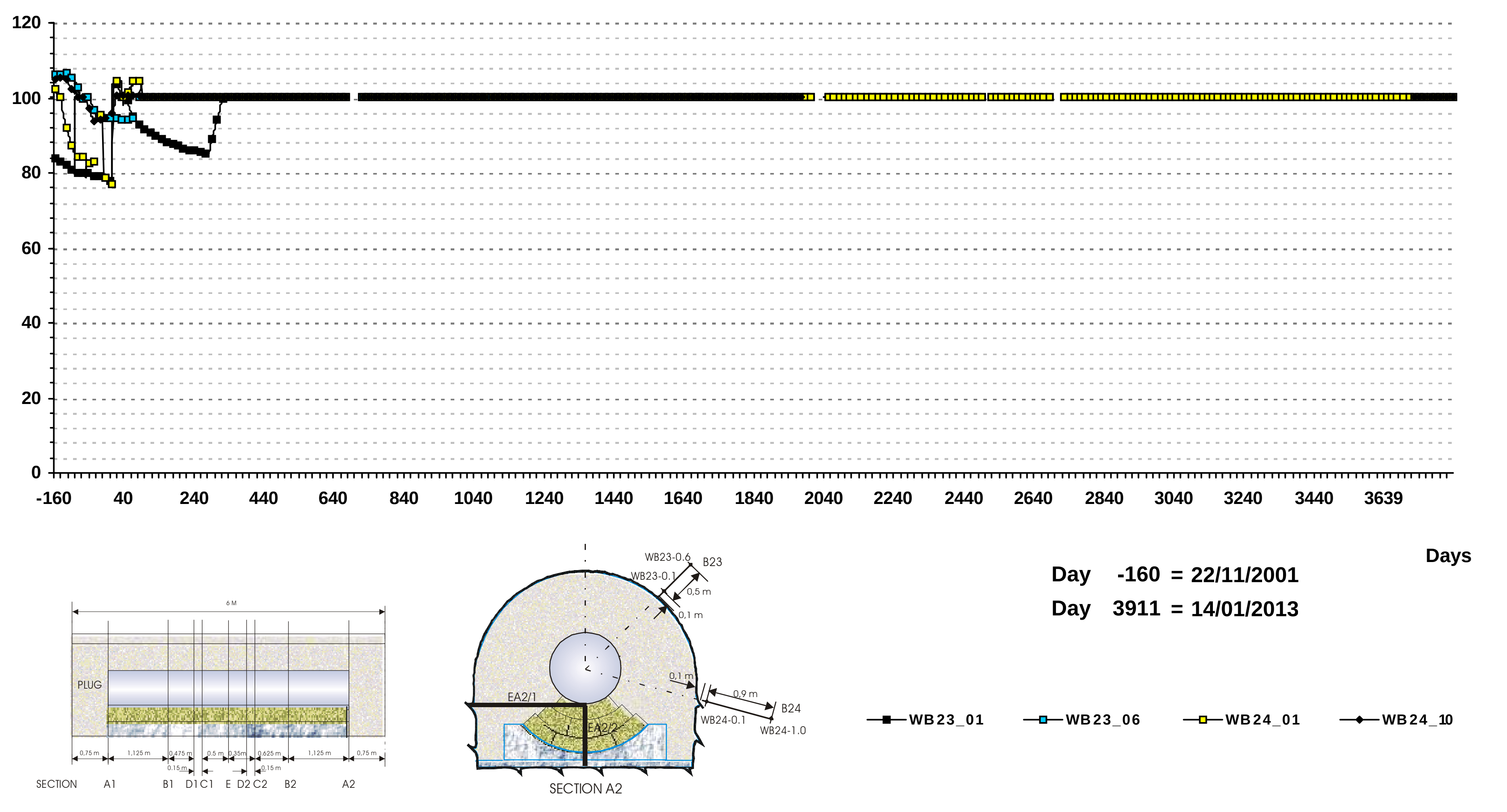

COMMENTS:

Sensors installed 20 November 2001. Data available from 22 November 2002 (day -160).

No data from 28th April to 5th May 2003 (days -3 to 4) during connection of sensors to Data Acquisition System.

WB24-1.0: Data not reliable from 5th October 2007 (day 1983). Data eliminated from graph.

LOCATION **Section A1**

SENSOR TYPE: Displacement (Canister) **UNITS: mm**

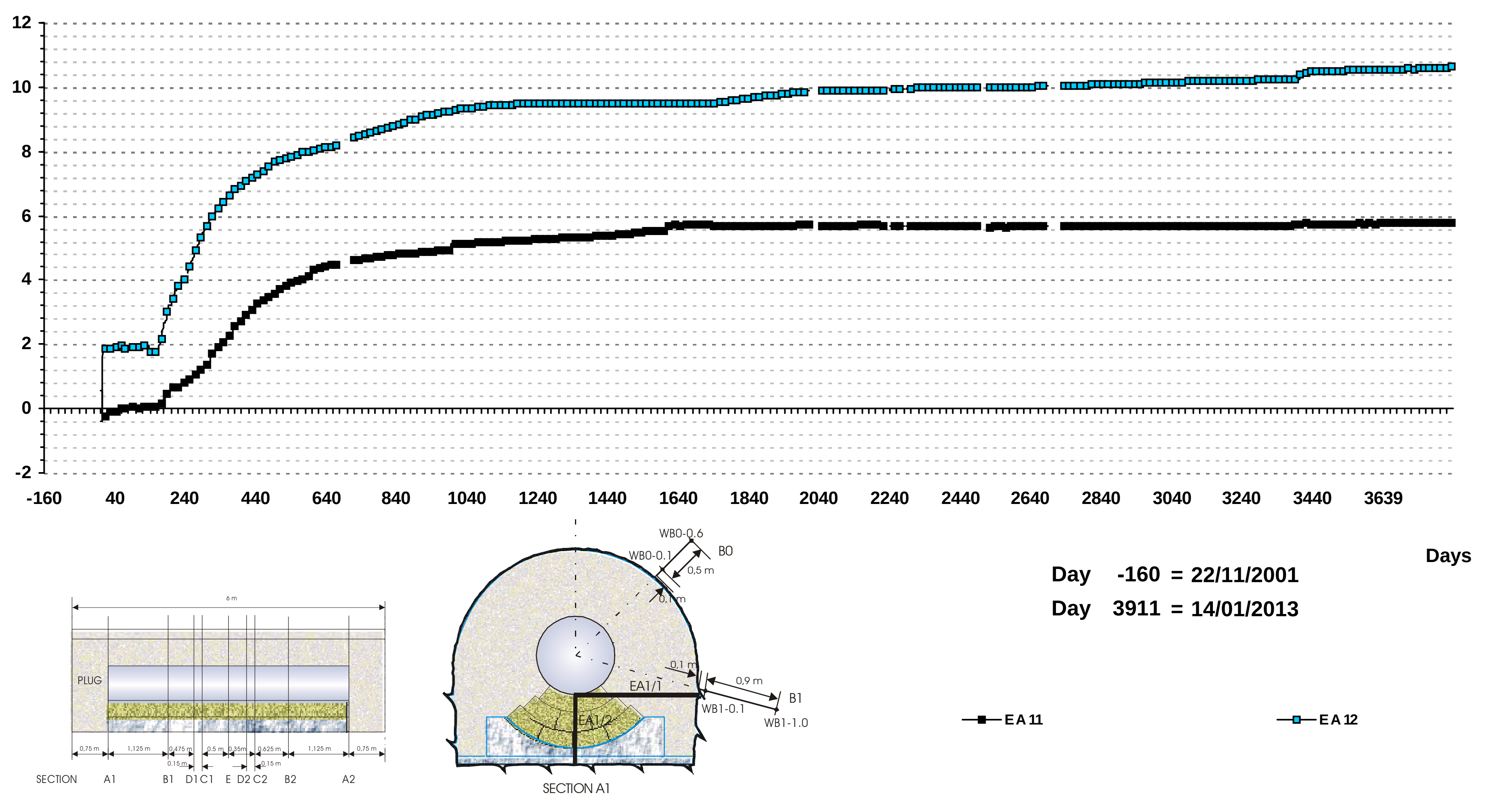

COMMENTS:

Sensors installed February 2002. Data available from 30 April 2002 (day -1).

LOCATION ***Section A2***

SENSOR TYPE: Displacement (Canister) ***UNITS: mm***

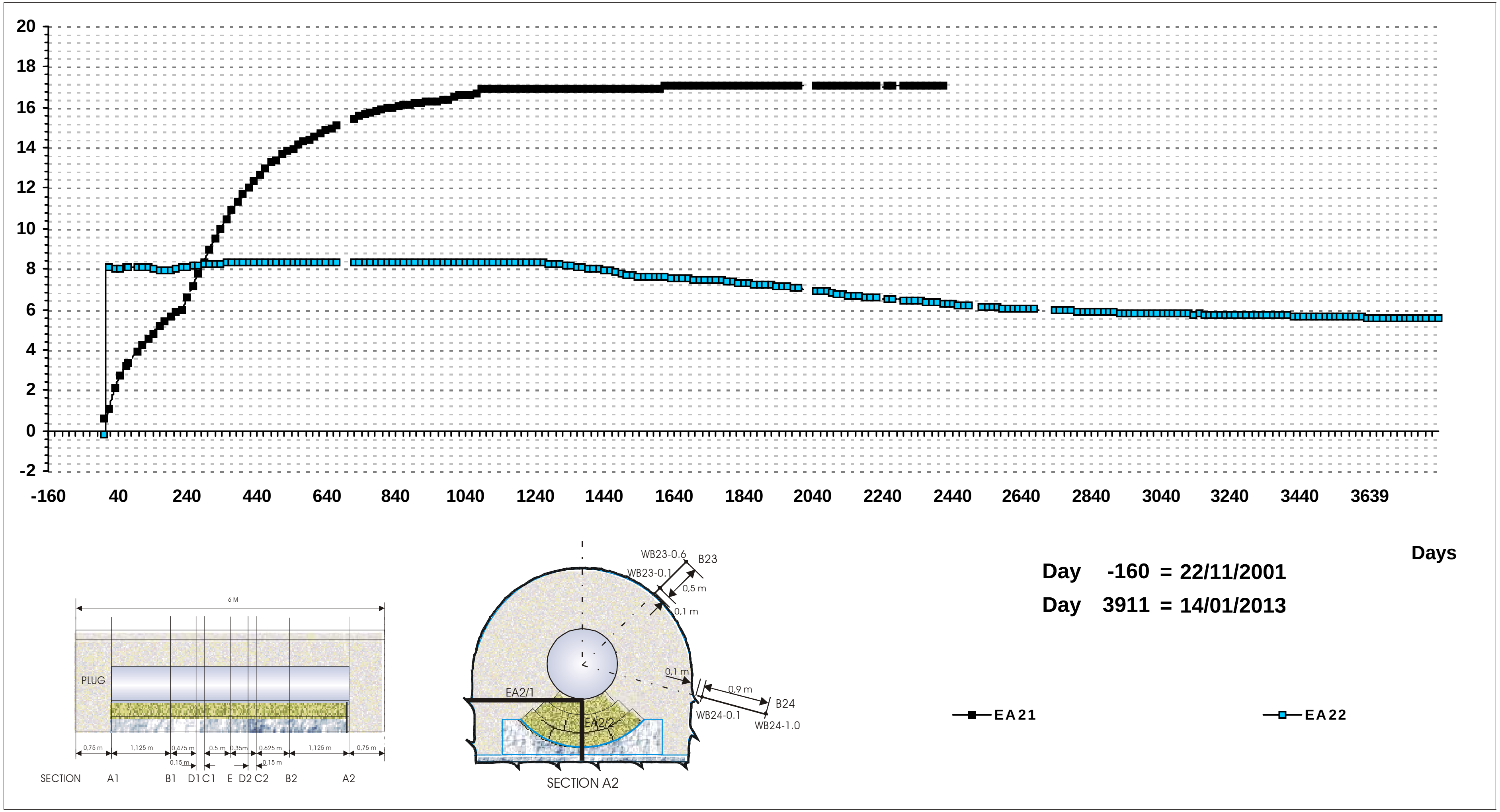

COMMENTS:

Sensors installed February 2002. Data available from 30 April 2002 (day -1).

EA2/1: No data from 12th December 2008 (day 2386).

LOCATION **Section E**

SENSOR TYPE: Displacement (Rock) **UNITS: mm**

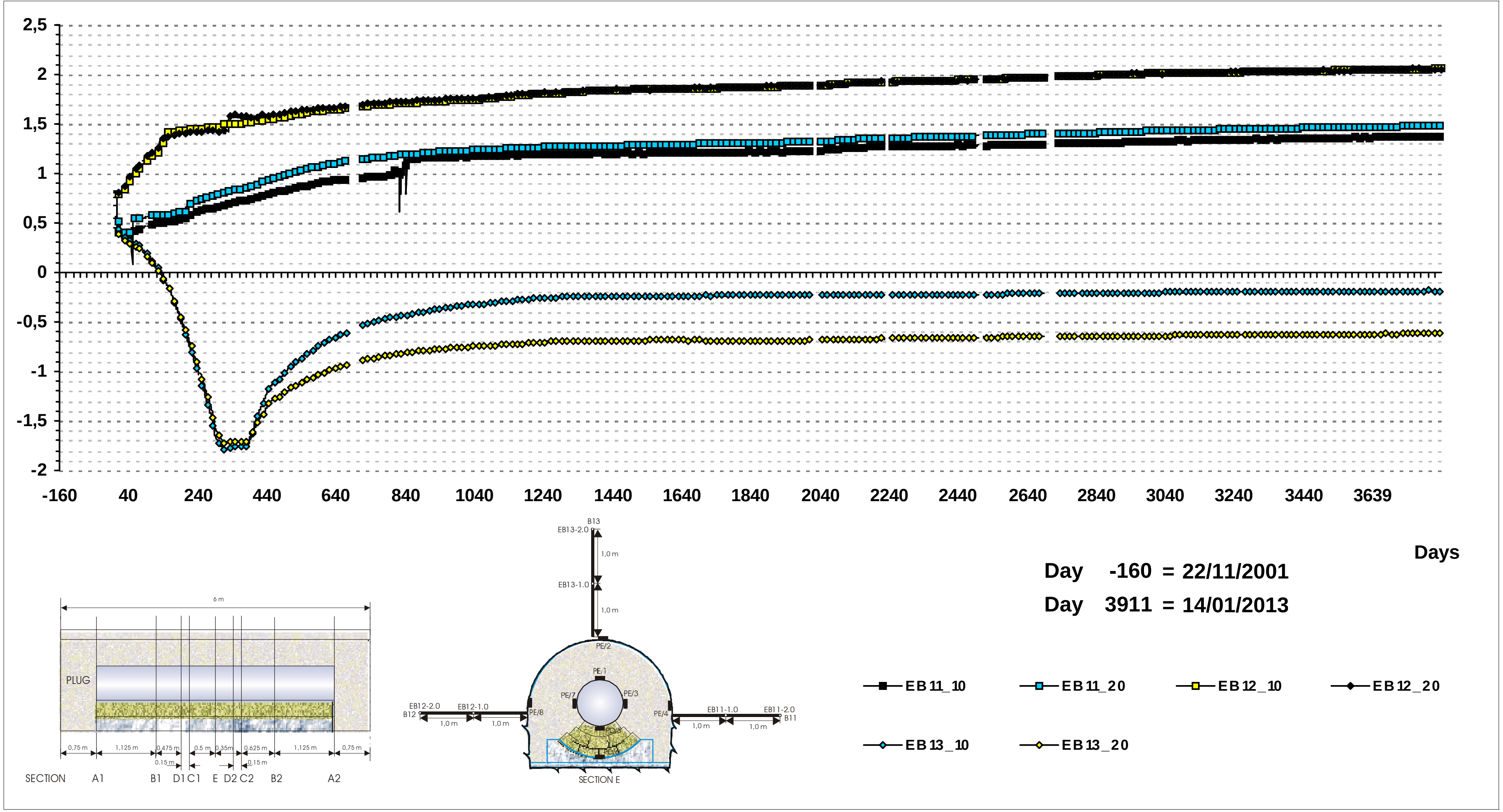

COMMENTS:

Sensors installed February 2002. Data available from 30 April 2002 (day -1).

EB12_2.0: Data not reliable from 20th March to 4th April 2003 (days 323 to 338).

LOCATION BEB-2

SENSOR TYPE: Pore pressure (Rock) **UNITS: bar abs.**

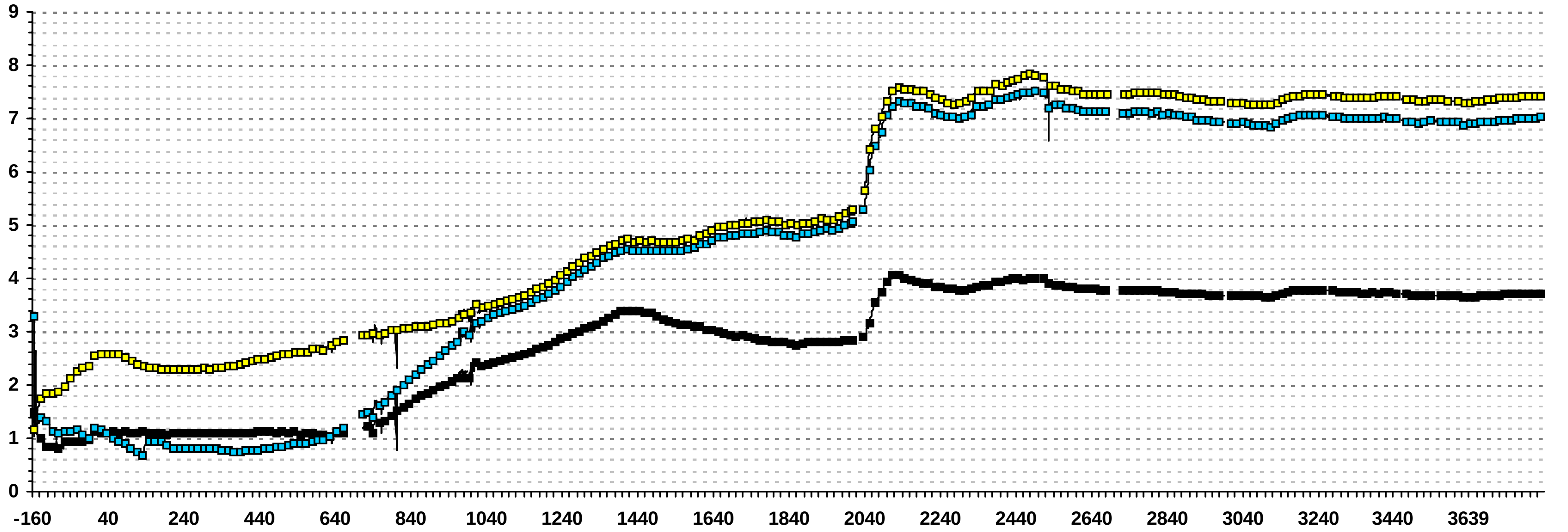

Day -160 = 22/11/2001
Day 3911 = 14/01/2013

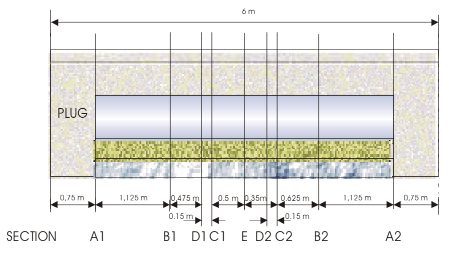

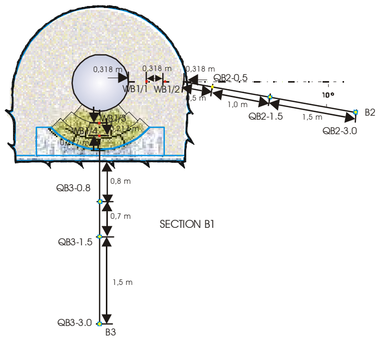

COMMENTS:
Sensors installed November 2001. Data available from 27 November 2001 (day -155).
No data from 28th April to 5th May 2002 (days -3 to 4) during connection of sensors to Data Acquisition System.

LOCATION BEB-3

SENSOR TYPE: Pore pressure (Rock) UNITS: bar abs.

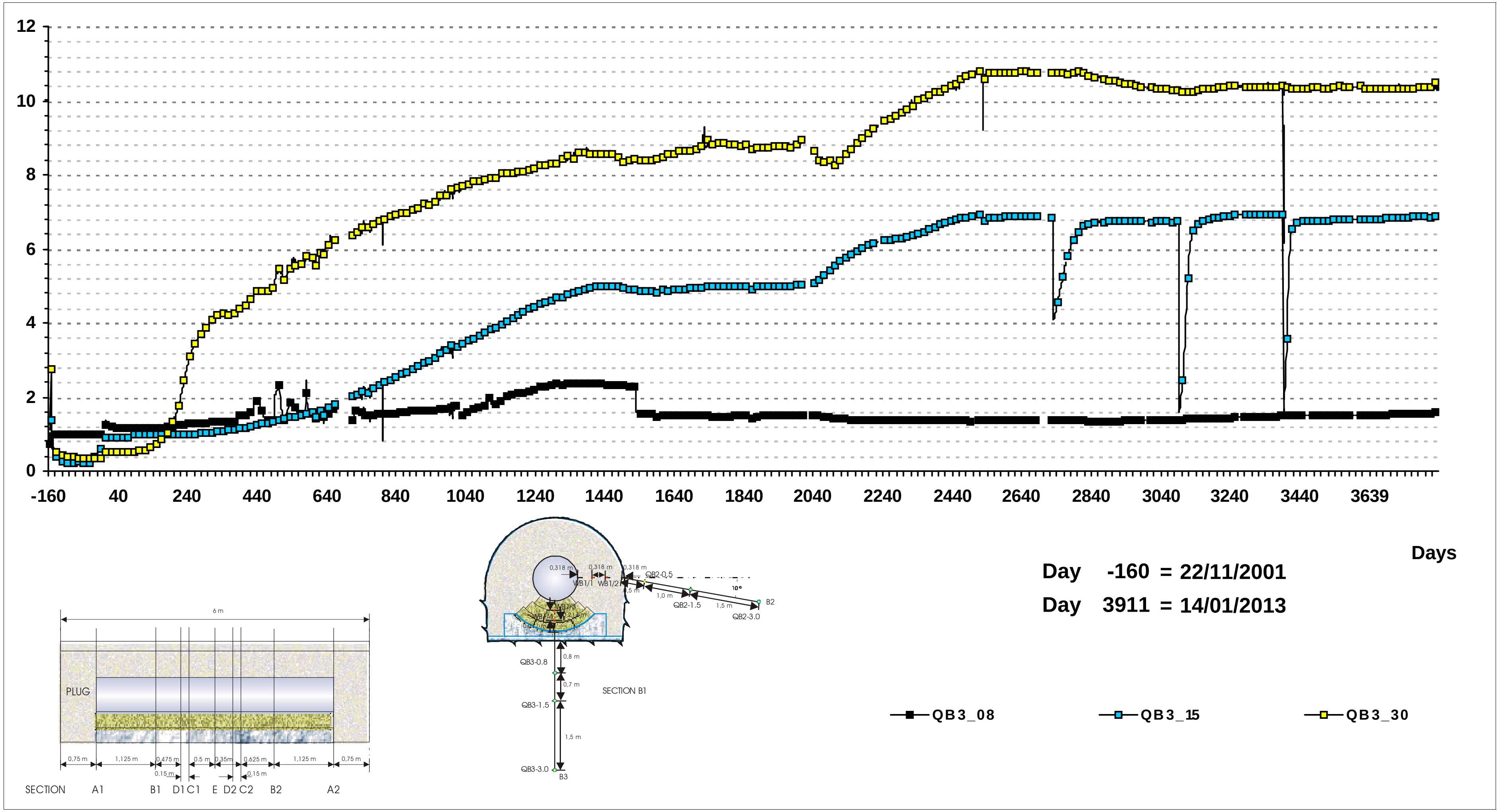

COMMENTS:

Sensors installed November 2001. Data available from 27 November 2001 (day -155).

No data from 28th April to 5th May 2002 (days -3 to 4) during connection of sensors to Data Acquisition System.

LOCATION BEB-21

SENSOR TYPE: Pore pressure (Rock) **UNITS: bar abs.**

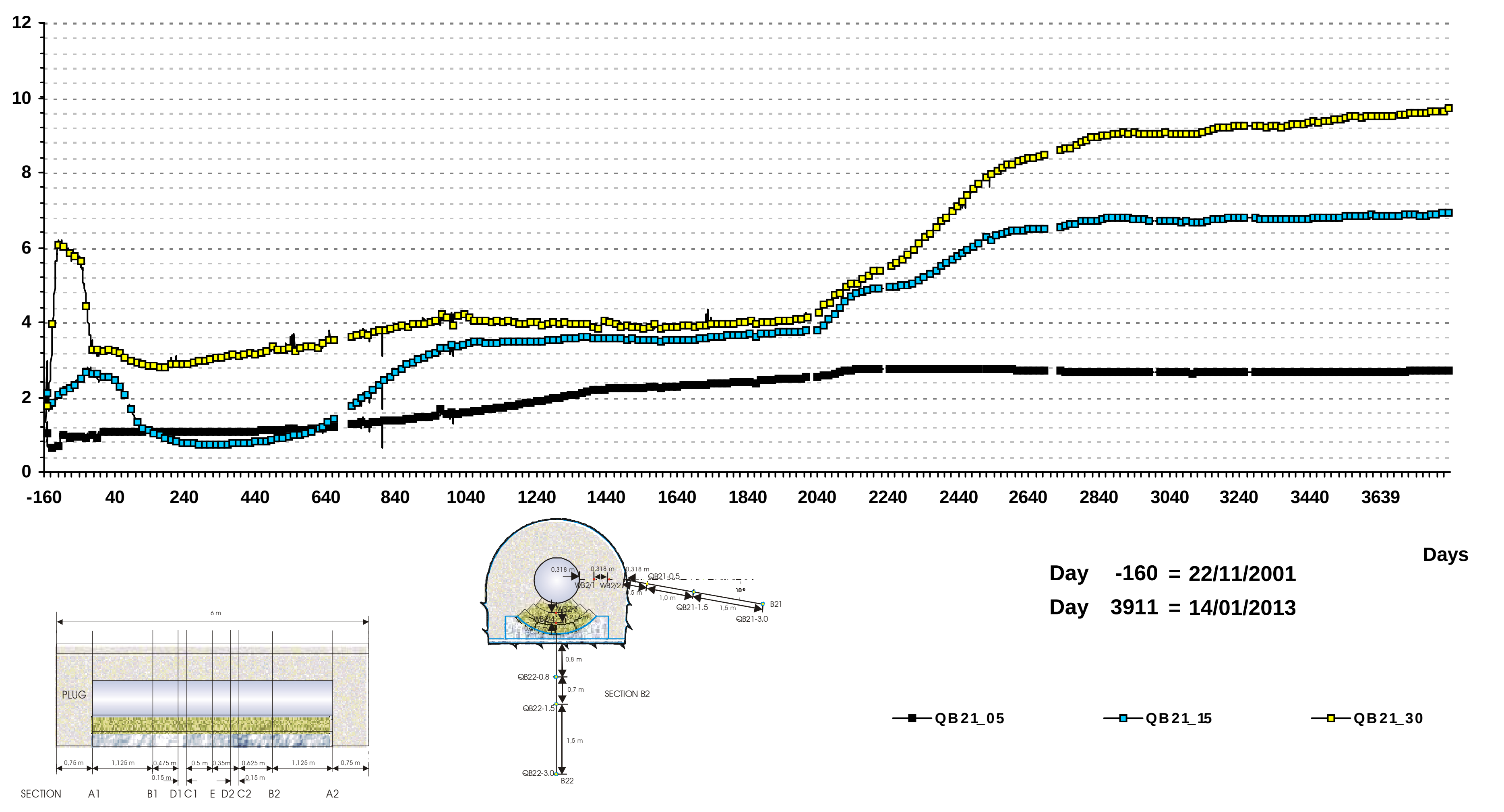

COMMENTS:

Sensors installed November 2001. Data available from 27 November 2001 (day -155).

No data from 28th April to 5th May 2002 (days -3 to 4) during connection of sensors to Data Acquisition System.

LOCATION BEB-22

SENSOR TYPE: Pore pressure (Rock) **UNITS: bar abs.**

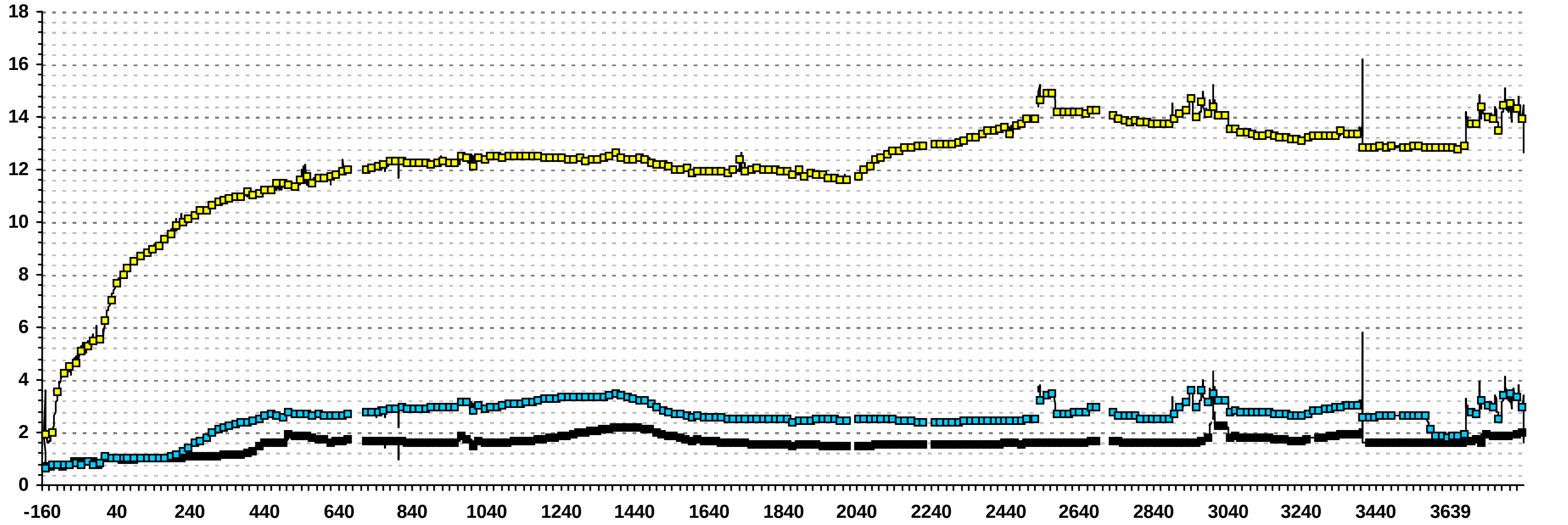

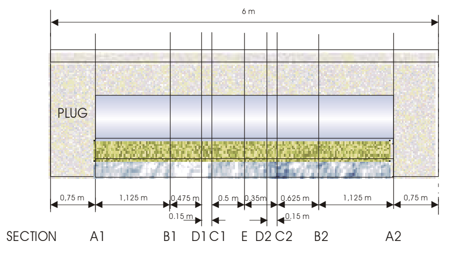

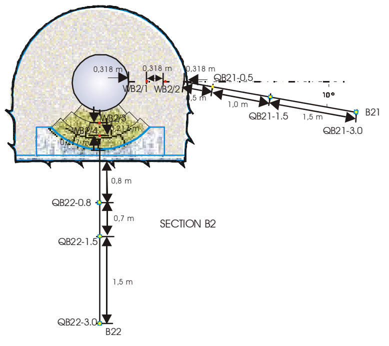

COMMENTS:

Sensors installed November 2001. Data available from 27 November 2001 (day -155).

No data from 28th April to 5th May 2002 (days -3 to 4) during connection of sensors to Data Acquisition System.

Data from 2nd April to 19th May 2009 (days 2528 to 2571): Noisy data after restart of driver. Data will be filtered if the trend does not continue.

LOCATION ***Section C1***

SENSOR TYPE: Pore pressure (Rock) ***UNITS: bar abs.***

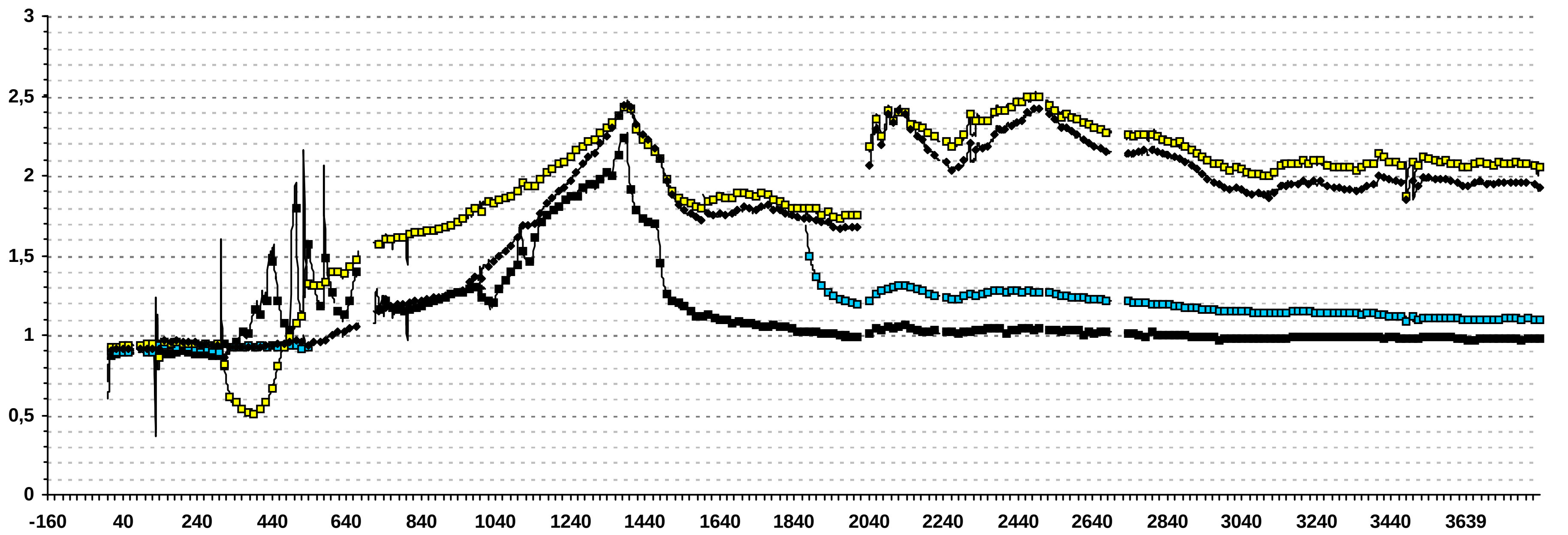

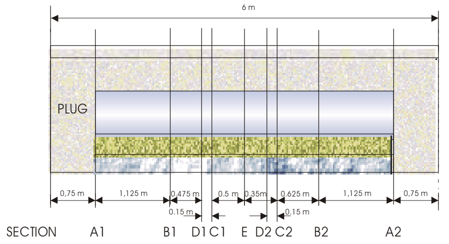

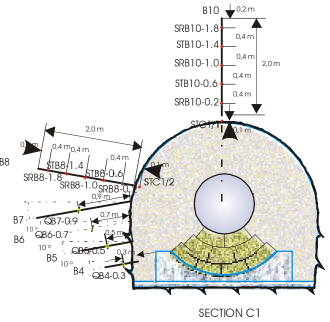

COMMENTS:

Sensors installed 26 September 2001. Data available from 30 April 2002 (day -1).

QB5-0.5: No data from 10th October 2003 (day 527) to 16th June 3007 (day 1872).

LOCATION Section C2

SENSOR TYPE: Pore pressure (Rock) ***UNITS: bar abs.***

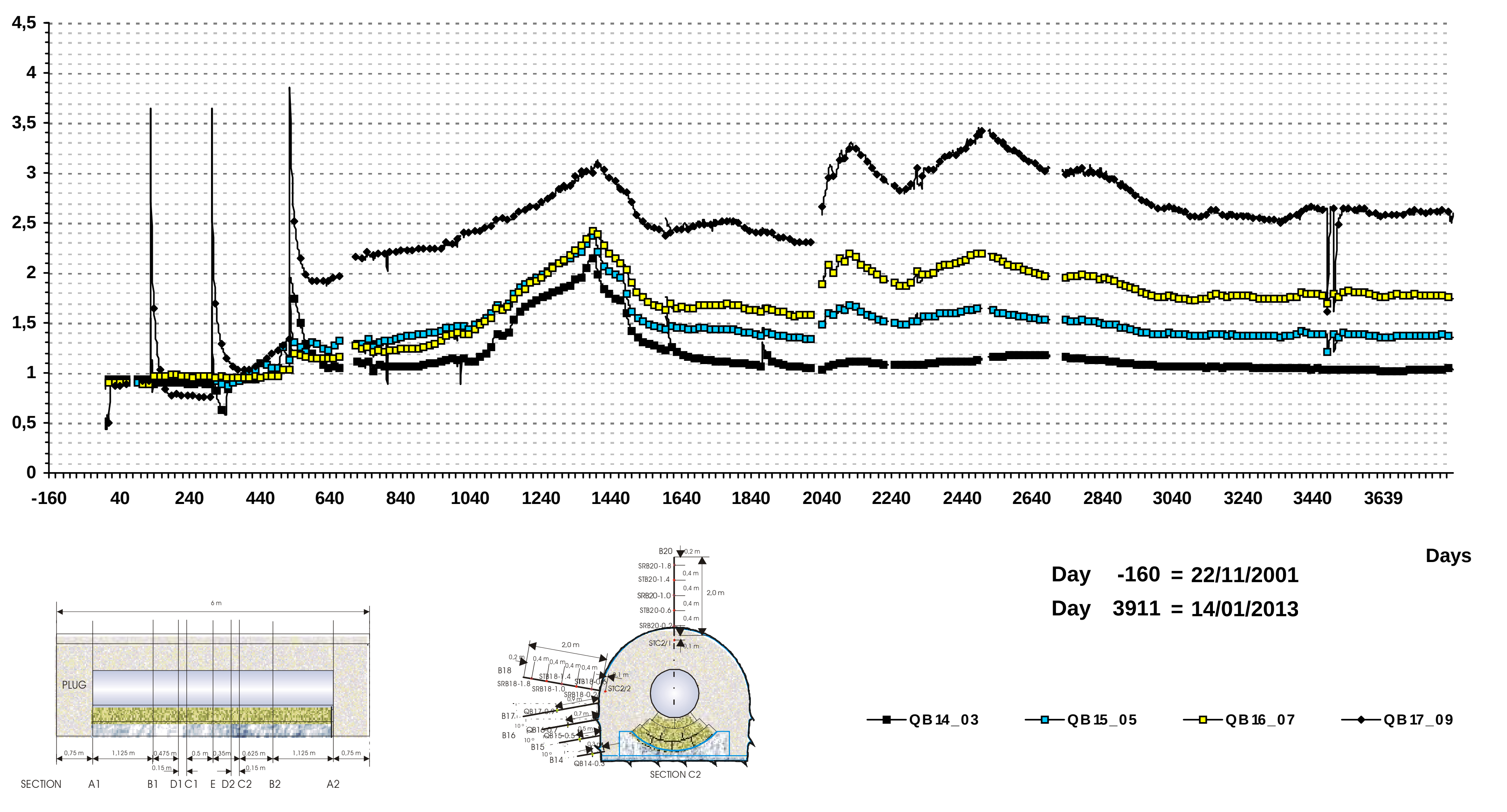

COMMENTS:

Sensors installed 26 September 2001. Data available from 30 April 2002 (day -1).

LOCATION **Section E**

SENSOR TYPE: Total pressure (Buffer) **UNITS: bar abs.**

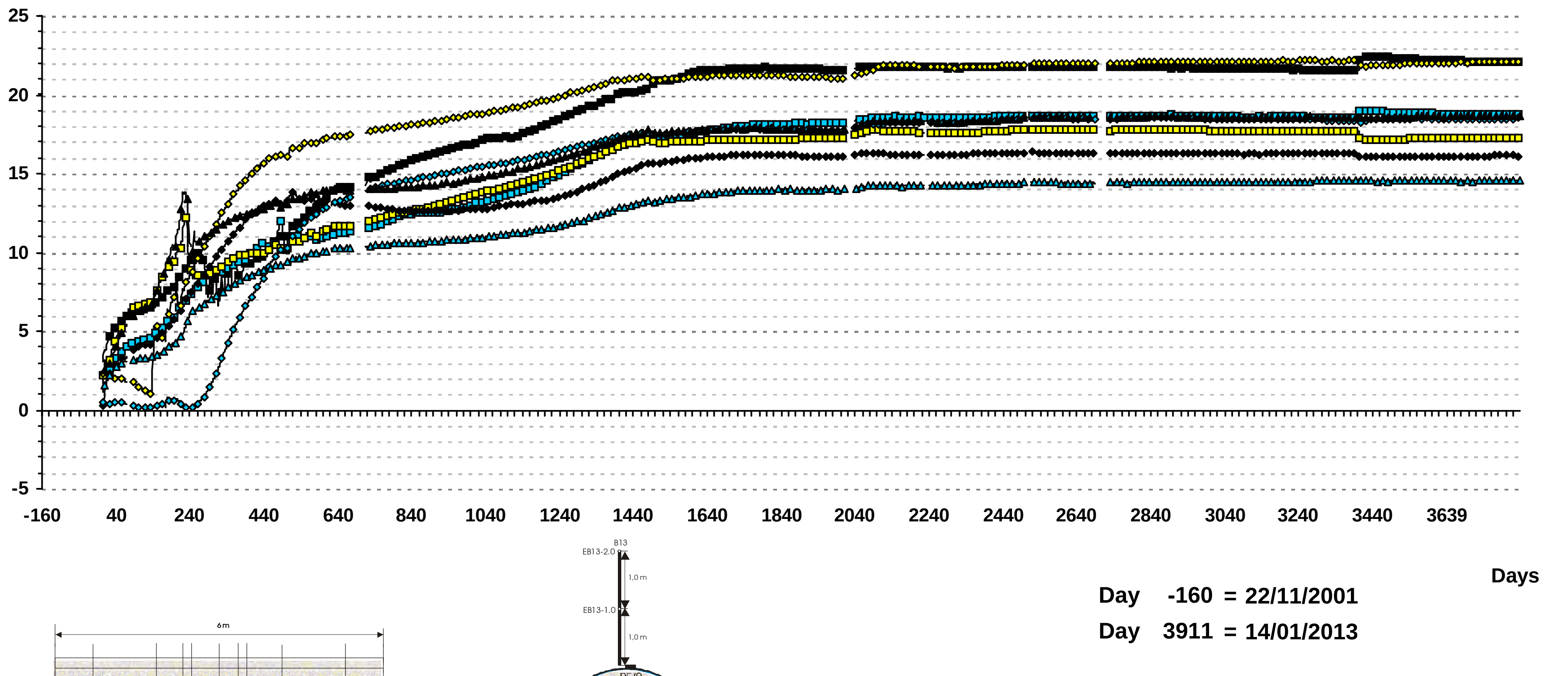

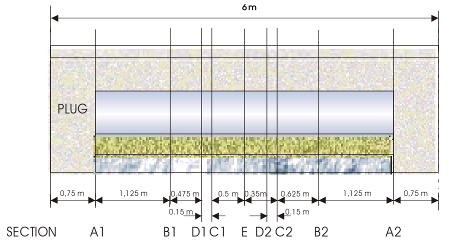

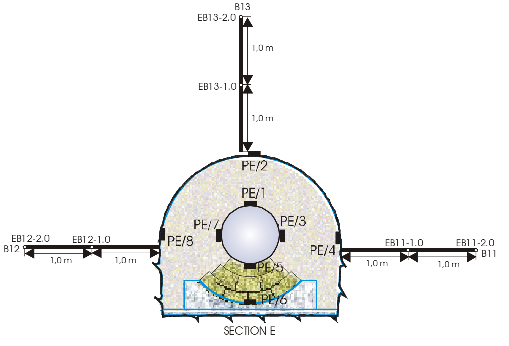

COMMENTS:
Sensors installed February 2002. Data available from 30 April 2002 (day -1).

10 APPENDIX IV EB EXPERIMENT. CONTRIBUTION OF CIEMAT

EUROPEAN COMMISSION

Community research

Long-term Performance of Engineered Barrier Systems

PEBS

Long-term Performance of Engineered Barrier Systems PEBS

EB experiment
Contribution of CIEMAT to EB dismantling report. Physical state of the bentonite

(CONTRIBUTION TO DELIVERABLE-N°: D2.1-4)

Contract (grant agreement) number: FP7 249681

CIEMAT Technical Report CIEMAT/DMA/2G210/04/2013

Author(s): M.V. Villar

Reporting period:
Date of issue of this report: June 20th 2013

Start date of project: 01/03/10 Duration : 48 Months

Project co-funded by the European Commission under the Seventh Euratom Framework Programme for Nuclear Research &Training Activities (2007-2011)		
Dissemination Level		
PU	Public	**PU**
RE	Restricted to a group specified by the partners of the [acronym] project	
CO	Confidential, only for partners of the [acronym] project	

PEBS

EURATOM

Contents

1 Introduction: the EB experiment

The EB experiment (ENRESA 2005), was run by ENRESA at the Mont Terri Underground Research Laboratory in Switzerland, starting in October 2000, with the aim of demonstrating that automated production of a Granular Bentonite Material (GBM) and its emplacement in the upper part of a clay barrier were feasible. The EB niche excavated in the Opalinus clay was 15 m long and had a geometry of a horseshoe section, 2.55 m high and 3 m wide (Figure 1).

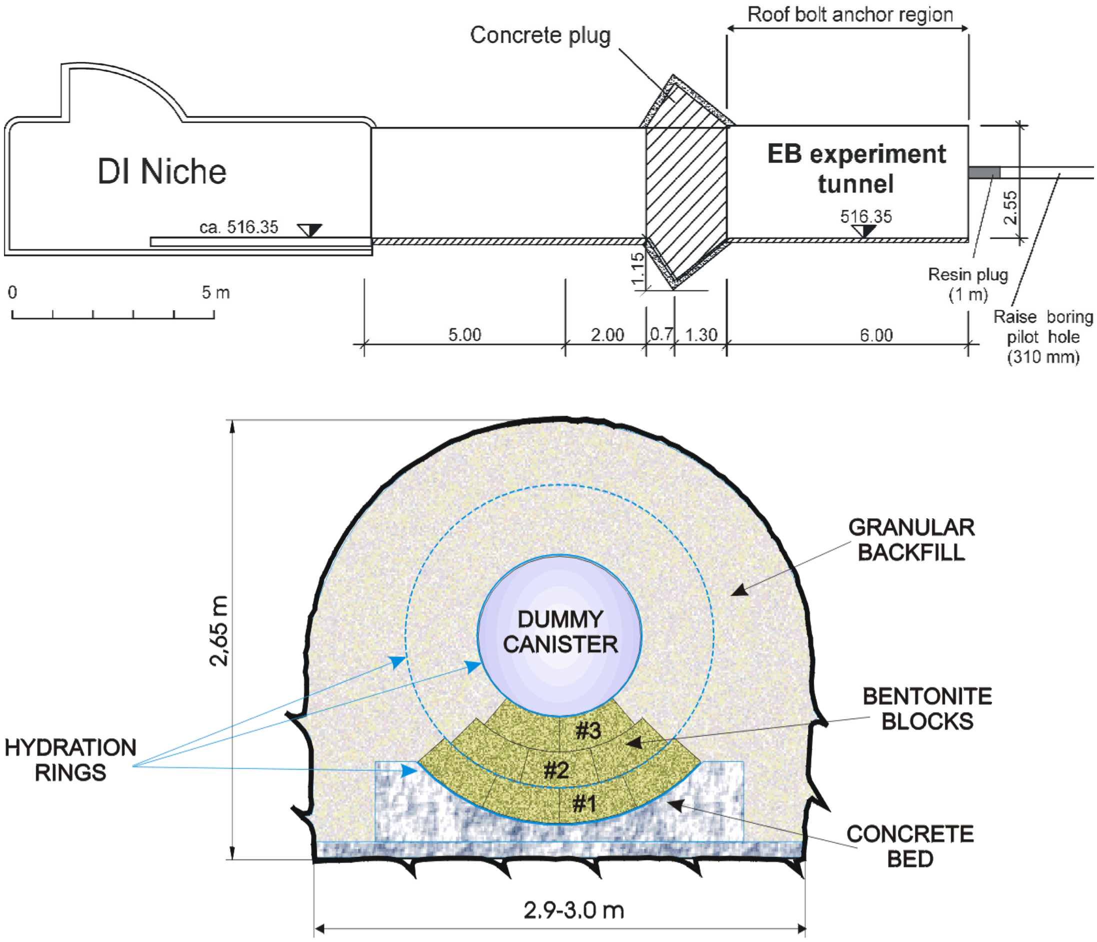

Figure 1: EB niche at Mont Terri URL, longitudinal and cross sections (ENRESA 2005)

According to the measurements performed during installation, in the EB test section an average dry density of 1.36 g/cm^3 of the emplaced GBM was obtained, although some segregation during the emplacement and density inhomogeneities were acknowledged. According to the laboratory characterization of the GBM (ENRESA 2005), for this dry density value it was estimated that the hydraulic conductivity was lower than $5 \cdot 10^{-12}$ m/s and the swelling pressure about 1.3 MPa. The artificial hydration of the buffer material started on May 2002 through a series of porous tubes that crossed along the GBM and the bentonite blocks as shown in Figure 2. To enhance the water homogeneous distribution, the concrete bed, the surface of the container and the three rings of bentonite blocks were covered with geotextile. Hydration was carried out with Pearson water coming from a deposit. The Pearson water is a sodium-rich solution and has a composition similar to the Opalinus Clay formation pore water. It has a density of 1.020 g/cm^3 (Pearson 1998) and its chemical composition is indicated in Table I.

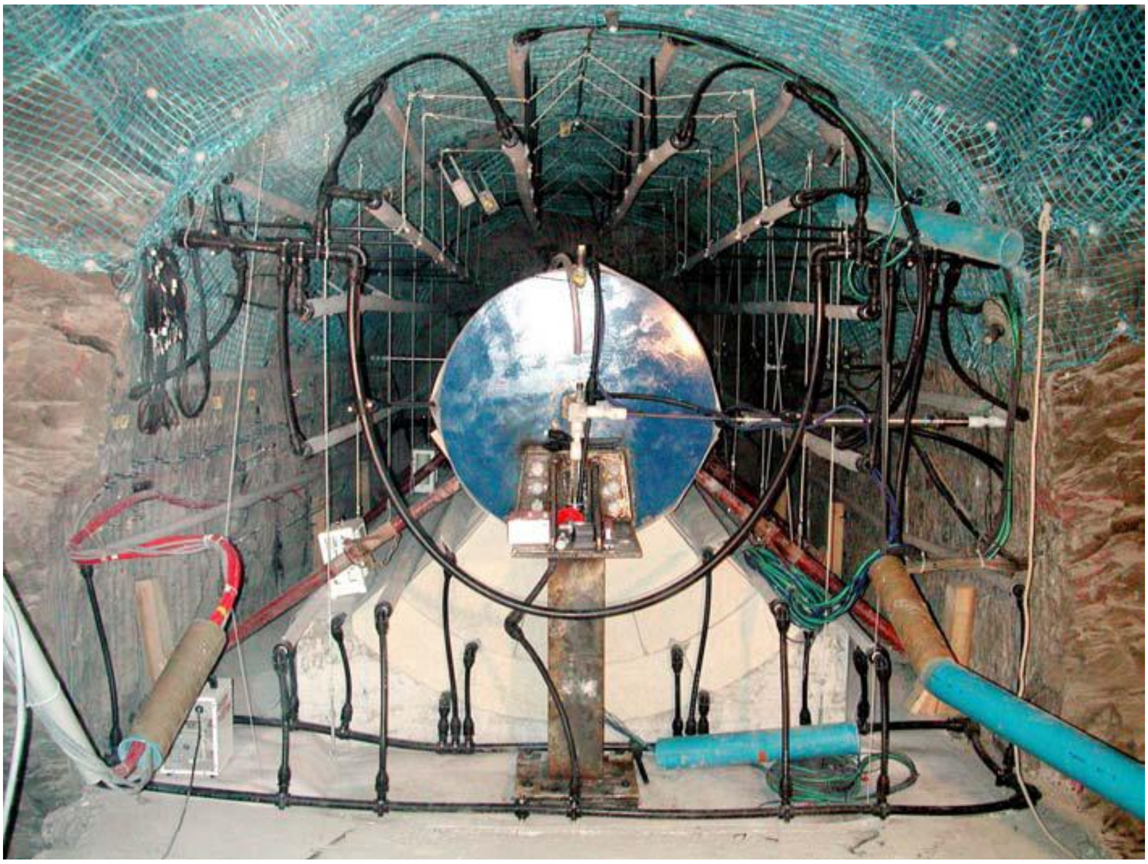

Figure 2: Appearance of the concrete and bentonite blocks bed, dummy canister and hydration system before the installation of the GBM (ENRESA 2005)

Table I: Chemical composition of Pearson water (mg/L)

Cl^-	SO_4^{2-}	HCO_3^-	Mg^{2+}	Ca^{2+}	Na^+	K^+	Sr^+	pH
10635.90	1354.41	25.75	413.19	1034.06	5550.01	62.95	44.69	7.6

2 Dismantling and sampling

The test run under isothermal conditions (average temperature 16°C) for 10.5 years. The dismantling of the test started on October 2012 with the demolition of the concrete plug, which took almost a month, and went on until February 2013. Figure 3 shows the appearance of the GBM and the bentonite blocks as the test was dismantled, as well as details of the GBM-block contact. The GBM looked completely homogeneous and every void in the barrier had been filled. The contact between the blocks and the GBM was easily recognisable, since the blocks presented a coarse-grained texture, whereas no grains could be identified in the GBM. The pictures show also the numerous tubes and cables that crossed the barrier and the blocks, the appearance of the steel container, the concrete bed and the geotextile layers that separated the three rings of blocks.

Figure 3: Appearance of the GBM (left up), the bentonite blocks (right up), and the GBM-blocks contact (bottom) upon dismantling.

Samples of the GBM, the bentonite blocks, the concrete bed and the concrete plug, the Opalinus clay, and other materials were taken for analysis in the laboratory. Additionally, dry density and water content determinations of the bentonite were performed on site by the AITEMIN team. These determinations were also performed at CIEMAT in bentonite samples that were quickly packed after being taken and sent to CIEMAT laboratories. The packing consisted of a plastic film and two aluminium foil bags that were vacuumed before being closed.

The bentonite samples analysed at CIEMAT laboratories belong to the sampling sections A1-25, CMT1, CMT2, E, B2 and CMT3 (Figure 5). The samples were taken following approximately radii, as shown in Figure 4. Initially only the sections CMT1, CMT2 and CMT3 were to be sampled for CIEMAT (AITEMIN 2012), but once the dismantling started it was decided to take samples from the other sections in order to crosscheck the water content and dry density values obtained on site.

This report summarises the results obtained concerning the physical state of the samples. Additional analyses were performed at CIEMAT, including permeability, thermal conductivity, swelling capacity, geochemical and mineralogical determinations. Those will be reported in separate documents.

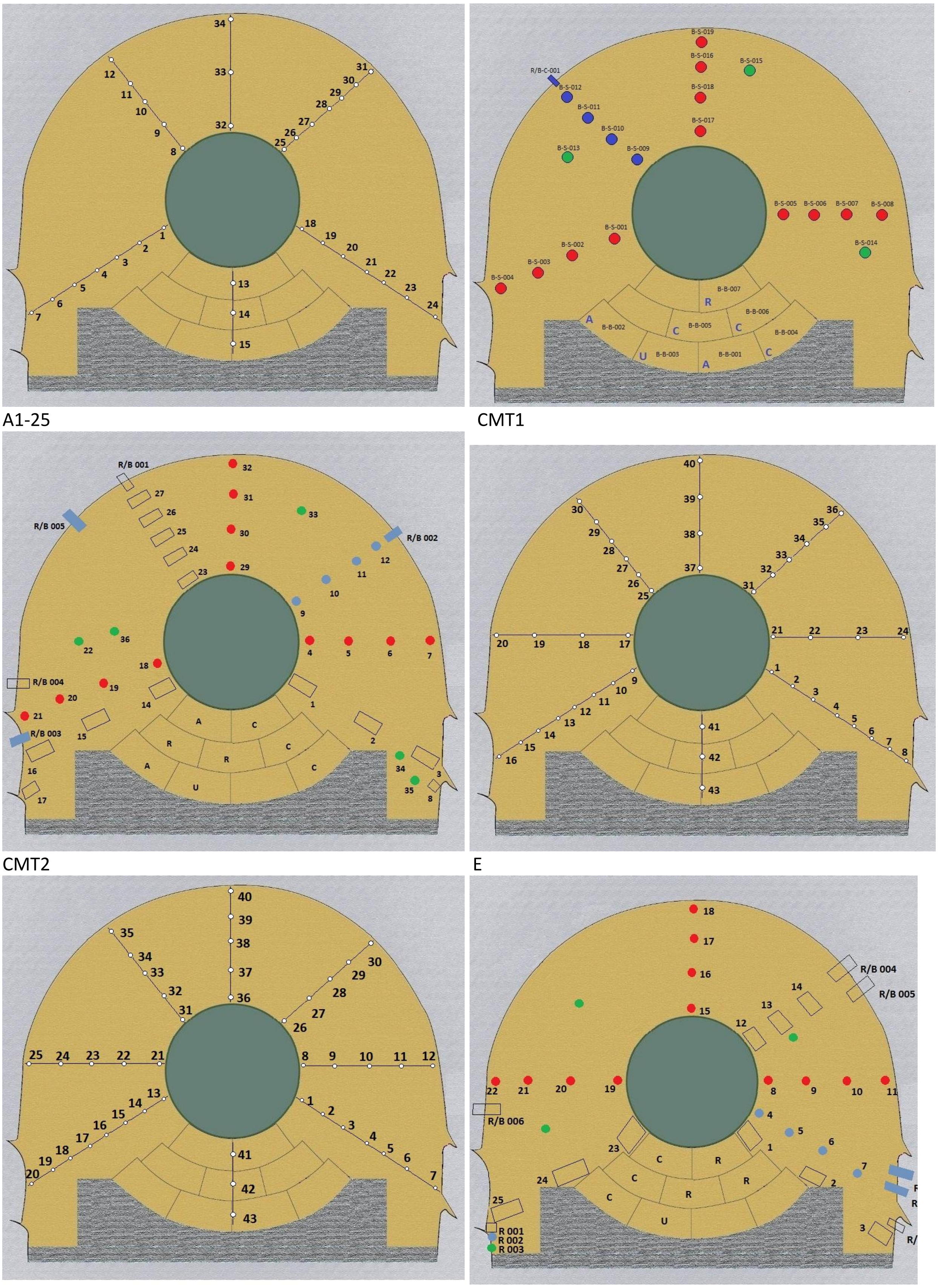

A1-25 CMT1

CMT2 E

B2 CMT3

Figure 4: Cross section of the sampling sections showing the location of the bentonite samples (in sections CMT1, CMT2 and CMT3 the GBM samples sent to CIEMAT are indicated with red circles or a rectangle and the blocks with a C) (AITEMIN 2012)

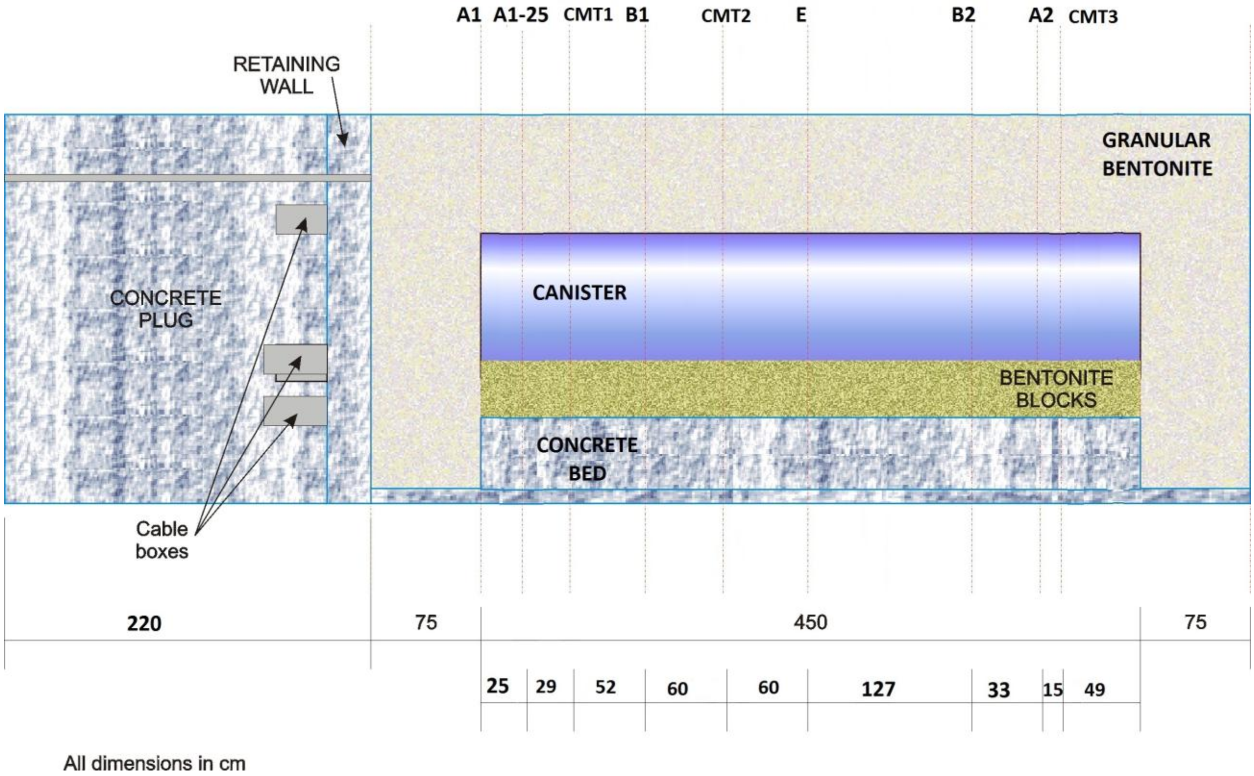

Figure 5: Bentonite sampling sections (AITEMIN 2012)

3 Material

The GBM used in the EB experiment was prepared from FEBEX bentonite dried and milled in a three-step process to produce a fine grade powder with a water content of 3.3%. Later, a commercial plant with an in-line highly automated briquetting process produced coarse (>7 mm) and fine (0.4-2 mm) grained materials with dry densities of 2.11 and 2.13 g/cm^3, respectively. These two grain size fractions were subsequently combined after several trials to produce a material with a granulometric Simonis curve, which was used for the *in situ* emplacement (ENRESA 2005). On the other hand, the blocks used came from the series that was manufactured for the FEBEX *in situ* test in 1997, and had a dry density of 1.69 g/cm^3 and a water content of 14.4%.

The physico-chemical properties of the FEBEX bentonite, as well as its most relevant thermo-hydro-mechanical and geochemical characteristics obtained during the projects FEBEX I and II were summarised in the final report of the project (ENRESA 2006). The FEBEX bentonite was extracted from the Cortijo de Archidona deposit (Almería, Spain). The processing at the factory consisted of disaggregation and gently grinding, drying at 60°C and sieving by 5 mm, and this was the material used for the laboratory characterisation.

The montmorillonite content of the FEBEX bentonite is above 90 wt.%. The smectitic phases are actually made up of a smectite-illite mixed layer, with 10-15 wt.% of illite layers. Besides, the bentonite contains variable quantities of quartz, plagioclase, K-felspar, calcite, and cristobalite-trydimite. The liquid limit of the bentonite is 102±4%, the plastic limit 53±3%, the specific gravity 2.70±0.04, and 67±3 percent of particles are smaller than 2 μm. The hygroscopic water content is 13.7±1.3 percent. The total specific surface area obtained using the Keeling hygroscopicity method is 725 m^2/g. The cation exchange capacity is 102±4 meq/100g, the main exchangeable cations being calcium, magnesium and sodium. The predominant soluble ions are chloride, sulphate, bicarbonate and sodium.

4 Methodology of laboratory tests

Until their analysis, the samples sent from Mont Terri were kept at CIEMAT facilities in a storage room in which the temperature was between 7 and 16°C and the relative humidity between 70 and 90%. The samples were taken one at a time out of the storage room and unpacked in the laboratory. The size and condition of the samples was very variable. Most of the blocks kept their original shape, but some of them came in pieces (Figure 6). Overall, the samples from the GBM looked homogeneous, but occasionally they presented blue spots or areas of different grain size (Figure 7).

Figure 6: Appearance of blocks after unpacking

Figure 7: Appearance of some GBM samples

The samples for the water content and dry density determinations were prepared by trimming regular specimens of the right size, with volumes of between 6 and 13 cm^3 (Figure 8). Two specimens were trimmed and analysed from each GBM sample. The subsamples from the blocks were taken at three different distances from the container (up, middle, down), and for each distance at least two specimens were used. To section the blocks, knives and hammers were used (Figure 9). The process of trimming took some minutes, and during this time some drying of the sample could have taken place, because the samples remained exposed to drier room conditions than those in the barrier. This was evaluated and the results obtained are shown in the section "Methodology impact on results".

Figure 8: Trimming of a sample in the laboratory for water content and dry density determination

Figure 9: Sectioning of blocks to obtain subsamples

The gravimetric water content (w) is defined as the ratio between the weight of water and the weight of dry solid expressed as a percentage. The weight of water was determined as the difference between the weight of the sample and its weight after oven drying at 110°C for 48 h (weight of solid). Dry density (ρ_d) is defined as the ratio between the weight of the dry sample and the volume occupied by it prior to drying. The volume of the specimens was determined by immersing them in a recipient containing mercury and by weighing the mercury displaced, as established in UNE Standard 7045 "Determination of soil porosity". The same samples whose volumes had been determined were used for the water content determination. Additionally, in some cases larger samples were used just for water content determination.

In some samples the relative humidity and temperature were measured using either a capacitive sensor or a psychrometer (Figure 10, Figure 11). Since the degree of saturation of the samples was very high, the measurement range of the capacitive sensors was not suitable, because their accuracy for relative humidities between 90 and 100% is 2%. Consequently, it was decided to use exclusively psychrometers. In both cases the sensors were inserted in holes drilled in the bentonite and sealed with the bentonite itself. The samples were kept wrapped in plastic films or in bags to avoid water content lost during the measurements. The equilibration time for the capacitive sensors was less than 2 hours and for the psychrometers of at least 24 hours. The suction in the pores of the sample (s, in MPa) is related to the relative humidity (RH, %) and the temperature (T, absolute temperature) measured by the sensors by means of Kelvin's law:

$$s = -10^6 \frac{R \times T}{V_w} \ln\left(\frac{HR}{100}\right) \qquad [1]$$

where R is the universal constant of the gases (8.3143 J/mol·K) and V_w is the molar volume of the water ($1.80 \cdot 10^{-5}$ m^3/mol).

Figure 10: Insertion of capacitive sensors in blocks for measurement of RH and *T*

Figure 11: Measurement of relative humidity and temperature with psychrometers

Thermal conductivity measurements, mercury intrusion porosimetry tests, determination of the specific surface area and measurement of the basal spacing of the smectite were done also in all the subsamples, but the results are reported elsewhere.

5 Results

5.1 METHODOLOGY IMPACT ON RESULTS

Since most of the samples analysed had very high water contents, much higher than hygroscopic, their manipulation at laboratory conditions (temperature of 22±1°C, relative humidity of 35±6%, corresponding to a suction of 146±24 MPa) could imply certain drying. In order to determine how this drying could affect the values of water content obtained, some samples were let after unpacking in room conditions and their weight change was checked periodically, before putting the samples in the oven to determine their dry mass. The evolution of their water content during exposure to laboratory conditions is shown in Figure 12, and in

Figure 13 in terms of percent water content loss. In the latter the average results of a similar test performed on site by AITEMIN during the dismantling are shown. In this case the ambient conditions were different, since the relative humidity and temperature at the gallery of the Mont Terri URL where the determinations were done were 48% and 17°C. The preparation of the samples for dry density and water content measurements took on average less than 20 minutes. According to Figure 13 this would mean that the decrease of water content during manipulation in the laboratory could be of between 0.7 and 1.5%. This could imply a certain decrease in the degrees of saturation obtained, of 2% in the worst cases.

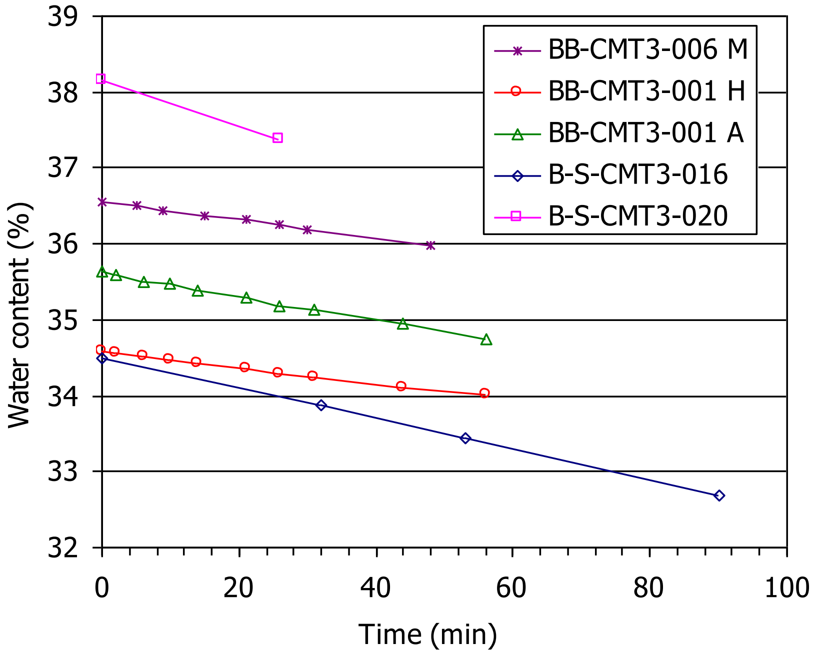

Figure 12: Evolution of water content in samples kept at laboratory conditions after unpacking

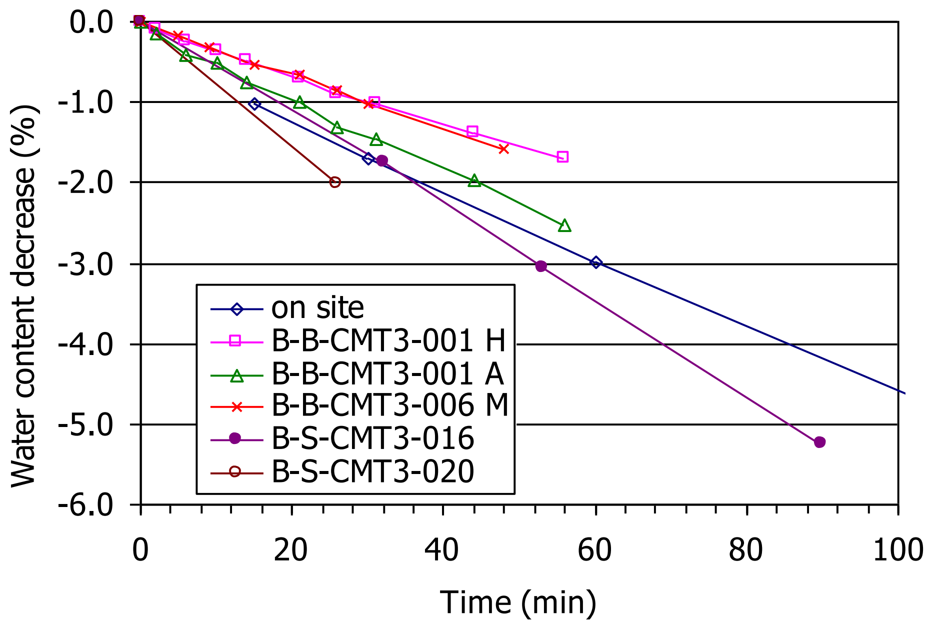

Figure 13: Decrease of water content in samples exposed to room conditions at CIEMAT's laboratory and on site (average of several data of AITEMIN)

5.2 SIZE OF BLOCKS

Some of the blocks received were measured upon unpacking, in order to compare their dimensions to the original ones and evaluate their deformation. The results obtained are shown in Table II according to the key given in Figure 14. The expansion of all the blocks is clear, particularly in those of section CMT1, which is the one closer to the concrete plug. In this section the height of the samples increased up to a 56%, which indicates the longitudinal expansion of the bentonite bed. In the two other sections the average height increase was of 4%. The other dimensions increased also between 6 and 14% in section CMT1. The dimension c increased an average of 7% in sections CMT2 and CMT3, indicating the uplift of the canister.

When these measurements are compared with those taken by AITEMIN during dismantling (also included in the Table), it is observed that the measurements taken in the laboratory are larger, which could mean that the expansion of the blocks continued after excavation. The difference between both measurements is particularly large for the blocks in sections CMT2 and CMT3. At these two sections the GBM was removed long before the blocks were extracted, and this would have allowed more time for them to swell once the overload of the GBM was removed. Besides, the time between excavation and sampling at the laboratory was longer for the blocks in section CMT3.

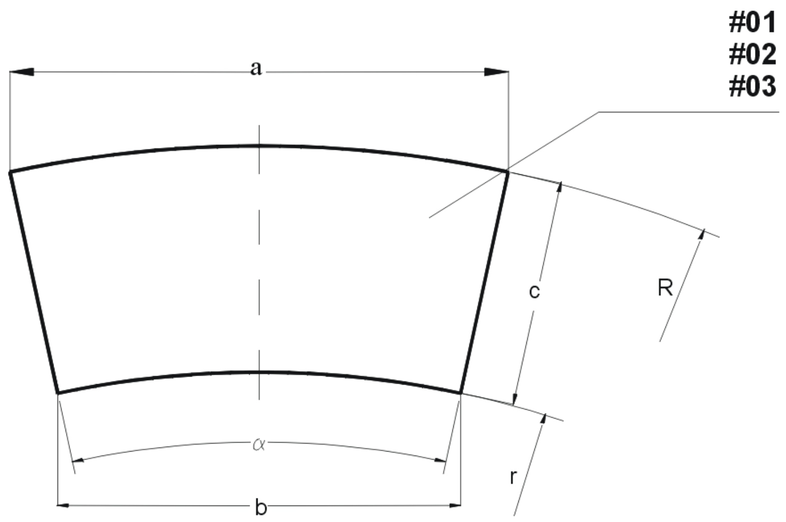

Figure 14: Block dimensions (ENRESA 2005)

Table II: Dimensions of the blocks sampled in the laboratory (refer to Figure 1 and Figure 14). The initial height (h) was 12.5 cm and the dimension c 21.4 cm for all types of blocks

Reference	Block Type	Initial (cm)		Final (cm)				
		a	b	h	a	b	c	c[a]
B-B-CMT1-006	2	47.3	36.1	16.0	51	41	24.3	24.3
B-B-CMT1-004	1	47.0	38.0	19.5	50	45	23.8	22.0
B-B-CMT2-002	3			12.8			22.0	22.0
B-B-CMT2-005	2			13.0			23.0	21.0
B-B-CMT2-009	1			13.0			23.0	21.0
B-B-CMT3-006	1			13.0			23.0	21.8

[a] taken on site during dismantling

5.3 DRY DENSITY AND WATER CONTENT

The samples for the water content and density determinations were taken following approximately sampling radii in the GBM, as shown in Figure 4. The results are shown in the Tables in Appendix 1 and are plotted in terms of water content, dry density and degree of saturation as a function of the distance to the container axis in Figure 15 to Figure 17. The points joint by lines in these Figures belong to the same sampling radius. Each point is the average of two measurements. As the dismantling operation started it was observed that the bottom part of the barrier, particularly the zones closer to the concrete bed, looked wetter than the rest of the GBM, and it was decided to analyse also samples taken from this part of the barrier and not belonging to any particular radius. These are the samples having higher water contents (higher than 45%) and lower dry densities and located farther away from the container axis in Figure 15 and Figure 16. In general, only the sampling radii located in the lower half of the barrier showed a trend to higher water contents towards the external part of the barrier, *i.e*. towards the bottom. In the sampling radii located in the upper half of the barrier, no trend with respect to water content or dry density was observed. Regarding the degrees of saturation, no trends along the GBM were observed, most of the values being between 96 and 100%.

The results obtained in bentonite blocks are detailed in Tables in Appendix 1 and plotted in Figure 18 and Figure 19. Each point in the Figures is the average of two or three measurements. In sections CMT1 and CMT2 the water content tended to increase and the dry densities to decrease towards the bottom, that is, away from the container and towards the concrete bed. However, in section CMT3 these trends were not observed. In terms of degree of saturation there are not clear spatial trends. The values measured were between 95 and 101%.

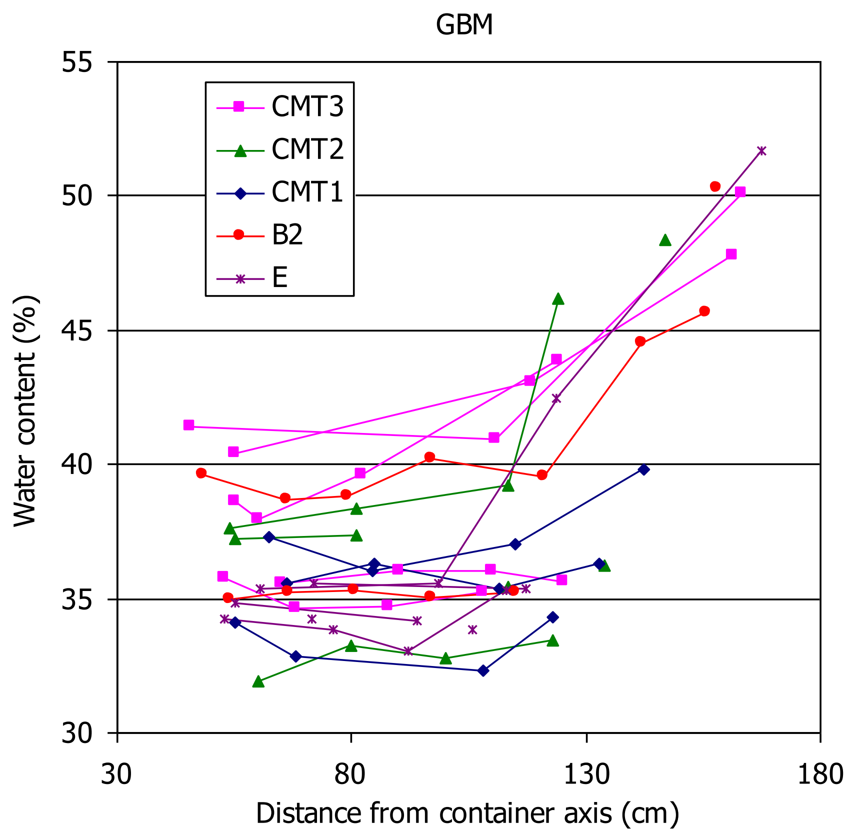

Figure 15: Water content of GBM samples from different sampling sections as measured in the laboratory

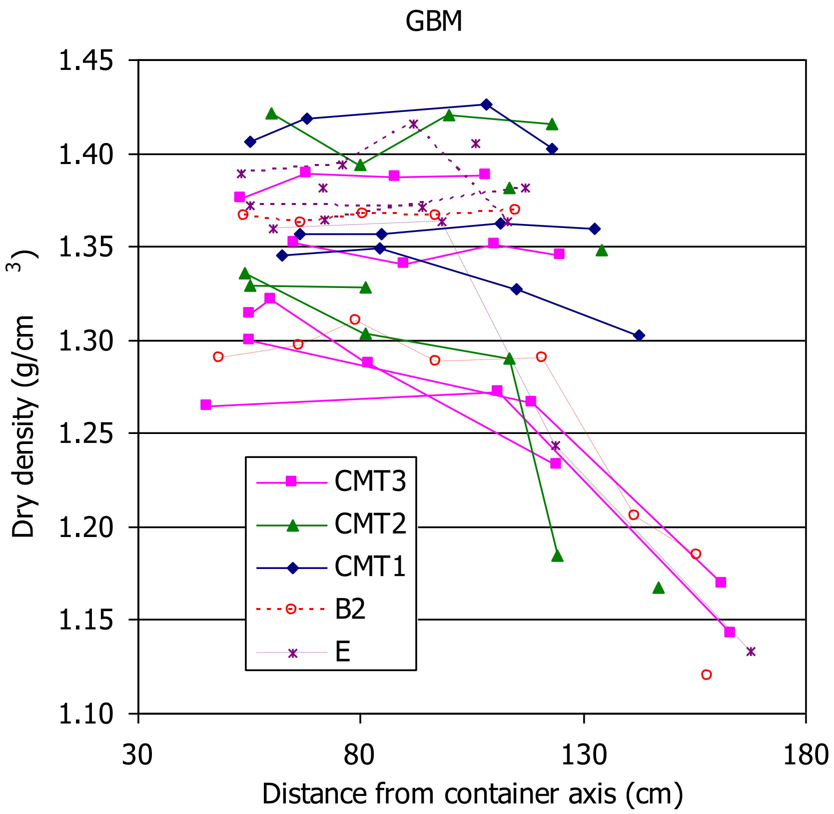

Figure 16: Dry density of GBM samples from different sampling sections as measured in the laboratory

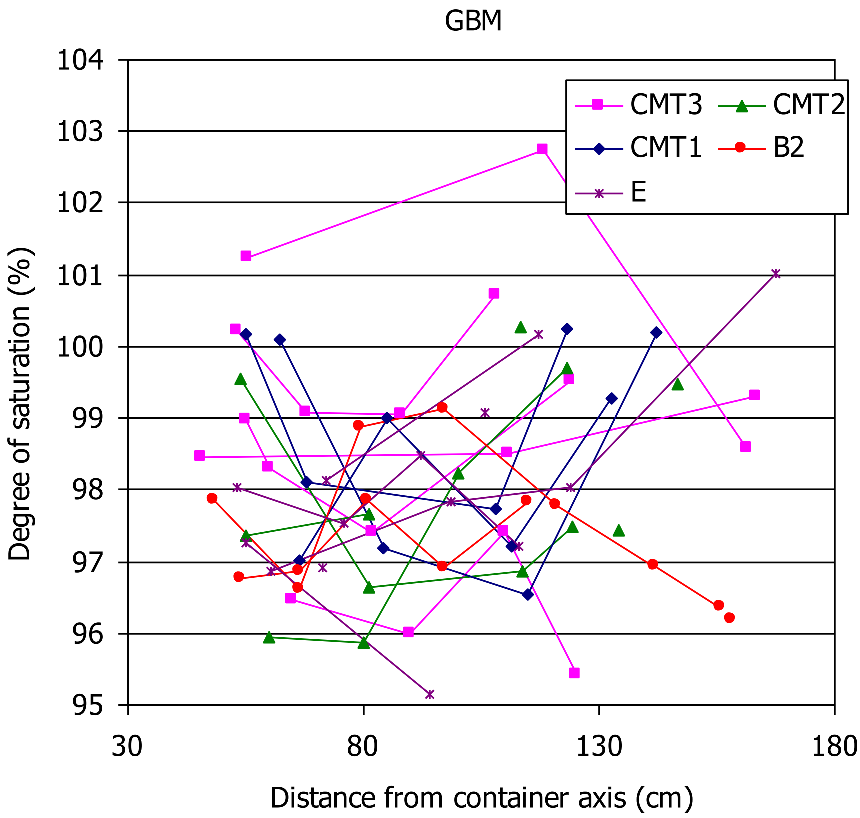

Figure 17: Degree of saturation of GBM samples from different sampling sections as measured in the laboratory

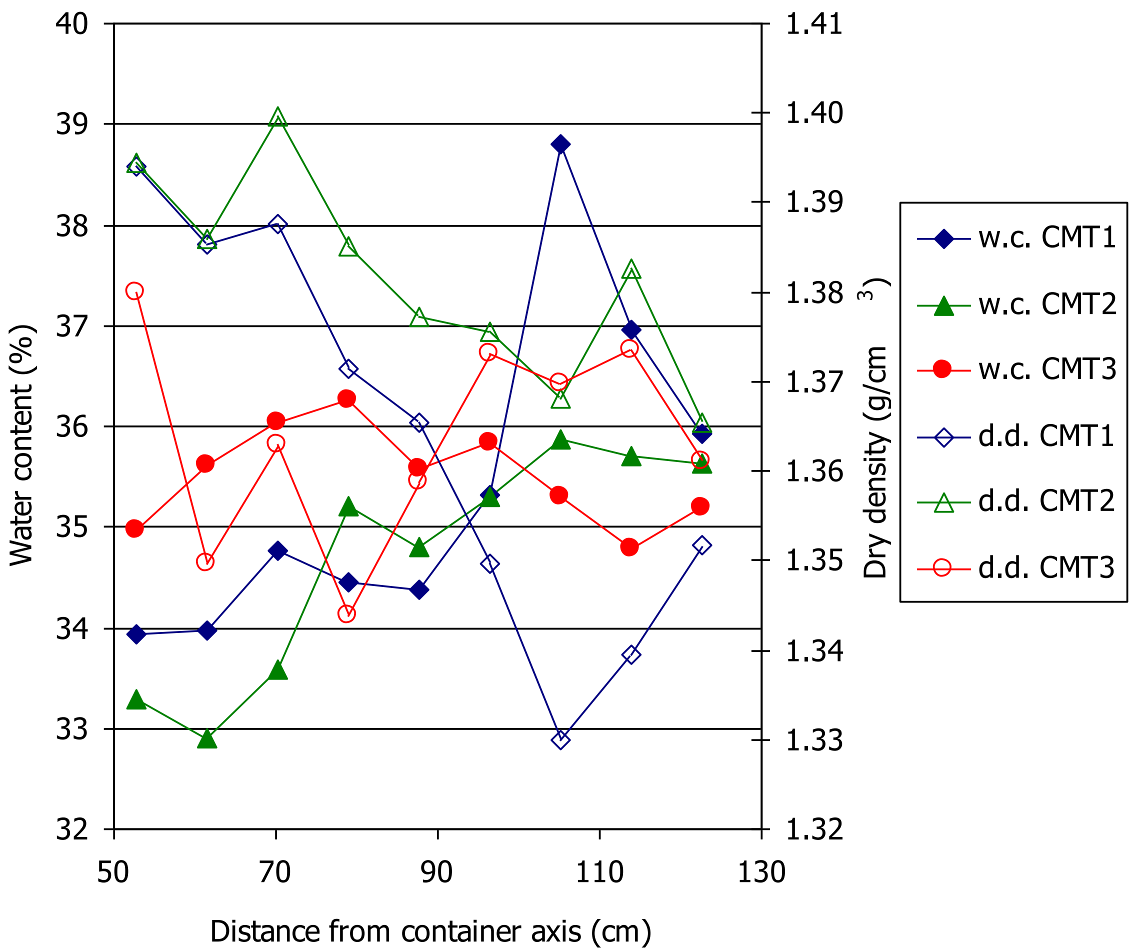

Figure 18: Water contents and dry densities measured in blocks from three sampling sections

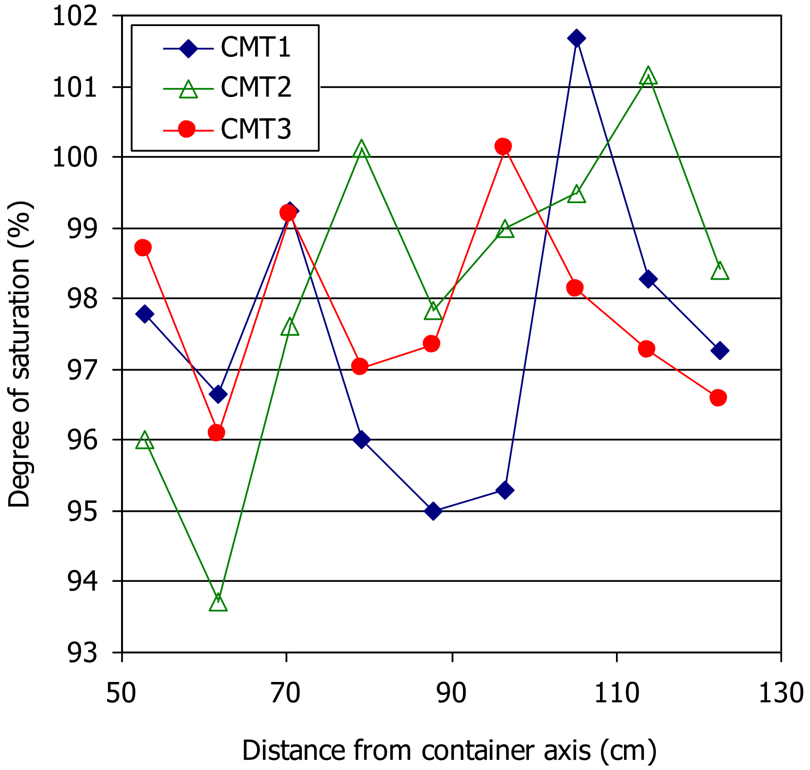

Figure 19: Degrees of saturation measured in blocks from three sampling sections

Table III shows average values for each sampling section grouped according to the position of the samples in the barrier: upper, intermediate and lower part of the GBM and blocks. These values are also plotted in Figure 20 to Figure 22. Inside the GBM the water content increased clearly towards the bottom, while the dry density decreased. These changes were not reflected in the degrees of saturation, which did not show any clear spatial trend. The deviations with respect to the average values were higher towards the bottom of the GBM because the increase in water content towards the bottom was sharper in the lower part of the GBM. The average values for the blocks were between those of the bottom and the upper part of the GBM and were similar for the three sampling sections. On the other hand, there were differences among sections in the GBM, and it seems that the average water content of the GBM increased towards the bottom part of the gallery (from section CMT1 to CMT3).

Table III: Average values according to the position of the samples in each section

Position	# samples	Dry density (g/cm^3)	Water content (%)	Degree of saturation (%)
CMT1 GBM upper	4	1.42±0.01	33.4±1.0	99±1
CMT1 GBM intermediate	4	1.36±0.00	35.9±0.05	98±1
CMT1 GBM lower	4	1.33±0.02	37.5±1.6	99±2
CMT1 blocks	12	1.36±0.02	35.4±1.6	97±2
CMT2 GBM upper	5	1.41±0.02	33.4±1.3	98±2
CMT2 GBM intermediate	5	1.35±0.02	36.6±1.0	98±1
CMT2 GBM lower	4	1.24±0.07	43.0±5.0	98±1
CMT2 blocks	12	1.38±0.01	34.7±1.1	98±2
CMT3 GBM upper	5	1.39±0.01	35.0±0.5	99±1
CMT3 GBM intermediate	8	1.32±0.04	37.9±2.8	97±2
CMT3 GBM lower	6	1.24±0.06	44.1±3.9	100±2
CMT3 blocks	12	1.36±0.01	35.5±0.5	98±1
A1_25 GBM lower	7	1.34±0.03	37.2±1.9	99±2
E GBM upper	6	1.39±0.02	34.2±0.7	98±1
E GBM intermediate	4	1.37±0.01	35.2±0.7	98±2
E GBM lower	4	1.27±0.11	41.3±7.7	99±2
B2 GBM upper	5	1.37±0.00	35.2±0.2	97±1
B2 GBM lower	8	1.25±0.07	42.2±4.2	98±1

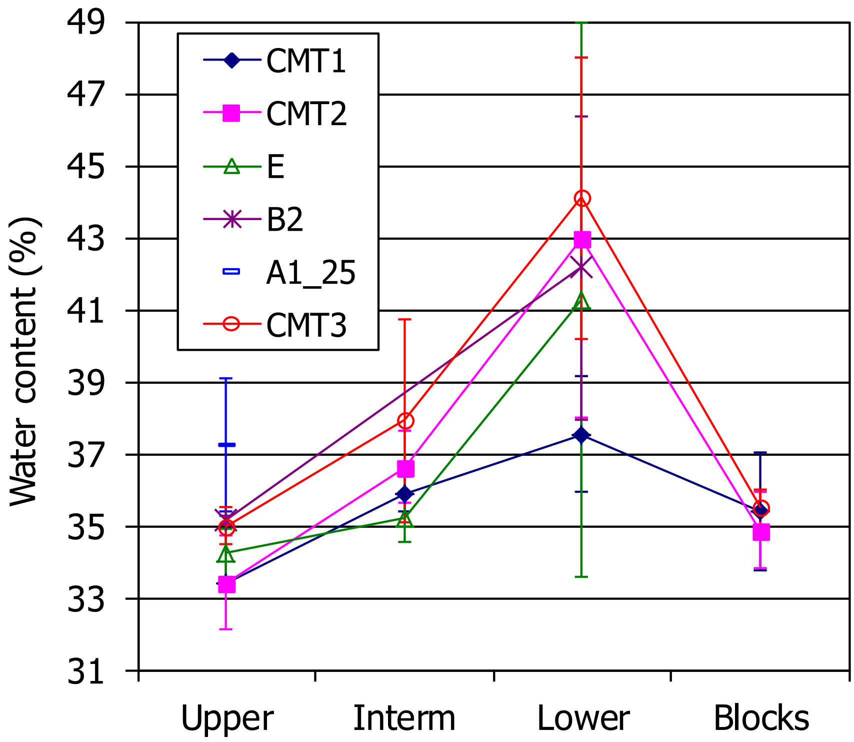

Figure 20: Average water content measured in the laboratory according to the position of the samples in the barrier and the sampling section

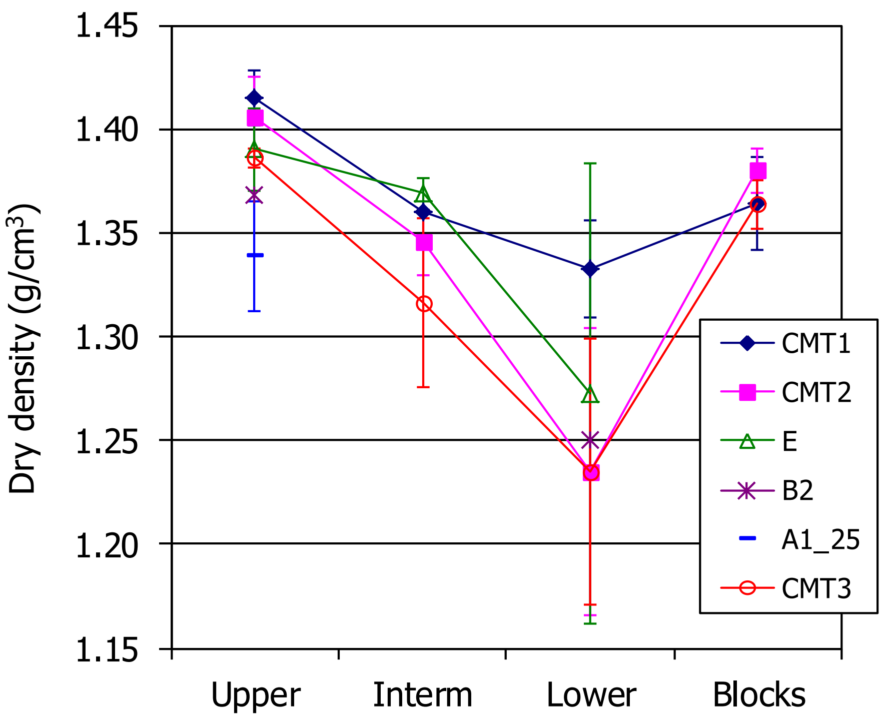

Figure 21: Average dry density measured in the laboratory according to the position of the samples in the barrier and the sampling section

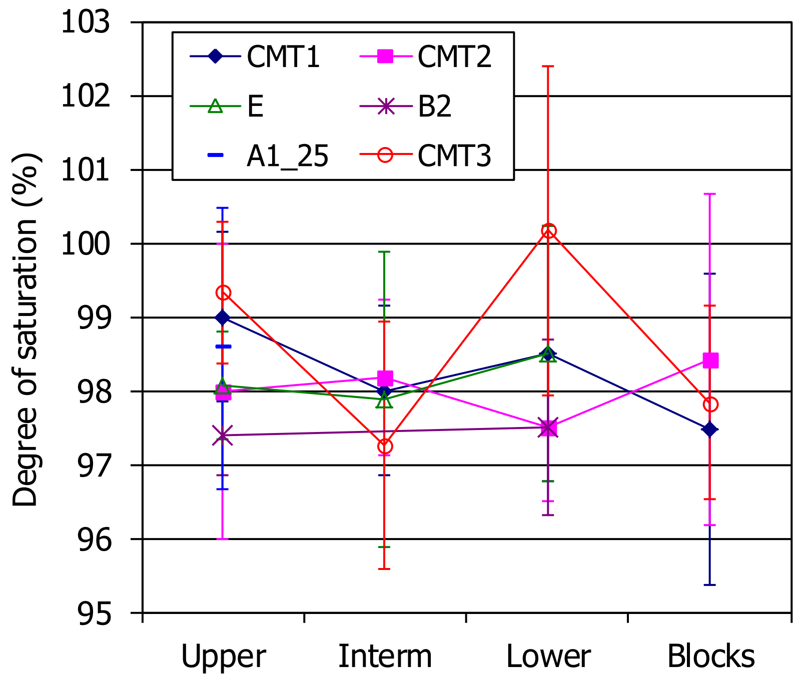

Figure 22: Average degree of saturation measured in the laboratory according to the position of the samples in the barrier and the sampling section

The results for the GBM are plotted again in Figure 23 and Figure 24 as a function of the coordinate y indicating the positions of the samples. The origin for this coordinate is the middle point of the bottom of the gallery. The trend for the water content to increase and the dry density to decrease towards the bottom is very clear and can even be fit to a potential expression.

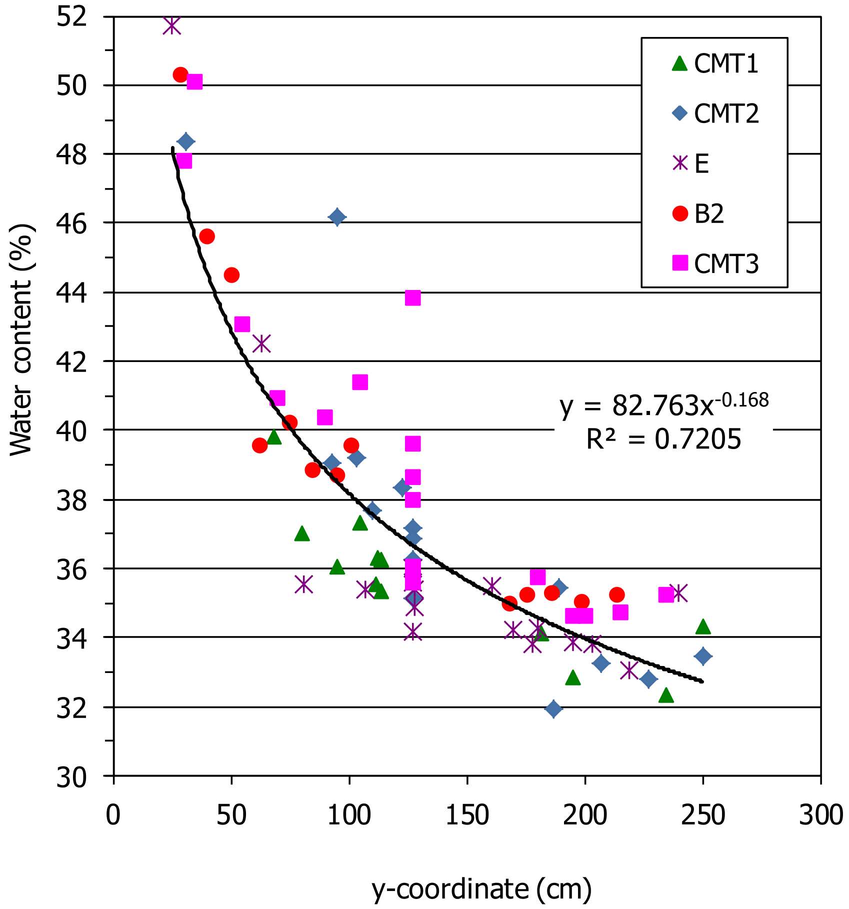

Figure 23: Water content measured in the GBM of different sections as a function of coordinate y

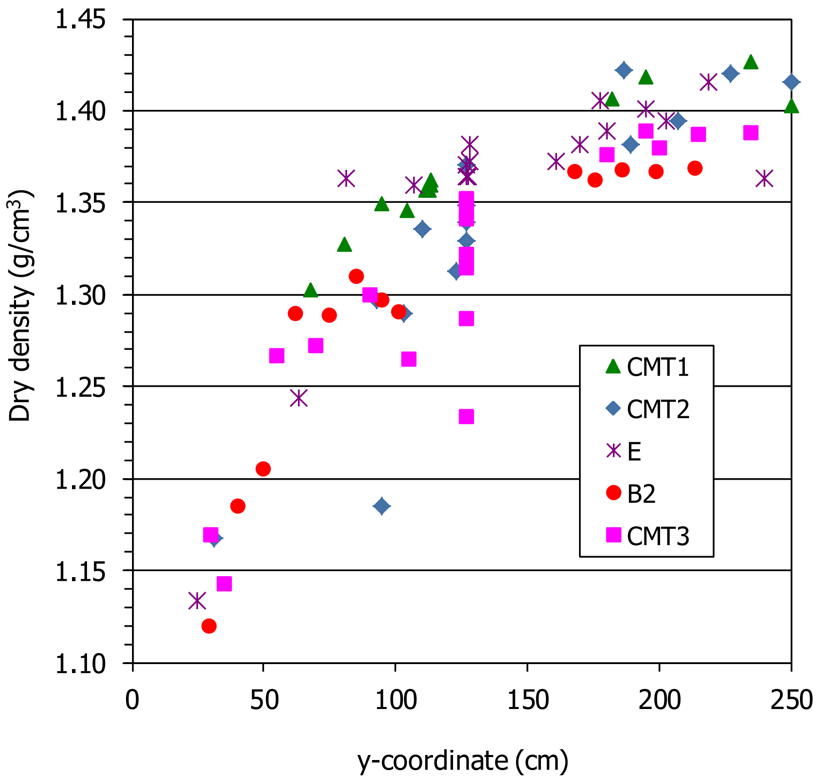

Figure 24: Dry density measured in the GBM of different sections as a function of coordinate y

5.4 LABORATORY SUCTION MEASUREMENTS

The suction of the samples was computed with Equation 1 from the relative humidity and temperature measured in the laboratory in samples of the blocks and the GBM. The values obtained with the psychrometers, which ranged between 2.1 and 4.7 MPa, are plotted in Figure 25 as a function of the water content of the bentonite for the different kinds of samples. Despite the large dispersion, the suction is seen to decrease with water content, and no difference could be found between the GBM and the blocks. The relationship between suction and dry density was inverse (Figure 26), but no clear relation with the degree of saturation could be verified.

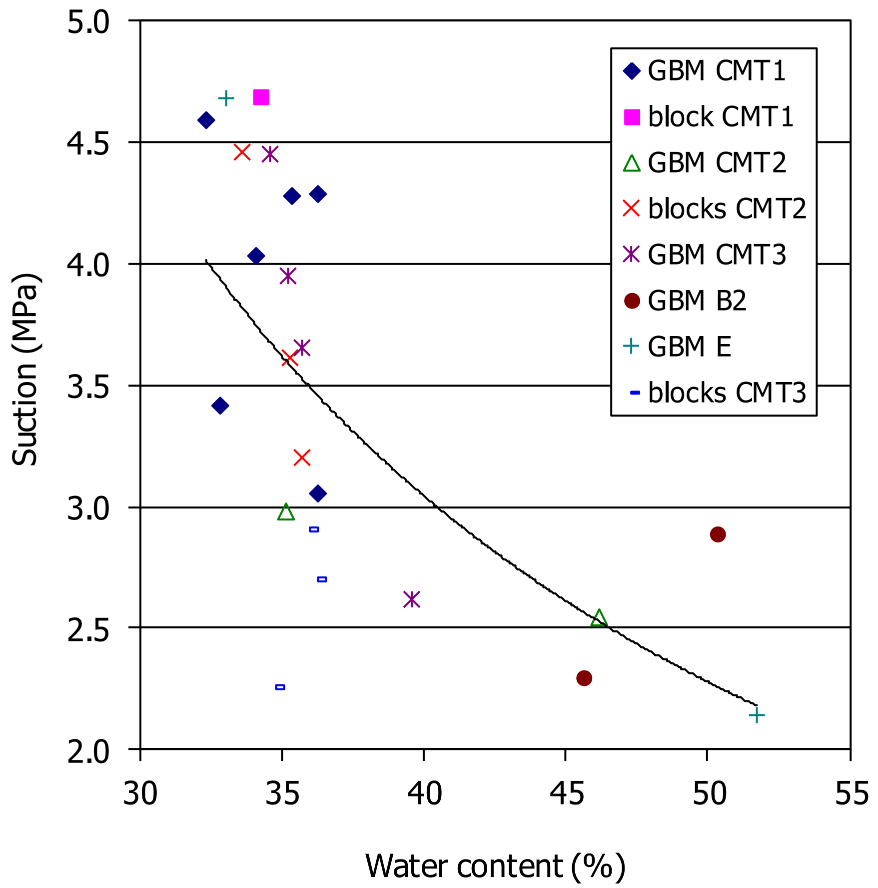

Figure 25: Suction computed from the psychrometer measurements in samples from different sampling sections as a function of the water content of the samples

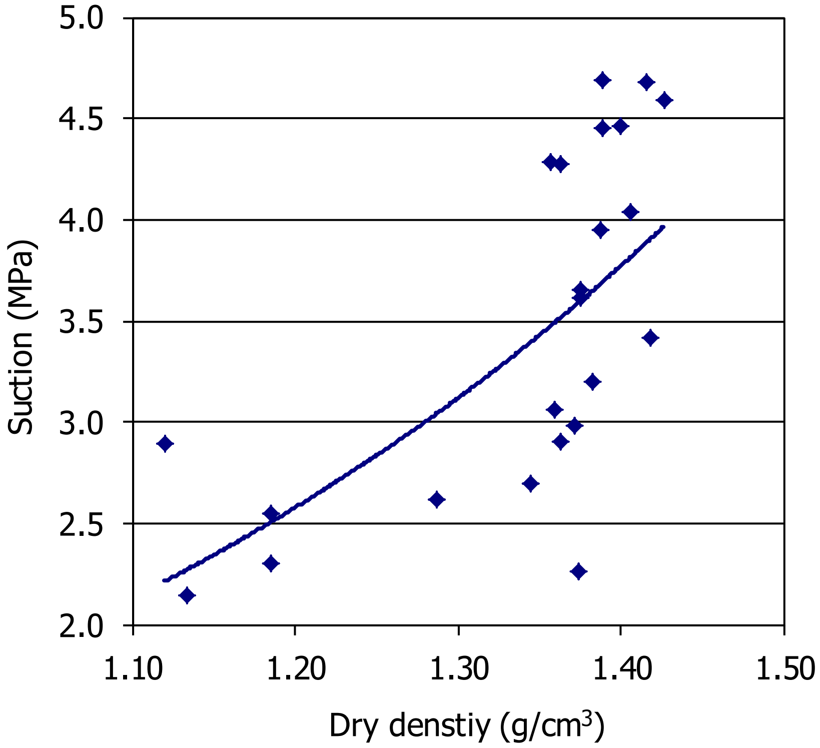

Figure 26: Suction computed from the psychrometer measurements in samples from different sampling sections as a function of the dry density of the samples

5.5 COMPARISON OF ON SITE AND LABORATORY DETERMINATIONS

A few samples from section A1_25 were cut in two, and one half was analysed on site by the AITEMIN team and the other half at CIEMAT laboratories, with the aim of fine tuning the on-site measurement methods. The results obtained by both are shown in Figure 27, where it can be observed that the water contents obtained in the laboratory were a 3.8% higher than those obtained on site and, consequently, the dry densities were lower (a 1.1%). This proved that the packing methods were good enough to keep the physical conditions of the samples upon extraction.

Additionally, twin samples were taken in sections E and B2, one of them was analysed on site and the other one was sent to CIEMAT. A total of 13 samples from section B2 (Table A- IX) and 17 from section E (Table A- VIII) were analysed. For section B2 the water contents obtained in the laboratory were on average a 0.7% higher than those obtained on site, and the dry densities a 0.2% higher. For section E the water contents obtained in the laboratory were on average the same as those obtained on site and the dry densities a 1.4% higher. The differences are very small, particularly regarding water content, consequently they are not considered significant.

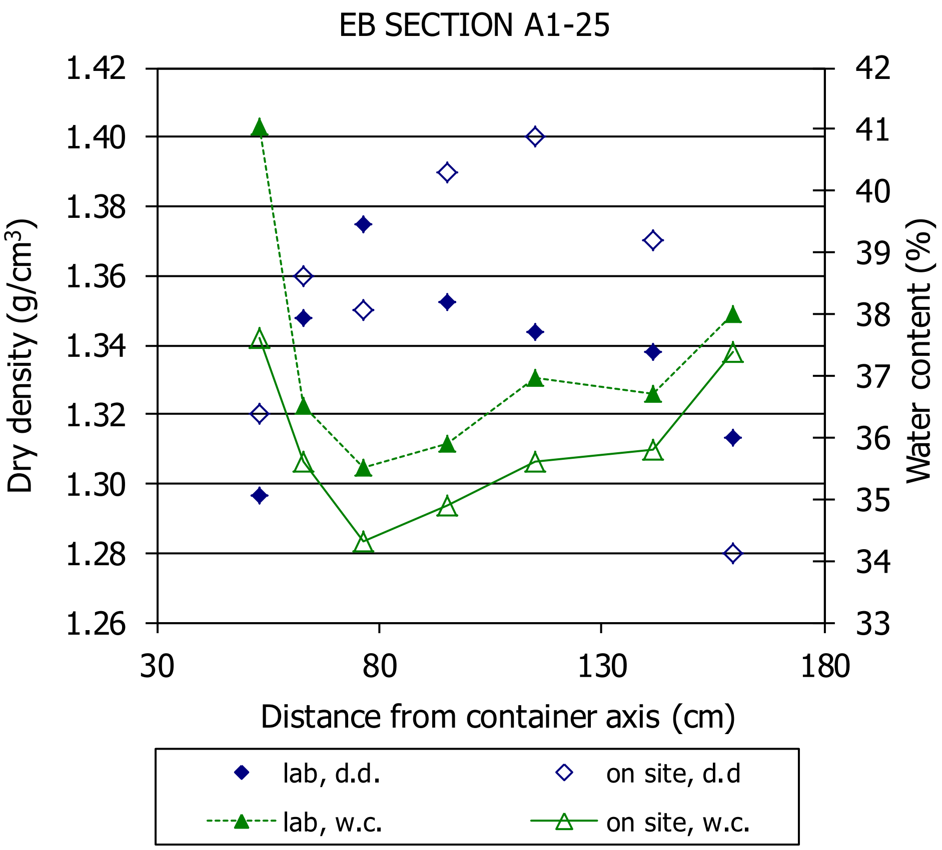

Figure 27: Water content and dry density measured in samples from section A1_25 on site and in the laboratory

Conclusions

This report summarises the physical characterisation performed at CIEMAT laboratories of bentonite samples taken during the EB experiment dismantling. Water content, dry density and degree of saturation values have been presented, along with some suction measurements.

The water contents ranged between 33 and 43% and the dry densities between 1.42 and 1.24 g/cm^3, with a clear trend for the water content to increase towards the bottom part of the barrier. Two factors could have played a role in this distribution. Firstly, during the installation of the GBM segregation occurred, the finer grains accumulating at the bottom, which would cause an initial density gradient in the barrier, with lower density at the bottom. Secondly, the effect of gravity on the water distribution seems to have been relevant. The accumulation of water in the lower part of the barrier took place probably at the beginning of the experiment, favoured by the higher initial porosity of the barrier bottom. The higher water contents in these zones were accompanied by a further reduction in dry densities, consequence of swelling. This swelling seems to have been irreversible, since the density difference among different parts of the barrier remained after 10 years of operation. The blocks had water contents similar to those of the adjacent GBM, and their density decreased from an initial value of 1.7 g/cm^3 to values close to 1.4 g/cm^3, similar to the average values found in the GBM. The increase in the dimensions of the blocks confirms that they swelled during the test and also after dismantling, when the pressures were released. The blocks closer to the concrete plug swelled mainly in the longitudinal direction, whereas in the rest of sections the change in blocks' vertical dimensions indicates the uplift of the canister.

The degrees of saturation of the barrier ranged between 95 and 101%. It is considered that the average pore water density in the barrier is close to 1.0 g/cm^3 due to the low average dry density of the bentonite.

Concerning the average values of water content and dry density there are not important differences among the different sampling sections.

The comparison between the values obtained on site and in the laboratory has shown a very good agreement, but all these observations have to be confirmed with the on site measurements, which involve a larger number of samples.

Acknowledgements

The research leading to these results received funding from the European Atomic Energy Community's Seventh Framework Programme (FP7/2007-2011) under Grant Agreement n^{o}249681, the PEBS project. This work was additionally financed by ENRESA through a CIEMAT-ENRESA General Agreement. The laboratory work was performed by Juan Aroz, Francisco Javier Romero and Ramón Campos, at CIEMAT. The psychrometers used for suction measurement were lent by AITEMIN.

References

AITEMIN 2012. Engineered Barrier Emplacement Experiment in Opalinus Clay "EB" Experiment. TEST PLAN. Madrid, 64 pp.

ENRESA 2005. "Engineered barrier emplacement experiment in Opalinus Clay for the disposal of radioactive waste in underground repositories" Final Report. *Publicación Técnica ENRESA* 02/05. Madrid, 101 pp.

ENRESA, 2006. FEBEX Full-scale Engineered Barriers Experiment, Updated Final Report 1994-2004. *Publicación Técnica ENRESA* 05-0/2006, Madrid, 590 pp.

PEARSON F. 1998. Artificial waters for use in laboratory and field experiments with Opalinus Clay. *Paul Scherrer Institut TM* 44-98-08

UNE 7045(1952): Determinación de la porosidad de un terreno.

Appendix 1 Laboratory measurements

Table A- I: Values measured in the laboratory in GBM samples from section A1_25 (z=320)

Sample reference	x	y	Position[a] (cm)	Dry density (g/cm^3)	Water content (%)	Degree of saturation (%)
B-S-A1_25-018	49	107	53	1.30	41.0	102
B-S-A1_25-019	57	100	63	1.35	36.5	98
B-S-A1_25-020	67	90	77	1.38	35.5	100
B-S-A1_25-021	83	80	95	1.35	35.9	97
B-S-A1_25-022	100	70	115	1.34	37.0	99
B-S-A1_25-023	125	60	142	1.34	36.7	97
B-S-A1_25-024	140	50	160	1.31	38.0	97
Average				1.34±0.03	37.2±1.9	99±2

[a] Approximate distance to canister centre

Table A- II: Values measured in the laboratory in block samples (two or three measurements per sample, average specimen volume 10±2 cm^3) from section CMT1 (z=355)

Sample reference	Position[a] (cm)	Dry density (g/cm^3)	Water content (%)	Degree of saturation (%)	Suction (MPa)
B-B-CMT1-007	53	1.39	33.9	98	4.7[c]
	62	1.39	34.0	97	
	70	1.39	34.8	99	
B-B-CMT1-006	79	1.37	34.4	96	
	88	1.37	34.4	95	
	96	1.35	35.3	95	
B-B-CMT1-004	105	1.33	38.8	102	
	114	1.34	37.0	98	0[b]
	123	1.35	35.9	97	0.5[b]
Average		1.36±0.02	35.4±1.6	97±2	

[a] Approximate distance to canister centre; [b] Measured in the laboratory with capacitive sensors; [c] Measured in the laboratory with psychrometers

Table A- III: Values measured in the laboratory in block samples (two or three measurements per sample, average specimen volume 11±2 cm^3) from section CMT2 (z=460)

Sample reference	Position[a] (cm)	Dry density (g/cm^3)	Water content (%)	Degree of saturation (%)	Suction[b] (MPa)
B-B-CMT2-002	53	1.39	33.3	96	
	62	1.39	32.9	94	
	70	1.40	33.6	98	4.5
B-B-CMT2-005	79	1.39	35.2	100	
	88	1.38	34.8	98	
	96	1.38	35.3	99	3.6
B-B-CMT2-009	105	1.37	35.9	99	
	114	1.38	35.7	101	
	123	1.37	35.6	98	3.2
Average		1.38±0.01	34.7±1.1	98±2	

[a] Approximate distance to canister centre; [b] Measured in the laboratory with capacitive sensors

Table A- IV: Values measured in the laboratory in block samples (two or three measurements per sample, average specimen volume 10±1 cm^3) from section CMT3 (z=650)

Sample reference	Position[a] (cm)	Dry density (g/cm^3)	Water content (%)	Degree of saturation (%)	Suction[b] (MPa)
B-B-CMT3-001	53	1.38	35.0	99	
	62	1.35	35.6	96	
	70	1.36	36.0	99	2.9
B-B-CMT3-003	79	1.34	36.3	97	2.7
	88	1.36	35.6	97	
	96	1.37	35.8	100	
B-B-CMT3-006	105	1.37	35.3	98	
	114	1.37	34.8	97	2.3
	123	1.36	35.2	97	
Average		1.36±0.01	35.5±0.5	98±1	

[a] Approximate distance to canister centre; [b] Measured in the laboratory with capacitive sensors; [c] Measured in the laboratory with psychrometers

Table A- V: Values measured in the laboratory in GBM samples (two measurements per sample, average specimen volume 12±3 cm^3) from section CMT1 (z=349)

Sample reference	x	y	Position[a] (cm)	Dry density (g/cm^3)	Water content (%)	Degree of saturation (%)	Suction[b] (MPa)
B-S-CMT1-001	-58	105	62	1.35	37.3	100	
B-S-CMT1-002	-78	95	84	1.35	36.0	97	
B-S-CMT1-003	-105	81	115	1.33	37.0	97	
B-S-CMT1-004	-130	68	142	1.30	39.8	100	2.0[b]
B-S-CMT1-005	65	112	66	1.36	35.6	97	
B-S-CMT1-006	84	113	85	1.36	36.3	99	1.2[b] / 4.3[c]
B-S-CMT1-007	111	114	111	1.36	35.3	97	4.3[c]
B-S-CMT1-008	132	114	133	1.36	36.3	99	3.1[c]
B-S-CMT1-017	0	182	55	1.41	34.1	100	4.0[c]
B-S-CMT1-018	0	195	68	1.42	32.8	98	3.4[c]
B-S-CMT1-016	0	235	108	1.43	32.3	98	
B-S-CMT1-019	0	250	123	1.40	34.3	100	2.2[b] / 4.6[c]
Average				1.37±0.04	35.6±2.0	99±1	

[a] Approximate distance to canister centre; [b] Measured in the laboratory with capacitive sensors; [c] Measured in the laboratory with psychrometers

Table A- VI: Values measured in the laboratory in GBM samples (two measurements per sample, average specimen volume 8±1 cm^3) from section CMT2 (z=460)

Sample reference	x	y	Position[a] (cm)	Dry density (g/cm^3)	Water content (%)	Degree of saturation (%)	Suction[b] (MPa)
B-S-CMT2-004	55	127	55	1.33	37.2	97	
B-S-CMT2-005	81	127	81	1.33	37.4	98	
B-S-CMT2-006	107	127	107	1.37	35.1	98	3.0
B-S-CMT2-007	134	127	134	1.35	36.2	97	
B-S-CMT2-018	-53	110	56	1.34	37.7	100	
B-S-CMT2-019	-81	123	81	1.30	38.3	97	
B-S-CMT2-020	-111	103	114	1.29	39.2	97	
B-S-CMT2-021	-120	95	124	1.18	46.2	97	3.4
B-S-CMT2-029	0	187	60	1.42	32.0	96	
B-S-CMT2-030	0	207	80	1.39	33.3	96	
B-S-CMT2-031	0	227	100	1.42	32.8	98	
B-S-CMT2-032	0	250	123	1.42	33.5	100	
B-S-CMT2-026	95	189	113	1.38	35.5	100	
Average				1.35±0.07	36.4±3.7	98±1	
B-S-CMT2-017	-129	31	161	1.17	48.3	99	

[a] Approximate distance to canister centre; [b] Measured in the laboratory with psychrometers

Table A- VII: Values measured in the laboratory in GBM samples (two measurements per sample, average specimen volume 9±1 cm^3) from section CMT3 (z=695)

Sample reference	x	y	Position[a] (cm)	Dry density (g/cm^3)	Water content (%)	Degree of saturation (%)	Suction[b] (MPa)
B-S-CMT3-008	65	127	65	1.35	35.6	96	
B-S-CMT3-009	90	127	90	1.34	36.0	96	
B-S-CMT3-010	110	127	110	1.35	36.0	97	
B-S-CMT3-011	125	127	125	1.34	35.6	95	
B-S-CMT3-014	65	200	98	1.38	34.6	98	
B-S-CMT3-015	0	180	53	1.38	35.7	100	3.7
B-S-CMT3-016	0	195	68	1.39	34.6	99	4.5
B-S-CMT3-017	0	215	88	1.39	34.7	99	
B-S-CMT3-018	0	235	108	1.39	35.3	101	4.0
B-S-CMT3-019	-55	127	55	1.31	38.7	99	
B-S-CMT3-020	-60	127	60	1.32	38.0	98	
B-S-CMT3-021	-82	127	82	1.29	39.6	97	2.6
B-S-CMT3-022	-124	127	124	1.23	43.8	100	
Average[c]				1.34±0.05	36.8±2.6	98±2	
B-S-CMT3-001	41	90	55	1.30	41.3	103	
B-S-CMT3-002	94	55	118	1.27	43.1	103	
B-S-CMT3-003	129	30	161	1.17	47.8	99	
B-S-CMT3-023	-40	105	46	1.26	41.4	98	
B-S-CMT3-024	-95	70	111	1.27	40.9	99	
B-S-CMT3-025	-135	35	163	1.14	50.1	99	
Average[d]				1.31±0.07	39.3±4.6	99±2	

[a] Approximate distance to canister centre; [b] Measured in the laboratory with psychrometers; [c] Samples from the 3 sampling radii in the half upper part of the GBM; [d] Samples from the 5 sampling radii

Table A- VIII: Values measured in the laboratory in GBM samples (two measurements per sample, average specimen volume 7±1 cm^3) from section E (z=520)

Sample reference	x	y	Position[a] (cm)	Dry density (g/cm^3)	Water content (%)	Degree of saturation (%)	Suction[b] (MPa)
B-S-E-017	-67	128	67	1.37	34.9	97	
B-S-E-019	-112	127	112	1.37	34.2	95	
B-S-E-022	80	128	80	1.36	35.6	98	
B-S-E-023	94	127	94	1.36	36.0	99	
B-S-E-024	132	128	132	1.38	35.4	100	
B-S-E-028	68	161	76	1.37	35.5	99	
B-S-E-029	96	178	109	1.41	33.8	99	
B-S-E-032	-57	170	71	1.38	34.2	97	
B-S-E-034	-80	195	105	1.40	33.9	99	
B-S-E-037	0	180	53	1.39	34.3	98	
B-S-E-038	0	203	76	1.39	33.8	98	
B-S-E-039	0	219	92	1.42	33.1	98	4.7
B-S-E-040	0	240	113	1.36	35.3	97	
Average[c]				1.38±0.02	34.6±0.9	98±1	
B-S-E-010	-57	107	60	1.36	35.4	97	
B-S-E-012	-87	81	98	1.36	35.5	98	
B-S-E-014	-106	63	124	1.24	42.5	98	
B-S-E-016	-133	25	168	1.13	51.7	101	2.1
Average[d]				1.36±0.07	36.2±4.5	98±1	

[a] Approximate distance to canister centre; [b] Measured in the laboratory with psychrometers; [c] Samples from the half upper part of the GBM; [d] Samples from all the sampling radii

Table A- IX: Values measured in the laboratory in GBM samples (two measurements per sample, average specimen volume 8±2 cm^3) from section B2 (z=647)

Sample reference	x	y	Position[a] (cm)	Dry density (g/cm^3)	Water content (%)	Degree of saturation (%)	Suction (MPa)
B-S-B2-031	-35	168	54	1.37	35.0	97	
B-S-B2-032	-45	176	67	1.36	35.2	97	2.0[b]
B-S-B2-033	-55	186	81	1.37	35.3	98	
B-S-B2-034	-65	199	97	1.37	35.0	97	1.2[b]
B-S-B2-035	-75	214	115	1.37	35.2	98	
Average[d]				1.37±0.00	35.2±0.2	97±1	
B-S-B2-001	48	101	55	1.29	39.6	98	
B-S-B2-002	58	95	66	1.30	38.7	97	
B-S-B2-003	67	85	79	1.31	38.8	99	
B-S-B2-004	82	75	97	1.29	40.2	99	
B-S-B2-005	102	62	121	1.29	39.6	98	
B-S-B2-006	119	50	142	1.21	44.5	97	
B-S-B2-007	129	40	156	1.19	45.6	96	2.3[c]
B-S-B2-020	-124	29	158	1.12	50.3	96	2.9[c]
Average[e]				1.25±0.07	42.2±4.2	97±1	

[a] Approximate distance to canister centre; [b] Measured in the laboratory with capacitive sensors; [c] Measured in the laboratory with psychrometers; [d] Samples from the half upper part of the GBM; [e] Samples from the half lower part of the GBM